

NEW CARBOCYCLISATIONS OF POLYUNSATURATED HYDRAZONES CATALYSED BY RHODIUM(I)

Òscar Torres Antón

Per citar o enllaçar aquest document:

Para citar o enlazar este documento:

Use this url to cite or link to this publication:

<http://hdl.handle.net/10803/401739>

ADVERTIMENT. L'accés als continguts d'aquesta tesi doctoral i la seva utilització ha de respectar els drets de la persona autora. Pot ser utilitzada per a consulta o estudi personal, així com en activitats o materials d'investigació i docència en els termes establerts a l'art. 32 del Text Refós de la Llei de Propietat Intel·lectual (RDL 1/1996). Per altres utilitzacions es requereix l'autorització prèvia i expressa de la persona autora. En qualsevol cas, en la utilització dels seus continguts caldrà indicar de forma clara el nom i cognoms de la persona autora i el títol de la tesi doctoral. No s'autoritza la seva reproducció o altres formes d'explotació efectuades amb finalitats de lucre ni la seva comunicació pública des d'un lloc aliè al servei TDX. Tampoc s'autoritza la presentació del seu contingut en una finestra o marc aliè a TDX (framing). Aquesta reserva de drets afecta tant als continguts de la tesi com als seus resums i índexs.

ADVERTENCIA. El acceso a los contenidos de esta tesis doctoral y su utilización debe respetar los derechos de la persona autora. Puede ser utilizada para consulta o estudio personal, así como en actividades o materiales de investigación y docencia en los términos establecidos en el art. 32 del Texto Refundido de la Ley de Propiedad Intelectual (RDL 1/1996). Para otros usos se requiere la autorización previa y expresa de la persona autora. En cualquier caso, en la utilización de sus contenidos se deberá indicar de forma clara el nombre y apellidos de la persona autora y el título de la tesis doctoral. No se autoriza su reproducción u otras formas de explotación efectuadas con fines lucrativos ni su comunicación pública desde un sitio ajeno al servicio TDR. Tampoco se autoriza la presentación de su contenido en una ventana o marco ajeno a TDR (framing). Esta reserva de derechos afecta tanto al contenido de la tesis como a sus resúmenes e índices.

WARNING. Access to the contents of this doctoral thesis and its use must respect the rights of the author. It can be used for reference or private study, as well as research and learning activities or materials in the terms established by the 32nd article of the Spanish Consolidated Copyright Act (RDL 1/1996). Express and previous authorization of the author is required for any other uses. In any case, when using its content, full name of the author and title of the thesis must be clearly indicated. Reproduction or other forms of for profit use or public communication from outside TDX service is not allowed. Presentation of its content in a window or frame external to TDX (framing) is not authorized either. These rights affect both the content of the thesis and its abstracts and indexes.



Doctoral Thesis

**New carbocyclisations of polyunsaturated
hydrazones catalysed by rhodium(I)**

Òscar Torres Antón

2017

Doctoral Programme in Chemistry

Supervised by: Dr. Anna Pla Quintana and Prof. Anna Roglans Ribas

Tutor: Prof. Anna Roglans Ribas

Presented in partial fulfilment of the requirements for a **doctoral degree** from the **University of Girona**



Dr. Anna Pla Quintana and **Prof. Anna Roglans Ribas**, from the University of Girona

WE DECLARE:

That the thesis entitled “New carbocyclisations of polyunsaturated hydrazones catalysed by rhodium(I)” presented by **Òscar Torres Antón** to obtain a doctoral degree has been completed under our supervision and meets the requirements to opt for an International Doctorate.

For all intents and purposes, we hereby sign this document.

Dr. Anna Pla Quintana

Prof. Anna Roglans Ribas

Girona, 9th January, 2017

A mons pares i a la Teresa, qui m'omple la vida de colors meravellosos.

ACKNOWLEDGEMENTS

This work would not have been possible without the support from the following institutions and people:

- AGAUR of Generalitat de Catalunya for financial support through the project 2014-SGR-931 and for the Ph.D. Grant FI-DGR 2014.
- MINECO of Spain for financial support through projects CTQ2011-2312-P and CTQ2014-54306-P.
- Serveis Tècnics de Recerca from University of Girona and Dr. Teodor Parella from the Universitat Autònoma de Barcelona for technical support.
- Dr. Luca Gonsalvi from Consiglio Nazionale delle Ricerche (CNR) and Dr. Marko Hapke from Leibniz-Institut für Katalyse e. V. for hosting scientific visits, the latter supported by the MOB2015 from the UdG.

PUBLICATIONS

This doctoral thesis has resulted in the following publications:

- Enantioselective rhodium(I) donor carbenoid-mediated cascade triggered by a base-free decomposition of arylsulfonyl hydrazones. Torres, Ò.; Parella, T.; Solà, M.; Roglans, A.; Pla-Quintana, A. *Chem. Eur. J.* **2015**, *21*, 16240.
- An enantioselective cascade cyclopropanation reaction catalyzed by rhodium(I): asymmetric synthesis of vinylcyclopropanes. Torres, Ò.; Roglans, A.; Pla-Quintana, A. *Adv. Synth. Catal.* **2016**, *358*, 3512. This publication has been labelled as a Very Important Publication (VIP) by the journal and was illustrated on the inside cover of the issue.
- Unusual reactivity of rhodium(I) carbenes with allenes: an efficient asymmetric synthesis of methylenetetrahydropyran scaffolds. Torres, Ò.; Solà, M.; Roglans, A.; Pla-Quintana, A. *Submitted*.
- The rich reactivity of transition-metal carbenes with alkynes. Torres, Ò.; Pla-Quintana, A. *Tetrahedron Lett.* **2016**, *57*, 3881.

Contributions in other publications not included in this thesis

- Nickel(0) complexes of acyclic polyunsaturated aza ligands. Brun, S.; Torres, Ò.; Pla-Quintana, A.; Roglans, A.; Goddard, R.; Pörschke, R. K. *Organometallics*, **2013**, *32*, 1710.
- Stereoselective rhodium(I)-catalyzed [2+2+2] cycloaddition of linear allene-ene/yne-allene substrates: reactivity and theoretical mechanistic studies. Torres, Ò.; Haraburda, E.; Parella, T.; Solà, M.; Pla-Quintana, A. *Chem. Eur. J.*, **2014**, *20*, 5034.
- Computational insight into Wilkinson's complex catalyzed [2+2+2] cycloaddition mechanism leading to pyridine formation. Torres, Ò.; Roglans, A.; Pla-Quintana, A.; Luis, J. M.; Solà, M. *J. Organomet. Chem.*, **2014**, *768*, 15.
- Examining the factors that govern the regioselectivity in the rhodium-catalyzed alkyne cyclotrimerization. Torres, Ò.; Fernández, M.; Parera, M.; Pla-Quintana, A.; Roglans, A.; Solà, M. *Submitted*.

ABBREVIATIONS

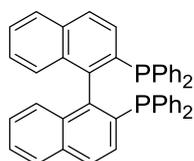
°C	Celsius degrees
ΔE	Electronic energy
ΔG	Gibbs free energy
δ	Charge density
ν (in IR)	Frequency (units: cm ⁻¹)
Ac	Acetyl
AcOEt	Ethyl acetate
aq.	Aqueous
Ar	Aryl
ATR (in IR)	Attenuated total reflectance
Bu	Butyl
cat.	Catalytic
CHPLC	Chiral high performance liquid chromatography
CSI-MS	Criospray ionisation mass spectrometry
cod	1,5-Cyclooctadiene
Cp*	Pentamethyl-η ⁵ -cyclopentadienyl
DCE	1,2-Dichloroethane
DCM	Dichloromethane
1,2-DCP	1,2-Dichloropropane
DMF	<i>N,N</i> -Dimethylformamide
DMSO	Dimethyl sulfoxide
DFT	Density functional theory
DOSP	<i>N</i> -(Dodecylbenzenesulfonyl)prolinate
EA	Elemental analysis
ee	Enantiomeric excess
equiv.	Equivalent
ESI-MS	Electrospray ionisation mass spectrometry
ESI-HRMS	Electrospray ionisation-high resolution mass spectrometry
esp	α,α,α',α'-Tetramethyl-1,3-benzenedipropionic acid
Et	Ethyl
EDG	Electron donating group
EtOH	Ethanol
EWG	Electron withdrawing group
DIAD	Diisopropyl azodicarboxylate
h	Hours
hfacac	Hexafluoroacetylacetonate
HPLC	High performance liquid chromatography
IBAZ	Isobutyl-2-oxaazetidincarboxylate

<i>i</i>Pr	<i>iso</i> -propyl
IPr	1,3-Bis(2,6-diisopropylphenyl)-1,3-dihydro-2H-imidazol-2-ylidene
IR	Infrared spectroscopy
K	Kelvin
kcal	Kilocalories
L	Ligand
LG	Leaving group
<i>m/z</i>	Mass to charge ratio
M	Molar
<i>m</i>-	Meta-
min	Minute
mL	Milliliter
m. p.	Melting point
Me	Methyl
MeOH	Methanol
Ms	Mesyl
MS	Molecular sieves
MS/MS	Tandem mass spectrometry
MW	Molecular weight
n. d.	Not-determined
Ns	Nosyl, 4-nitrobenzenesulfonyl
2-Ns	2-Nosyl, 2-nitrobenzenesulfonyl
<i>o</i>-	<i>Ortho</i> -
oct	Octane
<i>p</i>-	<i>Para</i> -
Ph	Phenyl
piv	Pivalate
por	Porphyrin
PTAD	4-Phenyl-1,2,4-triazoline-3,5-dione
rac	Racemic
r.t.	Room temperature
salen	<i>N,N'</i> -Bis(salicylidene)ethylenediamine
S	Spin state
T	Temperature
<i>t</i>Bu	<i>Tert</i> -butyl
TBAF	Tetrabutylammonium fluoride
TBDMS	<i>Tert</i> -butyldimethylsilyl
TBPTTL	3,3-Dimethyl-2-(tetrabromophthalimido)butyrate
TFA	Trifluoroacetic acid
Tf	Triflate, trifluoromethanesulfonyl
THF	Tetrahydrofuran

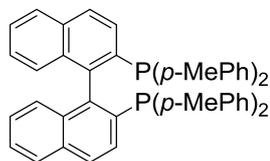
TLC	Thin layer chromatography
TM	Transition metal
Ts	Tosyl, 4-methylphenylsulfonyl

Biphosphines

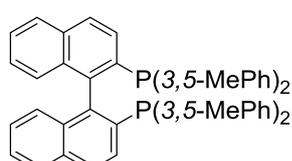
BINAP	2,2'-Bis(diphenylphosphino)-1,1'-binaphthalene
BIPHEP	2,2'-Bis(diphenylphosphino)-1,1'-biphenyl
DIFLUOROPHOS	5,5'-Bis(diphenylphosphanyl)-2,2,2',2'-tetrafluoro-4,4'-bi-1,3-benzodioxole
Dppf	1,1'-Bis(diphenylphosphino)ferrocene
DTBM-SEGPHOS	5,5'-Bis[di(3,5-di-tert-butyl-4-methoxyphenyl)phosphino]-4,4'-bi-1,3-benzodioxole
H₈-BINAP	2,2'-Bis(diphenylphosphino)-5,5',6,6',7,7',8,8'-octahydro-1,1'-binaphthyl
PPF-P^tBu₂	1-[2-(Diphenylphosphine)ferrocenyl]ethyl-di-tert-butylphosphine
SEGPHOS	5,5'-Bis(diphenylphosphine)-4,4'-bi-1,3-benzodioxole
Tol-BINAP	2,2'-Bis(di- <i>p</i> -tolyl)phosphine-1,1'-binaphthyl
Xylyl-BINAP	2,2'-Bis(3,5-dimethylphenyl)phosphine-1,1'-binaphthyl



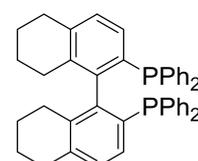
BINAP



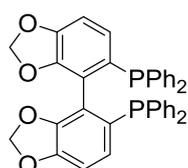
Tol-BINAP



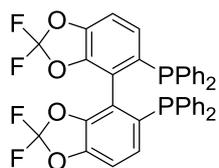
Xylyl-BINAP



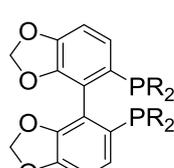
H₈-BINAP



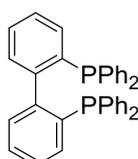
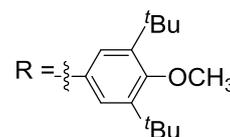
SEGPHOS



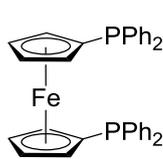
DIFLUOROPHOS



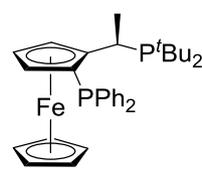
DTBM-SEGPHOS



BIPHEP



Dppf



PPF-P^tBu₂

Abbreviations used in Nuclear Magnetic Resonance (NMR)

δ	Chemical shift (units: ppm)
^{13}C NMR	Carbon-13 nuclear magnetic resonance
^1H NMR	Proton-1 nuclear magnetic resonance
^{31}P NMR	Phosphorous-31 nuclear magnetic resonance
1D	Monodimensional
2D	Bidimensional
abs	Absorption
ap	Apparent
br s	Broad signal
COSY	Correlation spectroscopy
d	Doublet
dd	Doublet of doublets
ddd	Doublet of doublet of doublets
dq	Doublet of quartets
DOSY	Diffusion ordered spectroscopy
HMBC	Heteronuclear multiple bond correlation
HSQCed	Edited heteronuclear single quantum coherence
J	Coupling constant
m	Multiplet
NOESY	Nuclear overhauser spectroscopy
ppm	Parts per million
q	Quartet
t	Triplet
s	Singlet

GRAPHICAL SUMMARY

Summary (Page 1)

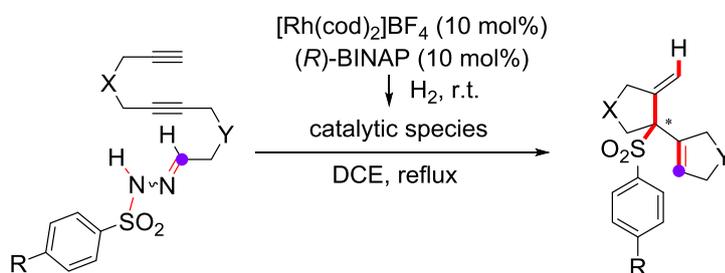
Resumen (Page 2)

Resum (Page 3)

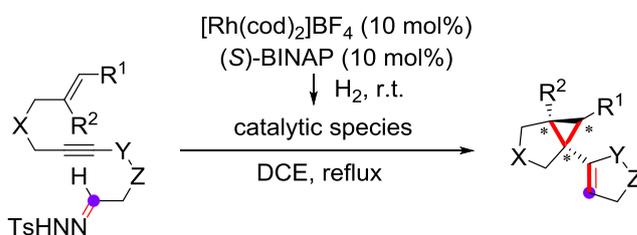
Chapter 1. General introduction (Page 5)

Chapter 2. Objectives (Page 25)

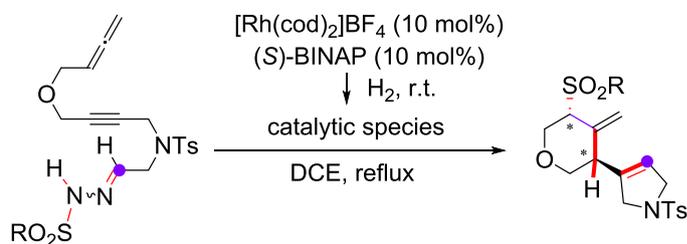
Chapter 3. Enantioselective rhodium(I) donor carbene-mediated cascade triggered by a base-free decomposition of arylsulfonylhydrazones (Page 29)



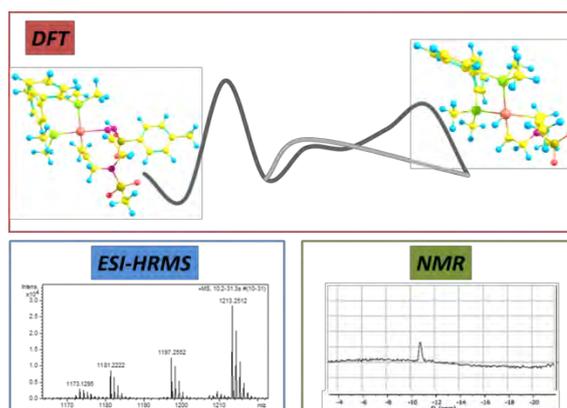
Chapter 4. Enantioselective cascade cyclopropanation reaction catalysed by rhodium(I): asymmetric synthesis of vinylcyclopropanes (Page 55)



Chapter 5. Unusual reactivity of rhodium(I) carbenes with allenes: an efficient asymmetric synthesis of methylenetetrahydropyran scaffolds (Page 71)



Chapter 6. Mechanistic insights into rhodium-carbene formation (Page 91)



Chapter 7. General conclusions (Page 109)

Chapter 8. Methods (Page 113)

Bibliography (Page 169)

SUPPLEMENTARY DATA

The material listed below is attached as supplementary data on the CD included in the thesis:

- **tota1de4.pdf**: Memory of the thesis.
- **tota2de4.pdf**: Selection of the ^1H NMR, ^2H NMR, ^{13}C NMR, IR and MS spectra and HPLC chromatograms of the products synthesised in Chapter 3 and cartesian coordinates of the stationary points.
- **tota3de4.pdf**: Selection of the ^1H NMR, ^2H NMR, ^{13}C NMR, IR and MS spectra and HPLC chromatograms and X-ray of the products synthesised in Chapter 4.
- **tota4de4.pdf**: Selection of the ^1H NMR, ^2H NMR and ^{13}C NMR spectra, HPLC chromatograms and X-ray of the products synthesised in Chapter 5 and cartesian coordinates of the stationary points.

TABLE OF CONTENTS

Summary	1
Resumen	2
Resum	3
Chapter 1. General introduction	5
1.1. Metal carbenes – generalities	7
1.2. Preparation of metal carbenes	9
1.3. Processes involving C _{alkyne} -H activation	13
1.4. Processes not involving C _{alkyne} -H activation	14
1.4.1. [2+1] Cycloaddition	14
1.4.2. Formal [3+2] cycloaddition	16
1.4.3. Carbene/alkyne metathesis – intramolecular processes	18
1.4.4. Carbene/alkyne metathesis – intermolecular processes	22
Chapter 2. Objectives	25
Chapter 3. Enantioselective rhodium(I) donor carbene-mediated cascade triggered by a base-free decomposition of arylsulfonylhydrazones	29
3.1. Retrosynthetic analysis of substrate 1aa	31
3.2. Synthesis of substrate 1aa	32
3.3. Reactivity studies	33
3.4. Computational studies.....	49
Chapter 4. Enantioselective cascade cyclopropanation reaction catalysed by rhodium(I): asymmetric synthesis of vinylcyclopropanes	55
4.1. Precedents in the synthesis of vinylcyclopropanes.....	57
4.2. Design and synthesis of the substrates 28	60
4.3. Reactivity studies	66
Chapter 5. Unusual reactivity of rhodium(I) carbenes with allenes: an efficient asymmetric synthesis of methylenetetrahydropyran scaffolds	71
5.1. Precedents in the reaction of metal carbenes and allenes	73
5.2. Retrosynthetic analysis of substrates 49 and 50a	74
5.3. Synthesis of substrates 49 and 50a	75
5.4. Reactivity studies	76
5.5. Computational studies.....	84

Chapter 6. Mechanistic insights into rhodium-carbene formation.....	89
6.1. Precedents in the mechanistic study of rhodium-carbene formation	91
6.2. NMR studies.....	92
6.3. ESI-HRMS studies	95
6.4. DFT calculations	101
Chapter 7. General conclusions	107
Chapter 8. Methods	111
8.1. General materials and instrumentation	113
8.1.1. General conditions.....	113
8.2. Experimental procedure for the products synthesised in Chapter 3.....	115
8.2.1. Synthesis of substrates.....	115
8.2.2. Experimental procedure for the rhodium(I)-catalysed cyclization of <i>N</i> -arylsulfonylhydrazones 1 and 23	125
8.3. Experimental procedure for the products synthesised in Chapter 4.....	130
8.3.1. Synthesis of substrates.....	130
8.3.2. Experimental procedure for the rhodium(I)-catalysed cyclisation of <i>N</i> -tosylhydrazone derivatives 28	147
8.4. Experimental procedure for the products synthesised in Chapter 5.....	151
8.4.1. Synthesis of substrates.....	151
8.4.2. Experimental procedure for the rhodium(I)-catalysed cyclisation of <i>N</i> -tosylhydrazone derivative 49	159
8.4.3. Experimental procedure for the rhodium(I)-catalysed cyclisation of <i>N</i> -sulfonylhydrazone derivatives 50	159
8.4.4. Deuterium labelling experiment	165
Bibliography.....	167

LIST OF FIGURES

Figure 1.1 Fischer and Schrock carbenes.....	7
Figure 1.2 Classification of metal carbenes species	8
Figure 1.3 Classification of rhodium carbene species	8
Figure 3.1 Model substrate tested in this study	31
Figure 3.2 Comparison between the expanded area of the ¹ H NMR spectrum (400 MHz) of 1aa (top) and 12aa in CDCl ₃ (bottom)	35
Figure 3.3 Expanded area of the HSQCed spectrum of 12aa in CDCl ₃	35
Figure 3.4 Assignment of ¹ H and ¹³ C NMR signals of 12aa	36
Figure 3.5 NOESY spectrum of 12aa (top) and its assignment (bottom)	36
Figure 3.6 Diphosphine ligands used in the optimisation process	37
Figure 3.7 Substrates designed and tested in this study	41
Figure 3.8 ¹ H NMR spectra of geometric isomers 1ba and 1ca	44
Figure 3.9 Expanded area corresponding to the ¹ H NMR spectrum (400 MHz) of 12ba in CDCl ₃ (top); Expanded area corresponding to the ¹ H NMR spectrum (400 MHz) of a mixture of 12ba and 12ba-D in CDCl ₃ (bottom)	48
Figure 3.10 Expanded area corresponding to the ¹ H NMR spectrum (400 MHz) of 12ca in CDCl ₃ (top); Expanded area corresponding to the ¹ H NMR spectrum (400 MHz) of a mixture of 12ca and 12ca-D in CDCl ₃ (bottom)	48
Figure 3.11 Expanded area of the ¹ H NMR spectrum (500 MHz) of a mixture of 12ca and 12ca-D in CDCl ₃ (bottom); ² H NMR spectrum (77 MHz) of a mixture of 12ca and 12ca-D in CDCl ₃ (top)	49
Figure 3.12 Gibbs energy profile (in kcal/mol) of the cyclisation of 24 to 26	50
Figure 3.13 Optimised structure (B3LYP/cc-pVDZ) for TS_BC . Distances in Å and angles in degrees	51
Figure 3.14 Optimised structure (B3LYP/cc-pVDZ) for TS_DE . Distances in Å and angles in degrees	51
Figure 3.15 Optimised structure (B3LYP/cc-pVDZ) for TS_EF . Distances in Å and angles in degrees	52
Figure 3.16 Optimised structure (B3LYP/cc-pVDZ) for TS_GH . Distances in Å and angles in degrees	52
Figure 3.17 Gibbs energy profile (in kcal/mol) for the different reaction pathways studied	53
Figure 3.18 Optimised structure (B3LYP/cc-pVDZ) for TS_BC (top-left), TS_DE (top-right) TS_E'F (bottom). Distances in Å and angles in degrees	53
Figure 4.1 Examples of compounds containing a bicyclo [3.1.0]-hexane ring system	57
Figure 4.2 Substrates designed and tested in this study	60
Figure 4.3 HPLC chromatogram of the crystallised 48a (top-left), the racemic mixture (top-right) and the fortified sample mixing the racemic mixture and the crystallised sample (bottom)	67

Figure 5.1 Substrates designed and tested in this study.....	74
Figure 5.2 ^1H NMR spectrum (400 MHz) of the mixture 2:1 of 53 and 53' in CDCl_3	77
Figure 5.3 ^1H NMR spectrum (400 MHz) of 54a in CDCl_3	79
Figure 5.4 ^1H NMR spectrum (400 MHz) of 55 in CDCl_3	79
Figure 5.5 Natural products containing functionalised tetrahydropyran rings	80
Figure 5.6 O-tethered substrates tested in this study.....	82
Figure 5.7 Gibbs energy profile (in kcal/mol) of the cyclisation of 56 to 57	85
Figure 5.8 Optimised structure (B3LYP/cc-pVDZ) for TS_BC . Distances in Å and angles in degrees	86
Figure 5.9 Trimethylene methane (TMM) structure	86
Figure 5.10 Optimised structure (B3LYP/cc-pVDZ) for TS_CD . Distances in Å	86
Figure 5.11 Optimised structure (B3LYP/cc-pVDZ) for TS_DE . Distances in Å.....	87
Figure 5.12 Optimised structure (B3LYP/cc-pVDZ) for TS_EF . Distances in Å.....	87
Figure 5.13 Optimised structure (B3LYP/cc-pVDZ) for TS_GH . Distances in Å	88
Figure 6.1 $^{31}\text{P}\{^1\text{H}\}$ NMR (101 MHz, 293 K, toluene- d_8 : $\text{CH}_2\text{Cl}_2 = 1:0.08$) of a mixture of $[\text{Rh}(\text{cod})_2]\text{BF}_4$ (1.1 equiv.) and BINAP (1.0 equiv.). (1) Before bubbling H_2 gas (1 atm); (2) after bubbling H_2 at room temperature for 30 minutes; (3) after addition of the <i>N</i> -tosylhydrazone 1aa at room temperature.....	94
Figure 6.2 $^{31}\text{P}\{^1\text{H}\}$ NMR (101 MHz, toluene- d_8 : $\text{CH}_2\text{Cl}_2 = 1:0.08$) (left) and ^1H NMR (300 MHz) (negative range, right) of the mixture between $[\text{Rh}(\text{cod})(\text{BINAP})]\text{BF}_4$ and the <i>N</i> -tosylhydrazone 1aa (1:1). Initial mixture before heating (bottom) and spectrum of the mixture after five minutes of heating recorded at 253 K (top).....	95
Figure 6.3 ESI-HRMS spectrum after 5 minutes of reaction	96
Figure 6.4 Possible structures of $[\text{RhH}(\text{BINAP})(\text{58aa})]^{2+}$	97
Figure 6.5 Experimental (top) and calculated (bottom) isotopic pattern for $[\text{Rh}(\text{BINAP})(\text{58aa})]^+$	98
Figure 6.6 ESI-HRMS spectrum after 5 minutes of reaction	99
Figure 6.7 Expected fragmentations of the peak with $m/z = 1299.2031$	100
Figure 6.8 Gibbs energy profile (in kcal/mol) of the rhodium-carbene formation	102
Figure 6.9 Optimised structure (B3LYP/cc-pVDZ) for TS_CF . Distances in Å.....	102
Figure 6.10 Effective oxidation state of intermediates C and F	103

LIST OF SCHEMES

Scheme 1.1 Synthesis of (-)-serotobenine	8
Scheme 1.2 Formation of metal carbenes from diazo compounds	9
Scheme 1.3 Formation of metal carbenes from 1,2,3-triazoles	9
Scheme 1.4 Generation of metal carbenes from cyclopropenes	9
Scheme 1.5 Formation of metal carbenes from ene-yne derivatives	10
Scheme 1.6 Formation of metal carbenes from enynyl ketones or imines	10
Scheme 1.7 Generation of metal carbenes from alkynes	10
Scheme 1.8 Synthesis of diazo compounds from <i>N</i> -tosylhydrazones	11
Scheme 1.9 Products of the base-promoted decomposition of <i>N</i> -tosylhydrazones	11
Scheme 1.10 Transformations of metal carbenes	12
Scheme 1.11 Transformations of metal carbenes	12
Scheme 1.12 Copper-catalysed activation of terminal alkynes	13
Scheme 1.13 Copper-catalysed synthesis of allenolates	13
Scheme 1.14 Use of <i>N</i> -tosylhydrazones as a source of diazo compounds for the copper-catalysed synthesis of allenes	14
Scheme 1.15 Metal-catalysed [2+1] cycloadditions of diazo compounds and terminal alkynes	15
Scheme 1.16 Metal-catalysed [2+1] cycloadditions of diazo compounds and internal alkynes	16
Scheme 1.17 Metal-catalysed [3+2] cycloadditions of diazo compounds and terminal alkynes	17
Scheme 1.18 Metal-catalysed [3+2] cycloadditions of alkynes and β -keto- α -diazoesters	17
Scheme 1.19 Possible operating mechanisms in the formal [3+2] cycloaddition of alkynes and α -diazocarbonyl compounds	18
Scheme 1.20 Rhodium-catalysed synthesis of multisubstituted thiophenes	18
Scheme 1.21 Carbene/alkyne metathesis	19
Scheme 1.22 First metal-catalysed intramolecular carbene/alkyne metathesis	19
Scheme 1.23 Rhodium- and palladium-carbene metathesis	19
Scheme 1.24 Rhodium-catalysed carbene metathesis	19
Scheme 1.25 Molybdenum-catalysed metathesis of dienyne	20
Scheme 1.26 Rhodium-catalysed metathesis of dienyne	20
Scheme 1.27 Rhodium-catalysed C-H insertions after carbene/alkyne metathesis	21
Scheme 1.28 Rhodium-catalysed C-H insertions after carbene/alkyne metathesis	21
Scheme 1.29 Cascade processes after carbene/alkyne metathesis	22
Scheme 1.30 Synthesis of pyrroles after carbene/alkyne metathesis	22
Scheme 1.31 Ruthenium-catalysed intermolecular carbene/alkyne metathesis	23
Scheme 1.32 Metal-catalysed cascade involving dienes and phenyl rings	24
Scheme 1.33 Cascade processes involving ruthenium-carbene/alkyne metathesis	24
Scheme 2.1 General objectives	27

Scheme 3.1 Retrosynthetic analysis of <i>NTs</i> -linked substrate 1aa	31
Scheme 3.2 Synthesis of the <i>NTs</i> -tethered substrate 4a	32
Scheme 3.3 Synthesis of the <i>NTs</i> -tethered compound 1aa	32
Scheme 3.4 1,3-Dipolar cycloaddition of derivative 1aa to afford compound 13	34
Scheme 3.5 Rhodium(I)-carbene catalysed cyclopropanation	38
Scheme 3.6 Rhodium(I)-carbene catalysed ylide transformation	39
Scheme 3.7 Rhodium(I)-carbene catalysed C-C bond insertion	39
Scheme 3.8 Rhodium(I)-carbene catalysed B-H bond insertion	39
Scheme 3.9 Rhodium(I)-carbene catalysed Si-H bond insertion	40
Scheme 3.10 Enantioselective rhodium(II) catalysed carbene/alkyne process	40
Scheme 3.11 Synthesis of 2- <i>Ns</i> -tethered derivative 4b	41
Scheme 3.12 Preparation of malonate-tethered compound 4c	42
Scheme 3.13 Synthesis of <i>O</i> -tethered compound 4d	42
Scheme 3.14 Preparation of the non-terminal alkyne 21	42
Scheme 3.15 Synthesis of sulfonylhydrazides 3c and 3d	43
Scheme 3.16 Scope of the rhodium(I)-catalysed cyclisation of diynearylhydrazones 1	45
Scheme 3.17 Competitive experiments	46
Scheme 3.18 Competitive experiments	47
Scheme 3.19 Deuterium-labelling experiments	47
Scheme 3.20 Comparison between the experimental conditions (top) and the model reaction (bottom)	49
Scheme 3.21 Proposed mechanism for the rhodium-catalysed cyclisation reaction	54
Scheme 3.22 Rhodium-catalysed cyclisation of the substrate 14 , which contains two internal alkynes...	54
Scheme 4.1 Synthesis of vinylcyclopropanes by metal-catalysed vinyl diazo decomposition	57
Scheme 4.2 Selected example of vinyl diazo compounds decomposition to afford vinylcyclopropanes	58
Scheme 4.3 Synthesis of vinylcyclopropanes by metal-catalysed ring-opening of cyclopropenes	58
Scheme 4.4 Synthesis of vinylcyclopropanes by metal-catalysed rearrangement of propargylic esters	58
Scheme 4.5 Selected examples of syntheses of vinylcyclopropanes by metal-catalysed rearrange- ment of propargylic esters	59
Scheme 4.6 Enantioselective rhodium-catalysed intramolecular cyclopropanation of enynones	59
Scheme 4.7 Synthesis of <i>O</i> -tethered enyneacetals 31	61
Scheme 4.8 Synthesis of <i>NSO₂Ar</i> -tethered compounds 31	62
Scheme 4.9 Synthesis of malonate-tethered 31e	63
Scheme 4.10 Synthesis of compound 31h	63
Scheme 4.11 Synthesis of aldehyde 39i	64
Scheme 4.12 Retrosynthetic analysis of compounds 28f and 28g	65
Scheme 4.13 Synthesis of enynes 42 and 43	65

Scheme 4.14 Synthesis of phenyl-tethered compounds 41a and 41b	66
Scheme 4.15 Synthesis of phenyl-tethered <i>N</i> -tosylhydrazones 28f and 28g	66
Scheme 4.16 Rhodium-catalysed cyclisation of enyne <i>N</i> -tosylhydrazones 28a	66
Scheme 4.17 Scope of the rhodium(I)-catalysed cyclisation of enyne <i>N</i> -tosylhydrazones 28	68
Scheme 4.18 Rhodium(I)-catalysed cyclisation of enyne <i>N</i> -tosylhydrazones 28i and 28j	68
Scheme 4.19 Proposed mechanism for the rhodium-catalysed cyclisation reaction	70
Scheme 5.1 Reported metal carbene/allene reactions.....	73
Scheme 5.2 Selected examples of enantioselective cyclopropanation of allenes using diazocompounds	73
Scheme 5.3 Selected examples of gold-catalysed [3+2] cycloadditions using diazocompounds	74
Scheme 5.4 Possible products of the cyclisation.....	74
Scheme 5.5 Retrosynthetic analysis of compounds 4a and 4d	75
Scheme 5.6 Synthesis of allene-yne <i>N</i> -tosylhydrazones 49 and 50a	75
Scheme 5.7 Mechanism of allene formation in Crabbé homologation	76
Scheme 5.8 Postulated mechanism for the formation of 53 and 53'	78
Scheme 5.9 Cyclisation reaction of compound 50a	78
Scheme 5.10 Rhodium-catalysed asymmetric cyclisation of 50	83
Scheme 5.11 Comparison between the experimental conditions (top) and the model reaction (bottom)..	85
.....	85
Scheme 5.12 Deuterium-labelling experiments	88
Scheme 6.1 Rhodium carbene cascade reactions obtained in Chapters 3, 4 and 5.....	91
Scheme 6.2 Bamford-Stevens reaction	91
Scheme 6.3 Postulated mechanism for the formation of metal carbenes from diazocompounds	92
Scheme 6.4 Rhodium-catalysed cyclisation studied by NMR	93
Scheme 6.5 Reactions observed in the NMR experiment.....	93
Scheme 6.6 Rhodium-catalysed cyclisation studied by ESI-HRMS	96
Scheme 6.7 Possible observed fragmentations of the intermediate [RhH(BINAP)(58aa)]²⁺	97
Scheme 6.8 Observed fragmentations of the peak with <i>m/z</i> = 1181.2216.....	98
Scheme 6.9 Rhodium-catalysed cyclisation studied by ESI-HRMS	99
Scheme 6.10 Possible observed fragmentations of the intermediate [RhH(Tol-BINAP)(58ba)]²⁺	100
Scheme 6.11 Rhodium-catalysed cyclisation studied by DFT.....	101
Scheme 6.12 Iron- and copper-catalysed synthesis of sulfones	104
Scheme 6.13 Base-free rhodium-catalysed synthesis of sulfones	104
Scheme 6.14 Rhodium-catalysed synthesis of sulfones	104

LIST OF TABLES

Table 1.1 Optimisation of the rhodium(I)-catalysed cyclisation of the diyne <i>N</i> -tosylhydrazone 1aa	33
Table 3.2 Optimisation of the rhodium(I)-catalysed cyclisation of the diyne <i>N</i> -tosylhydrazone 1aa	38
Table 3.3 Synthesis of diynehydrazones 1 and 14 from diyneacetals 4 and 21	43
Table 4.1 Synthesis of enyne- <i>N</i> -tosylhydrazones 28 from enyneacetals 31	64
Table 4.2 Optimisation of the rhodium(I)-catalysed cyclisation of the compound 28k	69
Table 5.1 Optimisation of the cyclisation of <i>NTs</i> -tethered substrate 49	77
Table 5.2 Optimisation of the rhodium(I)-catalysed cyclisation of the allene-yne <i>N</i> -tosylhydrazone 50a	81
Table 5.3 Synthesis of <i>N</i> -sulphonylhydrazones 50	83

SUMMARY

Some of the most powerful methods for synthesizing complex organic molecules with high levels of chemo-, diastereo- and enantioselectivity rely on metal carbene chemistry. These compounds are versatile reaction intermediates that can react with a wide variety of functional groups.

This doctoral thesis, which is divided into eight different chapters, is based on the methodological study of enantioselective rhodium(I) carbene-mediated cascade reactions comprising a carbene/alkyne metathesis step, triggered by base-free decomposition of sulfonylhydrazones. Chapter 1 contains a general introduction to the metal carbenes and their reactivity. Chapter 2 sets out the general objectives of the thesis. In Chapter 3 the reaction of diyne arylsulfonyl hydrazone substrates giving access to sulfonated azacyclic frameworks in a highly enantioselective manner is described. In Chapter 4, *N*-tosylhydrazone-yne-ene substrates affording the stereoselective synthesis of vinylcyclopropanes are evaluated. In Chapter 5, the use of allenes as unsaturated partners provides an efficient asymmetric synthesis of methylenetetrahydropyran scaffolds. Chapter 6 presents further evidence of the reaction mechanism that accounts for the formation of the rhodium-carbene found as the common initial intermediate. Chapter 7 draws general conclusions from the results of these studies. Finally, Chapter 8 contains the experimental procedure and the characterisation data for the different compounds that have been synthesised throughout the thesis.

RESUMEN

Algunos de los métodos más eficientes utilizados en la síntesis de compuestos orgánicos con estructuras complejas y con altos niveles de quimio-, diastereo- y enantioselectividad están basados en la química de los carbenos metálicos. Estos compuestos son intermedios muy versátiles en diferentes reacciones químicas, pudiendo reaccionar con una gran variedad de grupos funcionales.

Esta tesis doctoral, dividida en ocho capítulos diferentes, se basa en el estudio metodológico de reacciones en cascada enantioselectivas a través de metátesis carbeno/alquino, catalizadas por carbenos de rodio(I) obtenidos mediante la descomposición, en ausencia de base, de sulfonilhidrazonas. El Capítulo 1 contiene una introducción general de los carbenos metálicos y su reactividad. En el Capítulo 2 se definen los objetivos generales de la tesis. En el Capítulo 3 se describe la reacción de sustratos derivados de diiminoarilsulfonilhidrazonas, los cuales permiten la obtención de compuestos azacíclicos sulfonados de manera enantioselectiva. En el Capítulo 4 se evalúa la reactividad de los compuestos que contienen una *N*-tosilhidrazona, un triple y un doble enlace, conduciendo a la síntesis enantioselectiva de vinilciclopropanos. En el Capítulo 5, el uso de alenos como insaturación proporciona de manera asimétrica compuestos con estructura tipo metileno tetrahidropirano. En el Capítulo 6 se muestran más evidencias sobre el mecanismo de reacción, el cual podría explicar la formación del carbeno de rodio responsable de la química observada. En el Capítulo 7 se muestran las conclusiones generales a partir de los resultados de estos estudios. Finalmente, el Capítulo 8 contiene los procedimientos experimentales y la caracterización de los compuestos sintetizados en esta tesis.

RESUM

Alguns dels mètodes més poderosos emprats per a la síntesi de compostos orgànics amb estructures complexes i amb als nivells de quimio-, diastereo- i enantioselectivitat estan basats en la química dels carbens metàl·lics. Aquests compostos són intermedis de reacció molt versàtils, amb capacitat d'actuar vers una gran varietat de grups funcionals.

Aquesta tesi doctoral, dividada en vuit capítols diferents, es basa en l'estudi metodològic de reaccions en cascada enantioselectives a través de metàtesi carbè/alquí, catalitzada per carbens de rodi(I) obtinguts mitjançant la descomposició, en absència de base, de sulfonilhidrazones. El Capítol 1 conté una introducció general dels carbens metàl·lics i de la seva reactivitat. En el Capítol 2 es defineixen els objectius generals de la tesi. En el Capítol 3 es descriu la reacció de compostos derivats de diarilsulfonilhidrazones, les quals permeten l'obtenció de derivats azacíclics sulfonats de manera enantioselectiva. En el Capítol 4 s'avalua la reactivitat dels compostos que contenen *N*-tosilhidrazona, un triple i un doble enllaç, conduint a la síntesi enantioselectiva de vinilciclopropan. En el Capítol 5, s'obtenen de manera asimètrica compostos amb estructura tipus metiletetrahidropirà mitjançant l'ús d'al·lens com a insaturacions. En el Capítol 6 es mostren més evidències pel que fa al mecanisme de reacció, el qual podria explicar la formació del carbè de rodi responsable de la química observada. En el Capítol 7 es mostren les conclusions generals a partir dels resultats d'aquests estudis. Finalment, el Capítol 8 conté els procediments experimentals i la caracterització dels compostos sintetitzats en aquesta tesi.

Chapter 1. General introduction

1.1. Metal carbenes – generalities

The development of efficient syntheses for organic molecules of all shapes and sizes from readily available building blocks has a tremendous impact on numerous areas, such as biomedical, pharmaceutical and agrochemical sciences. In the case of processes that are already known, it is especially important to increase the selectivity and the number of substrates to which a specific reaction can be applied. However, there is also a real need for fundamentally new reactions to be discovered and developed. These new reactions should enable novel, more step- and atom-economical, synthetic strategies both to known and structurally original chemical libraries ideally providing benefits in safety, cost, resource utilisation, and in reducing environmental impact.

Within this context, metal-mediated reactions allow for the assembly of complex molecules, often in an enantioselective fashion, by employing only catalytic amounts of well-defined structurally simple mediators. Among the wealth of transition metal intermediates, transition metal carbene intermediates are capable of undergoing a range of unconventional reactions.

Metal carbenes have been typically classified, depending on their reactivity, into Fischer-type and Schrock-type carbenes. Whereas Fischer-type carbenes are electrophilic at the carbene carbon, Schrock-type carbene complexes generally behave as carbon nucleophiles. Fischer-type carbenes, formally derived from singlet carbenes, consist of low-valent, 18 electron complexes, with strong π -acceptor ligands at the metal which confer electrophilic behavior at the carbene carbon atom. Schrock carbenes, formally derived from triplet carbenes, are typically high-valent complexes with fewer than 18 valence electrons and without π -accepting ligands thus causing the carbene carbon atom to act as a nucleophile (Figure 1.1).

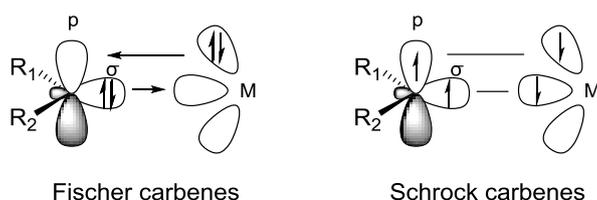


Figure 1.1 Fischer and Schrock carbenes.

However it is not always possible to predict whether a carbene complex will behave as an electrophile or as a nucleophile because not all of the real cases can be unequivocally identified with one of these model carbene types. The reactivity is best accounted for by a continuum ranging from a metal-stabilised singlet carbene to a metal coordinated carbocation as shown in Figure 1.2. The position of a given carbene species on this continuum depends on the ability of the metal fragment to release electrons into the empty p orbital of the carbene carbon atom but it is also strongly influenced by the electronic properties of the substituents on the carbene carbon.

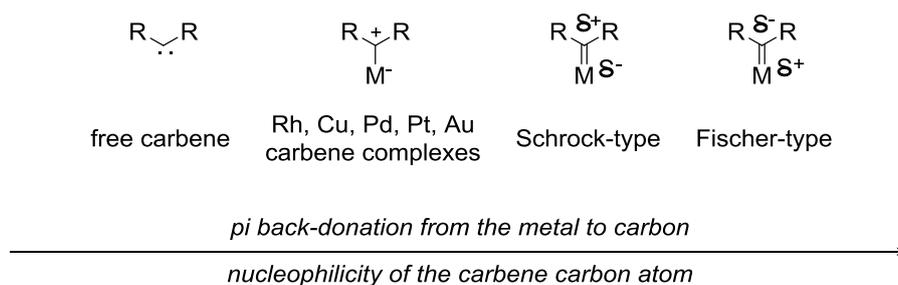


Figure 1.2 Classification of metal carbenes species.

Regarding to rhodium carbenes, Davies proposed a classification¹ based on the electronic character of the substituents on the carbene carbon. Whereas acceptor/acceptor and acceptor metal carbenes are extremely reactive and behave as highly electrophilic species, donor/acceptor substituted metal carbenes give more chemoselective and stereoselective reactions due to the ability of the donor group to moderate their reactivity (Figure 1.3).

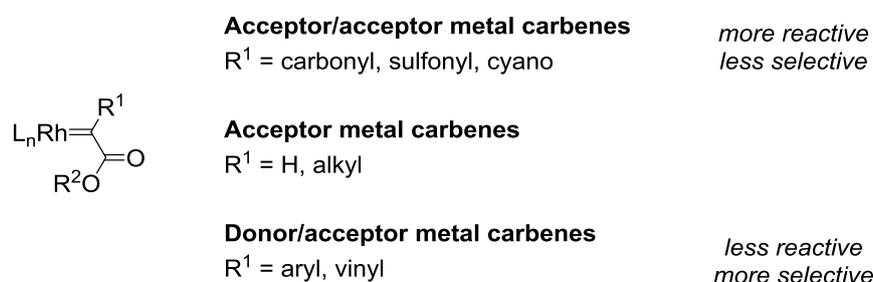
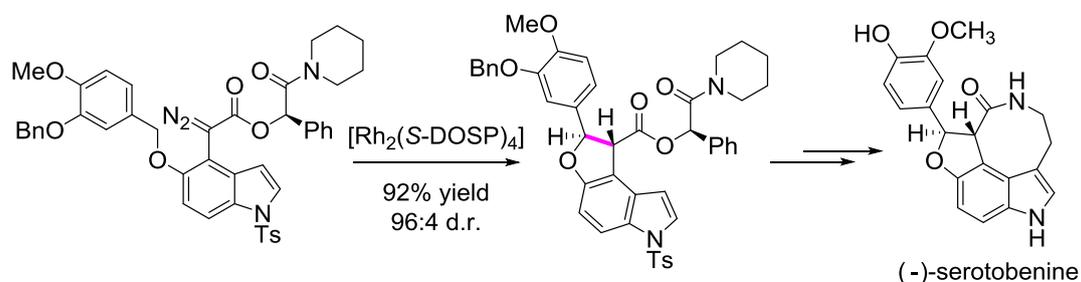


Figure 1.3 Classification of rhodium carbene species.

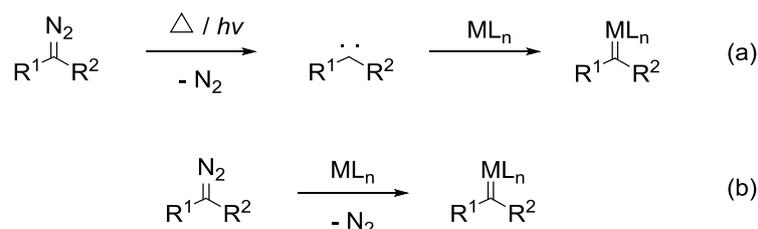
Donor/acceptor metal carbenes have been extremely useful in the synthesis of natural compounds, especially undergoing C-H insertion reactions.² As an example, Fukuyama et al. synthesised (-)-serotobenine using an indolyldiazoacetate as substrate (Scheme 1.1).³ The acceptor/donor metal carbene generated from $[\text{Rh}_2(\text{S-DOSP})_4]$, was able to catalyse the C-H insertion reaction of the indolyldiazoacetate generating a fused dihydrobenzofuran in 92% yield, with high asymmetric induction.



Scheme 1.1 Synthesis of (-)-serotobenine.

1.2. Preparation of metal carbenes

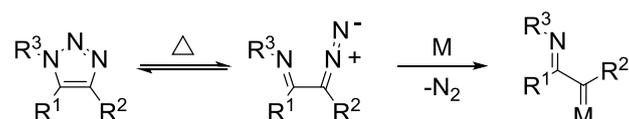
Among the different compounds that can be used as sources to generate metal carbenes, diazo compounds are the most commonly used. These compounds are molecules which contain two linked nitrogen atoms as a terminal functional group with four different resonance structures, which enable the creation of carbenes upon thermal or photochemical induced expulsion of molecular nitrogen (Scheme 1.2, a). Alternatively, transition metal-catalysed dediazonation generates metal carbene complexes (Scheme 1.2, b).



Scheme 1.2 Formation of metal carbenes from diazo compounds.

Diazo compounds are typically labelled as hazardous and potentially explosive, which limits their use on a large scale. However, those having at least one electron-withdrawing group are sufficiently stable and safe as to be manipulated with reasonable precautions. New safer methods have been developed as alternative sources of metal carbenes. The most commonly used sources include triazoles, cyclopropenes, enynes, alkynes, and *N*-tosylhydrazones.⁴

Triazoles, which exist in equilibrium upon heating with their diazoimine tautomer, may serve as precursors for α -iminyl metal carbenes under metal catalysis (Scheme 1.3).



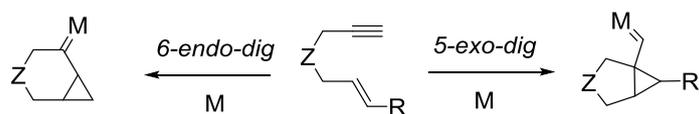
Scheme 1.3 Formation of metal carbenes from 1,2,3-triazoles.

Cyclopropenes can also generate metal carbene intermediates under quite mild conditions due to their intrinsic ring strain (Scheme 1.4).



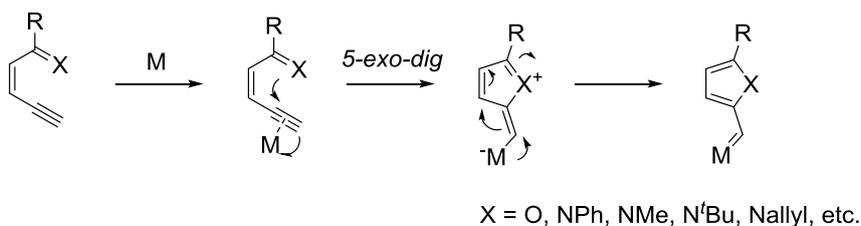
Scheme 1.4 Generation of metal carbenes from cyclopropenes.

1,*n*-Enynes (*n* = 5, 6, 7, etc.) can also generate metal carbenes whereby the C=C bond attacks as the nucleophile (Scheme 1.5). Products not easily available from diazo compounds can be obtained by careful design of the stable and readily available substrates.



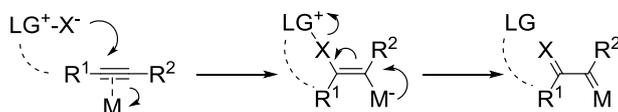
Scheme 1.5 Formation of metal carbenes from ene-yne derivatives.

Enynyl-substituted ketones or imines are another reliable approach for the generation of 2-furyl or 2-pyrrolyl metal carbenes under metal catalysis through 5-*exo-dig* cyclisation (Scheme 1.6).



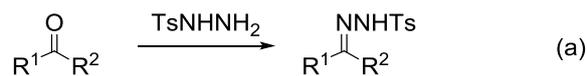
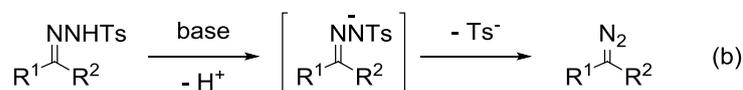
Scheme 1.6 Formation of metal carbenes from enynyl ketones or imines.

The attack of alkynes by a nucleophilic entity containing a leaving group is another type of readily available precursor for the generation of metal carbenes via the intermediacy of vinyl metal species, which bear a negative charge at the metal centre, triggering the elimination of a leaving group (LG) to form the metal carbene bearing an α -C=X unit (Scheme 1.7).

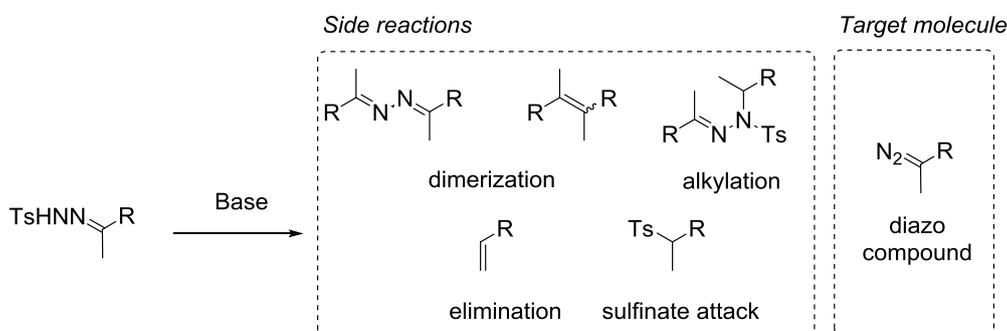


Scheme 1.7 Generation of metal carbenes from alkynes.

Finally, *N*-tosylhydrazones have shown themselves to be excellent candidates as a safe source of diazo compounds due to their stability and the fact that they can be isolated and stored, as well as easily handled and prepared. Furthermore, they are readily available from the corresponding ketone or aldehyde (Scheme 1.8, a). The decomposition of *N*-tosylhydrazones was discovered in 1952 by W. R. Bamford and T. S. Stevens and needs the presence of a base (Scheme 1.8, b).⁵ The only by-products generated in the reaction are nitrogen – the driving force of the process – and *p*-toluenesulfinate anions.

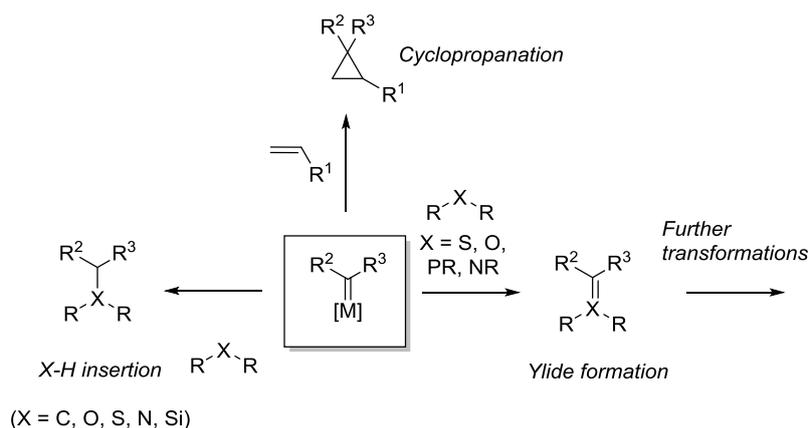
N-Tosylhydrazone synthesis*Bamford-Stevens reaction***Scheme 1.8** Synthesis of diazo compounds from *N*-tosylhydrazones.

However, the generation of diazo compounds can sometimes be difficult due to the variety of side-products that can be generated: dimerisation, alkylation, elimination, and the formation of sulfinate products (Scheme 1.9).

**Scheme 1.9** Products of the base-promoted decomposition of *N*-tosylhydrazones.

Many efforts have to be dedicated to obtain the optimal conditions in terms of the solvent, phase-transfer catalyst (when reactions are carried out at temperatures below 50°C), and the temperature. The choice of the base, and even its counterion, has also been demonstrated to be of great importance.⁶ Thus, there is a growing interest in the generation of diazo compounds in such a way that side reactions can be reduced.

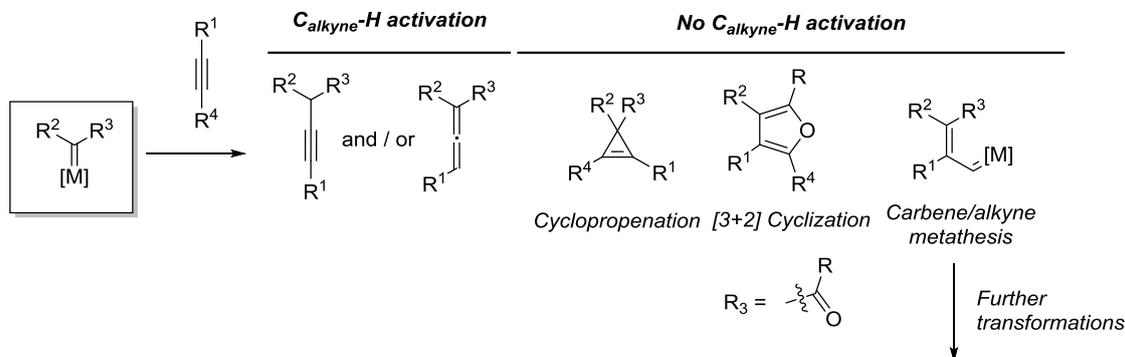
On the other hand, *N*-tosylhydrazones have been used in many metal-catalysed transformations, showing their importance in metal carbene chemistry. In this respect, acceptor-substituted metal carbenes can participate in various transformations, such as X-H insertions (X = C, O, S, N, Si), cyclopropanations and ylide formation followed by rearrangements (Scheme 1.10).⁴



Scheme 1.10 Transformations of metal carbenes.

The X-H insertion reactions have been widely studied for X = O, S, N, Si, and C. This reaction has become of great interest due to the combination of carbon-carbon bond formation and the low bond polarity of C-H bonds in comparison with O-H, S-H and N-H. On the other hand, cyclopropanation using metal carbenes has become a common reaction in organic synthesis, especially in the synthesis of natural products due to the presence of cyclopropane rings in many synthetic intermediates.⁷ There has been a considerable growth of interest in recent years in the use of α -diazoketone reagents for this purpose, whose stability has allowed their involvement in key steps of many synthetic routes in the last few decades. Furthermore, many studies have been focused on the diastereo- and enantioselective synthesis of these three-membered rings. Finally, ylides have been shown to be competent intermediates in a large variety of transformations. Although these reactions will not be covered in detail in this introduction, the most common ylides are from ammonium, azomethine, nitrile, oxonium, carbonyl, sulfonium, and thiocarbonyl.

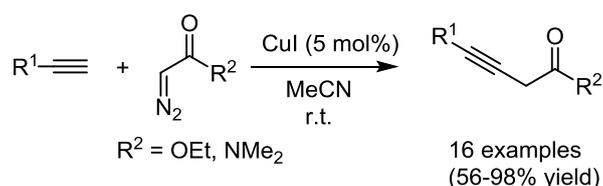
Despite the fact that metal carbenes can react with a large number of functional groups, alkynes show a particularly diverse reactivity (Scheme 1.11). Transformations involving alkynes can be classified by whether or not a C_{alkyne} -H activation of a terminal alkyne is involved, as will be explained in the following sections.



Scheme 1.11 Transformations of metal carbenes.

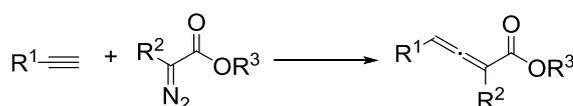
1.3. Processes involving C_{alkyne}-H activation

Alkynes can react with metal carbenes in a process that involves C_{alkyne}-H activation forming either internal alkynes and/or allenes. The copper-catalysed decomposition of diazo compounds in the presence of terminal acetylenes to produce allenes and alkynes has been reported in seminal works although with generally moderate yields and harsh reaction conditions.⁸ It was not until 2004 that Fu et al. described a practical method for the synthesis of 3-alkynoates by coupling terminal alkynes with ethyl diazoacetate under CuI catalysis in non-basic conditions at room-temperature (Scheme 1.12).⁹ A small quantity of the allene isomer of the 3-alkynoate was observed as a by-product. The reaction was efficient with aryl, alkyl, and silyl-substituted alkynes and was also extended to a diazoamide.



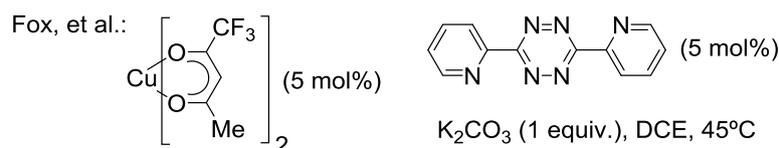
Scheme 1.12 Copper-catalysed activation of terminal alkynes.

Some years later, Fox et al. reported the coupling of α -substituted- α -diazoesters with terminal alkynes with selectivity that was complementary to Fu's method.¹⁰ Allenates were obtained as main products with small traces of the alkynoates when Cu(trifluoroacetylacetonate)₂ and 3,6-di(2-pyridyl)-s-tetrazine as the ligand were used as the catalytic system in DCE (Scheme 1.13). The authors found that the use of potassium carbonate improved the selectivity for allenolate products. Wang et al., who have been particularly active in researching this topic, reported the same transformation as Fox but using CuI and phenanthroline in acetonitrile at 80°C under base-free conditions (Scheme 1.13). However, it should be noted that this finding^{11a} was a later correction to the originally published paper,^{11b} which had described furans as being obtained.



Fox, et al.: 12 examples (44-80% yield)

Wang, et al.: 13 examples (55-95% yield)

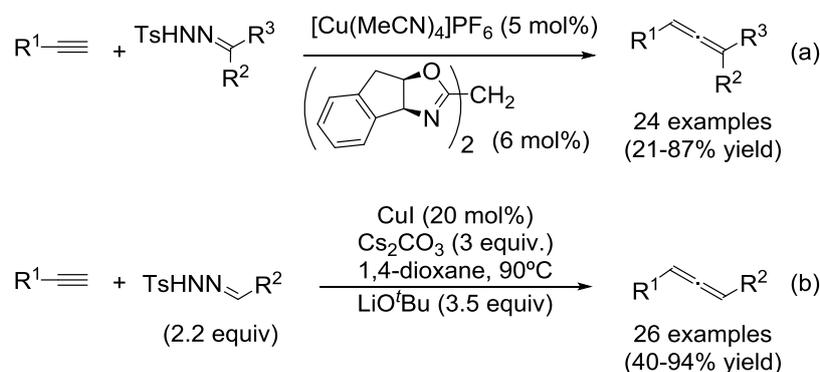


Wang, et al.: CuI (5 mol%), phenanthroline (5 mol%), MeCN, 80°C

Scheme 1.13 Copper-catalysed synthesis of allenates.

Wang et al. then introduced the use of *N*-tosylhydrazones as metal carbene sources for coupling to terminal alkynes. The combination of [Cu(MeCN)₄]PF₆ with a racemic bis(benzoxazole) ligand

provided an efficient catalytic system for the synthesis of trisubstituted allenes in basic conditions (Scheme 1.14, a).¹² *N*-Tosylhydrazone substrates derived from alkyl and aryl ketones reacted smoothly although in moderate yields. The reaction was not efficient with *N*-tosylhydrazones derived from aldehydes but the same authors later reported a modification which was efficient for these substrates.¹³ By using CuI without a ligand, 1,3-disubstituted allenes were obtained in moderate to good yields (Scheme 1.14, b). It was possible to scale up the synthesis to gram-scale.



Scheme 1.14 Use of *N*-tosylhydrazones as a source of diazo compounds for the copper-catalysed synthesis of allenes.

Further reactivity of the compounds formed through this $C_{alkyne}\text{-H}$ activation has provided important molecule families including benzofurans and indoles,¹⁴ phenanthrenes¹⁵, 2H-chromenes¹⁶, and pyridotriazoles.¹⁷

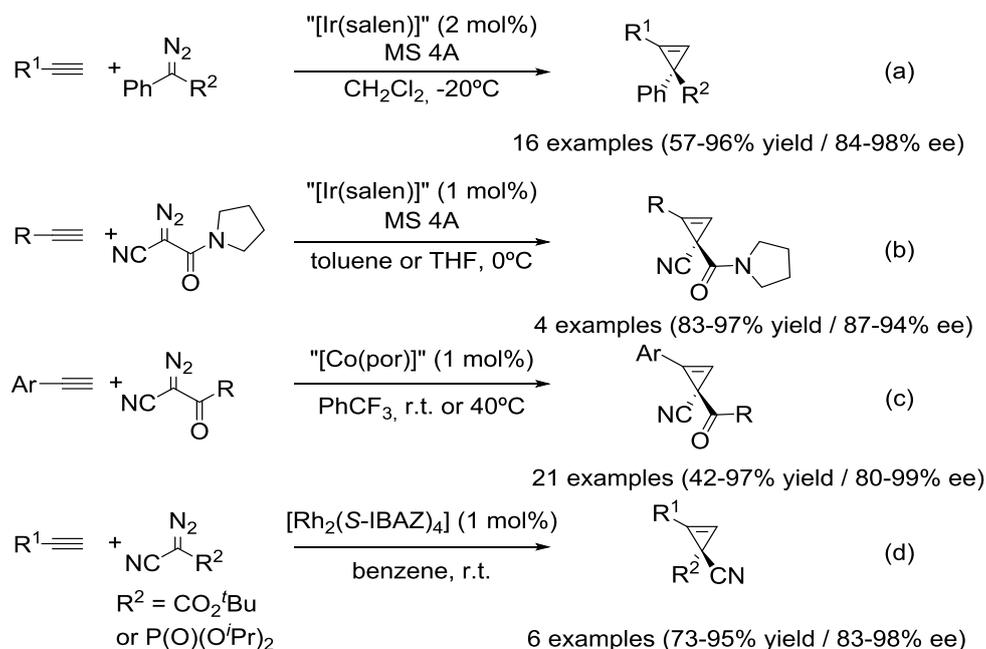
1.4. Processes not involving $C_{alkyne}\text{-H}$ activation

Processes not involving $C_{alkyne}\text{-H}$ activation have been subdivided into three categories. The first two groups can be described in general terms as cycloaddition reactions: [2+1] and formal [3+2]. The third contains the processes that are postulated as involving a carbene/alkyne metathesis as a key step.

1.4.1. [2+1] Cycloaddition

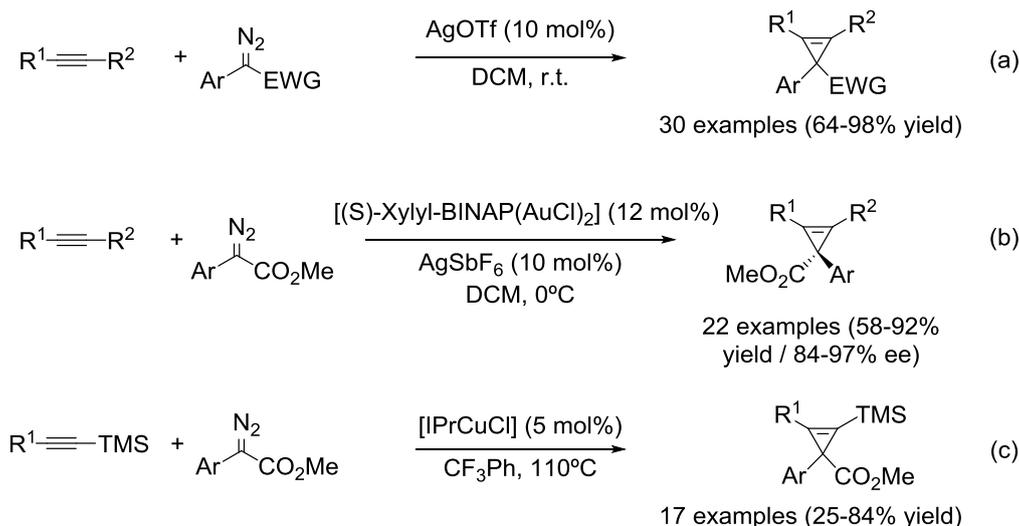
The preparation of cyclopropenes from a [2+1] cycloaddition reaction of diazo compounds and alkynes is a widely used, efficient methodology. The reaction is catalysed by transition metals, mainly based on copper and rhodium.¹⁸ Some recent findings in this field will be presented. Katsuki et al. reported in 2011 the synthesis of enantioenriched cyclopropenes containing a quaternary asymmetric carbon by the reaction of terminal alkynes or arylacetylenes with diazo compounds.¹⁹ The reaction was catalysed by an [Ir(salen)] complex that the same authors have also used in cyclopropenation and C-H reactions involving diazo compounds. Apart from the widely used ester and sulfonyl groups, phosphonate and trifluoromethyl groups were also engaged as the acceptor counterpart in the diazo precursor (Scheme 1.15, a). α -cyano- α -diazoacetamides that are reluctant to participate in cyclopropenation reactions due to the acceptor nature of both substituents of the diazo compound were also used as substrates under

the modified reaction conditions (Scheme 1.15, b). These acceptor/acceptor-substituted metal carbenes were generalised as substrates in enantioselective cyclopropenation reactions by Zhang et al. (Scheme 1.15, c).²⁰ They use a chiral metalloradical porphyrin cobalt(II) complex that operates through a distinct radical mechanism. Two years later, Charette et al.²¹ also contributed to the topic by developing a stereoselective rhodium-catalysed cyclopropenation of alkynes with diaceptor diazo compounds (Scheme 1.15, d).



Scheme 1.15 Metal-catalysed [2+1] cycloadditions of diazo compounds and terminal alkynes.

Whereas cyclopropenation of alkynes is efficient with the highly reactive acceptor metal carbenes, it was not until 2011 that Davies et al. achieved its cyclopropenation with donor/acceptor diazo compounds. In a first paper, they described the use of silver triflate to afford tetrasubstituted cyclopropenes (Scheme 1.16, a).²² The asymmetric version was subsequently reported by the same authors switching from silver to gold catalysis.²³ Gold(I) catalysts bearing BINAP ligands and activated with AgSbF_6 , efficiently promoted the enantioselective cyclopropenation reaction (Scheme 1.16, b). Coleman et al. also tackled the cyclopropenation of internal alkynes but using copper as the catalyst. After preliminary results showing that donor/acceptor diazo acetate reacted with 1-(*p*-methoxy)phenylprop-1-yne under CuI catalysis to afford tetrasubstituted cyclopropenes,²⁴ the authors applied the methodology to internal alkynylsilanes to yield 1-silylcyclopropenes that are useful starting materials for various transition metal-catalysed transformations.²⁵ (1,3-Bis-(diisopropylphenyl)imidazole-2-ylidene) copper(I) chloride (IPrCuCl) was the catalyst of choice for the aforementioned transformation (Scheme 1.16, c).

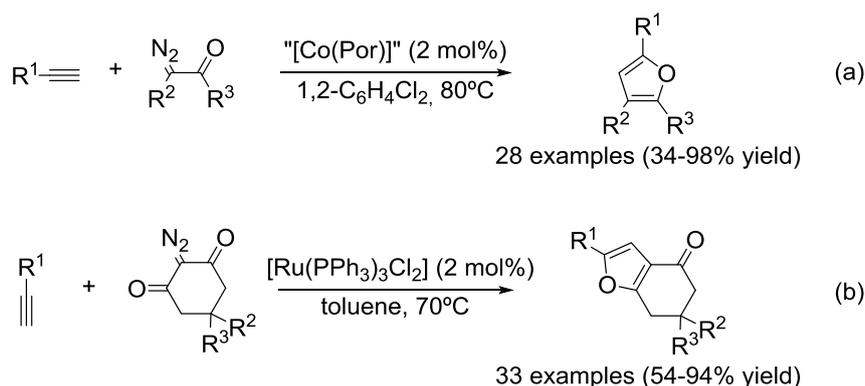


Scheme 1.16 Metal-catalysed [2+1] cycloadditions of diazo compounds and internal alkynes.

1.4.2. Formal [3+2] cycloaddition

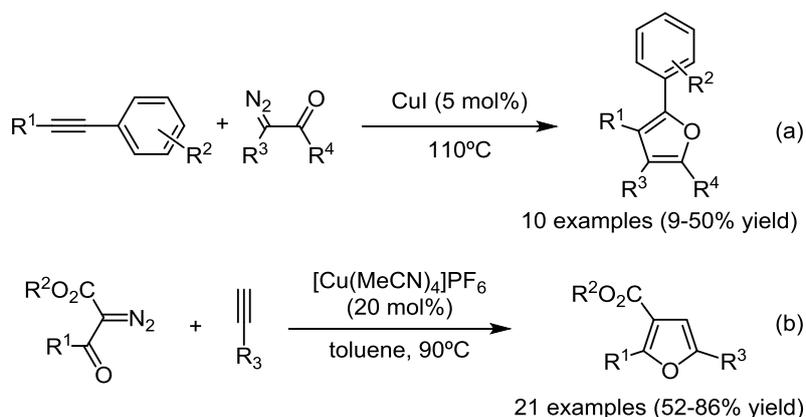
Alkynes can also react with α -diazocarbonyl compounds under transition metal catalysis in a formal [3+2] cycloaddition to furnish furan derivatives. This method is a highly convenient general protocol for the assembly of polysubstituted furans.²⁶

There are several interesting recent findings in this field. Although furan synthesis is generally catalysed by rhodium or copper complexes, other transition metals have also been used. Zhang et al. described the use of metalloradical cobalt(II)-porphyrin complexes [Co(Por)], which had already proved to be useful for the cyclopropanation reaction,²⁰ as catalysts for the formal [3+2] cyclisation of alkynes with α -diazocarbonyl compounds (Scheme 1.17, a).²⁷ In cases where different carbonyl types were available for reaction, cyclisation occurred preferentially on ketone or aldehyde carbonyl rather than the ester carbonyl. Both aromatic and aliphatic terminal alkynes were efficient substrates for the reaction. On the other hand, internal alkynes were inefficient for the transformation, which the authors take advantage of to develop an iterative synthesis toward oligofurans by reacting a bifunctional ketodiazooacetate bearing a TMS-protected internal alkyne. Lee et al. reported the use of ruthenium for the reaction of terminal aryl alkynes and symmetrically substituted cyclic diazodicarbonyl compounds to afford fused bicyclic furan derivatives (Scheme 1.17, b).²⁸

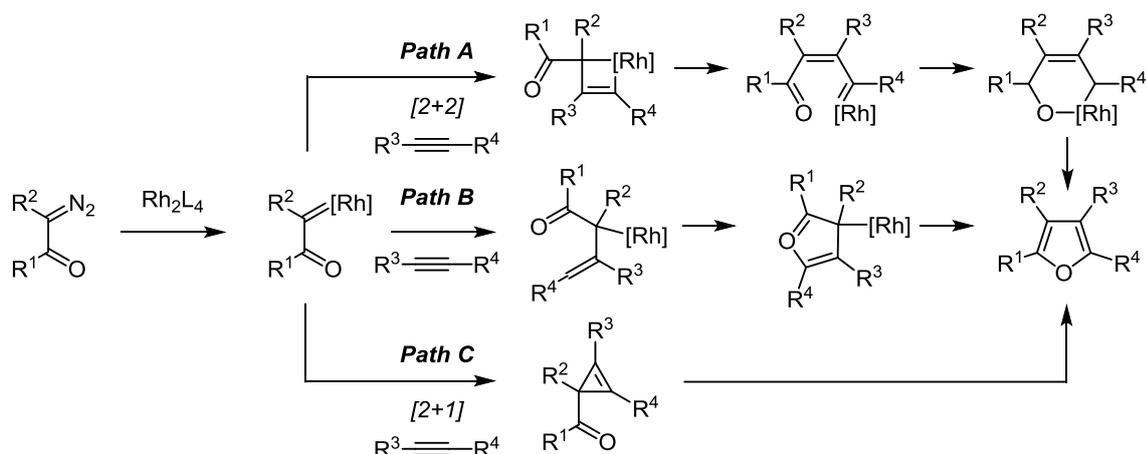


Scheme 1.17 Metal-catalysed [3+2] cycloadditions of diazo compounds and terminal alkynes.

Coleman et al. tackled the reaction with the less reactive internal alkynes.²⁴ Using CuI as the catalyst in neat conditions, tetrasubstituted furans were obtained in moderate yields (Scheme 1.18, a). Also using copper, Wang et al. reported the copper(I)-catalysed reaction of terminal alkynes with β -keto- α -diazooesters as a straightforward synthesis of 2,3,5-trisubstituted furans (Scheme 1.18, b).²⁹

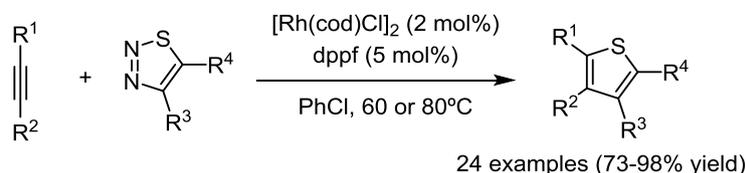
**Scheme 1.18** Metal-catalysed [3+2] cycloadditions of alkynes and β -keto- α -diazooesters.

There is controversy as to which mechanism operates in the formal [3+2] cycloaddition of alkynes and α -diazocarbonyl compounds. Different possibilities have been proposed that involve ylide intermediates, by nucleophilic attack of the alkyne onto the metal carbene (Scheme 1.19, Path B), or the reaction starting with either a [2+1] (Scheme 1.19, Path C) or a [2+2] cycloaddition of the metal carbene (Scheme 1.19, Path A), involving cyclopropenes or metallacyclobutenes as intermediates, respectively.²⁶ The prevalence of one or other of these pathways is probably dependent on the catalyst used and the electronic and steric properties of the reagents.

**Scheme 1.19** Possible operating mechanisms in the formal [3+2] cycloaddition of alkynes and α -diazocarbonyl compounds.

The examples commented until now describe the cyclisation of metalla-oxavinyl carbenes for the formation of furans. Gevorgyan et al. have recently described the synthesis of multisubstituted

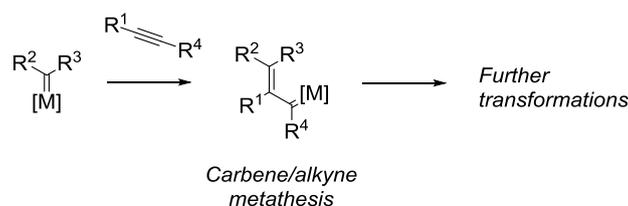
thiophenes, via an analogous process that involved the intermediacy of a rhodium thiavinyl carbene rather than the metallaoxavinyl carbene.³⁰ 1,2,3-thiadiazoles were used as an in situ source for the thiavinyl carbene that was trapped with rhodium and reacted with terminal alkynes, and even an internal one, to efficiently afford the desired polysubstituted thiophenes (Scheme 1.20). The use of a rhodium(I) catalyst was key to the success of the reaction.



Scheme 1.20 Rhodium-catalysed synthesis of multisubstituted thiophenes.

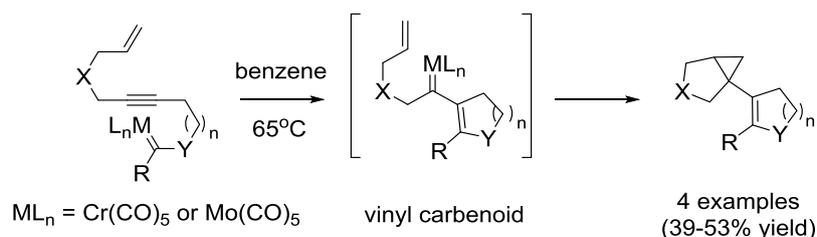
1.4.3. Carbene/alkyne metathesis – intramolecular processes

Carbene/alkyne metathesis refer to the processes in which a metal carbene reacts with an alkyne, generating a new intermediate in which the carbene-like character is transferred to the β -carbon of the alkyne and a double bond is formed between the metal carbene carbon and the α -carbon of the alkyne (Scheme 1.21). The vinyl metal carbene thus formed may then be involved in typical carbene reactions such as cyclopropanation, C-H insertion or ylide generation, setting up cascade processes (also known as tandem or domino reactions). The difference between sequential or one-pot reactions and cascade processes is that in cascade processes, as defined Tietze in 1993, “the subsequent reactions result as a consequence of the functionality formed by bond formation or fragmentation in the previous step.”³¹



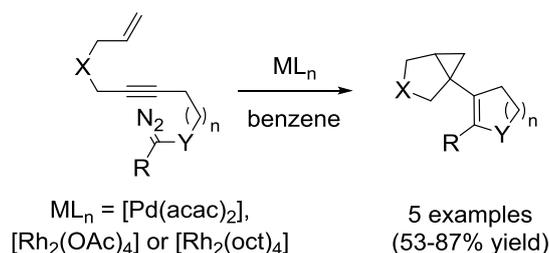
Scheme 1.21 Carbene/alkyne metathesis.

This reactivity mode was first described by Hoye's group in 1988,³² who described the chromium-mediated cyclisation of an enyne-tethered to a chromium Fischer carbene (Scheme 1.22). The first carbene/alkyne metathesis affords a vinyl metal carbene intermediate that can intramolecularly cyclopropanate the remaining double bond giving a vinylcyclopropane. Making use of molybdenum as the stoichiometric metal, Harvey et al. reported a pair of analogous transformations.³³



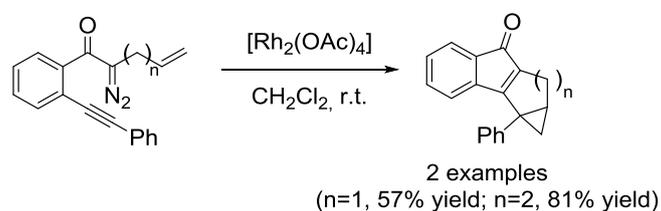
Scheme 1.22 First metal-catalysed intramolecular carbene/alkyne metathesis.

Hoye's and Padwa's groups later developed similar reactions of enynes-tethered to an α -diazocompound with catalytic amounts of either palladium³⁴ or rhodium³⁵ (Scheme 1.23).



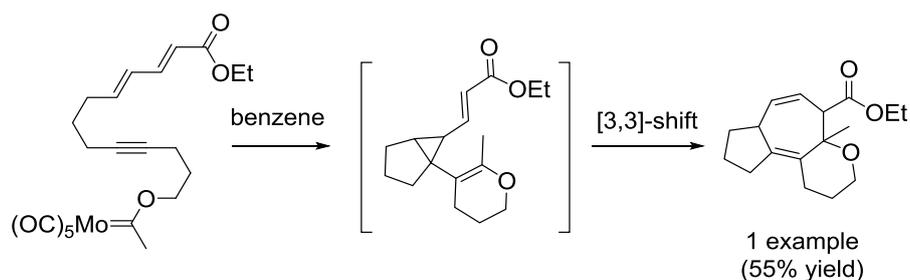
Scheme 1.23 Rhodium- and palladium-catalysed carbene metathesis.

Switching the order of unsaturations in the substrate – placing the metal carbene in a central position – a single tetrafused structure was efficiently obtained by Padwa et al. (Scheme 1.24).³⁶

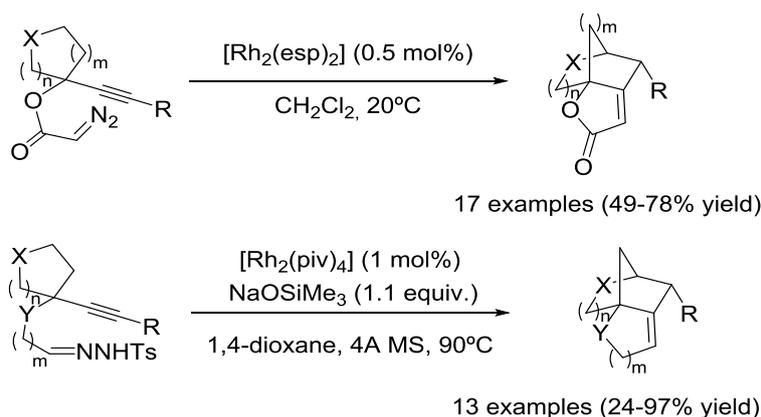


Scheme 1.24 Rhodium-catalysed carbene metathesis.

Further reactivity was obtained by changing the alkene for a diene. In this first example a stoichiometric amount of the metal was used. The vinylcyclopropane formed could not be isolated because of a [3,3]-shift affording an heptadiene (Scheme 1.25).³³

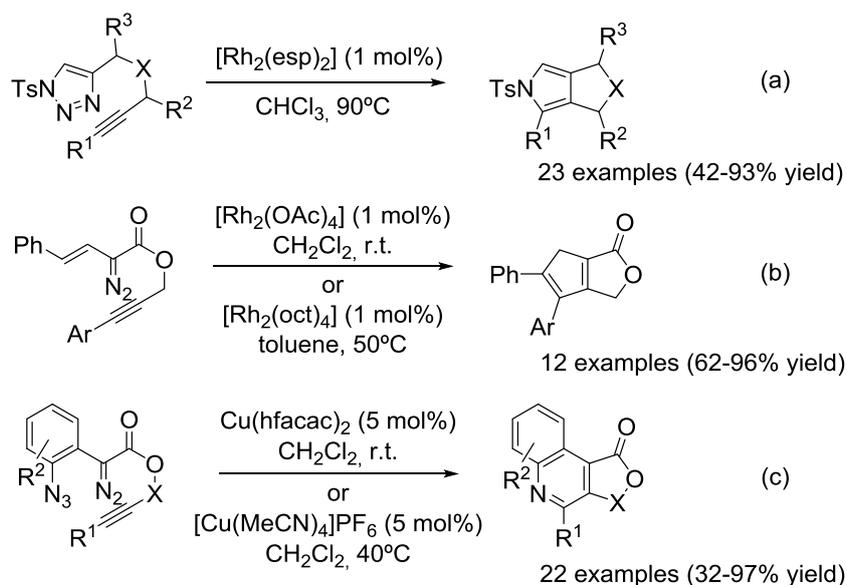


Scheme 1.25 Molybdenum-catalysed metathesis of dienynes.



Scheme 1.28 Rhodium-catalysed C-H insertions after carbene/alkyne metathesis.

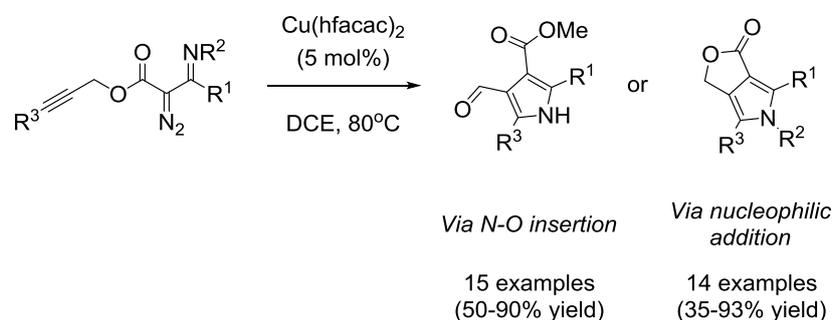
Gevorgyan et al. described the construction of 5,5-fused pyrrole units from alkynyl triazoles.⁴⁰ The rhodium-imino carbene generated from ring-opening of the *N*-sulfonyl-1,2,3-triazole, suffers a carbene/alkyne metathesis, followed by a nucleophilic attack of the imino N atom at the rhodium carbene to achieve the intramolecular transannulation reaction (Scheme 1.29, a). Mao, Xu et al. reported a similar transformation that starting from alkynyl-tethered styryl diazoesters accomplished the construction of bicyclic cyclopentadiene scaffolds.⁴¹ The transformation, which is only efficient for aryl alkynes, involved a carbene/alkyne metathesis followed by a formal [3+2] cycloaddition and a subsequent [1,5]-H shift (Scheme 1.29, b). The same group described the use of a transannular cyclisation to obtain 4-carboxyl quinolines through a carbene/alkyne metathesis that terminated in the reaction of the vinyl carbene that was formed with the azide.⁴² Whereas rhodium was only moderately efficient for quinoline formation, replacement by copper greatly improved the yield (Scheme 1.29, c).



Scheme 1.29 Cascade processes after carbene/alkyne metathesis.

Very recently, Xu et al. developed a cascade divergent reaction of alkynyl-tethered α -iminodiazooacetates, providing access to a broad scope of pyrroles (Scheme 1.30).⁴³ The reaction,

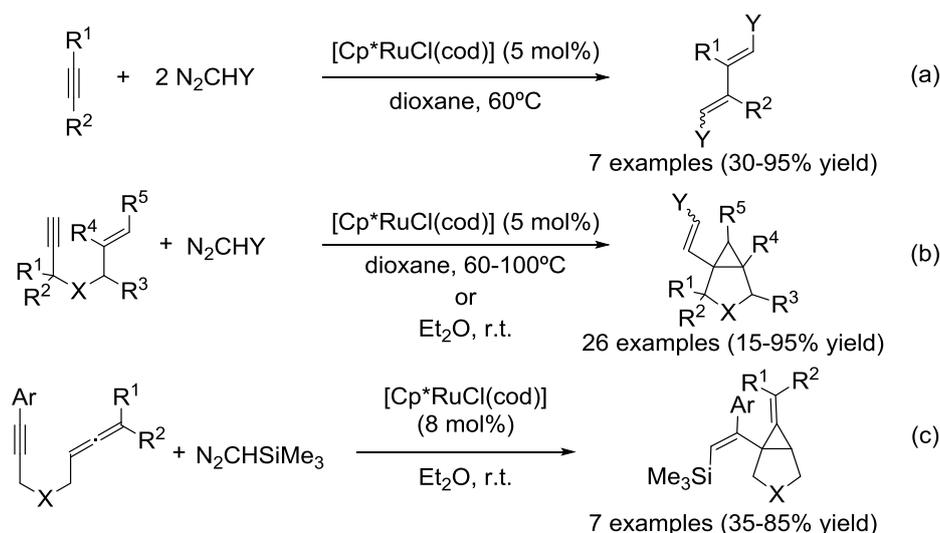
after a first carbene/alkyne metathesis, can undergo an N-O insertion or a nucleophilic addition. The formation of these two possible products could efficiently be controlled through the substituents on the substrates.



Scheme 1.30 Synthesis of pyrroles after carbene/alkyne metathesis.

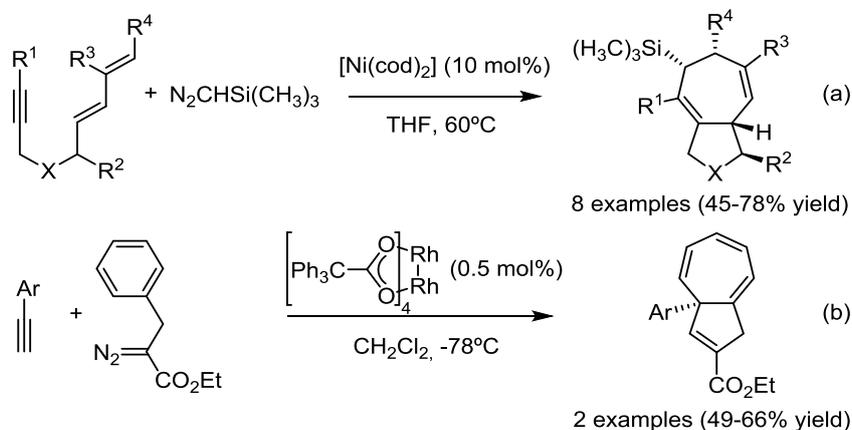
1.4.4. Carbene/alkyne metathesis – intermolecular processes

Intermolecular versions of the carbene/alkyne metathesis reaction have been described by several groups. Dixneuf et al. studied the intermolecular formation of ruthenium vinyl carbenes and their subsequent transformations. One of the topics they explored was the formation of dienes.⁴⁴ In a first paper, they reported their synthesis by a carbene/alkyne metathesis followed by the coupling of the vinyl metal carbene formed with another equivalent of the diazoalkane (Scheme 1.31 a).^{44a} Two other papers followed that involved the reaction of propargylic carbonates and silyl diazo compounds.^{44b-c} Although a mechanism involving an initial Rautenstrauch rearrangement (metal carbene catalysed isomerisation of 1-ethynyl-2-propenyl derivatives to cyclopentenones) could not be unequivocally excluded, the authors propose a mechanism involving initial carbene/alkyne metathesis followed by acetate migration. The same catalytic system, which inhibits the enyne metathesis, was efficient for the transformation of enynes into bicyclic vinylcyclopropanes.⁴⁵ The diazoalkane intermolecularly reacts with the alkyne in the enyne to form the ruthenium vinyl metal carbene that intramolecularly cyclopropanates the tethered alkene (Scheme 1.31, b). This transformation has also been applied to the synthesis of bicyclic amino acid derivatives.^{45c} Later on, the same authors extended the methodology to the cyclisation of allenynes into alkenyl alkylidene bicyclo[3.1.0]hexane derivatives (Scheme 1.31, c).⁴⁶



Scheme 1.31 Ruthenium-catalysed intermolecular carbene/alkyne metathesis.

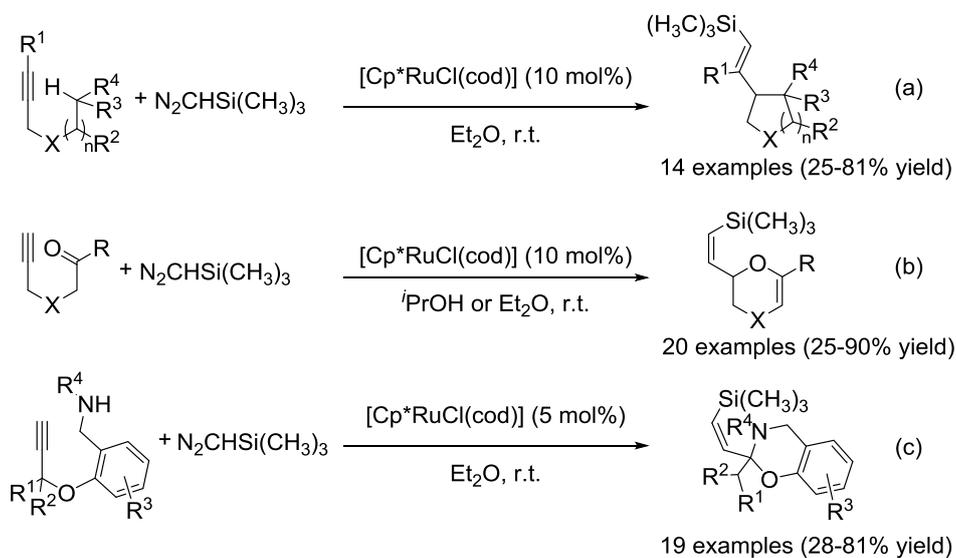
Montgomery et al. reacted a silyldiazo compound with a dienyne to develop a formal [4+2+1] cycloaddition.⁴⁷ Trimethyldisilyldiazomethane intermolecularly reacted under nickel catalysis with the diene-yne to initially afford divinylcyclopropanes that were transformed to bicyclo-[3.5.0]-decane derivatives upon [3,3] sigmatropic rearrangement (Scheme 1.32, a). Seven-membered rings could also be accessed by the rhodium-catalysed cascade involving a carbene/alkyne metathesis followed by a Büchner ring expansion, as reported by Fox et al (Scheme 1.32, b).⁴⁸



Scheme 1.32 Metal-catalysed cascade involving dienes and phenyl rings.

Saá et al.⁴⁹ used the conditions established by Dixneuf et al.⁴⁴ for the preparation of ruthenium vinyl metal carbene to set up varied cascade processes (Scheme 1.33). In a first report,^{49a} they described a cascade that formed 5- or 6-membered rings through a C-H insertion onto activated positions (Scheme 1.33, a). In a second paper, they reported the synthesis in mild reaction conditions of 2-vinyldihydropyrans and dihydro-1,4-oxazines (Scheme 1.33, b) in a process in which the initially formed ruthenium vinyl carbene suffers a nucleophilic attack by the carbonyl group to afford a zwitterionic intermediate.^{49b} A final paper in the series, introduces the N-H insertion as a key step to

the cascade to achieve the synthesis of 1,3-benzoxazines (Scheme 1.33, c).^{49c} The presence of an oxygenated tether is crucial for the rearrangement that follows the N-H insertion.

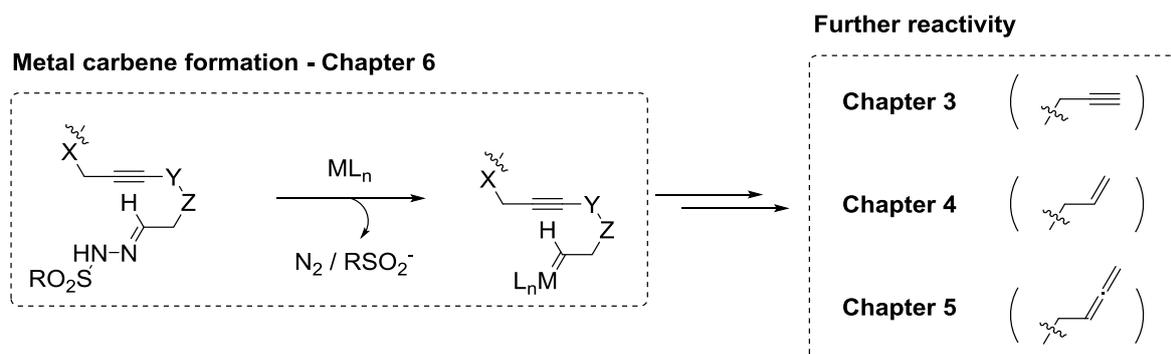


Scheme 1.33 Cascade processes involving ruthenium-carbene/alkynes metathesis.

Despite of the multiple bonds generated in the reactions showed above, none of them is created in an enantioselective way. Moreover, when using substrates bearing diazo compounds, the group has to be stabilised with an electron-withdrawing group, limiting the scope of the reactions. Therefore, carbene/alkyne reactions, as well as the use of new surrogates of diazo compounds and non-stabilised substrates, still remain a challenge.

Chapter 2. Objectives

On the basis of the previous examples, the aim of this thesis is to develop novel chemical transformations for the efficient and sustainable preparation of complex polycyclic compounds from linear substrates using carbene/alkyne metathesis and involving chiral metal carbenes derived from *N*-tosylhydrazones. Three main group of molecules will be used for this propose: diynehydrazones (Chapter 3), yne-ene-hydrazones (Chapter 4) and allene-yne-hydrazones (Chapter 5). Mechanistic studies that account for those transformations will be developed in Chapter 6 on bases of DFT methods and detection of intermediates by ESI-MS and ^1H NMR.

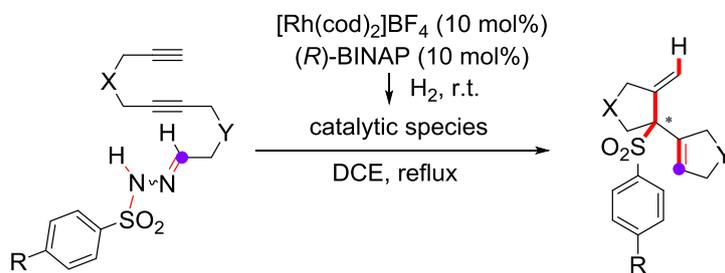


Scheme 2.1 General objectives.

Chapter 3. Enantioselective rhodium(I) donor carbene-mediated cascade triggered by a base-free decomposition of arylsulfonylhydrazones

This chapter has been published on:

Torres, Ò.; Parella, T.; Solà, M.; Roglans, A.; Pla-Quintana, A. *Chem. Eur. J.* **2015**, *21*, 16240.



After looking at the precedents found in the literature on the use of metal carbenes in carbocyclisation reactions, which have been highlighted in Chapter 1, the main objective of this chapter was established. This consisted of the synthesis of substrates bearing two alkynes and an *N*-sulfonylaryldiazene in order to study their cyclisation reactions to obtain high-value cyclic compounds. The completely intramolecular version was chosen to decrease regio- and chemoselectivity problems and NTs tethers were used between the different reacting units in the first attempts to facilitate the synthesis of these compounds and to increase their molecular weight, making them easier to handle as solid and crystalline molecules. This resulted in the design of substrate **1aa** (Figure 3.1) as a model to test whether or not a double carbene/alkyne metathesis could effectively lead to polycyclic compounds.

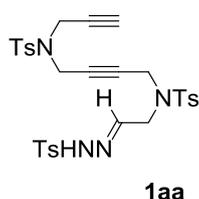
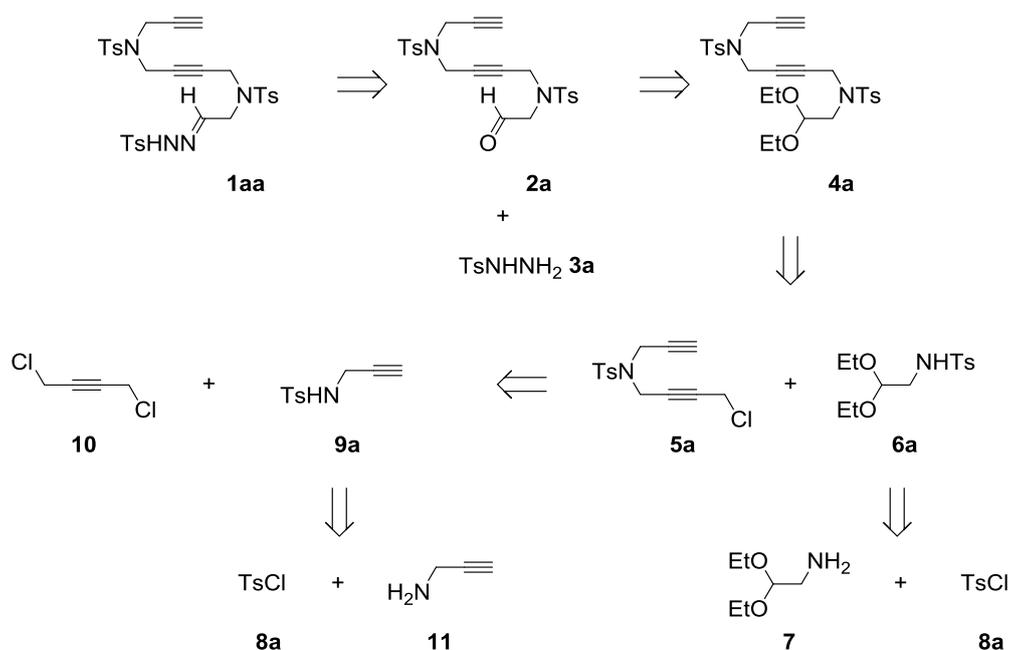


Figure 3.1 Model substrate tested in this study.

3.1. Retrosynthetic analysis of substrate **1aa**

Our retrosynthetic analysis of compound **1aa** was based on the late stage-installation of *N*-tosylhydrazone moiety on an aldehyde which is protected in an acetal form throughout the synthesis (Scheme 3.1).

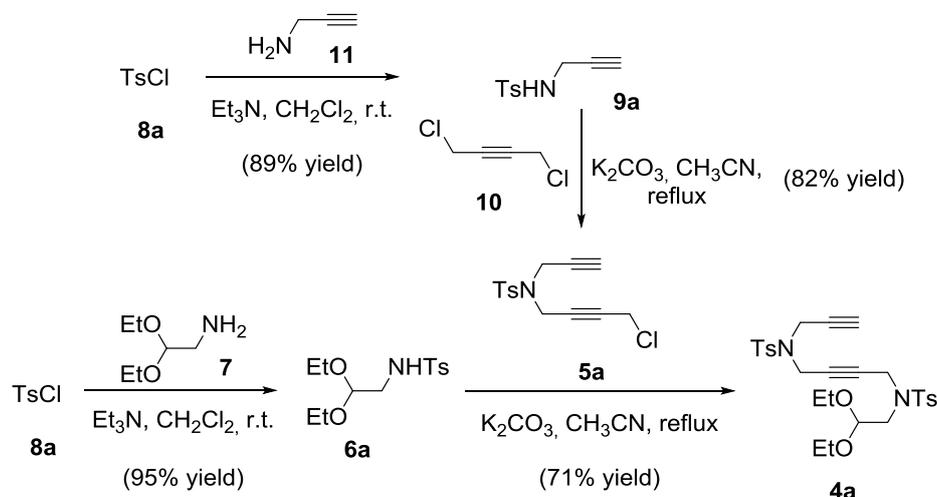


Scheme 3.1 Retrosynthetic analysis of *NTs*-linked substrate **1aa**.

The hydrazone moiety can be assembled by deprotection of the aldehyde and the condensation with commercially available tosylhydrazine (Scheme 3.1, **4a** → **2a** → **1aa**). It is expected that appropriate conditions for this deprotection will be established through experimentation. Several nucleophilic substitutions will be used to assemble the linear diyne precursor **4a** (Scheme 3.1). *N*-Tosylamides **6a** and **9a** were further disconnected via the N-S bond to afford commercially available starting materials.

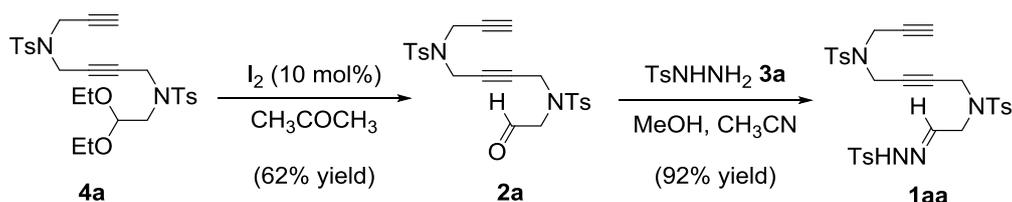
3.2. Synthesis of substrate **1aa**

Based on this retrosynthetic analysis, the synthesis of diyneacetal **4a** was tackled, as detailed in Scheme 3.2.



Scheme 3.2 Synthesis of the *NTs*-tethered substrate **4a**.

The synthesis has 4-methylbenzene-1-sulfonyl chloride (TsCl) **8a** as the common initial reagent. Derivative *N*-tosylprop-2-yn-1-amine **9a**, which contains the first unsaturation, and **6a**, which will finally be transformed to the *N*-tosylhydrazone, were obtained in high yields by treatment of TsCl **8a** in anhydrous dichloromethane and triethylamine as a base with propargylamine **11** and 2,2-diethoxyethanamine **7**, respectively. *N*-Tosylprop-2-yn-1-amine **9a** was further reacted with 1,4-dichloro-2-butyne **10** and potassium carbonate in acetonitrile at reflux to obtain diyne derivative **5a**. An 82% yield was obtained when excess of the dichloride reagent was used to avoid the dialkylation. Acetal **6a** was then reacted with chloride derivative **5a**, which contains two unsaturations, to obtain **4a** with a 71% yield using the same alkylation conditions as were used for the preparation of **5a**. The next step was to remove the acetal protecting group of derivative **4a** (Scheme 3.3).



Scheme 3.3 Synthesis of the *NTs*-tethered compound **1aa**.

The reaction was first attempted using hydrochloric acid and tetrahydrofuran but the product was obtained as an inseparable mixture with secondary products. For this reason, we changed the conditions using acetone and a catalytic amount of iodine, following a procedure described in the literature by Hu et al.⁵⁰ This alternative methodology furnished the aldehyde **2a** with a 62% yield (Scheme 3.3). After having accessed the aldehyde form, **2a** was reacted with *N*-tosylhydrazide **3a** in methanol and the minimum amount of acetonitrile in order to solubilize the aldehyde completely to form *N*-tosylhydrazone compound **1aa**. The desired product **1aa** was obtained with a 92% yield.

3.3. Reactivity studies

After synthesizing the diyne-*N*-tosylhydrazone model substrate **1aa**, its reactivity was evaluated with a series of rhodium catalysts (Table 3.1).

Table 1.1 Optimisation of the rhodium(I)-catalysed cyclisation of the diyne *N*-tosylhydrazone **1aa**.^[a]



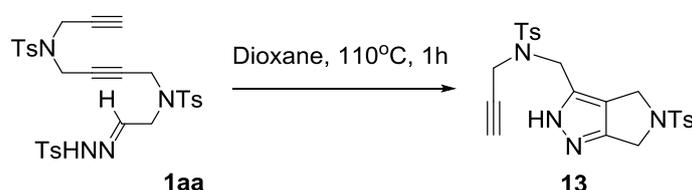
Entry	Rh complex	Biphosphine	Solvent, T	Base	Yield ^[b]
1	[Rh ₂ (OAc) ₄]	-	DCE, reflux	-	- ^[c]
2	[RhCl(PPh ₃) ₃]	-	Toluene, reflux	-	- ^[d]
3	[RhCl(PPh ₃) ₃]	-	EtOH, reflux	-	- ^[d]
4	[RhCl(PPh ₃) ₃]	-	DCE, reflux	-	- ^[d]
5	[RhCl(cod)] ₂	-	DCE, reflux	-	- ^[d]
6	[Rh(OH)(cod)] ₂	-	DCE, reflux	-	- ^[d]
7	[Rh(cod) ₂]BF ₄	<i>rac</i> -BINAP	DCE, reflux	KO ^t Bu (3 equiv.)	- ^[d]
8	[Rh(cod) ₂]BF ₄	<i>rac</i> -BINAP	DCE, reflux	K ₂ CO ₃ (3 equiv.)	47%
9	[Rh(cod) ₂]BF ₄	<i>rac</i> -BINAP	DCE, reflux	.	46%
10	[Rh(cod) ₂]BF ₄	BIPHEP	DCE, reflux	-	- ^[d]
11	-	-	Dioxane, 110°C	K ₂ CO ₃ (1.5 equiv.)	- ^[e]
blank	-	-	DCE, reflux	-	Recovery of 1aa

[a] Reaction conditions: **1aa** (0.10 mmol, 0.03M), 1 hour. [b] Isolated yield after column chromatography. [c] Initial **1aa** was recovered. [d] A complex mixture of unidentified products was obtained. [e] Product corresponding to the 1,3-dipolar addition **13** (Scheme 3.4) is formed.

No reaction took place when the rhodium(II) dimer [Rh₂(OAc)₄] was used even when the reaction time was prolonged to 24 hours (Entry 1). This catalyst has shown great potential in metal carbene transformations.⁵¹ Changing to rhodium(I) sources by the use of Wilkinson's catalyst, also failed to afford the desired product despite different solvents being tested (entries 2-4). Degradation was observed when a phosphine-free rhodium source such as [RhCl(cod)]₂ was used (Entry 5). The use of

$[\text{Rh}(\text{OH})(\text{cod})]_2$ either alone or in combination with bases such as KO^tBu also led to product **1aa** being degraded (Entry 6).

The use of a combination of BINAP with a cationic rhodium source such as $[\text{Rh}(\text{cod})_2]\text{BF}_4$ in the presence of potassium *tert*-butoxyde only led to the decomposition of the starting material (Entry 7) but changing the base to potassium carbonate effectively furnished a new cyclisation product **12aa** after 1.5 hours of reaction (Entry 8). To our delight, performing the reaction without a base furnished the same product with the same yield (Entry 9). The ligand change to a BIPHEP was detrimental to the reaction (Entry 10). Treatment of **1aa** in dioxane at 110°C in the presence of K_2CO_3 and without a rhodium catalyst afforded a bicyclic pyrazole **13** as similarly observed by other authors (Scheme 3.4).⁵² A blank reaction without a transition metal catalyst only allowed the recovery of the starting material, indicating that the catalyst is needed for the reaction to proceed.



Scheme 3.4 1,3-Dipolar cycloaddition of derivative **1aa** to afford compound **13**.

The obtained product **12aa** was analysed by ESI-HRMS. The ESI-HRMS spectrum in the positive ion mode showed a peak at $m/z = 613.0$, which corresponds to the mass of the starting material **1aa** but with a loss of 28 units, possibly corresponding to N_2 . Furthermore, elemental analysis fitted with the formula $\text{C}_{30}\text{H}_{32}\text{N}_2\text{O}_6\text{S}_3$, confirming the loss of diatomic nitrogen from **1aa**. We then proceed to analyze the whole range of monodimensional and bidimensional NMR spectra. Comparison of the ^1H NMR of the diynetylsulfonylhydrazone **1aa** and the obtained product **12aa** gave us some clues as to the structure of the new product formed (Figure 3.2). In the aromatic region, we were able to check that three magnetically unequivalent 4-methylphenyl groups were still in the molecule (Figure 3.2, 7.18 to 7.76 ppm). The signals were slightly modified and especially one of the doublets was shifted upfield to 7.19 ppm. It was possible to corroborate the presence of the three unequivalent tosyl groups by the three singlets observed around 2.4 for the methyls (Figure 3.2, 2.43, 2.45 and 2.47 ppm). Continuing with the analysis of the ^1H NMR spectrum, we could see two new signals integrating three protons in the region of the alkenes (Figure 3.2, 5.41 to 5.66 ppm). The analysis of the region between 3.31 and 4.40 ppm, where the methylenic protons next to the NTs groups appeared, also proved to be interesting. Whereas the signals appeared as a doublet and overlapped signals integrating 2 and 6 protons in diynetylsulfonylhydrazone **1aa**, in the new product eight signals could be clearly observed. This is evidence that **12aa** has conformationally restricted cycles with diastereotopic protons.

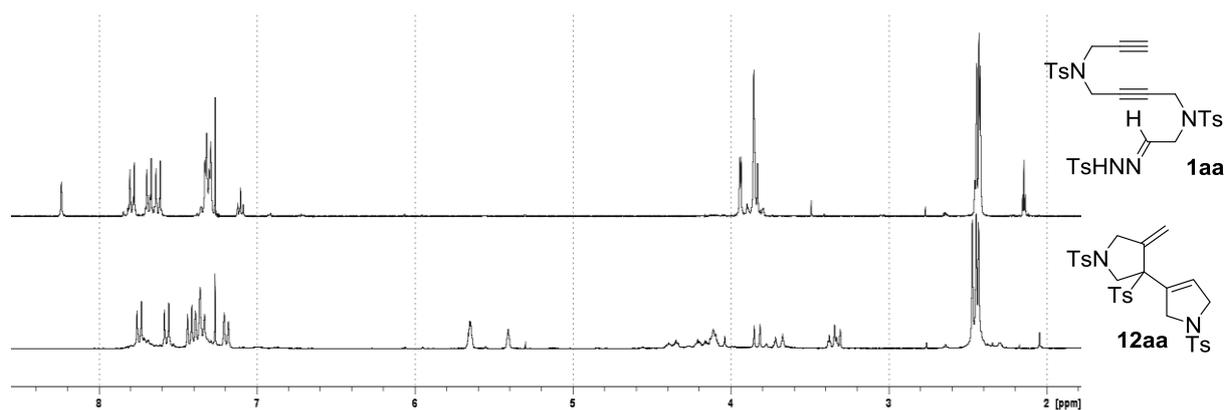


Figure 3.2 Comparison between the expanded area of the ¹H NMR spectrum (400 MHz) of **1aa** (top) and **12aa** in CDCl₃ (bottom).

Further information was obtained on analyzing the HSQCed. In Figure 3.3 we can see an expansion of the HSQCed for the new compound that allowed us to analyze the region between 5.3 and 5.7 ppm for the ¹H NMR dimension. Two of the alkenic protons at 5.41 and 5.66 ppm are attached to the same carbon at 116.47 ppm and so it can be concluded that they constitute a pair of diastereotopic protons on a terminal alkene. The third proton at 5.65 ppm is attached to the carbon at 129.10 ppm. Finally, we were also able to determine that the carbon at 73.89 ppm is quaternary.

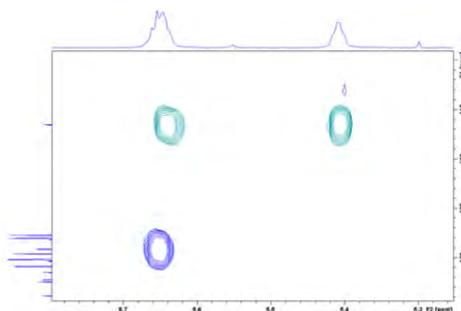


Figure 3.3 Expanded area of the HSQCed spectrum of **12aa** in CDCl₃.

Based on the information provided and a detailed analysis of the HSQCed, HMBC and NOESY correlation, we determined that the structure of the product formed consists of the bicyclic structure shown in Figure 3.4. In this case, NOESY is extremely useful to assign peaks from the tosyl groups using the couplings that are observed (Figure 3.5).

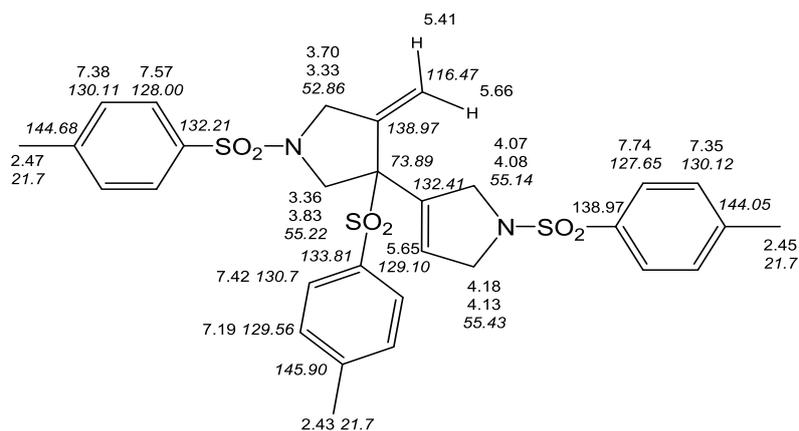


Figure 3.4 Assignment of ^1H - and ^{13}C NMR signals of 12aa.

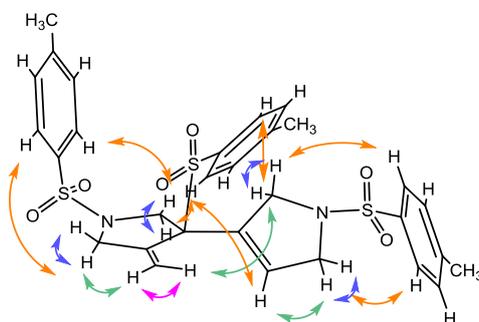
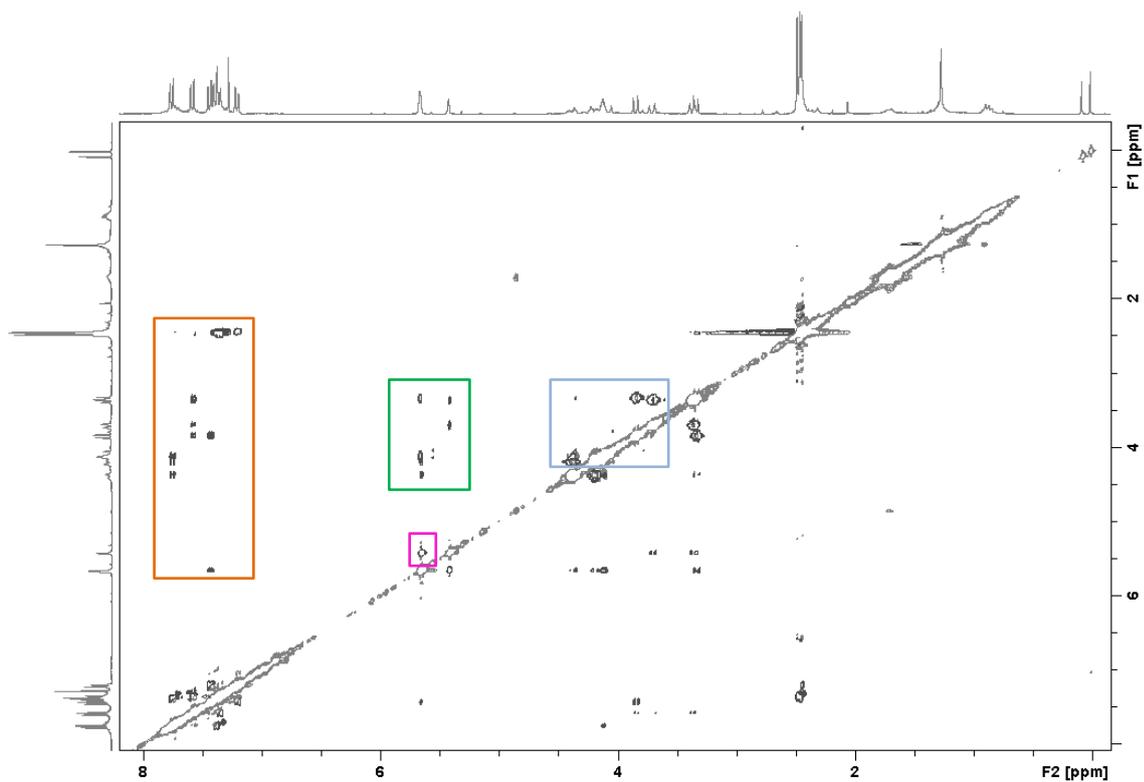


Figure 3.5 NOESY spectrum of 12aa (top) and its assignment (bottom).

Therefore, under rhodium(I) catalysis, the diynetosylhydron **1aa** has suffered a carbocyclisation reaction forming two new C-C bonds through carbene/alkyne metathesis, a migration of a hydrogen atom forming a C-H bond and a migration of a tosyl forming a C-S bond, accompanied by a loss of nitrogen, which has resulted in the formation of the bicyclic structure **12aa**. As mentioned in the introduction, *N*-tosylhydrazones can be a safe source of diazo compounds and can undergo different kinds of reaction when a metal is placed in the reaction. Unlike examples presented in the literature, the base was not necessary to obtain this reactivity, showing that the rhodium is somehow able to decompose the *N*-tosylhydrazone (this will be discussed in Chapter 6).

The formation of the C-S bond generates a quaternary asymmetric carbon, so we then attempted to run the process enantioselectively. To this end we used a combination of various BINAP-type chiral diphosphine ligands in combination with $[\text{Rh}(\text{cod})_2]\text{BF}_4$ (Figure 3.6).

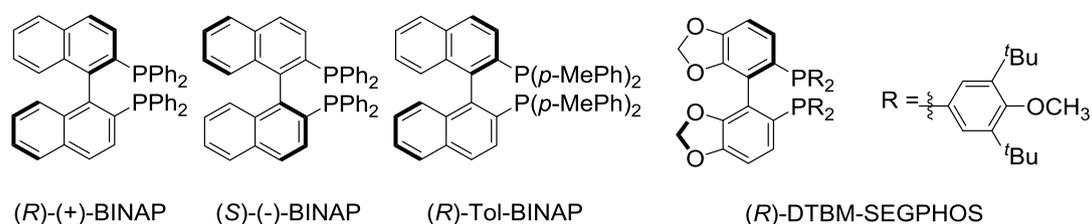
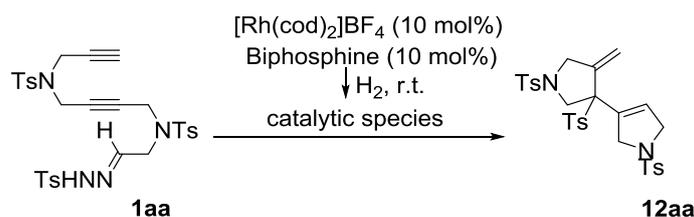


Figure 3.6 Diphosphine ligands used in the optimisation process.

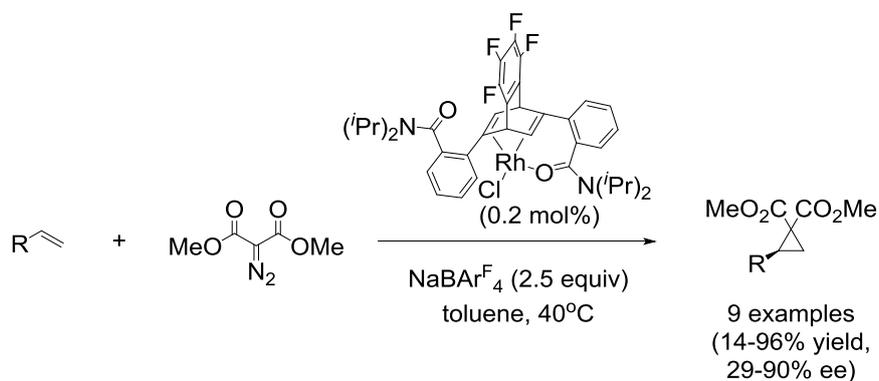
The use of either (*R*)- or (*S*)-BINAP allowed the isolation of two enantiomeric cycloadduct products in excellent enantiomeric excesses (Entries 2 and 3, Table 3.2). When a bulkier biphosphine such as DTBM-Seghos was tested, it resulted in a complete loss of reactivity (Entry 4). (*R*)-Tol-BINAP, on the other hand, gave analogous results to those obtained with (*R*)-BINAP (Entry 5). Increasing the temperature to 110 °C whether by conventional or microwave heating (Entries 6 and 7) or changing the concentration of the reaction mixture did not improve the yield (Entry 8).

Table 3.2 Optimisation of the rhodium(I)-catalysed cyclisation of the diyne *N*-tosylhydrazone **1aa**.^[a]

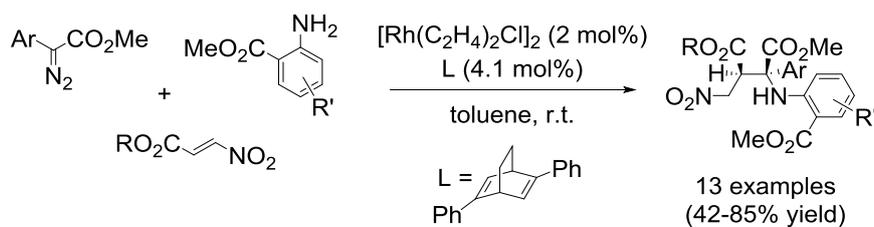
Entry	Biphosphine	Solvent, T, t	Yield ^[b]	ee
1	<i>rac</i> -BINAP	DCE, reflux, 1h	46%	-
2	(<i>R</i>)-BINAP	DCE, reflux, 1h	58%	> 99%
3	(<i>S</i>)-BINAP	DCE, reflux, 1h	45%	> 99% ^[c]
4	(<i>R</i>)-DTBM-SEGPHOS	DCE, reflux, 1h	-	-
5	(<i>R</i>)-Tol-BINAP	DCE, reflux, 1h	55%	> 99%
6	(<i>R</i>)-Tol-BINAP	Chlorobenzene, reflux, 10 min	43%	n.d.
7	(<i>R</i>)-Tol-BINAP	Chlorobenzene, MW 110°C, 10 min	48%	n.d.
8 ^[d]	(<i>R</i>)-Tol-BINAP	DCE, reflux, 1h	51%	n.d.

[a] Reaction conditions: $[\text{Rh}(\text{cod})_2]\text{BF}_4$ (10 mol%), **1aa** (0.10 mmol, 0.03M). [b] Isolated yield after column chromatography. [c] The reaction forms the opposite enantiomer to the one obtained with (*R*)-BINAP. [d] Reaction run at a concentration of 0.01M.

Although rhodium(I) complexes are well known to mediate in various asymmetric reactions,⁵³ the development of stereoselective processes making use of rhodium(I)-carbene chemistry has been little explored. Only four examples can be found in the literature. In 2010, Hayashi et al. reported the use of a cationic chiral diene-rhodium(I) complex for the asymmetric cyclopropanation of alkenes with dimethyl diazomalonate (Scheme 3.5).⁵⁴

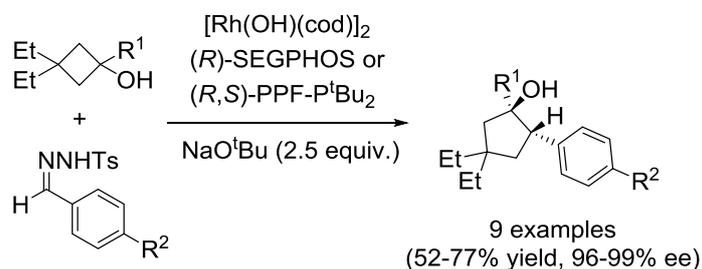
**Scheme 3.5** Rhodium(I)-carbene catalysed cyclopropanation.

Hu et al. also used a rhodium(I) complex with a chiral diene ligand to promote an enantioselective three-component reaction that formed an ylide intermediate, which was subsequently involved in a Michael addition-type reaction (Scheme 3.6).⁵⁵



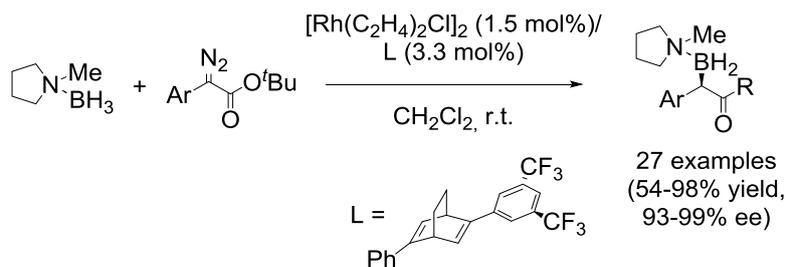
Scheme 3.6 Rhodium(I)-carbene catalysed ylide transformation.

In 2014, Murakami *et al.* reported the enantioselective insertion of cyclopentanols promoted by rhodium(I)-carbene stabilised with diphosphine ligands formed upon decomposition of *N*-tosylhydrazones (Scheme 3.7).⁵⁶



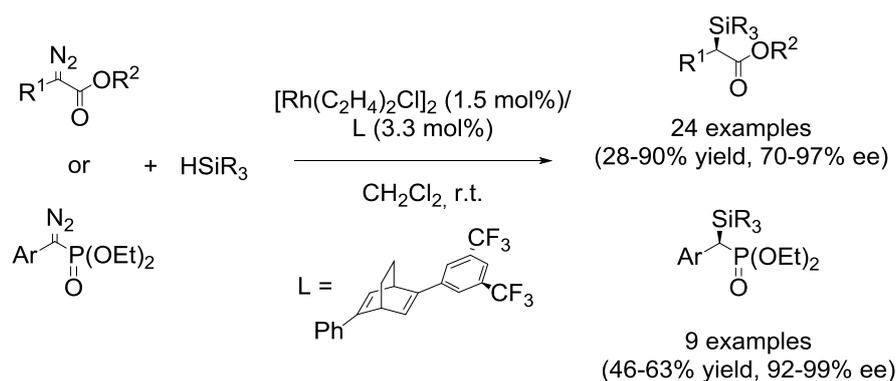
Scheme 3.7 Rhodium(I)-carbene catalysed C-C bond insertion.

Xu *et al.* in 2015 reported the asymmetric carbene insertion into B-H bonds giving access to functionalised organoboranes, again using a chiral diene rhodium(I) complex (Scheme 3.8).⁵⁷ It should be noted that this last example is the only one in which an enantioselective process is achieved without the presence of electronwithdrawing groups in the molecule and using *N*-tosylhydrazones as the metal carbene source.



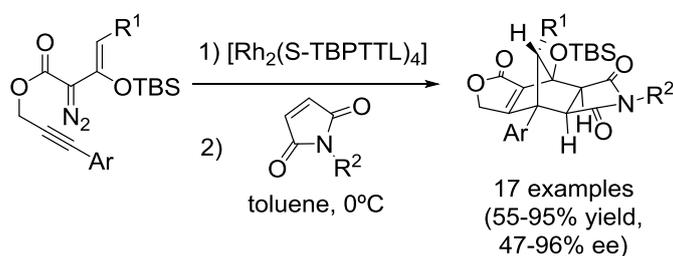
Scheme 3.8 Rhodium(I)-carbene catalysed B-H bond insertion.

These conditions were used by the same authors one year later to report an analogous insertion of α -diazoesters and α -diazophosphonates to silanes (Scheme 3.9).⁵⁸



Scheme 3.9 Rhodium(I)-carbene catalysed Si-H bond insertion.

Therefore, the enantioselective cyclisation of **1aa** represented the **first example of an enantioselective process in which a carbene/alkyne metathesis was involved not only using rhodium(I) catalysts but also considering other transition metal catalysts**. It should be noted, however, that soon after our work was published, Bao, Xu, et al. reported an enantioselective rhodium(II) catalysed carbene/alkyne process that made it possible to prepare cyclopentadienes by a cascade reaction of alkynyl-tethered enol diazoacetates (Scheme 3.10).⁵⁹ Chiral cyclopentadienes were obtained under rhodium(II) catalysis, which were in situ trapped with *N*-phenylmaleimide to afford bridged polycyclic compounds.



Scheme 3.10 Enantioselective rhodium(II) catalysed carbene/alkyne process.

Having developed an extremely interesting new process, we wished to examine how broadly this transformation could be applied. We first proceeded to synthesize a series of substrates in which this chemistry could be explored, modifying the electronics of the hydrazone (**1aa-1ad**) and the tether groups (**1ba-1da**), and using a non-terminal alkyne (**14**) (Figure 3.7).

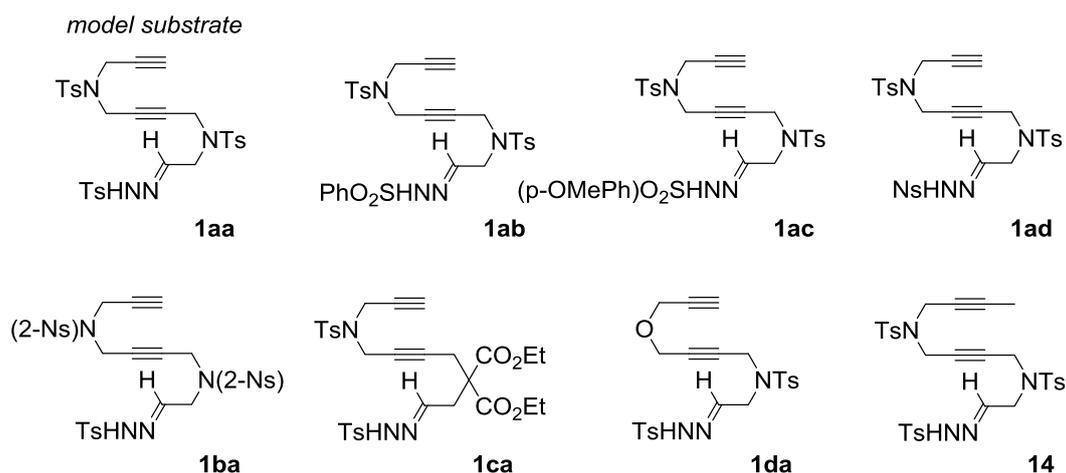
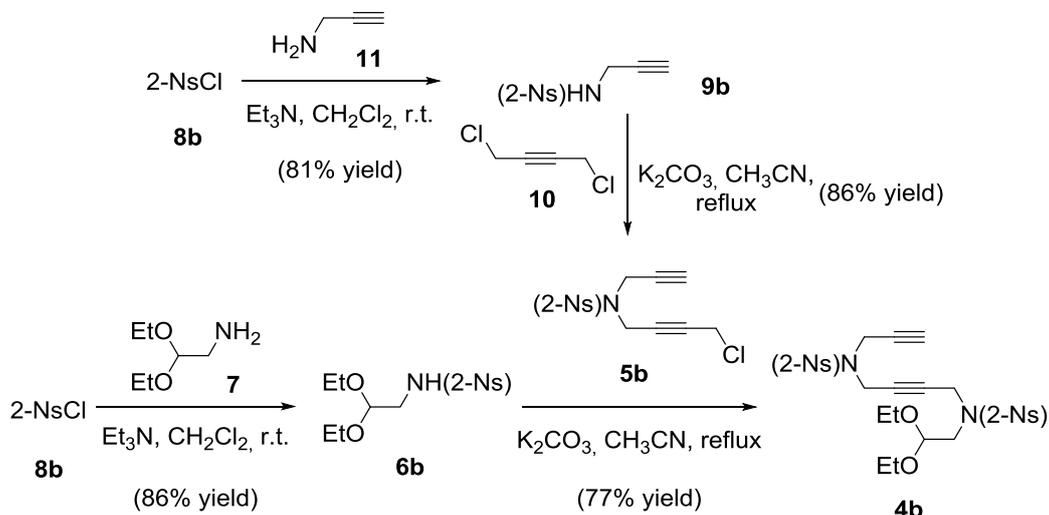


Figure 3.7 Substrates designed and tested in this study.

The synthesis of these substrates was planned following synthetic pathways that were analogous to the one developed for **1aa**, in which the *N*-tosylhydrazone is installed at the end of the synthesis by condensation of the acetal-protected aldehyde. With regards to the synthesis of acetal-protected intermediates **4**, these were adapted depending on the tethers used between the different unsaturations.

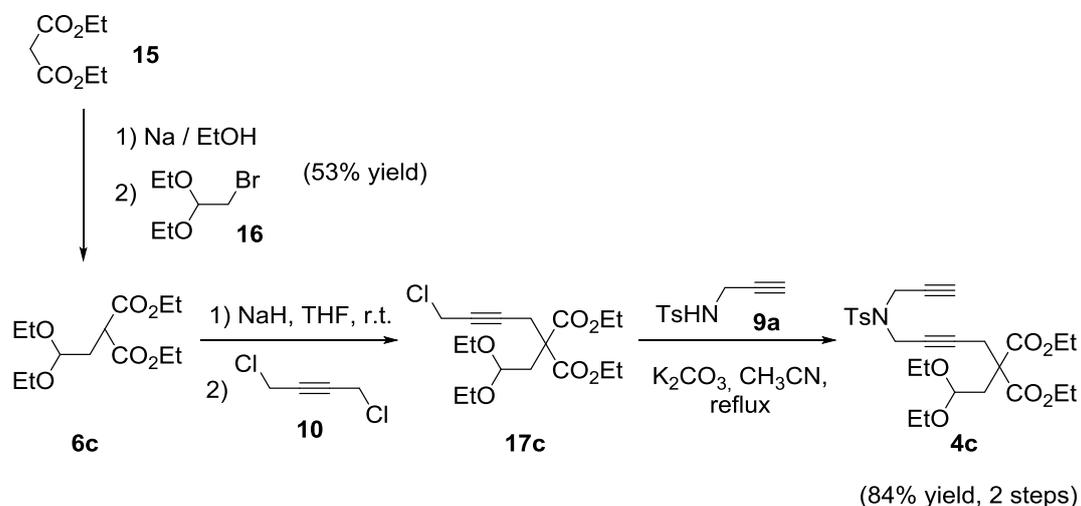
In the case of product **4b** – an intermediate for the synthesis of **1ba** and with 2-nosyl groups as tethers – a synthetic route analogous to the one used for **4a** was employed (Scheme 3.11).



Scheme 3.11 Synthesis of 2-*Ns*-tethered derivative **4b**.

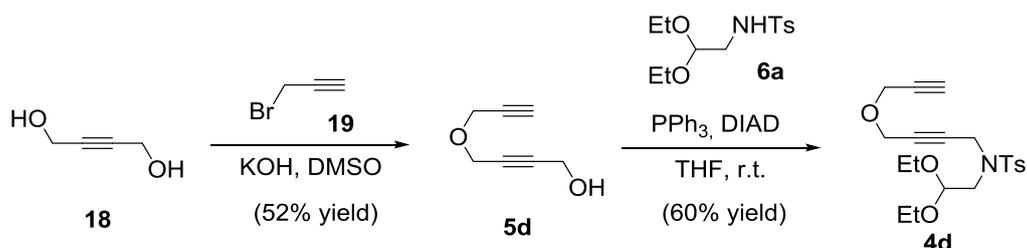
The synthesis of malonate-tethered substrate **4c**, towards the synthesis of **1ca**, was started with the in situ generation of sodium ethoxide, which is able to deprotonate the commercially available diethylmalonate **15**. The enolate that is formed attacks the 2-bromo-1,1-diethoxyethane **16** (Scheme 3.12). Remarkably, this method from the literature⁶⁰ allowed the formation of monoalkylated product **6c** on its own in a 53% yield. The next step was the monosubstitution of 1,4-dichloro-2-butyne **10** with **6c** to obtain **17c**. Although an excess of 1,4-dichloro-2-butyne **10** was used to avoid the disubstitution in the nucleophilic substitution, **17c** was obtained as an inseparable mixture with traces of the

disubstituted compound. Its subsequent alkylation afforded a mixture of **4c** and the disubstituted compound, which could be separated by column chromatography. Derivative **4c** was isolated with an 84% yield after two reaction steps.



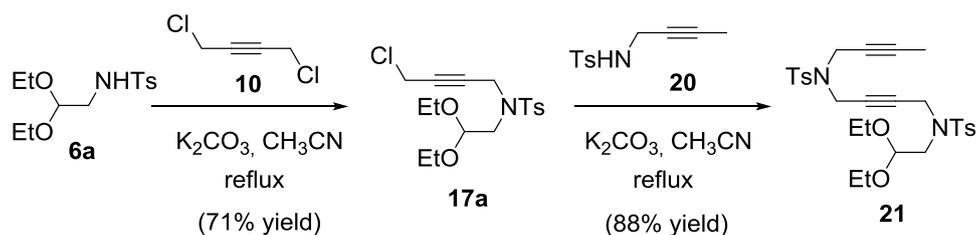
Scheme 3.12 Preparation of malonate-tethered compound **4c**.

The synthesis of the *O*-tethered acetal **4d** – as an intermediate for the synthesis of **1da** – was carried out as outlined in Scheme 3.13. The first step consisted in the nucleophilic substitution of propargyl bromide **19** with an excess of butyne-1,4-diol **18** using potassium hydroxide as the base. In order to avoid the formation of the dialkylated product, propargyl bromide was added dropwise for 1 hour. Compound **5d** was obtained in a 52% yield.⁶¹ A Mitsunobu reaction was used in the next step to alkylate in neutral conditions the previously prepared compound **6a** affording a 60% yield of derivative **4d** (Scheme 3.13).



Scheme 3.13 Synthesis of *O*-tethered compound **4d**.

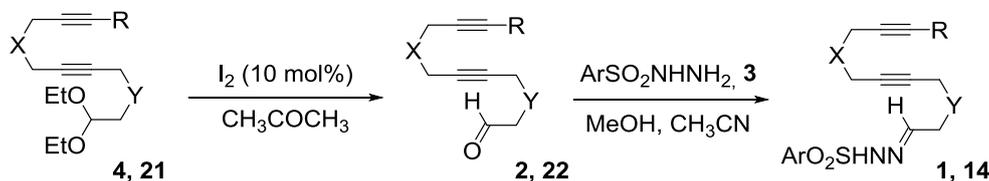
Finally, the synthesis of compound **14**, which has two internal alkynes, was tackled. Similar strategies to those described above allowed us to obtain the non-terminal alkyne **21** (Scheme 3.14).



Scheme 3.14 Preparation of the non-terminal alkyne **21**.

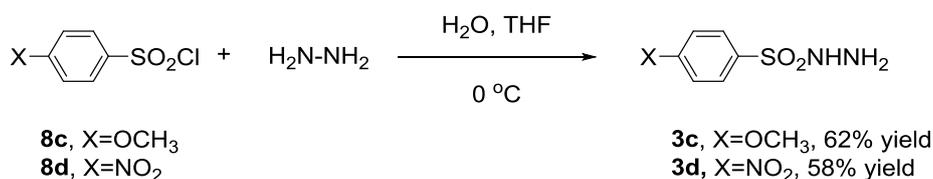
Once all the acetal-protected derivatives **4** and **21** were prepared, the aldehyde deprotection and condensation of the corresponding *N*-sulfonylphenylhydrazide **3** to yield the corresponding hydrazones **1** and **23** was carried out (Table 3.3).

Table 3.3 Synthesis of diynehydrazones **1** and **14** from diyneacetals **4** and **21**.



Acetal	Aldehyde (yield)	X	Y	R	<i>N</i> -Sulfonylaryl-hydrazones (yield)	Ar
4a	2a (62%)	NTs	NTs	H	1aa (92%)	<i>p</i> -CH ₃ Ph
4a	2a	NTs	NTs	H	1ab (96%)	Ph
4a	2a	NTs	NTs	H	1ac (66%)	<i>p</i> -OCH ₃ Ph
4a	2a	NTs	NTs	H	1ad (42%)	<i>p</i> -NO ₂ Ph
4b	2b (67%)	N(2-Ns)	N(2-Ns)	H	1ba (97%)	<i>p</i> -CH ₃ Ph
4c	2c (85%)	NTs	C(CO ₂ Et) ₂	H	1ca (100%)	<i>p</i> -CH ₃ Ph
4d	2d (66%)	O	NTs	H	1da (79%)	<i>p</i> -CH ₃ Ph
21	22 (65%)	NTs	NTs	CH ₃	14 (100%)	<i>p</i> -CH ₃ Ph

Whereas *p*-toluenesulfonylhydrazide and phenylsulfonylhydrazide are commercially available, *p*-methoxyphenylsulfonylhydrazide and *p*-nitrophenylsulfonylhydrazide were prepared from the corresponding arylsulfonyl chloride and hydrazine (Scheme 3.15).



Scheme 3.15 Synthesis of sulfonylhydrazides **3c** and **3d**.

The yields of the deprotection of the different acetals were between 62 and 85% (Table 3.3). More differences can be observed in the hydrazone condensation due to the necessity of purification by column chromatography of the product from other subproducts formed (Table 3.3, Ar= *p*-OCH₃Ph and *p*-NO₂Ph). These low yields could also be explained by the insufficient purity of the prepared *N*-sulfonylarylhydrazides and the resulting need to purify the hydrazones. All the products formed were characterised by NMR and MS spectroscopies. An important effect that was observed by ¹H NMR spectroscopy was the formation of geometric isomers on the N=C bond of the hydrazone in some of the substrates (Figure 3.8).

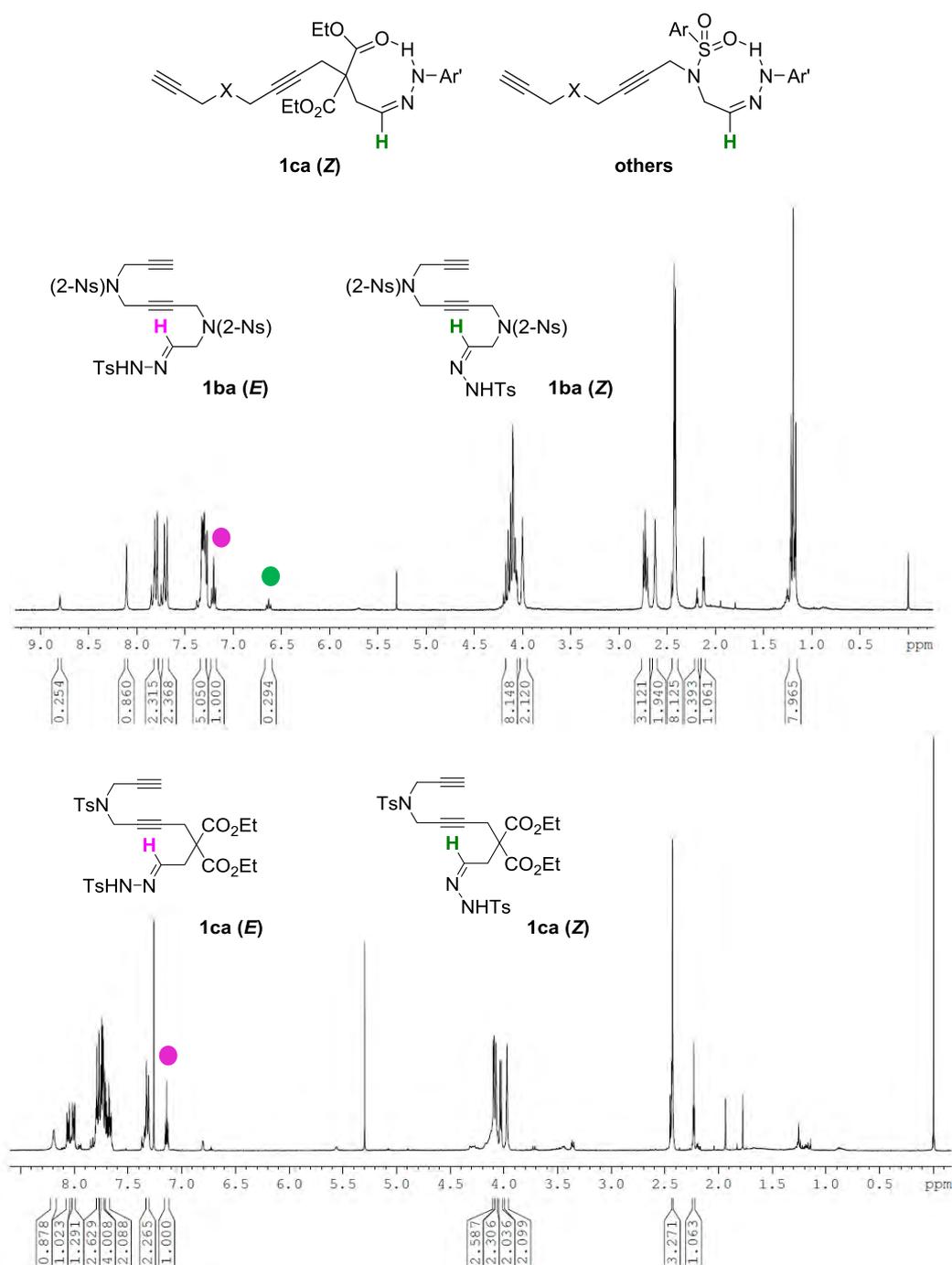
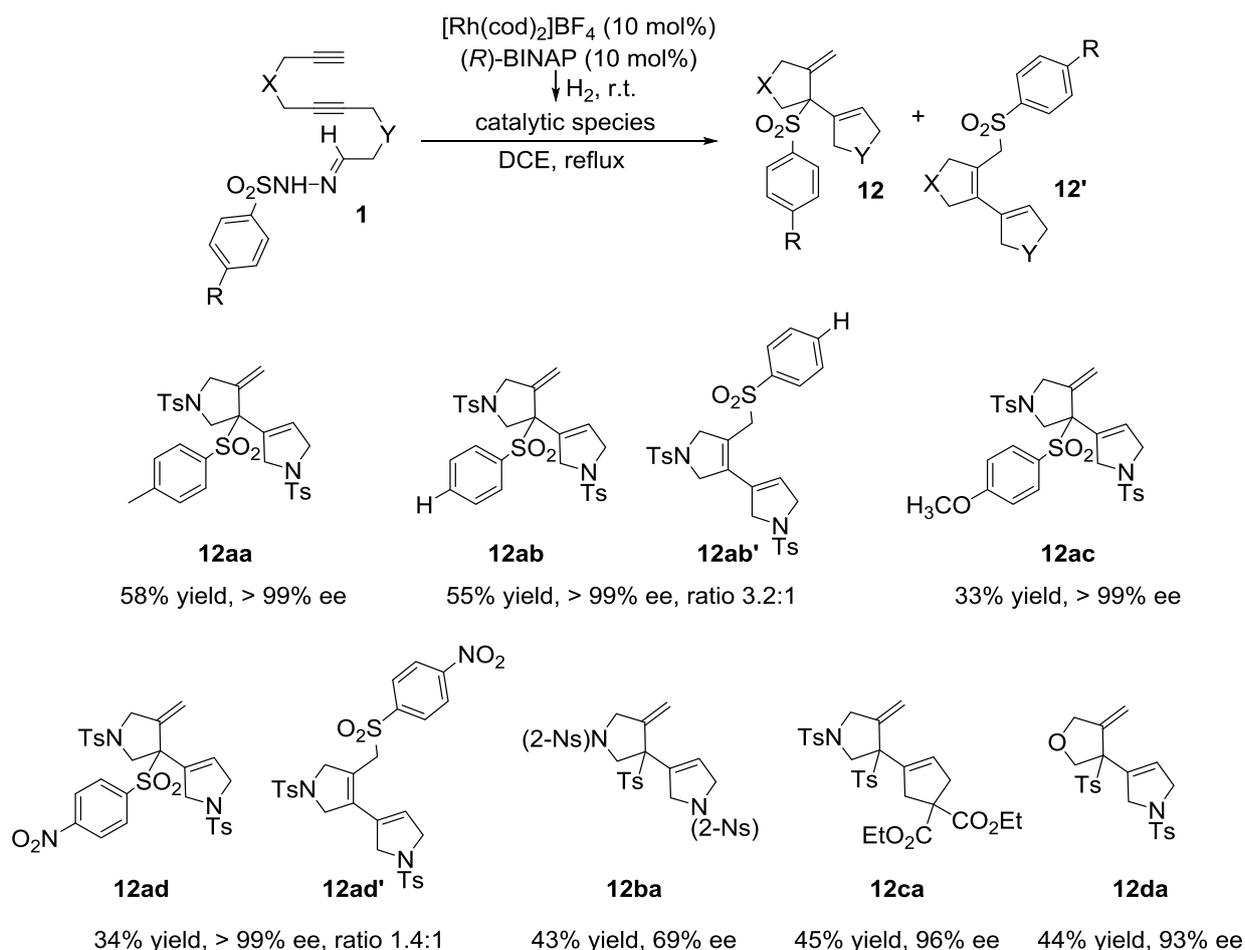


Figure 3.8 ^1H NMR spectra of geometric isomers **1ba** and **1ca**.

Whereas the substrates that have NSO_2Ar as the Y tether show *Z/E* ratios ranging from 23/77 (see for instance the spectrum for hydrazone **1ba** at the top of Figure 3.8) to 8/92, compound **1ca** shows a ratio of 0/100 (see the bottom of Figure 3.8, where the signal in green corresponding to the *cis* hydrazone is negligible). The *Z* isomer of the hydrazone bond is stabilised by intramolecular hydrogen bonding, and our hypothesis is that whereas the arylsulfonyl tethers stabilize the *Z* form, the malonate-tethered substrates are not able to do so. Furthermore, the quantity of *Z* isomer is maximum for compound **1ba**, which has $\text{NSO}_2(2\text{-NO}_2\text{Ph})$ as the tether, and so the greater the electronwithdrawing character of the tether, the stronger the H-bond that is formed.

The nature of the tether used has also a clear influence on the chemical shift of the signals in the NMR spectrum. For example, the methylenic protons next to the *N*-tethered derivatives appear around δ 3.8 ppm, whereas in the case of *O*-tethered compounds the signals are shifted downfield up to a chemical shift of around δ 4.0 ppm. On the other hand, the malonate-tethered substrate decreases the chemical shift and the corresponding methylenic protons appear around δ 2.6 ppm. The same behaviour can be observed in the ^{13}C NMR.

After the synthesis of starting compounds **1** and **14**, the optimised conditions found for the formation of **12aa** were applied to the other substrates (Scheme 3.16).

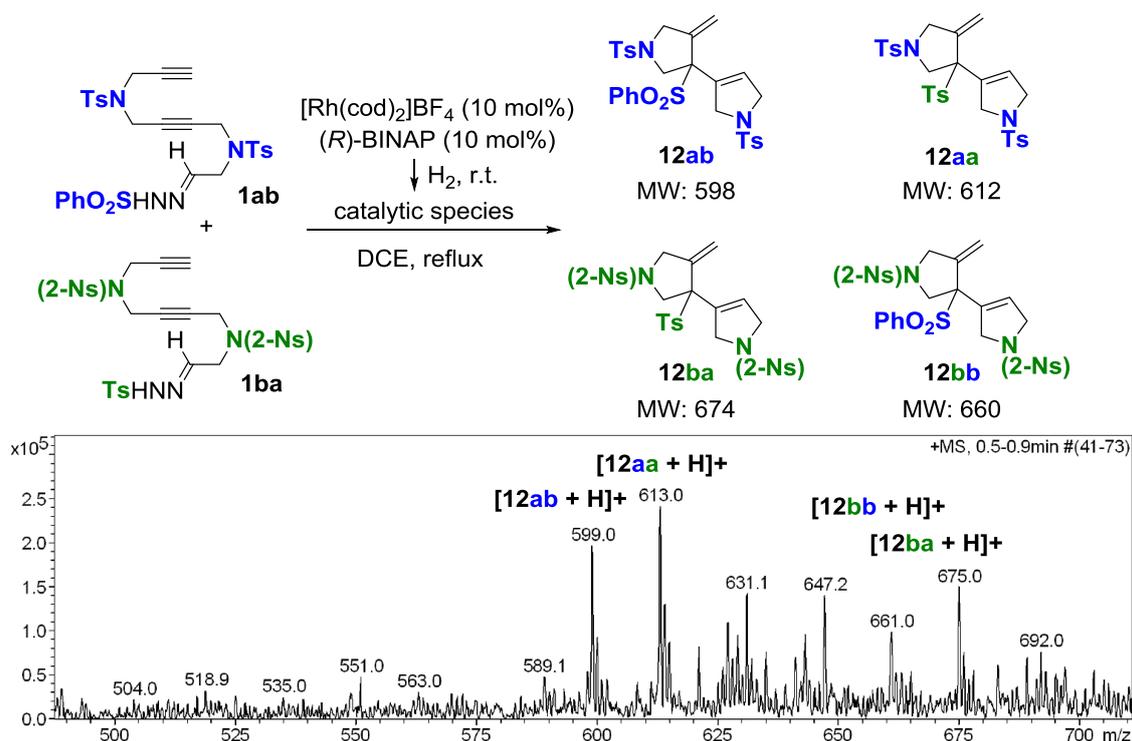


Scheme 3.16 Scope of the rhodium(I)-catalysed cyclisation of diynarylhydrazones **1**.

In contrast with **12aa**, changing the *p*-toluenesulfonyl ring of the hydrazone moiety to a phenylsulfonyl promoted the formation of two isomers, **12ab** and **12ab'**, in a 3.2:1 ratio, resulting in variation in the positions to which the phenylsulfonyl group migrated. Switching to an electrodonating group such as -OMe in the phenyl ring gave the product **12ac** regioselectively. On the other hand, an electron withdrawing group such as -NO₂ favoured the attack on the less hindered position and a 1.4:1 ratio of regioisomers **12ad** and **12ad'** was afforded, allowing us to conclude that the regioselectivity is improved when electron-rich sulfonyl groups are used. The influence of the tether group was then studied. Changing the tosyl to a 2-nitrophenylsulfonyl ring (N(2-Ns)) in the tether gave bicycle **12ba** with slightly lower enantioselectivity. The cycloaddition of substrates in which one of the nitrogenated

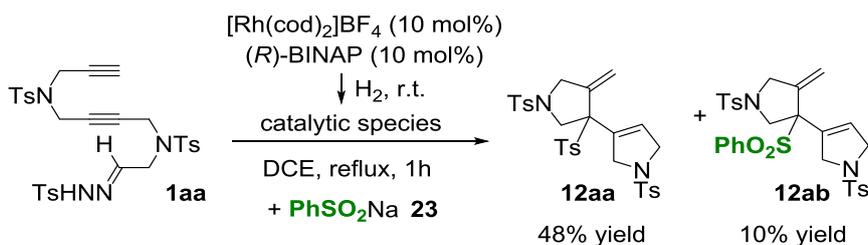
tethers was substituted by either a malonate (**1ca**) or oxygen (**1da**) also furnished the corresponding cycloadducts in a regioselective and highly enantioselective way.

We were eager to gain further understanding of the mechanism of the reaction to shed light on its particularities and explore the potential of the transformation. We first focused our attention on establishing whether the shift of the sulfonyl group occurred in an intramolecular or intermolecular pathway. A crossover experiment between equimolar amounts of reactants **1ab** and **1ba**, differing in the tethers and in the aryl group of the hydrazone, was conducted. The reaction yielded the four possible products, clearly indicating that migration proceeds in an intermolecular manner (Scheme 3.17).

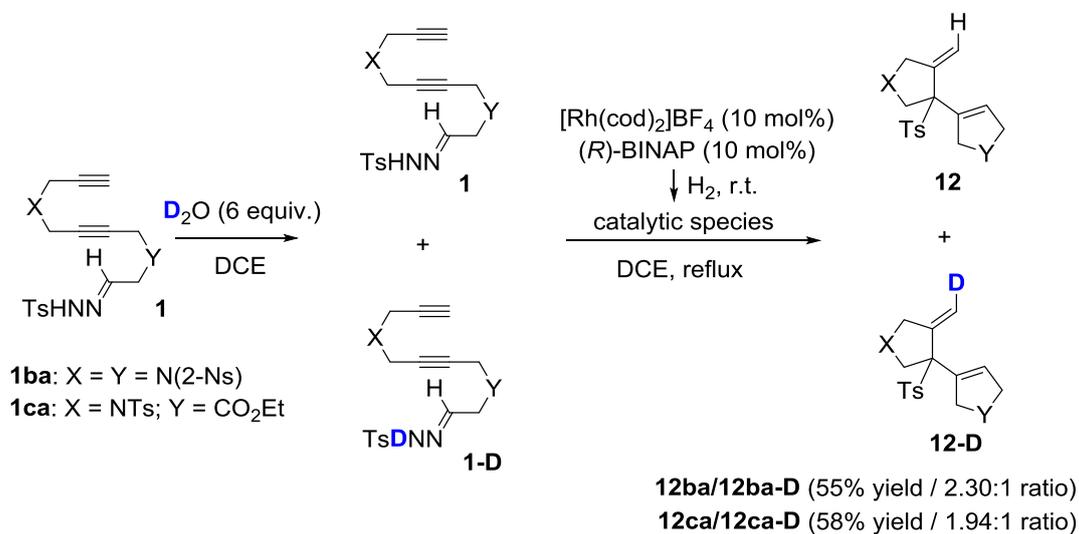


Scheme 3.17 Competitive experiments.

To verify the form in which the sulfonyl group was transferred, a further competitive experiment was performed by adding sodium phenylsulfinate **23** to the cyclisation reaction of **1aa**, which has a tosylhydrazone (Scheme 3.18). Mass spectrometry and NMR revealed that the reaction affords a mixture of the expected product **12aa** with the competitive product **12ab**. The competition of the external sulfinate anion indicates that the decomposition of the hydrazone generates a sulfinate anion in situ.


Scheme 3.18 Competitive experiments.

We then turned our attention to the CH bond which is also formed in the cyclisation reaction. The working hypothesis was that the hydrogen on the *N*-tosylhydrazone was transferred to the terminal alkyne. To confirm this point, deuterium labelling experiments were conducted. By stirring the corresponding substrate **1** in anhydrous dichloroethane in the presence of 6 equivalents of D_2O , the NH was partially exchanged (1:6.1 **1**: **1-D** ratio as monitored by ^1H NMR) leading to a deuterium enriched sample (Scheme 3.19).


Scheme 3.19 Deuterium-labelling experiments.

^1H - and ^2H NMR revealed the incorporation of the deuterium stereoselectively in the olefinic *trans* position on cyclisation reaction under the optimised conditions. If we first take a look at the ^1H NMR spectrum of the reaction mixture obtained from the partially deuterated substrate and compare it with the product obtained when no deuteration has been performed, we can see that there is a clear difference in signal integration, confirming the presence of deuterium in compounds **12ba-D** (Figure 3.9) and **12ca-D** (Figure 3.10).

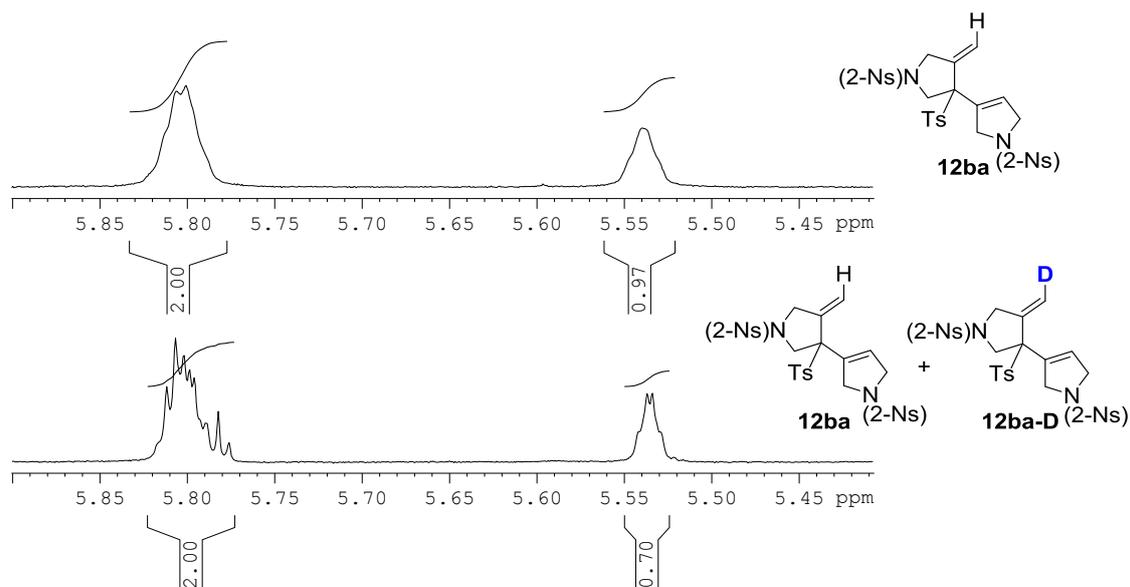


Figure 3.9 Expanded area corresponding to the ^1H NMR spectrum (400 MHz) of **12ba** in CDCl_3 (top); Expanded area corresponding to the ^1H NMR spectrum (400 MHz) of a mixture of **12ba** and **12ba-D** in CDCl_3 (bottom).

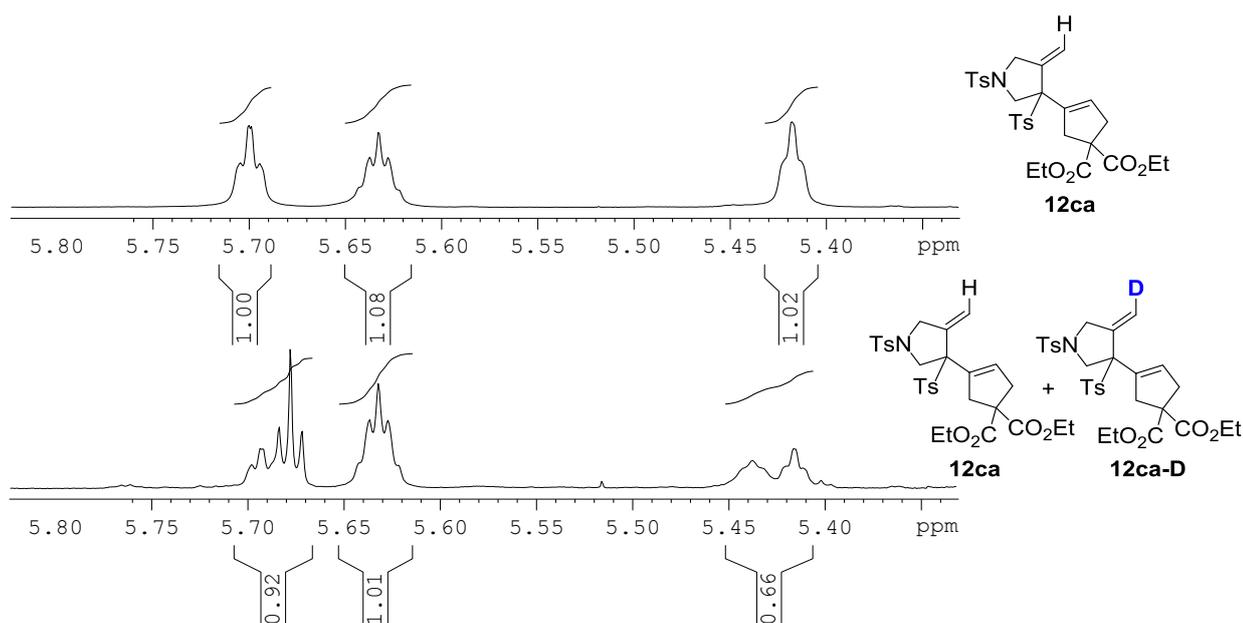


Figure 3.10 Expanded area corresponding to the ^1H NMR spectrum (400 MHz) of **12ca** in CDCl_3 (top); Expanded area corresponding to the ^1H NMR spectrum (400 MHz) of a mixture of **12ca** and **12ca-D** in CDCl_3 (bottom).

Further confirmation was gained by acquiring the ^2H NMR spectrum. The signal at 5.45 ppm confirms the deuteration at the *trans* position whereas no signal is observed at 5.75 ppm, *cis* position (Figure 3.11).

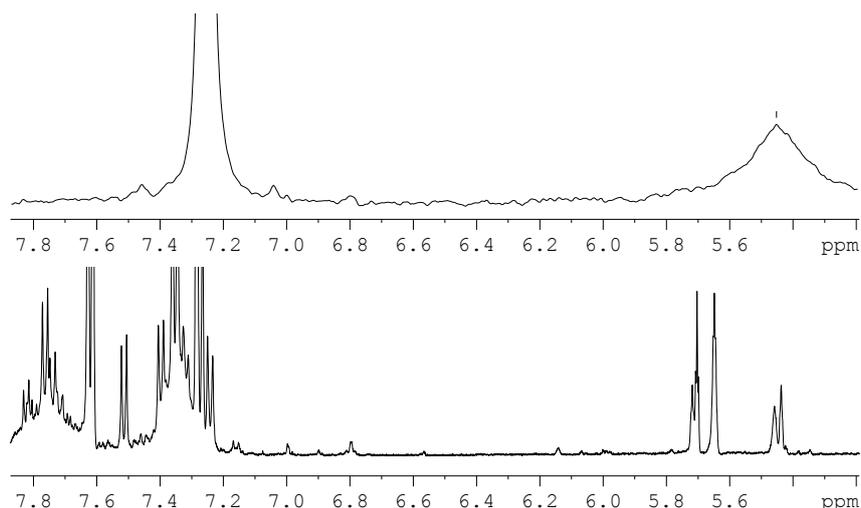
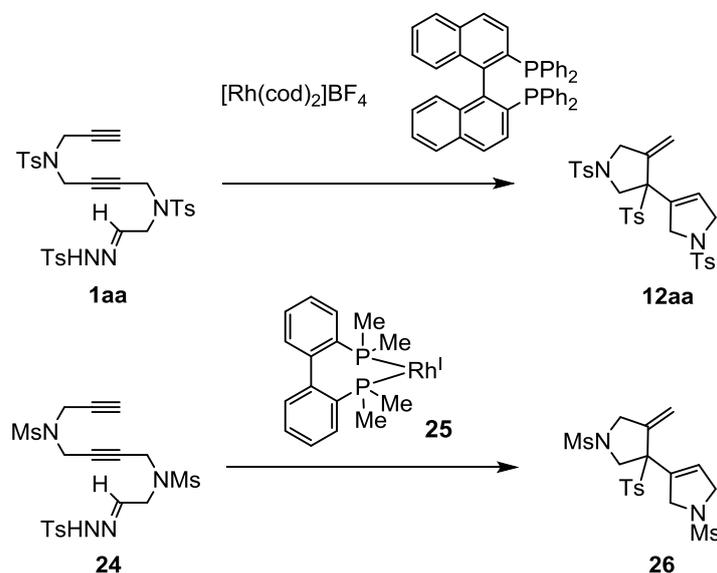


Figure 3.11 Expanded area of the ^1H NMR spectrum (500 MHz) of a mixture of **12ca** and **12ca-D** in CDCl_3 (bottom); ^2H NMR spectrum (77 MHz) of a mixture of **12ca** and **12ca-D** in CDCl_3 (top).

3.4. Computational studies

In order to look for a mechanism which could account for the whole set of experimental results, DFT calculations were performed with the B3LYP functional (Scheme 3.20).



Scheme 3.20 Comparison between the experimental conditions (top) and the model reaction (bottom).

Reported Gibbs energies are B3LYP/cc-pVDZ-PP electronic energies corrected with ZPEs, thermal energies, entropy effects, and solvent effects (dichloroethane solution). The calculations were carried out on a model substrate in which the two Ar groups of the two Ts = $\text{SO}_2\text{-Ar}$ moieties present in the experimental tethers were substituted by a CH_3 to yield Ms = $\text{SO}_2\text{-CH}_3$ group in order to reduce the computational cost of the calculations. The influence of the tether group was found to be rather small and therefore we believe that this does not significantly change the results. The migrating Ts group was included in the calculations without any simplification. To save computational time, the four Ph

groups of the diphenylphosphino groups in the BINAP catalysts were also substituted by methyl groups and two rings of the ligand were removed.

The results are summarised in the Gibbs energy profile of Figure 3.12.

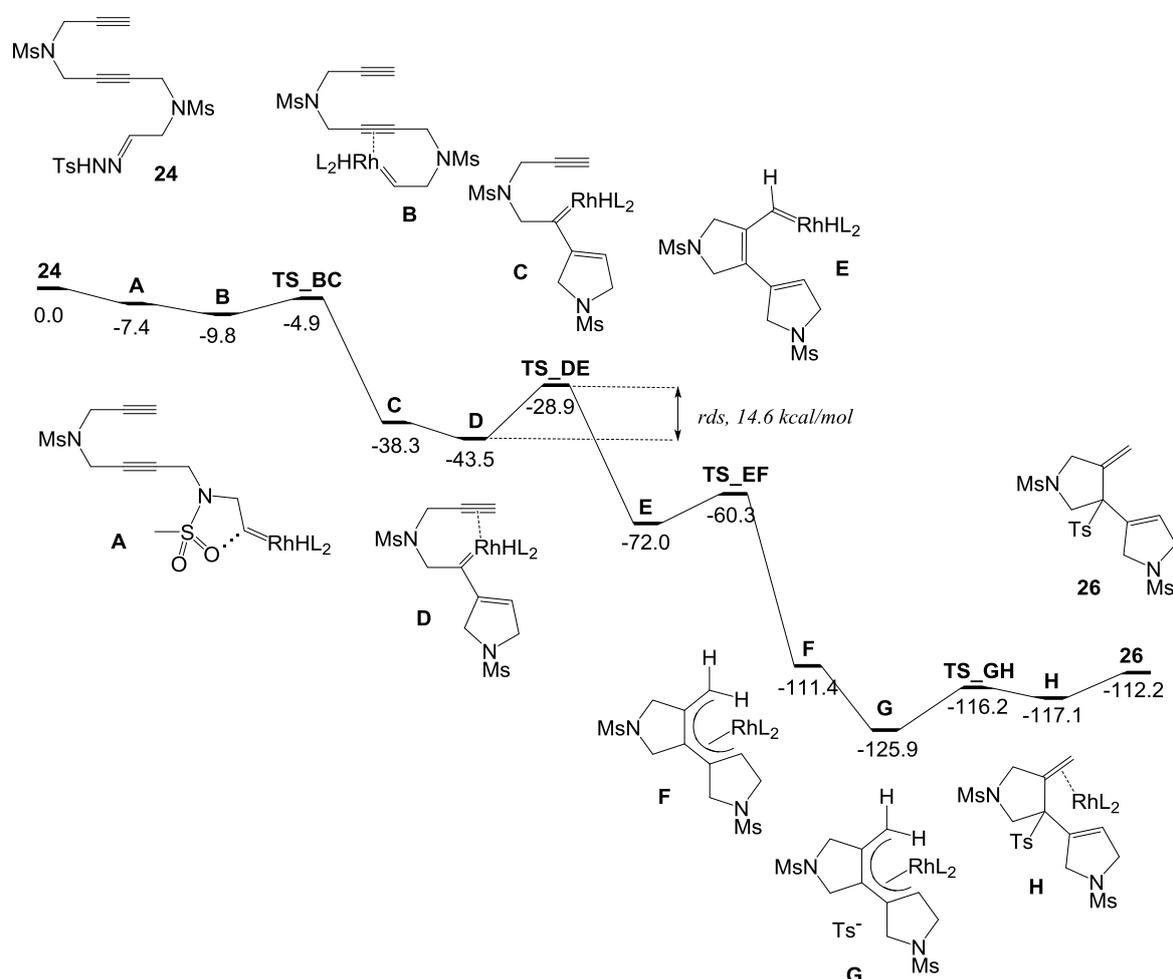


Figure 3.12 Gibbs energy profile (in kcal/mol) of the cyclisation of **24** to **26**.

The first step involves the reaction of the arylsulfonylhydrazone of substrate **24** with the rhodium catalytic species **25**, $\text{Rh}^{\text{I}}\text{L}_2$ (L_2 = biphosphine). Rhodium carbene complex **A**, which is stabilised by coordination of one of the oxygens of the sulfonamide moiety with the carbenic carbon, is formed. The release of N_2 and arylsulfinate, is exergonic by 7.4 kcal/mol in a transformation that will be further discussed in Chapter 6. Subsequent η^2 -coordination of rhodium to the central alkyne group ($\text{Rh}-\text{C}$ distances of 2.375 and 2.639 Å) leads to the rhodium carbene **B** in a process that is slightly exergonic by 2.4 kcal/mol. The next step corresponds to a $[\pi_2\text{s} + \pi_2\text{a}]$ addition of the central alkyne to the rhodium carbene double bond and simultaneous electrocyclic opening of the rhodacyclobutene formed to yield a new vinylrhodium(I) carbene **C**. The opening of the rhodacyclobutene has already been described in a cobaltacyclobutene complex.⁶² Transformation of **B** to **C** takes place through a low Gibbs energy barrier of 4.9 kcal/mol and releases 28.5 kcal/mol. The 16-electron complex **C** rearranges to 18-electron complex **D** in which the terminal alkyne group is η^2 -coordinated to rhodium.

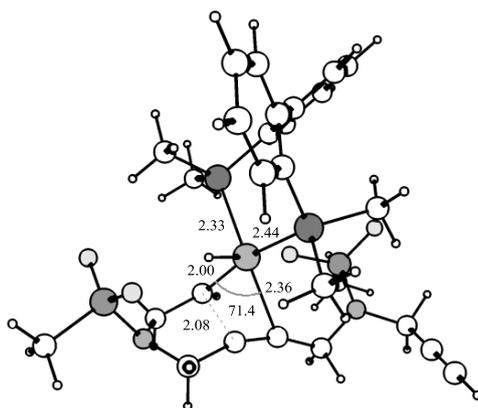


Figure 3.13 Optimised structure (B3LYP/cc-pVDZ) for **TS_{BC}**. Distances in Å and angles in degrees.

D then reacts with the terminal alkyne forming vinylrhodium(I) carbene **E**. The transformation of **D** to **E** follows the same reaction pathway as the process that converts **B** to **C**. It is exergonic by the same energy as **B** to **C** reaction (28.5 kcal/mol) and has to surmount a Gibbs energy barrier of 14.6 kcal/mol. The **D** to **E** conversion is the rate determining step (rds), **D** and the transition state from **D** to **E** being the rate-determining intermediate and transition state, respectively.⁶³ Subsequent metal carbene migratory insertion, in which the hydrogen migrates from the metal to the carbenic carbon, leads to a η^5 -pentadienyl rhodium intermediate **F**.

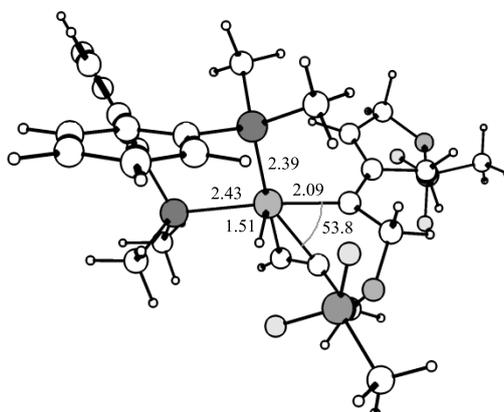


Figure 3.14 Optimised structure (B3LYP/cc-pVDZ) for **TS_{DE}**. Distances in Å and angles in degrees.

Transformation of **E** to **F** is thermodynamically very favorable (39.4 kcal/mol) and takes place through a barrier of 11.7 kcal/mol.

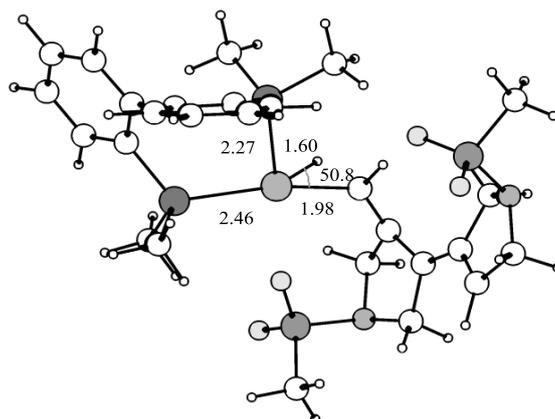


Figure 3.15 Optimised structure (B3LYP/cc-pVDZ) for **TS_{EF}**. Distances in Å and angles in degrees.

In the final part of the reaction mechanism, the *p*-methylphenylsulfinate intermolecularly attacks the η^5 -pentadienyl rhodium intermediate **G**, which is **F** interacting with Ts^- , in a stereoselective way to furnish the final cyclisation product **26** and regenerating the catalytically active species. This last part of the reaction is slightly endergonic (13.2 kcal/mol).

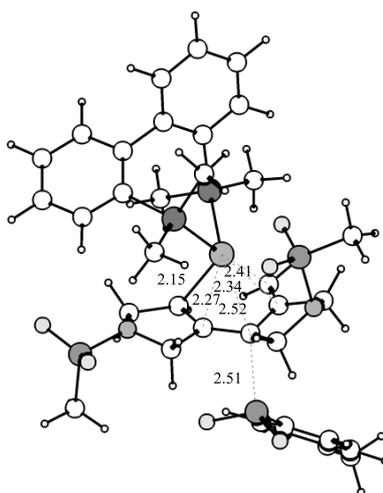


Figure 3.16 Optimised structure (B3LYP/cc-pVDZ) for **TS_{GH}**. Distances in Å and angles in degrees.

As found in deuterium-labeling experiments, the final product **26** has the transferred H in the olefinic *trans* position. We have calculated an alternative pathway that leads to the same final product **26** but with the transferred H in the olefinic *cis* position (Figure 3.17, green and Figure 3.18). This latter path occurs with a higher energy barrier (24.1 kcal/mol) and its rate-determining step is the transformation from **E** to **F**. Moreover complex **E** with the H in *cis* can be easily transformed to complex **E** with H in *trans*. The latter, which is more stable than the *cis* conformer by 2.3 kcal/mol, evolves rapidly to the final product.

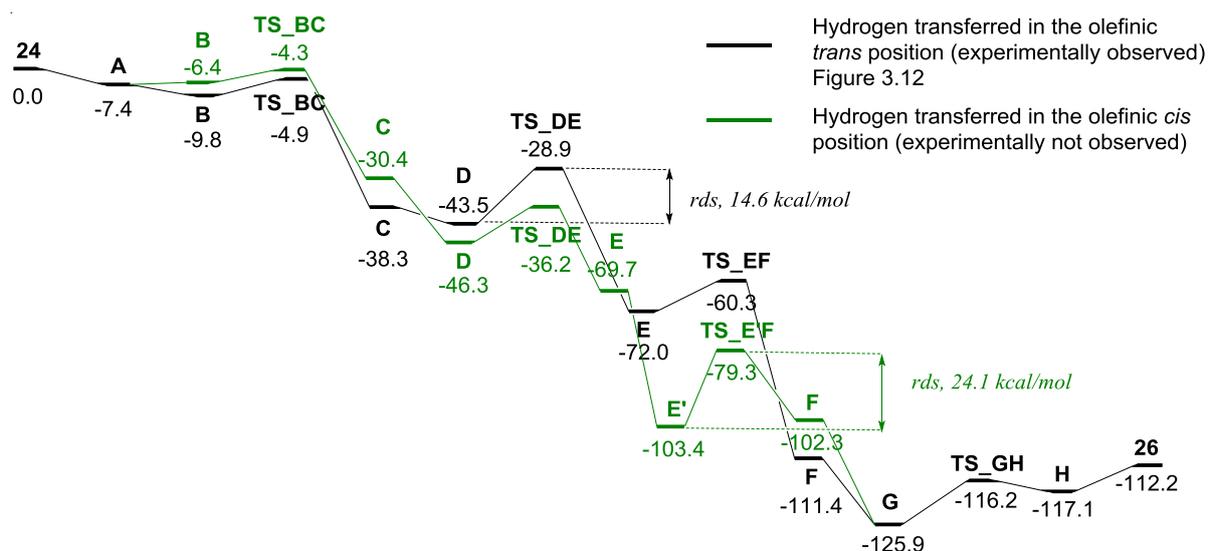


Figure 3.17 Gibbs energy profile (in kcal/mol) for the different reaction pathways studied.

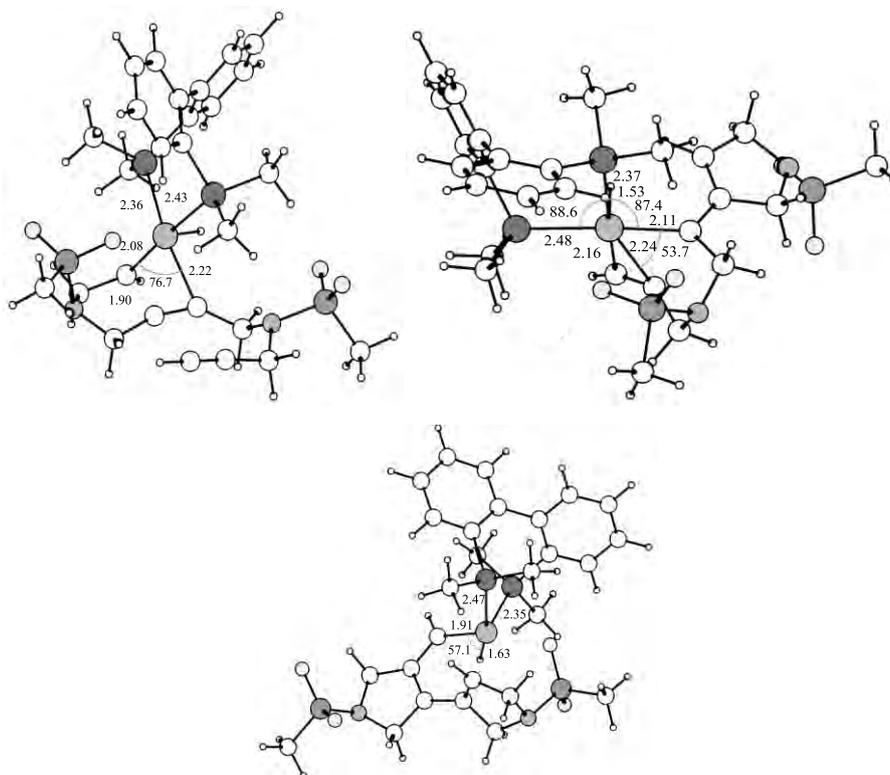
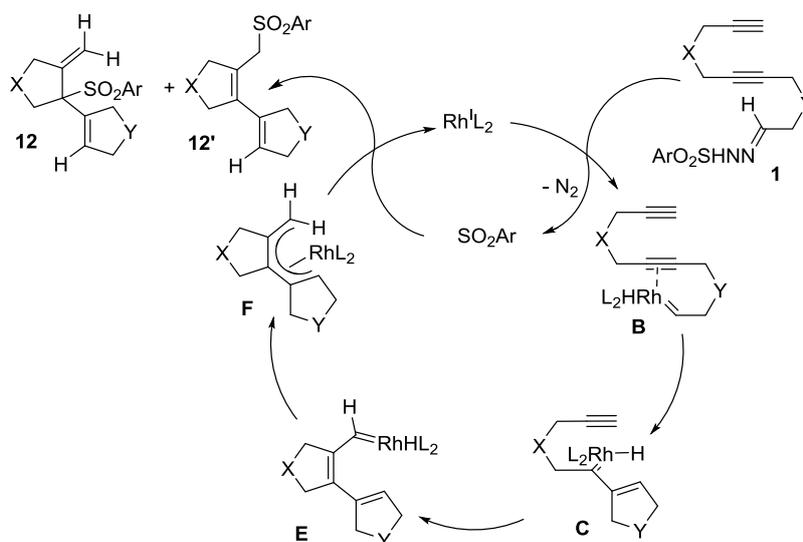


Figure 3.18 Optimised structure (B3LYP/cc-pVDZ) for **TS_{BC}** (top-left), **TS_{DE}** (top-right) **TS_{E'F}** (bottom). Distances in Å and angles in degrees.

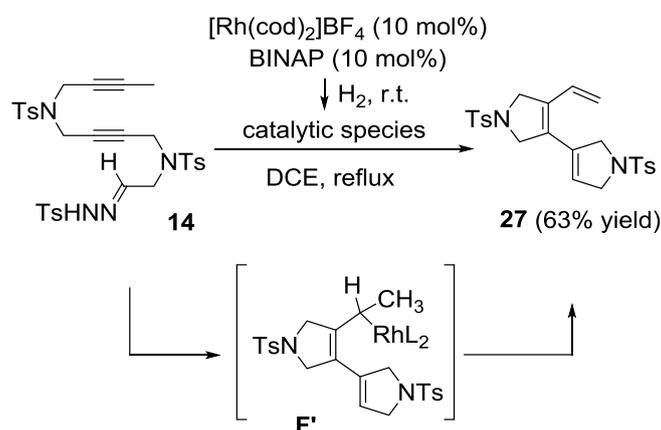
Overall, our data suggest that the rhodium-catalysed cyclisation proceeds via the mechanism depicted in Scheme 3.21. Rhodium(I) carbene is formed releasing nitrogen and arylsulfinate, which through a $[\pi 2_s + \pi 2_a]$ addition to the alkyne and simultaneous electrocyclic opening of the rhodacyclobutene – both of which take place on two consecutive occasions – generates vinylrhodium carbenes **C** and **E**. A metal-to-carbene migratory insertion then leads to the η^5 -pentadienyl rhodium intermediate **F** which is

intermolecularly and stereoselectively attacked by the arylsulfinate to furnish the final cyclisation product **12** and/or **12'**, regenerating the catalytically active species.



Scheme 3.21 Proposed mechanism for the rhodium-catalysed cyclisation reaction.

To obtain further information about the mechanism, we evaluated the reactivity of a substrate featuring a methyl substituent at the terminal alkyne in which β -hydrogen elimination could efficiently compete after the metal-to-carbene migratory insertion. Substrate **14** (Scheme 3.22) was reacted under the optimised conditions to afford product **27** in which the sulfonyl was not incorporated. Trienic product **27** arises from a β -hydrogen elimination of one of the hydrogens of the methyl group of intermediate **F'**, which is formed upon metal-to-carbene H migratory insertion.



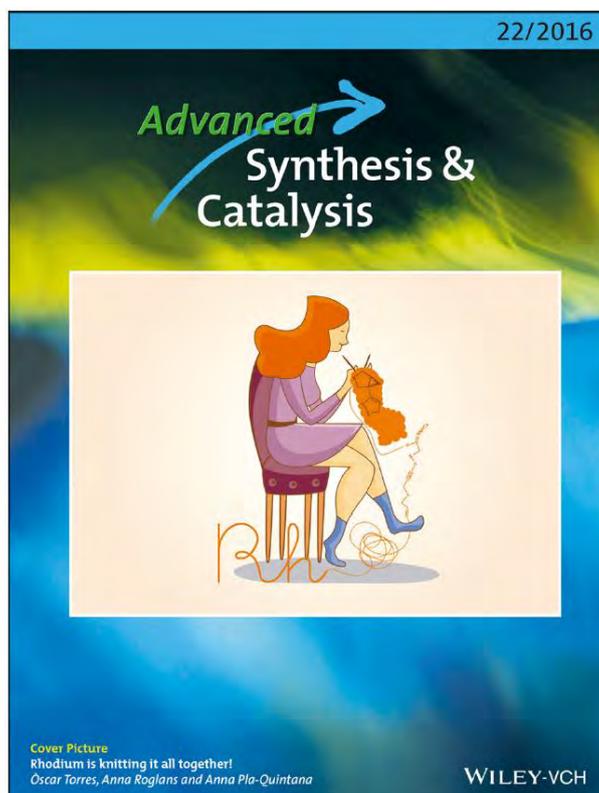
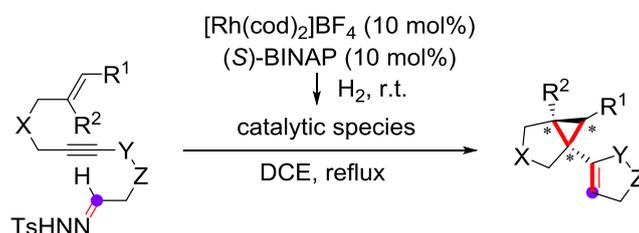
Scheme 3.22 Rhodium-catalysed cyclisation of the substrate **14**, which contains two internal alkynes.

Overall, we have described a new stereoselective cascade reaction that affords a sulfonated azacyclic framework through a process in which two C-C bonds are formed and both a hydrogen atom and a sulfonyl group migrate in a stereoselective manner. We propose, with the support of DFT calculations, that this mechanism, which has also been studied by competitive and isotope-labeling experiments, takes place through rhodium(I)-carbene intermediates and involves a metal-to-carbene migratory insertion step.

Chapter 4. Enantioselective cascade cyclopropanation reaction catalysed by rhodium(I): asymmetric synthesis of vinylcyclopropanes

This chapter has been published in:

Torres, Ò.; Roglans, A.; Pla-Quintana, A. *Adv. Synth. Catal.* **2016**, 358, 3512.



4.1. Precedents in the synthesis of vinylcyclopropanes

The construction of polycyclic structures with proper stereochemical control is a major challenge in organic synthesis. Among these structures, small ring-containing compounds – cyclopropane and cyclopropane-containing polycyclic derivatives – attract considerable interest due to their presence in bioactive substances.⁶⁴ This is the case of bicyclo[3.1.0] derivatives (Figure 4.1), which are found at the core of Eglumegad, a drug that is effective in treating anxiety symptoms and in relieving the symptoms of drug withdrawal,⁶⁵ and also of bicifadine and DOV21947, which are studied for the treatment of chronic pain and depression, respectively.⁶⁶ (-)-Nardoaristolone B, which exhibits protective activity in injuries of neonatal rat cardiomyocytes,⁶⁷ and (+)-Sarcandralactone A,⁶⁸ a vinylcyclopropane derivative, constitute further examples of compounds containing this moiety at the core.

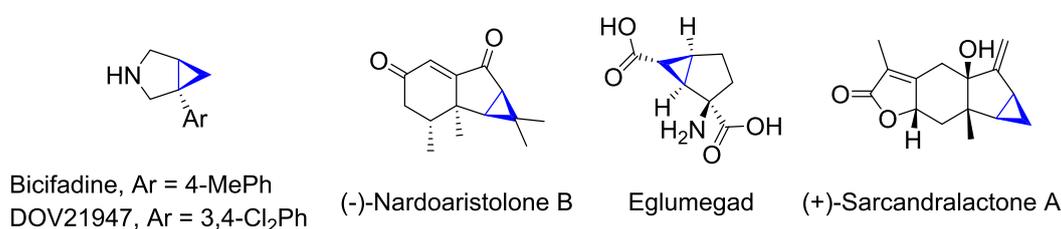
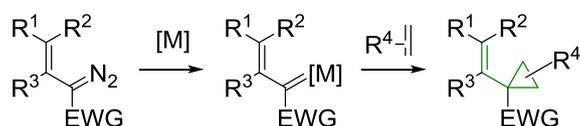


Figure 4.1 Examples of compounds containing a bicyclo [3.1.0]-hexane ring system.

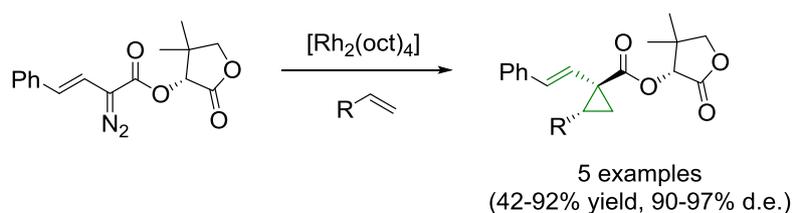
Cyclopropane-containing compounds are also recognised for their rich reactivity that, either through ring-opening or rearrangement, allow for the synthesis of a multitude of topologically different compounds.⁶⁹ The synthetic applications of cyclopropane-containing compounds are enhanced when the derivatives bear activating groups that can facilitate their ring-opening or offer opportunities for further transformations, as occur in the case of vinylcyclopropanes (VCP).⁷⁰

The asymmetric cyclopropanation of olefins stands out as one of the most versatile and straightforward methods for the stereoselective synthesis of cyclopropanes,⁷¹ and metal carbenes⁷² are among the most efficient cyclopropanating agents. When metal vinyl carbenes are used for this purpose, vinylcyclopropanes can be obtained directly (Scheme 4.1).



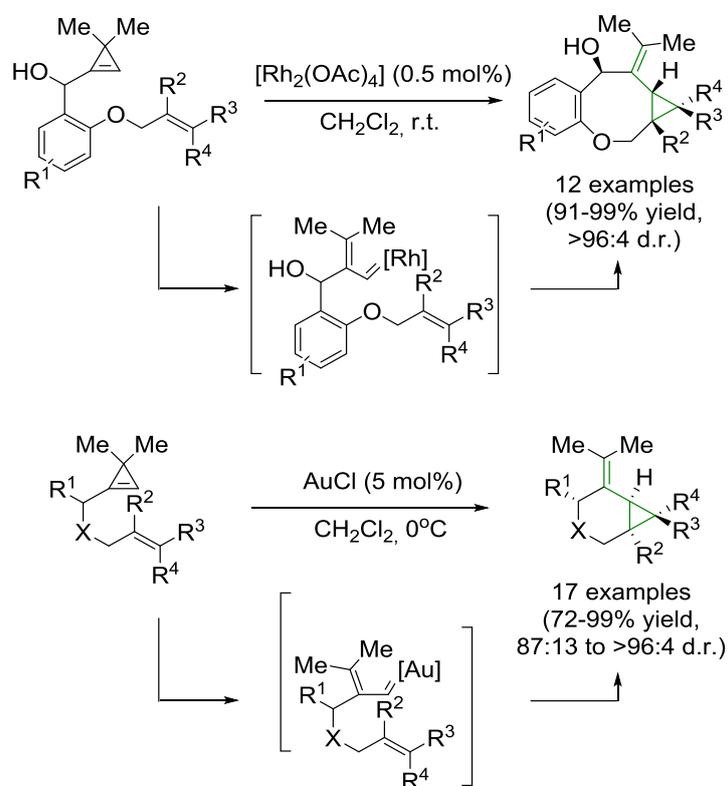
Scheme 4.1 Synthesis of vinylcyclopropanes by metal-catalysed vinyl diazo decomposition.

There are several examples in which the decomposition of vinyl diazo compounds has been used as a source of vinyl carbenes, which make enantioselective cyclopropanation reactions possible (Scheme 4.2).⁷³ This strategy has been used in the enantioselective synthesis of natural products.⁷⁴ However, an electron-withdrawing group adjacent to the diazo compounds is necessary to facilitate their synthesis, inhibit side reactions and achieve high stereoselectivity.



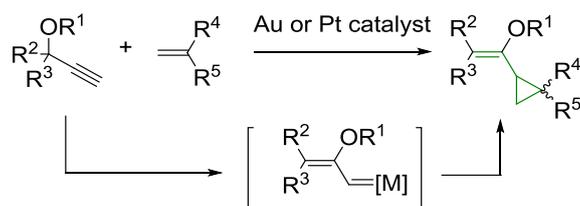
Scheme 4.2 Selected example of vinyl diazo compounds decomposition to afford vinylcyclopropanes.

Another strategy is to use transition metal-catalysed ring-opening of cyclopropenes to afford transition metal vinyl carbenes in mild conditions due to their intrinsic ring strain. When properly substituted cyclopropenes are reacted, regioselective ring-opening takes place. However, no enantioselective cyclopropanation has been achieved so far (Scheme 4.3).⁷⁵



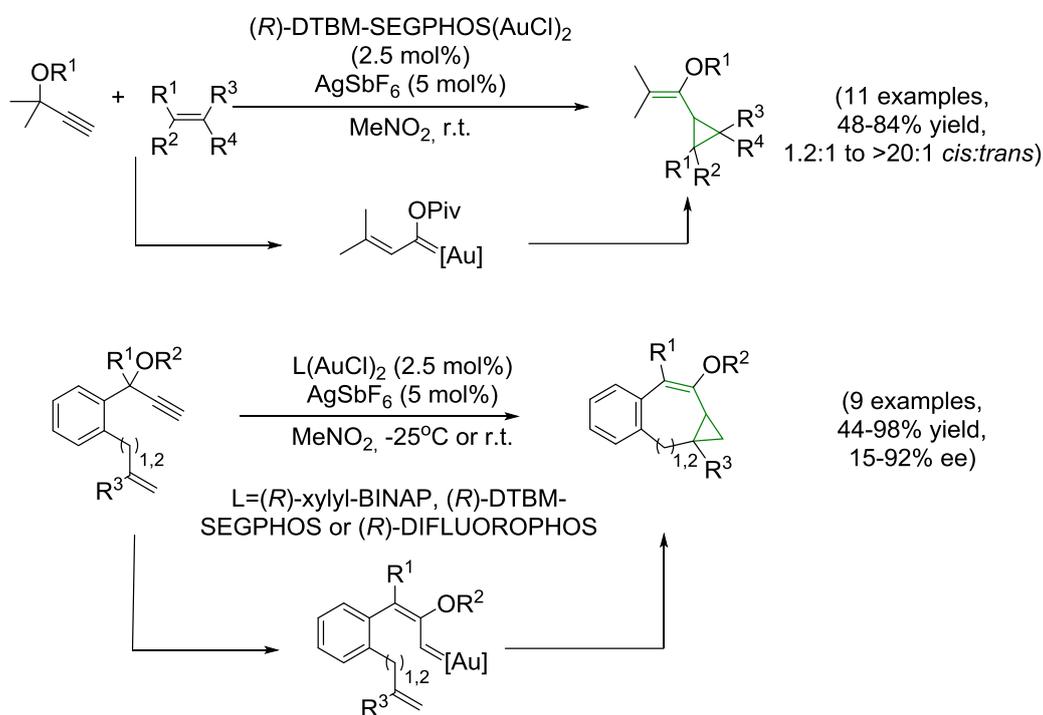
Scheme 4.3 Synthesis of vinylcyclopropanes by metal-catalysed ring-opening of cyclopropenes.

The transition metal-catalysed rearrangement of propargylic esters, providing access to metal vinyl carbenes when a *5-exo-dig* cyclisation takes place (also referred to as a 1,2-shift), has also been explored (Scheme 4.4).⁷⁶



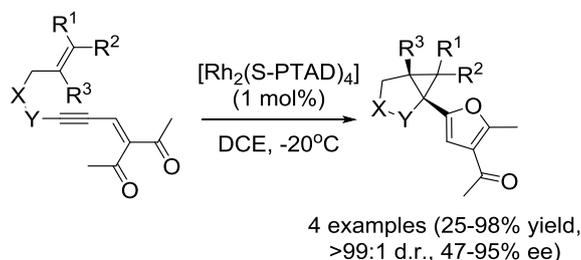
Scheme 4.4 Synthesis of vinylcyclopropanes by metal-catalysed rearrangement of propargylic esters.

Remarkably, Toste et al. reported the enantioselective synthesis of vinylcyclopropanes using a gold vinyl carbene generated by transition metal-induced rearrangement of a propargyl ester that either intra- or intermolecularly reacted with an alkene (Scheme 4.5).⁷⁷



Scheme 4.5 Selected examples of syntheses of vinylcyclopropanes by metal-catalysed rearrangement of propargylic esters.

Finally, very recently Zhu et al. managed to obtain furan-substituted bicyclic cyclopropanes in an enantioselective manner through the intramolecular cyclopropanation of enynones (Scheme 4.6).⁷⁸ It is important to highlight the fact that despite the formation of a cyclopropane ring, the reaction does not take place through a vinylcarbene intermediate. The rhodium carbene is formed after an initial intramolecular nucleophilic attack of the carbonyl to the C-C triple bond, which is promoted by the coordination of the transition metal. This strategy has been widely studied for the non-diazo approach to gold carbenes,⁷⁹ and has enabled different kinds of reactivity, including the formation of cyclopropanes.



Scheme 4.6 Enantioselective rhodium-catalysed intramolecular cyclopropanation of enynones.

4.2. Design and synthesis of the substrates 28

As outlined in Chapter 3, a rhodium(I) catalytic system has been found that is able to catalyse the carbene/alkyne metathesis and subsequent stereoselective transformations. Therefore, we established the main goal of this chapter as being the development of a stereoselective synthesis of vinylcyclopropanes through a cascade process involving the formation of a rhodium vinyl carbene through carbene/alkyne metathesis, followed by an intramolecular cyclopropanation reaction. In order to achieve this goal, 11 different ene-yne-*N*-tosylhydrazone substrates were designed (Figure 4.2) that allow us to analyse different features of the reaction: the effect of the tether (**28a** to **28g**), the formation of a 6-membered ring (**28h**) and how the substitution of the double bond affects the reactivity (**28i**, **28j** and **28k**).

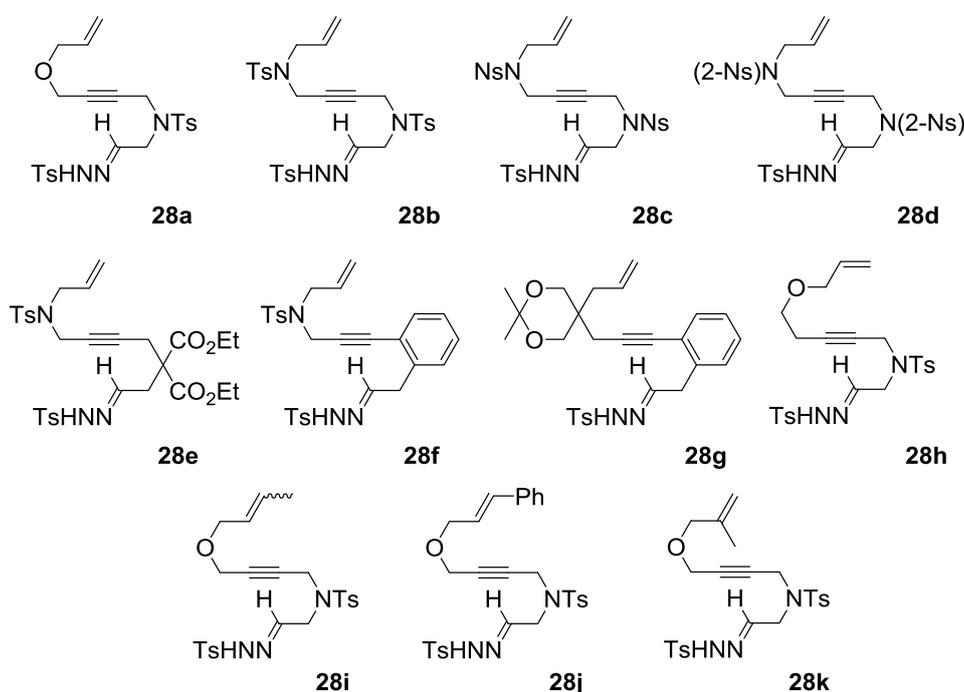
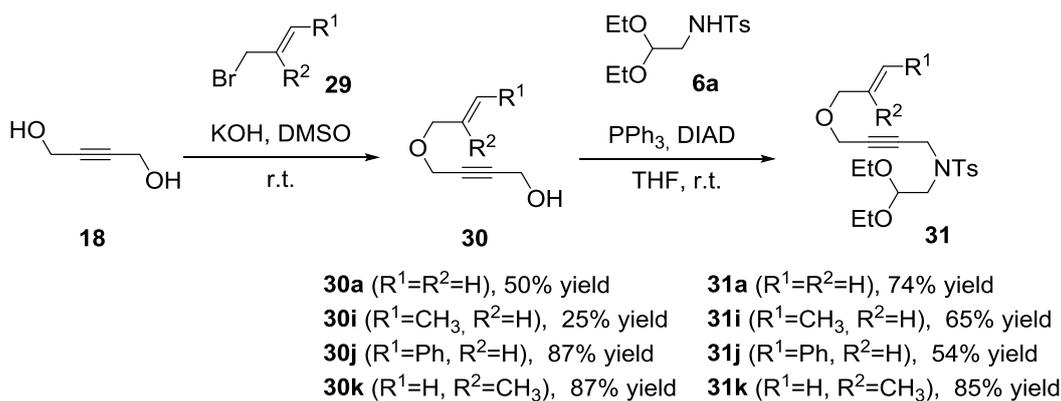


Figure 4.2 Substrates designed and tested in this study.

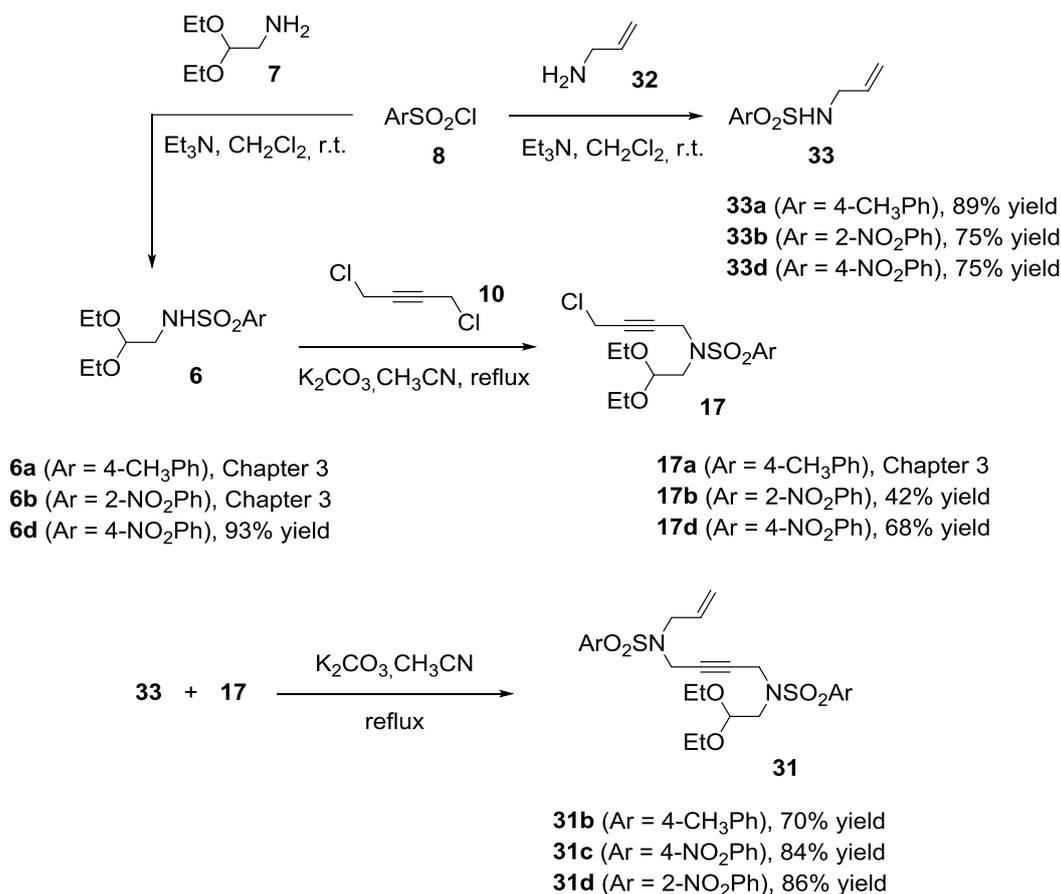
Except for compounds **28f** and **28g**, the strategy followed for the synthesis of the substrates was analogous to the one reported in Chapter 3. It consisted in the use of acetal derivatives as a protected form of aldehydes that at the end of the synthesis could be deprotected and coupled to the *N*-tosylhydrazide to form the corresponding *N*-tosylhydrazone. The synthesis of the different acetal protected derivatives will be presented first.

The synthesis of *O*-tethered derivatives **31** – as intermediates for the synthesis of substrates **28a**, **28i**, **28j** and **28k** – was started by alkylation of 1,4-butanediol **18** with the corresponding allylbromide **29** to afford compounds **30a,i-k**, which have already been described in the literature (Scheme 4.7).⁸⁰ Compound **30i** was obtained as an inseparable mixture of 1:9 *cis/trans* isomers as the commercial presentation of crotyl bromide (**29i**) is also a mixture. The next step consisted in a Mitsunobu reaction with the *N*-tosylprop-2-yn-1-amine **6a** prepared in Chapter 3. The reaction efficiently afforded compounds **31a**, **31i**, **31j** and **31k** in moderate to good yields.



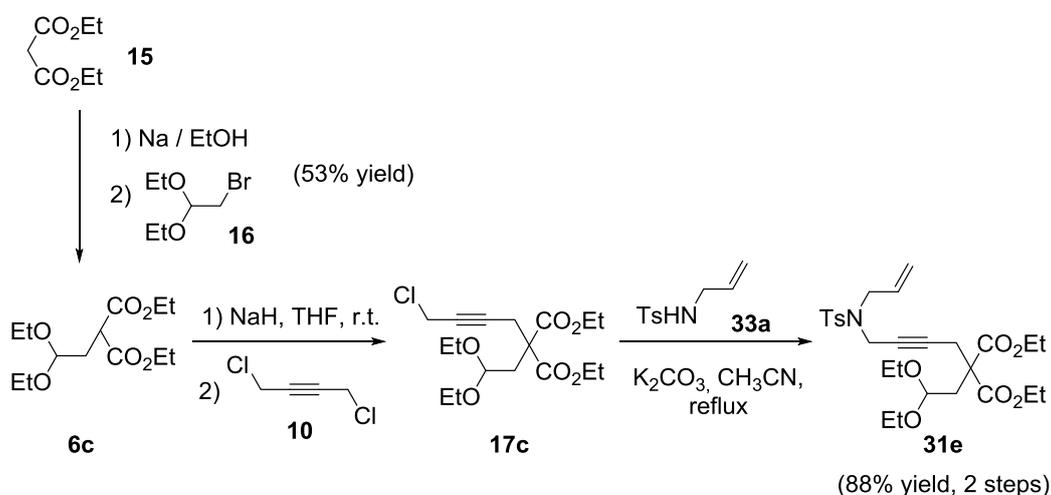
Scheme 4.7 Synthesis of O-tethered enyneacetals **31**.

NSO_2Ar -tethered compounds **31b-d** – intermediates for the synthesis of ene-yne-tosylhydrazone substrates **28b-d** – were prepared using a different arylsulfonylchloride **8**, as the common initial reagent, for each of the compounds. Monosubstituted sulfonamides **6** and **33** were obtained by condensation reaction of the arylsulfonylchloride with 2,2-diethoxyethanamine **7** or allylamine **32**, respectively. Sulfonamides **6** were monoalkylated by nucleophilic substitution using an excess of 1,4-dichloro-2-butyne **10** and potassium carbonate as the base with acetonitrile as the solvent. Compounds **32** and **17** were finally connected by nucleophilic substitution (Scheme 4.8). It should be noted that some of the compounds described in this synthetic route have been previously synthesised in Chapter 3.

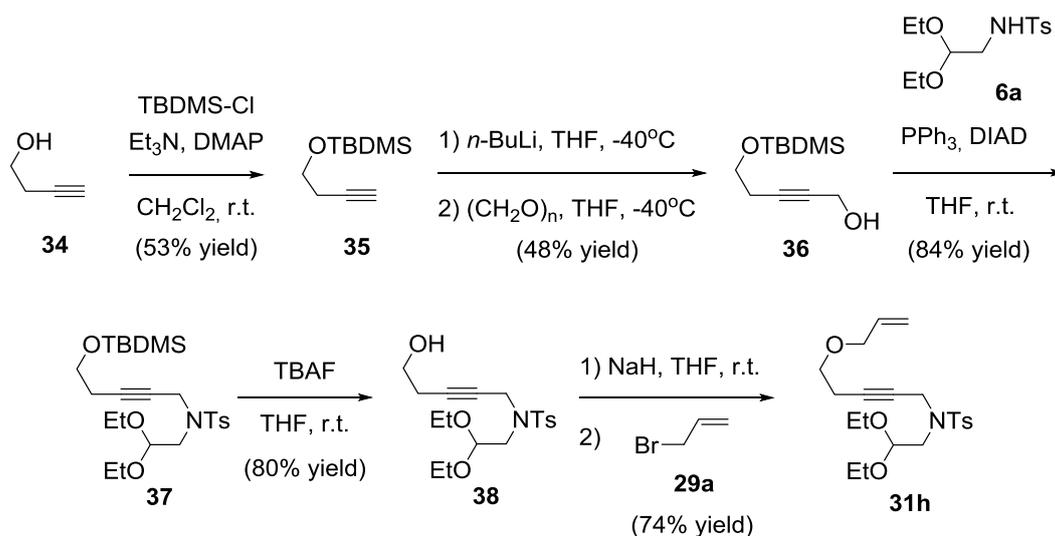


Scheme 4.8 Synthesis of NSO₂Ar-tethered compounds **31**.

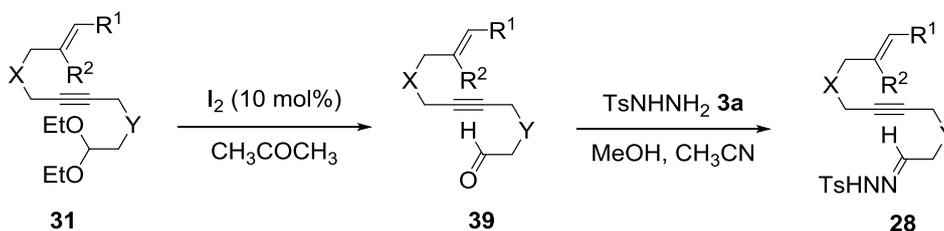
Similarly to Chapter 3, the synthesis of malonate tethered substrate **28e**, towards the synthesis of **31e**, was started with the formation of monoalkylated product **6c** (Scheme 4.9). The next step was the monosubstitution of 1,4-dichloro-2-butyne **10** with **6c** to obtain **17c**. Although an excess of 1,4-dichloro-2-butyne **10** was used to avoid the disubstitution in the nucleophilic substitution, **17c** was obtained as an inseparable mixture with small amounts of the disubstituted compound. The subsequent alkylation was performed with this mixture to afford a mixture of **31e** and the disubstituted compound, which could be separated by column chromatography. An 88% yield of derivative **31e** was isolated after two reaction steps.

**Scheme 4.9** Synthesis of malonate-tethered **31e**.

The synthesis of an ene-yne-acetal derivative **31h** with an extra methylenic group, followed a pathway analogous to the one depicted in Scheme 4.7, but required the protection of one of the alcohols to differentiate between the two inequivalent alcohol groups (Scheme 4.10). But-3-yn-1-ol **34** was protected using the TBDMS group to afford a 53% yield of compound **35**. The terminal hydrogen was then removed using *n*-BuLi as the base and the resulting organometallic intermediate was used as a nucleophile towards formaldehyde to obtain a 48% yield of 5-(*tert*-butyldimethylsilyloxy)-2-pentyn-1-ol **36**, whose spectroscopic data agrees with those described in the literature.⁸¹ Mitsunobu reaction was used to alkylate **6a** (previously prepared in Chapter 3) with alcohol **36** to obtain derivative **38** in an 84% yield. The TBDMS-protected alcohol was then deprotected using TBAF in THF affording an 80% yield of compound **38**. Finally, a nucleophilic substitution of the alcohol to allylbromide allowed the formation of compound **31h** in a 74% yield.


Scheme 4.10 Synthesis of compound **31h**.

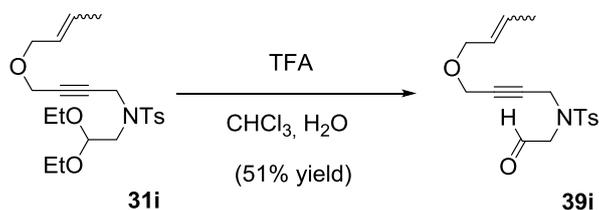
The last two steps, which consisted in the deprotection of the aldehyde and the formation of the *N*-tosylhydrazones, were carried out as previously explained in Chapter 3, affording compounds **28** (Table 4.1).

Table 4.1 Synthesis of enyne-*N*-tosylhydrazones **28** from enyneacetals **31**.


Acetal	Aldehyde (yield)	X	Y	R ¹	R ²	28 (yield)
31a	39a (69%)	O	NTs	H	H	28a (63%)
31b	39b (60%)	NTs	NTs	H	H	28b , (93%)
31c	39c (45%)	NNs	NNs	H	H	28c (100%)
31d	39d (41%)	N(2-Ns)	N(2-Ns)	H	H	28d (100%)
31e	39e (86%)	NTs	C(CO ₂ Et) ₂	H	H	28e (87%)
31h	39h (n.d.)	OCH ₂	NTs	H	H	28h (59%)
31i	39i (51%)	O	NTs	CH ₃	H	28i (87%)
31j	39j (15%)	O	NTs	Ph	H	28j (91%)
31k	39k (51%)	O	NTs	H	CH ₃	28k (82%)

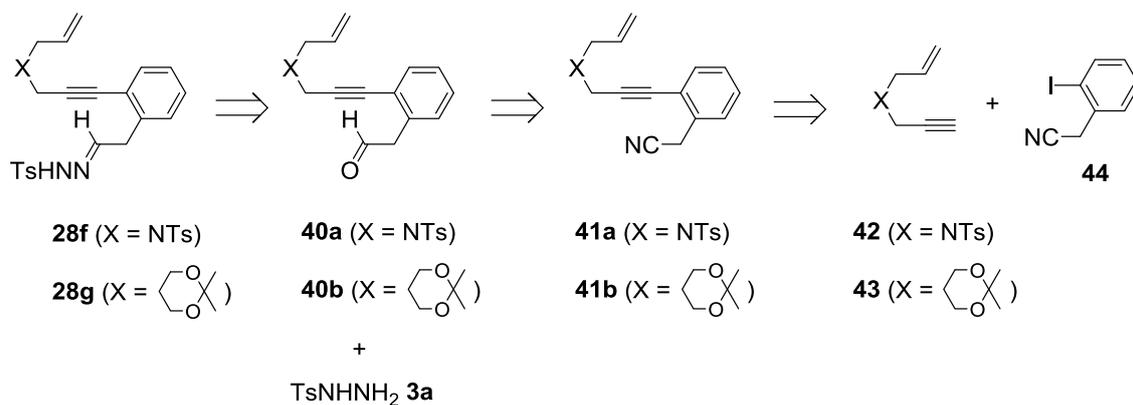
In the particular case of the deprotection of compound **31h**, **39h** could not be isolated in a pure form and was further reacted with the *N*-tosylhydrazide to afford compound **28h** with an overall 59% yield.

On the other hand, considering the low yield obtained for substrate **39j** in which the alkene was substituted, we decided to change the deprotection conditions. The use of trifluoroacetic acid in chloroform:water solvent mixture gave compound **31i** with an improved 51% yield (Scheme 4.11).



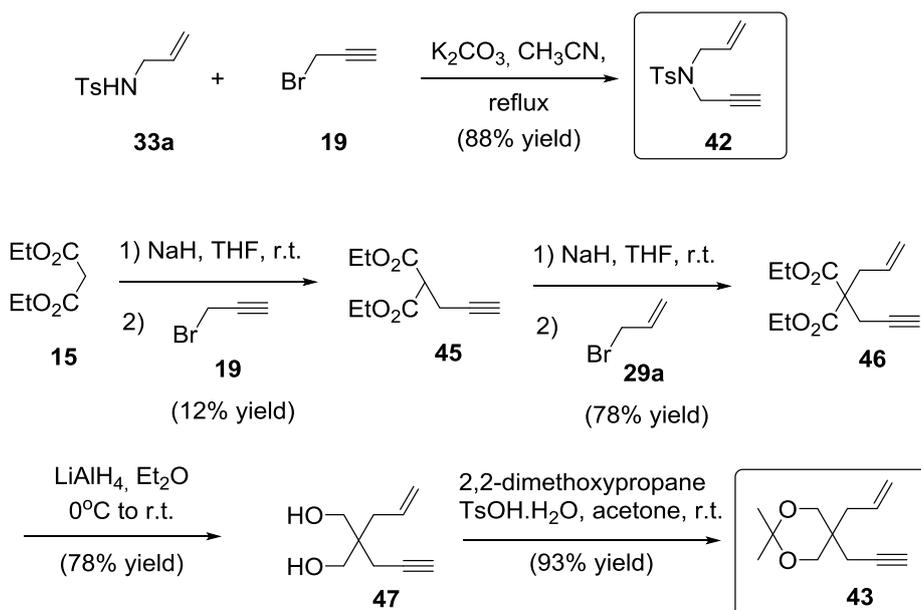
Scheme 4.11 Synthesis of aldehyde **39i**.

The retrosynthetic analysis of substrates **28f** and **28g** was planned by obtaining aldehyde **40** by the reduction of the ene-yne-cyano derivative **41** (Scheme 4.12). The latter can be obtained by a Sonogashira coupling between ene-yne compounds **42** or **43** and commercially available 2-iodophenylacetonitrile **44**.

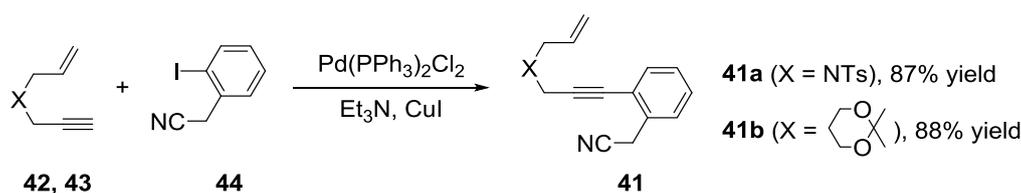


Scheme 4.12 Retrosynthetic analysis of compounds **28f** and **28g**.

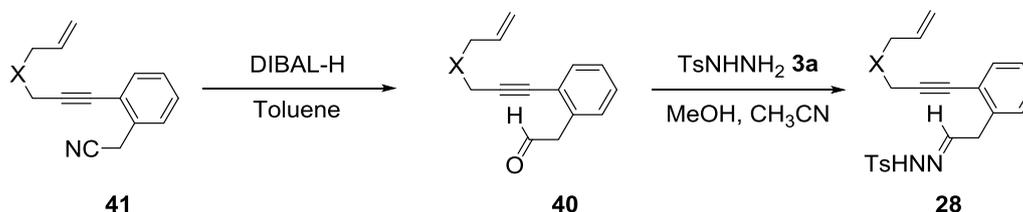
Ene-yne compounds **42** and **43** were prepared according to previously published procedures depicted in Scheme 4.13.⁸² Ene-yne derivative **42** was obtained by nucleophilic substitution of monosubstituted sulphonamide **33a** and propargyl bromide **19**. On the other hand, diethylmalonate **15** was first monoalkylated with propargyl bromide with a low yield because dialkylated derivative was also obtained. Dialkylated diethylmalonate **46** was then obtained by alkylation with allylbromide **29a**. The ester from tether group were reduced using lithium aluminium hydride with good yields and the resulting alcohols were converted to the corresponding acetal **43** form to avoid undesired reactions in further steps.


Scheme 4.13 Synthesis of enynes **42** and **43**.

These compounds were further reacted in a Sonogashira coupling with 2-iodophenylacetonitrile **44** to obtain phenyl-tethered ene-yne-cyano compounds **41a** and **41b** in 87 and 88% yields, respectively (Scheme 4.14).


Scheme 4.14 Synthesis of phenyl-tethered compounds **41a** and **41b**.

In this case, the aldehyde was obtained by the reduction of nitrile groups using diisobutylaluminum hydride in toluene. Compounds **40a** and **40b** were obtained with 30% and 35% yields, respectively (Scheme 4.15). Finally, the coupling with tosylhydrazide afforded the targeted ene-yne-*N*-tosylhydrazones **28f** and **28g**. Purification difficulties in the latter substantially dropped its yield.

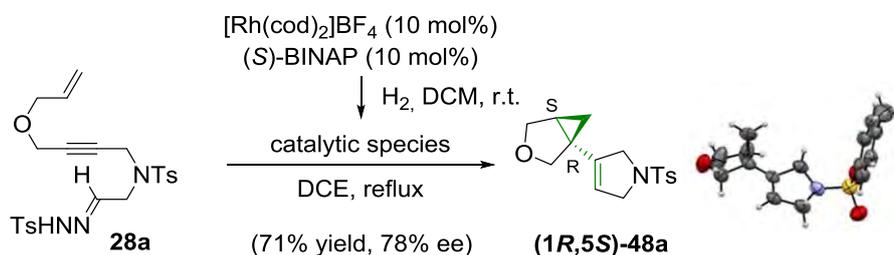


X	Nitrile	Aldehyde (yield)	Ene-yne- <i>N</i> -tosylhydrazone (yield)
NTs	41a	40a (30%)	28f (87%)
	41b	40b (35%)	28g (22%)

Scheme 4.15 Synthesis of phenyl-tethered *N*-tosylhydrazones **28f** and **28g**.

4.3. Reactivity studies

After the preparation of the substrates, we initially studied the cyclisation of substrate **28a** under the same conditions that triggered the cascade reaction in Chapter 3 (Scheme 3.17). In this case, the reaction worked efficiently affording a 71% yield of vinylcyclopropane **48a** with a 78% of enantiomeric excess (Scheme 4.16). As observed in our previous study, it is remarkable that the reaction works without the need to add a base to activate the *N*-tosylhydrazone. After considerable effort, single crystals of the cycloadduct were obtained from which the solid phase structure was solved and the absolute configurations (1*R*,5*S*) of the stereocentres were determined.⁸³ When the atropisomeric ligand of the rhodium was changed to (*R*)-BINAP, a 55% yield of (**1*S*,5*R***)-**48a** was isolated with an 89% enantiomeric excess.



Scheme 4.16 Rhodium-catalysed cyclisation of enyne *N*-tosylhydrazones **28a**.

The crystallised product corresponds to the major enantiomer of the sample as has been checked by chiral HPLC analysis upon injection of the crystallised (**1*R*,5*S***)-**48a** (Figure 4.3, top-left), comparing the chromatogram with the racemic mixture (Figure 4.3, top-right) and with the racemic mixture fortified with the crystallised sample (Figure 4.3, bottom).

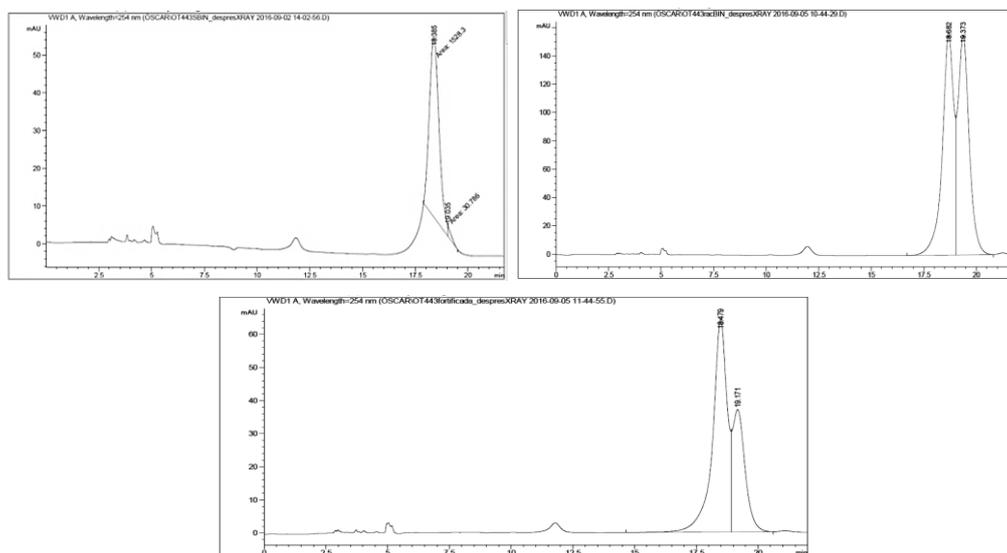
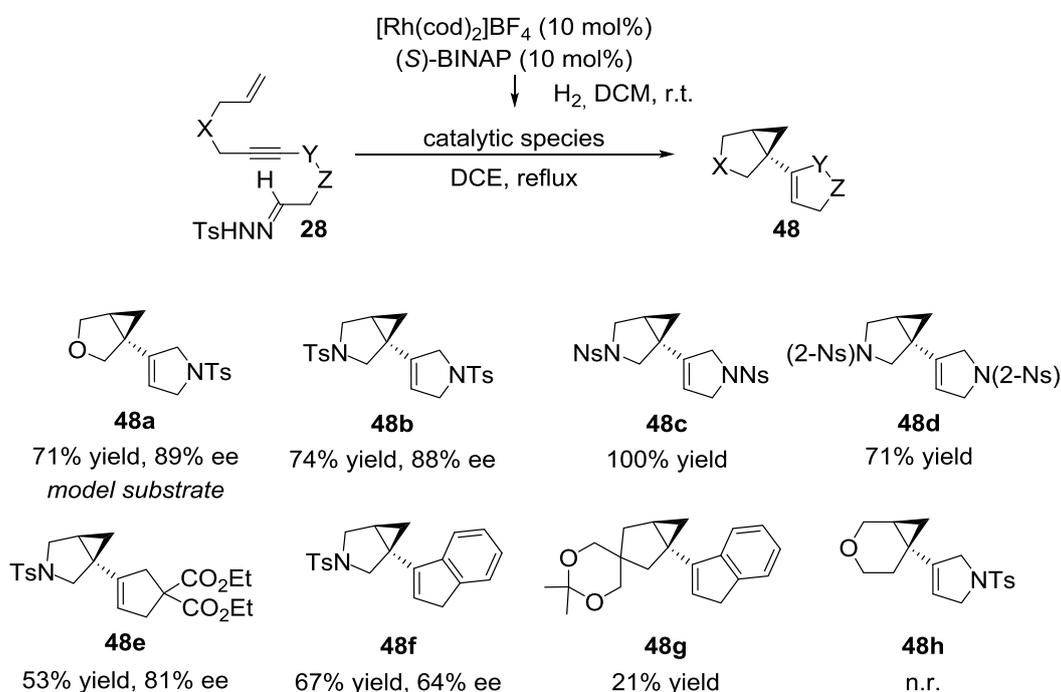


Figure 4.3 HPLC chromatogram of the crystallised **48a** (top-left), the racemic mixture (top-right) and the fortified sample mixing the racemic mixture and the crystallised sample (bottom).

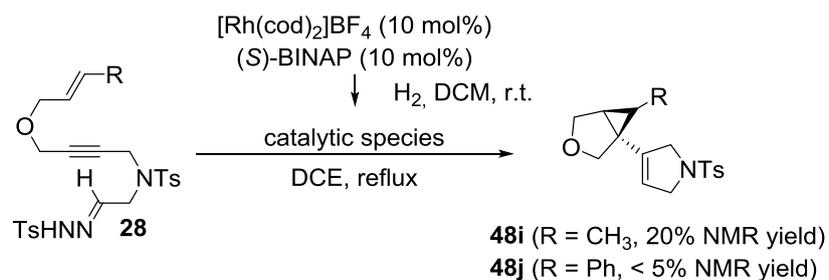
The reaction was then extended to substrates **28b-f**, which differ in the units tethering the different reactive moieties (Scheme 4.17). Substrates containing sulfonamide tethers, in both X and Z positions (**28b-d**), were successfully reacted under the cyclisation reaction conditions giving the cycloadducts in

good yields. Whereas the vinylcyclopropanes containing NTs tethers could be efficiently characterised, the low solubility of both the 4-nitrobenzenesulfonyl (Ns) **48c** and 2-nitrobenzenesulfonyl (2-Ns) **48d** tethers prevented the determination of the enantiomeric excess of the products obtained. A malonate tether was also introduced between the hydrazone and the alkyne and the cyclised product **48e** was obtained with moderate yield but high enantiomeric excess. By the reaction of substrates that feature a phenyl ring between the alkyne and the toluenesulfonylhydrazone, indenyl-substituted bicyclo[3.1.0] derivatives were also available. In the case that an NTs tether was placed in the enyne moiety, the cyclised product **48f** was efficiently obtained. When this moiety was linked through a cyclic ketal (2,2-dimethyl-1,3-dioxane), the reaction to provide product **48g** was only moderately efficient. Finally, on increasing the tether length in the enyne moiety no reaction was observed, as has also been the case in other studies.⁸⁴ The absolute stereochemistry of all the products shown in Scheme 4.17 was assigned by analogy with product **48a**.



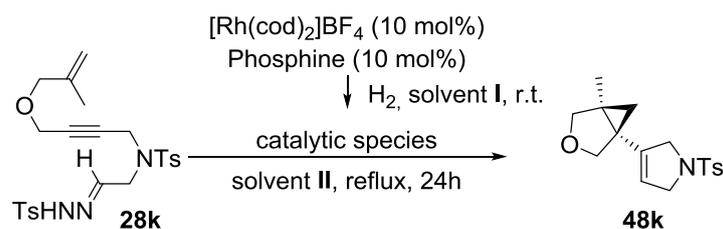
Scheme 4.17 Scope of the rhodium(I)-catalysed cyclisation of enyne *N*-tosylhydrazones **28**.

The substituents on the alkene group markedly affect the outcome of the carbene/alkyne metathesis-cyclopropanation sequence. When substrates **28i** and **28j**, which feature a *trans*-1,2-disubstituted alkene, were subjected to the reaction conditions, the efficiency of the reaction drastically dropped and only low quantities (**48i**) or traces (**48j**) of the corresponding vinylcyclopropanes were detected by NMR in the crude reaction mixture that contained a considerable amount of by-products (Scheme 4.18).



Scheme 4.18 Rhodium(I)-catalysed cyclisation of enyne *N*-tosylhydrazones **28i** and **28j**.

Reactivity of substrate **28k**, which has a 1,1-disubstituted alkene, was then evaluated. Only a 29% yield of vinylcyclopropane **48k** was isolated under the reaction conditions used for the unsubstituted alkenes, although with good enantioselectivity (Entry 1, Table 4.2). Since the reaction in this case was quite clean, we decided to optimize the reaction conditions. To begin with, the effect of an added base was evaluated (Entry 2) but on adding three equivalents of potassium carbonate to the reaction mixture only traces of the cyclised compound were formed. The reaction solvent was then switched to 1,2-dichloropropane (1,2-DCP) to increase the temperature but this resulted in a decrease in both the yield and the enantioselectivity (Entry 3).

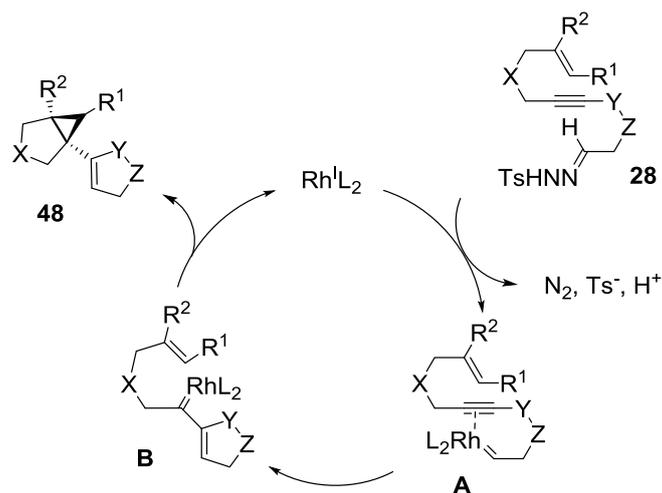
Table 4.2 Optimisation of the rhodium(I)-catalysed cyclisation of the compound **28k**.

Entry	Solvent I	Phosphine	Solvent II	Yield	ee
1	DCM	(<i>S</i>)-BINAP	DCE	29%	71%
2 ^[a]	DCM	(<i>S</i>)-BINAP	DCE	< 5%	n.d.
3	DCM	(<i>S</i>)-BINAP	1,2-DCEP	14%	53%
4	CH ₃ OH	(<i>S</i>)-BINAP	DCE	63%	74%
5	CH ₃ OH	(<i>R</i>)-H ₈ -BINAP	DCE	49%	73%
6	CH ₃ OH	(<i>R</i>)-DTBM-SEGPHOS	DCE	37%	23%
7 ^[b]	CH ₃ OH	(<i>S</i>)-BINAP	CH ₃ OH	73%	46%

[a] Reaction run with K₂CO₃ (3 equiv.). [b] The reaction was run for 1h 30m.

In these reactions, the catalytically active species are generated in situ by hydrogenation of a mixture of the cationic diolefin complex [Rh(cod)₂]BF₄ and the biphosphine in dichloroethane. Heller et al. have shown that the solvent in which this hydrogenation is carried out is crucial in determining the catalytically active species that are formed and their reactivity.⁸⁵ Given this, we decided to test the reaction with catalytically active species generated in methanol. To our delight, vinylcyclopropane **48k** was obtained in a much improved 63% yield and with a 74% ee (Entry 4). Other biphosphine ligands were then evaluated. Whereas H₈-BINAP was selective but less active in the cascade transformation developed (Entry 5), DTBM-SEGPHOS provided the product in lower yield and enantioselectivity (Entry 6). Finally, a reaction was run in which methanol was used as the solvent both in the activation of the catalyst and the cyclisation. This reaction gave vinylcyclopropane **48k** in a 73% yield in just 1.5 hours of reaction, but the enantioselectivity was considerably reduced (Entry 7). Best results are thus obtained by activating the catalyst in methanol whilst performing the reaction in DCE (Entry 4). These optimised conditions were tested in the reaction of selected substrates **28**, but the reactions were not improved.

Scheme 4.19 outlines the proposed catalytic cycle for this cascade reaction. The formation of the catalytic species from the cationic rhodium complex and the (*S*)-BINAP mixture precedes the formation of the rhodium carbene **A**. The *p*-methylphenylsulfonyl group is recovered at the end of the reaction as *p*-toluene-sulfoxy-*p*-toluenesulfonate, which has been already characterised.⁸⁶ The rhodium carbene then reacts with the alkyne in a carbene/alkyne metathesis process to afford the rhodium vinyl carbene **B** that intramolecularly cyclopropanates the tethered alkene in an enantioselective manner to furnish the chiral vinylcyclopropane **48** and recover the catalytic species.

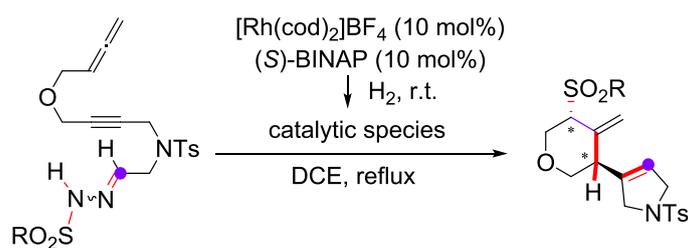


Scheme 4.19 Proposed mechanism for the rhodium-catalysed cyclisation reaction.

Therefore, in this Chapter 4 we have demonstrated that the chiral cationic rhodium(I) catalytic system is able to induce the formation of a rhodium carbene under base-free conditions, and catalyse the carbene/alkyne metathesis and enantioselective cyclopropanation cascade that enantioselectively forms vinylcyclopropanes. When 1,1-disubstituted olefins were reacted the cyclopropanation was more difficult. The use of methanol to hydrogenate the diolefin complex $[\text{Rh}(\text{cod})_2]\text{BF}_4$ and the biphosphine was crucial to improve the yield. The generation of methanol coordinated rhodium species facilitated the cyclopropanation, presumably stabilizing crucial reaction intermediates.

Chapter 5. Unusual reactivity of rhodium(I) carbenes with allenes: an efficient asymmetric synthesis of methylenetetrahydropyran scaffolds

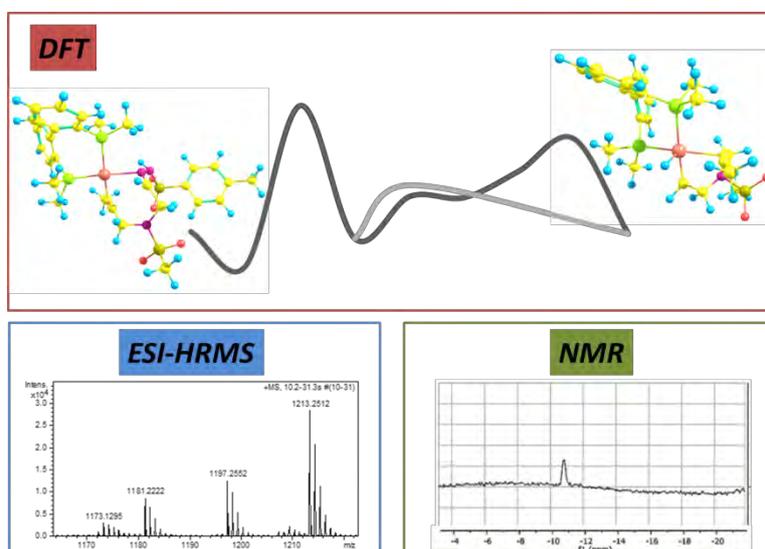
Torres, Ò.; Solà, M.; Roglans, A.; Pla-Quintana, A. *Submitted*.



Embargoed until publication

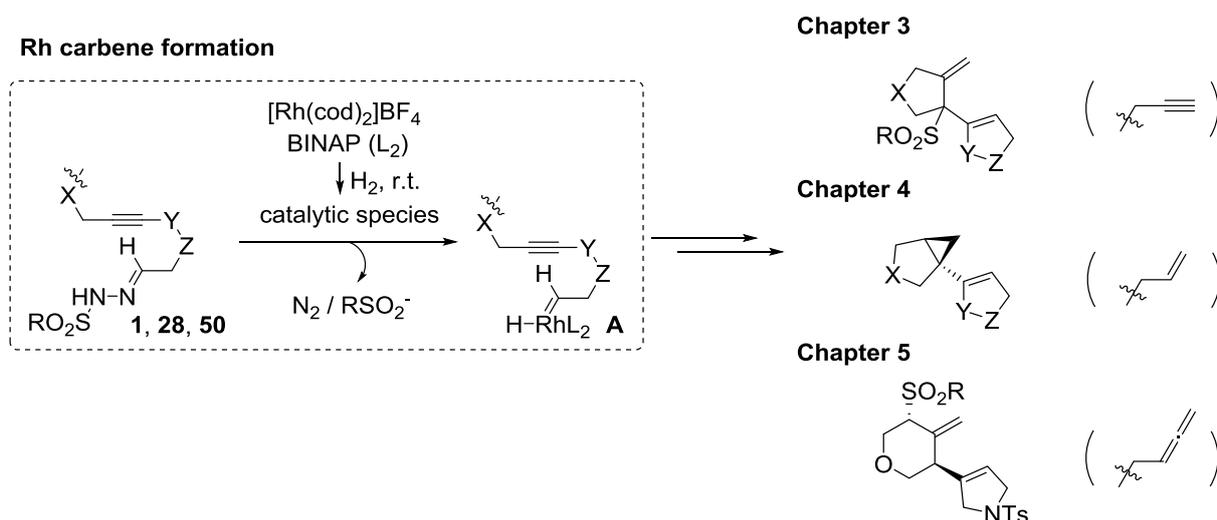
Torres, Ò.; Solà, M.; Roglans, A.; Pla-Quintana, A. "Unusual reactivity of rhodium(I) carbenes with allenes: an efficient asymmetric synthesis of methylenetetrahydropyran scaffolds". Manuscript submitted for publication

Chapter 6. Mechanistic insights into rhodium-carbene formation



6.1. Precedents in the mechanistic study of rhodium-carbene formation

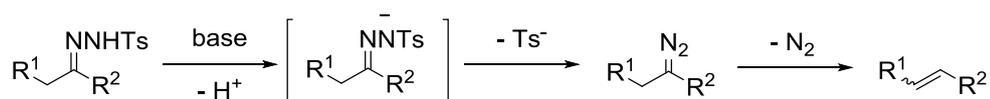
During the previous chapters of this thesis we have explained the development of three enantioselective rhodium donor carbene-mediated cascade reactions, all of which are triggered by a base-free decomposition of sulfonylhydrazones **1**, **28** and **50** (Scheme 6.1).



Scheme 6.1 Rhodium carbene cascade reactions obtained in Chapters 3, 4 and 5.

In all the processes, the catalytically active species were generated by mixing a rhodium(I) source and the BINAP ligand (L_2) before hydrogenating the whole mixture. Our hypothesis was that the three processes start similarly, by the formation of rhodium carbene species **A**. Despite having studied the mechanism of the reactions in Chapters 3 and 5 both experimentally and theoretically, the initial formation of the rhodium carbene had not been explored in detail.

As mentioned in the Introduction, *N*-tosylhydrazones have long been used as a source of diazo compounds by decomposition in the presence of a base, a process known as a Bamford-Stevens reaction (Scheme 6.2). The process involves an initial deprotonation followed by a *p*-toluenesulfinate anion dissociation. Diazo compounds can be isolated if mild temperatures ($< 60\text{ }^\circ\text{C}$) are employed, however, in most examples, the diazo compound thermally decomposes to form alkenes by loss of dinitrogen followed by a 1,2-hydrogen shift.



Scheme 6.2 Bamford-Stevens reaction.

When the decomposition is carried out in the presence of a metal that can trap the diazo compound, a metal carbene complex can be isolated. The formation of this metal carbene in the presence of rhodium(II) complexes has been studied, since rhodium(II) carbene complexes have been given a

wide range of applications in synthetic organic chemistry in recent decades, as detailed in Chapter 1. This mechanism has been postulated as taking place in two steps: the formation of a diazonium ion intermediate by complexation of the negatively polarised carbon of the diazo compound to the rhodium(II) complex (detected by optical spectroscopy and NMR),¹⁰⁴ and the irreversible extrusion of N₂, which is considered to be the rate-limiting step. Kinetic studies,¹⁰⁵ the observation of a negative Hammett ρ value for a series of substituted α -diazophenylacetate substrates¹⁰⁶ as well as computational studies¹⁰⁷ provides support for the proposed mechanism.



Scheme 6.3 Postulated mechanism for the formation of metal carbenes from diazocompounds.

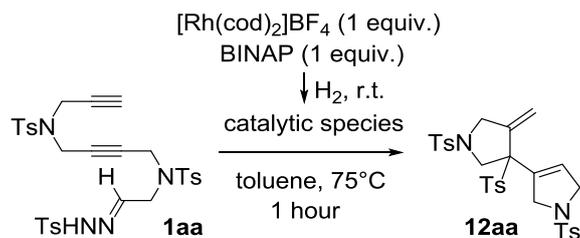
However, to the best of our knowledge, no reported studies have analysed the formation of metal carbene compounds directly from the *N*-tosylhydrazone in base-free conditions, as is the case of the methodologies that we have developed. Therefore, the aim of this last part of the thesis is to study this step in detail, attempting to resolve two doubts. Firstly, whether or not Rh-H intermediates are involved in the catalytic cycles that are postulated, and, secondly, why the use of a base is not necessary to obtain such reactivity and whether rhodium plays some role in this.

In Chapter 6 we will obtain further insights into the reaction mechanism through the use of experimental techniques such as NMR and ESI-HRMS combined with computational studies.

6.2. NMR studies

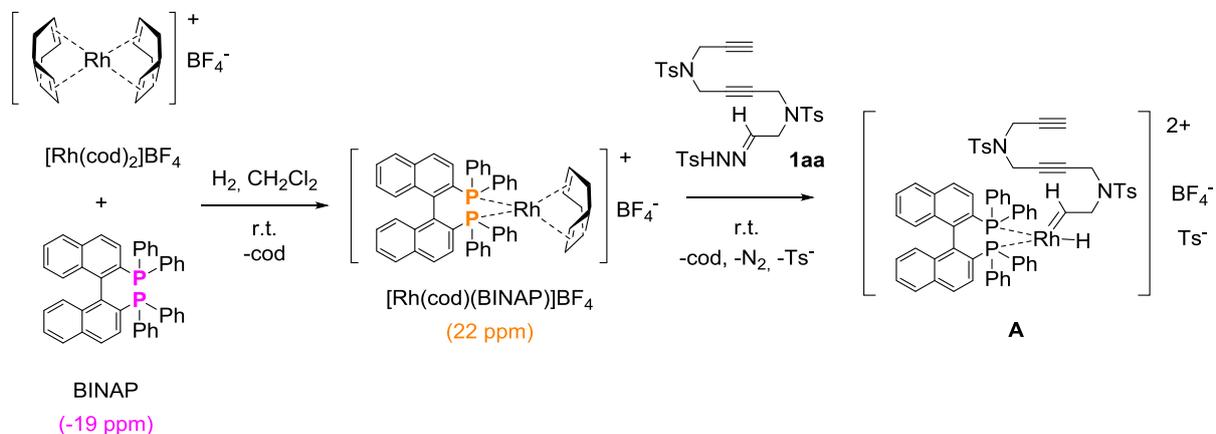
In a first step we wanted to detect the Rh-H species that were postulated in the mechanistic studies in Chapters 3 and 5. To this end, we collaborated with Prof. Luca Gonsalvi from the Consiglio Nazionale delle Ricerche (CNR), where I was able search for these Rh-H species by NMR spectroscopy.

Although the reaction conditions in the carbocyclisation reactions from Chapters 3, 4 and 5 are optimised with dichloroethane as a solvent, we wanted to test whether these reactions were also efficient using toluene, since its substantially lower melting point might enable the detection of the Rh-H NMR signal at lower temperatures. For this study we used the substrate bearing two alkynes and the *N*-tosylhydrazone **1aa** from Chapter 3 due to its stability and solubility in toluene and we run a reaction with a combination of BINAP and [Rh(cod)₂]BF₄, previously activated by bubbling H₂. The experiment showed that the cyclisation also takes place in toluene. We therefore decided to carry out the NMR study using a toluene solution with **1aa** and an equimolar mixture of the substrate and the catalyst in order to increase the concentration of the reactive intermediate species (Scheme 6.4).



Scheme 6.4 Rhodium-catalysed cyclisation studied by NMR.

The purpose of the first set of experiments was to verify the formation of the complex $[\text{Rh}(\text{cod})(\text{BINAP})]\text{BF}_4$ from the precursor $[\text{Rh}(\text{cod})_2]\text{BF}_4$ and BINAP and the role of hydrogen gas in this step (Scheme 6.5). An equimolar mixture of $[\text{Rh}(\text{cod})_2]\text{BF}_4$ and BINAP was dissolved in the minimum amount of CH_2Cl_2 and diluted with toluene- d_8 . The $^{31}\text{P}\{^1\text{H}\}$ NMR spectrum run at 293 K showed a partial formation of complex $[\text{Rh}(\text{cod})(\text{BINAP})]\text{BF}_4$, as shown by the presence of a doublet centred at ca. 22 ppm ($^1J_{\text{RhP}} = 145$ Hz) and a singlet at -19 ppm corresponding to the uncomplexed BINAP (Figure 6.1, 1). The tube was then removed and H_2 gas (1 atm) was bubbled through the solution for 30 minutes at room temperature. After this hydrogenation step, the sample was analysed again (Figure 6.1, 2). The signal due to the free ligand (-19 ppm, singlet) disappeared, suggesting complete formation of the $[\text{Rh}(\text{cod})(\text{BINAP})]\text{BF}_4$ complex. Another doublet, which could correspond to a $[\text{Rh}(\text{BINAP})_2]^+$ complex, centred at ca. 43 ppm ($^1J_{\text{RhP}} = 205$ Hz) appeared at a low intensity. No changes were observed when adding substrate **1aa** to the catalytic mixture at room temperature (Figure 6.1, 3) and no signals were observed in the negative ^1H NMR range under these conditions.



Scheme 6.5 Reactions observed in the NMR experiment.

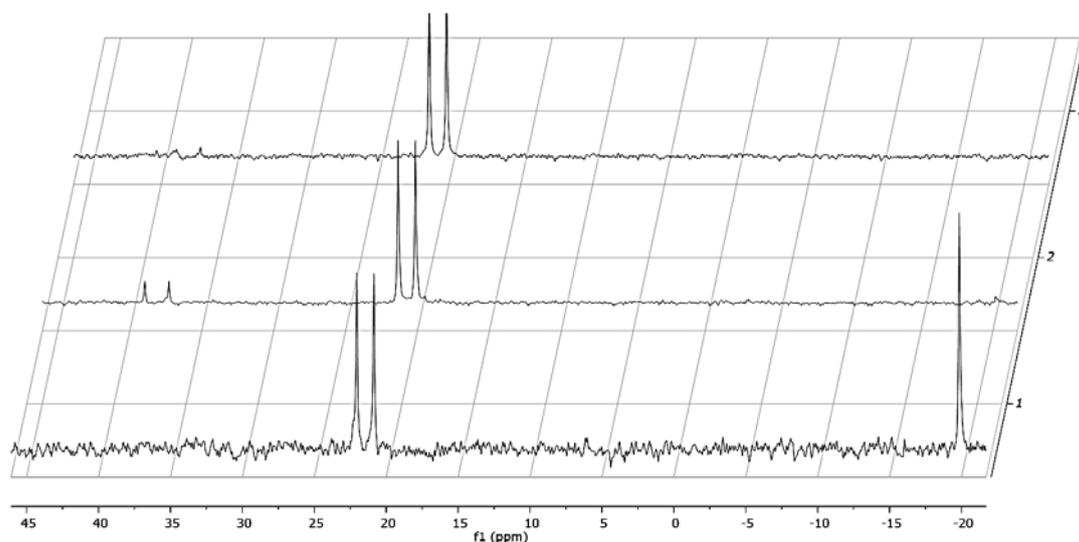


Figure 6.1 $^{31}\text{P}\{^1\text{H}\}$ NMR (101 MHz, 293 K, toluene- d_8 : $\text{CH}_2\text{Cl}_2 = 1:0.08$) of a mixture of $[\text{Rh}(\text{cod})_2]\text{BF}_4$ (1.1 equiv.) and BINAP (1.0 equiv.). (1) Before bubbling H_2 gas (1 atm); (2) after bubbling H_2 at room temperature for 30 minutes; (3) after addition of the *N*-tosylhydrazone **1aa** at room temperature.

A second set of experiments was aimed at monitoring the changes in ^1H and $^{31}\text{P}\{^1\text{H}\}$ NMR under the reaction conditions with the aim of detecting Rh-H signals. An equimolar mixture of $[\text{Rh}(\text{cod})_2]\text{BF}_4$ and BINAP was dissolved in CH_2Cl_2 and bubbled with H_2 for 30 minutes. It was then evaporated to dryness and toluene- d_8 was added. A few drops of CH_2Cl_2 were added to increase the solubility. Once the complete formation of $[\text{Rh}(\text{cod})(\text{BINAP})]\text{BF}_4$ complex was checked by $^{31}\text{P}\{^1\text{H}\}$ NMR spectroscopy, the *N*-tosylhydrazone **1aa** was added at room temperature. The NMR tube was then heated to 75 °C for ca. 5 minutes in an oil bath and the tube was then placed back into the NMR probe. $^{31}\text{P}\{^1\text{H}\}$ NMR and ^1H NMR spectrum were run initially at 293 K only showing the presence of the $[\text{Rh}(\text{cod})(\text{BINAP})]\text{BF}_4$ complex (Figure 6.2, bottom). However, when the temperature of the probe was decreased to 253 K, a broad singlet at ca. -10 ppm was observed in the ^1H NMR spectrum (Figure 6.2, top), which probably corresponded to the formation of a Rh-H bond, in agreement with the proposed mechanism (Scheme 6.5). In the corresponding $^{31}\text{P}\{^1\text{H}\}$ NMR spectrum, a mixture of $[\text{Rh}(\text{cod})(\text{BINAP})]\text{BF}_4$ and the unidentified complex (43 ppm, $^1J_{\text{RhP}} = 205$ Hz) observed before was obtained. According to the proposed mechanism (Figure 3.12 and Scheme 3.21), this signal might correspond to a single Rh-H species (i.e. intermediates **A** to **E** in Figure 3.12) or a mixture thereof. A mixture of multiple intermediates could explain why the Rh-H signal has no multiplicity despite being attached to the Rh ($S = 1/2$) and also why no phosphorous signals corresponding to this new complex formed appear in the spectrum. However, further studies will be required to make a final attribution.

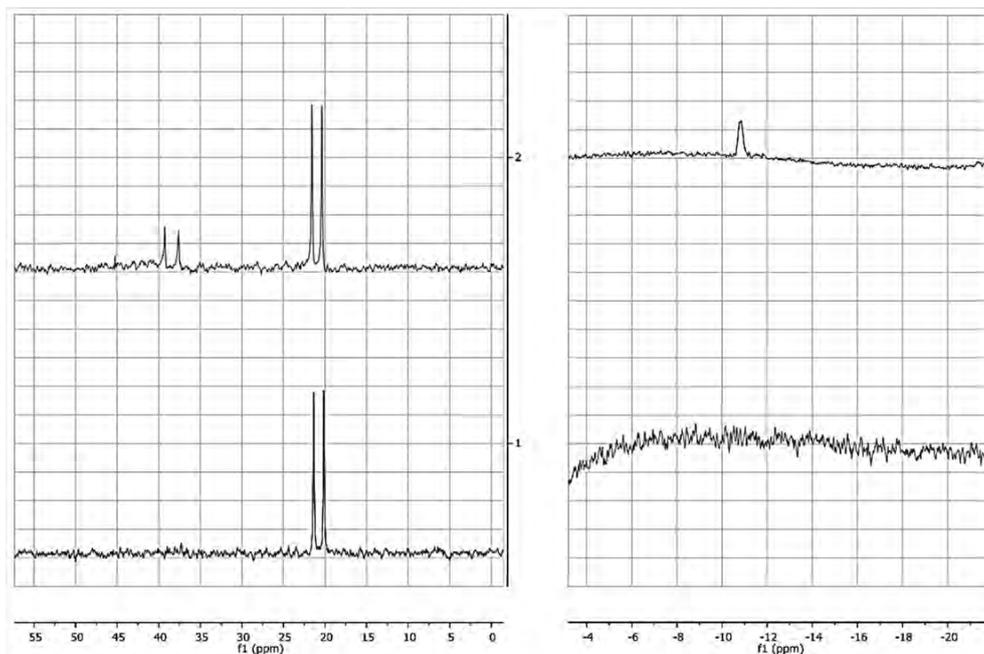


Figure 6.2 $^{31}\text{P}\{^1\text{H}\}$ NMR (101 MHz, toluene- d_8 : $\text{CH}_2\text{Cl}_2 = 1:0.08$) (left) and ^1H NMR (300 MHz) (negative range, right) of the mixture between $[\text{Rh}(\text{cod})(\text{BINAP})]\text{BF}_4$ and the *N*-tosylhydrazone **1aa** (1:1). Initial mixture before heating (bottom) and spectra of the mixture after five minutes of heating recorded at 253 K (top).

The experiment was continued by further heating the sample in the oil bath for an extra 5-10 minutes but this did not cause an increase in the amount of the intermediate being detected. The tube was then left at $-4\text{ }^\circ\text{C}$ (fridge) and checked again after three days but the putative intermediate had decomposed as no signals other than those belonging to complex $[\text{Rh}(\text{cod})(\text{BINAP})]\text{BF}_4$ were observed. No crystals were observed either, only dark red oily droplets.

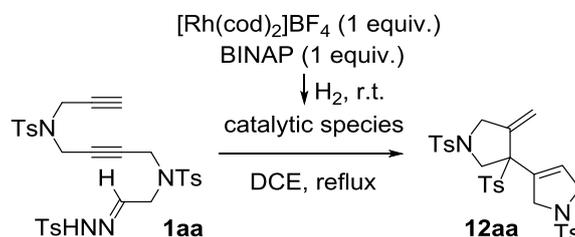
A final set of experiments was carried out with the aim of increasing the concentration of the Rh-H species in solution as much as possible, and to achieve better quality spectrum for the ^1H NMR broad singlet at ca. -10 ppm . The same conditions applied for the second experiment were used to prepare the sample but instead of heating in an oil bath, gradual heating was applied in a variable temperature VT NMR experiment (20 K steps). However, the signal at -10 ppm could not be observed under these experimental conditions.

In summary, it can be concluded that an Rh-H intermediate can be observed after heating a solution of $[\text{Rh}(\text{cod})(\text{BINAP})]\text{BF}_4$ and *N*-tosylhydrazone **1aa** and that the best way to do so is by heating the sample in an oil bath at 75°C for five minutes and then cooling down to a spectrum of 253 K to record the NMR spectrum.

6.3. ESI-HRMS studies

We next decided to use ESI-HRMS as a means of probing transient species from the reaction mixture, due to the cationic nature of the catalytically active species, and postulated reaction intermediates.

The *N*-tosylhydrazone **1aa** was again chosen to study the reaction by high resolution mass spectrometry in a Bruker micro Q-TOF spectrometer with a quadrupole-time-of-flight hybrid analyser of the Serveis Tècnics de Recerca of the University of Girona. An equimolar amount of the catalyst was also used to increase the concentration of intermediate species (Scheme 6.6).



Scheme 6.6 Rhodium-catalysed cyclisation studied by ESI-HRMS.

The reaction was carried out at the optimised temperature (85 °C) and after 5 minutes an aliquot was taken and analysed by ESI-HRMS. The sample, prepared under inert conditions, was diluted with methanol to facilitate ionisation and injected into the mass spectrometer.¹⁰⁸ We postulate that methanol is not only a better suited solvent for ESI-HRMS but also helps to stabilize the short-lived intermediates by forming solvent adducts or complexes that can be split in the ESI-HRMS source, facilitating their detection.¹⁰⁹ The spectrum showed high intensity peaks at the 700-900 *m/z* ratio region, which were assigned to species derived from the catalyst: $[\text{Rh}(\text{BINAP})]^+$ at 725.1049, $[\text{Rh}(\text{BINAP})(\text{H}_2\text{O})]^+$ at 743.1073, $[\text{Rh}(\text{BINAP})(\text{CH}_3\text{CN})]^+$ at 766.1337, $[\text{Rh}(\text{BINAP})(\text{cod})]^+$ at 833.2003, $[\text{Rh}(\text{BINAP}=\text{O})(\text{cod})]^+$ at 849.1844, and an unidentified species at 766.1337 (Figure 6.3). The oxidised species might have been formed in the same mass spectrometer because of the presence of traces of oxygen in the nebulizing nitrogen gas that was employed.

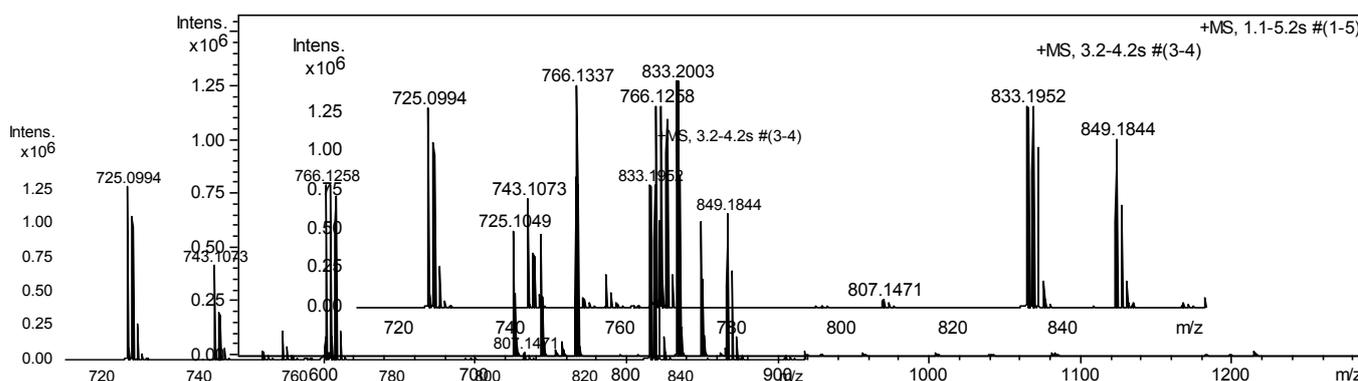
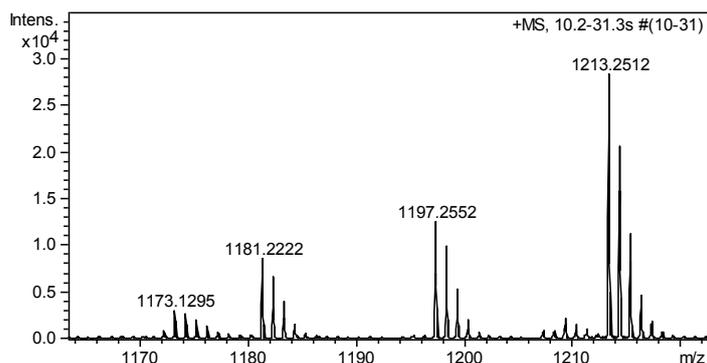
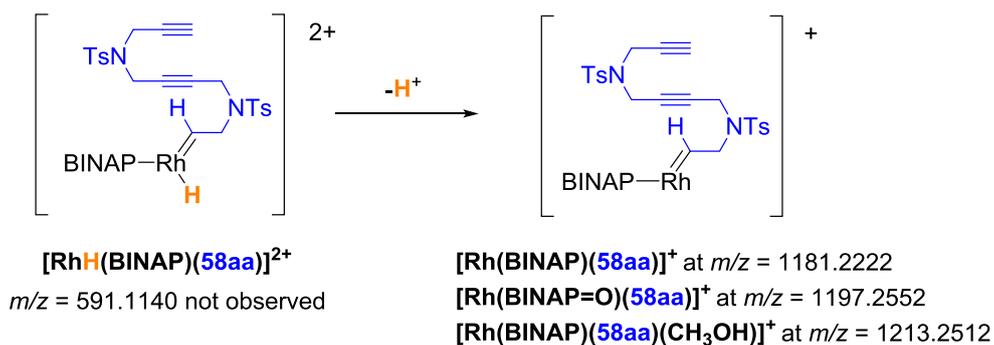


Figure 6.3 ESI-HRMS spectrum after 5 minutes of reaction.

More interestingly, low-intensity signals were also detected in the 1160-1230 *m/z* ratio region corresponding to the mass of the expected reaction intermediates. $[\text{Rh}(\text{BINAP})(\mathbf{58aa})]^+$ at 1181.2222, $[\text{Rh}(\text{BINAP}=\text{O})(\mathbf{58aa})]^+$ at 1197.2552 and $[\text{Rh}(\text{BINAP})(\mathbf{58aa})(\text{CH}_3\text{OH})]^+$ at 1213.2512 (Scheme 6.7).



Scheme 6.7 Possible observed fragmentations of the intermediate $[\text{RhH}(\text{BINAP})(\mathbf{58aa})]^{2+}$.

Considering the mechanism proposed in Chapter 3 (Figure 3.12 and Scheme 3.21), the intermediate $[\text{RhH}(\text{BINAP})(\mathbf{58aa})]^{2+}$ could also be different intermediate species from the catalytic cycle that have the same mass (Figure 6.4).

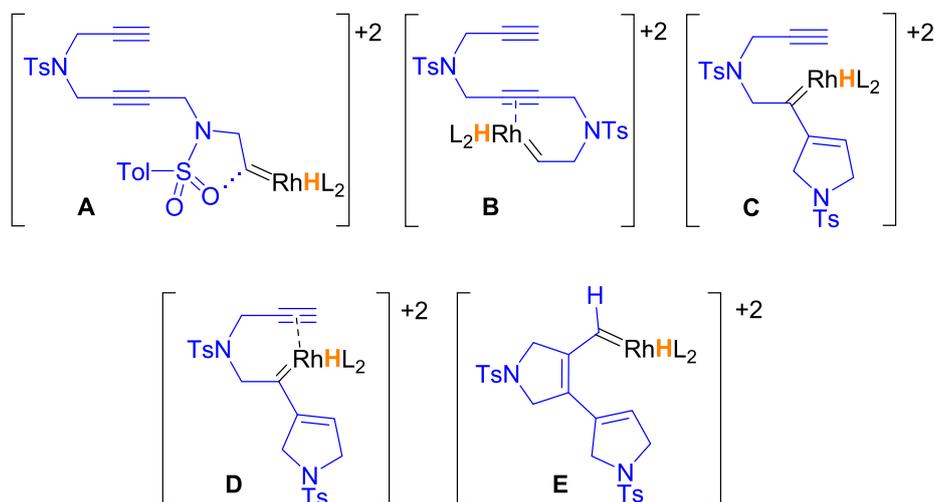


Figure 6.4 Possible structures of $[\text{RhH}(\text{BINAP})(\mathbf{58aa})]^{2+}$

The peak at 1181.2222 fits perfectly with the theoretical $[\text{Rh}(\text{BINAP})(\mathbf{58aa})]^+$ (Figure 6.5) that should be formed after a proton loss from the intermediates shown in Figure 6.4.

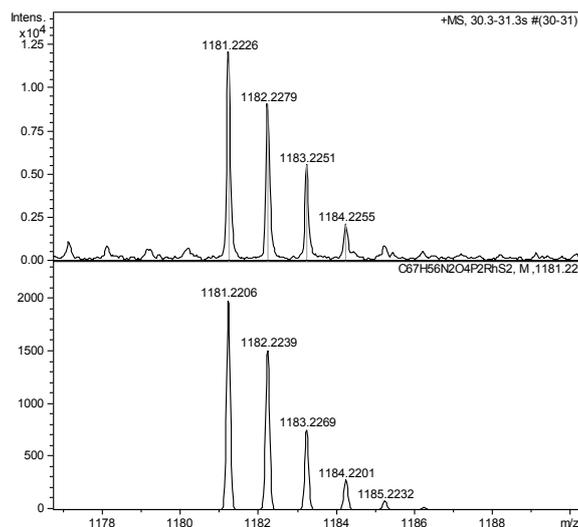
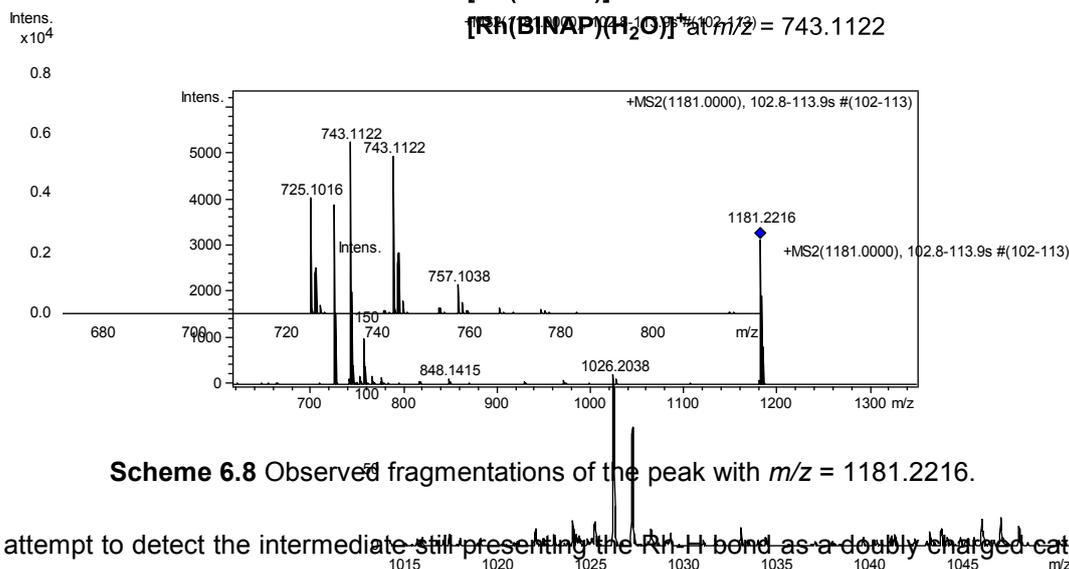
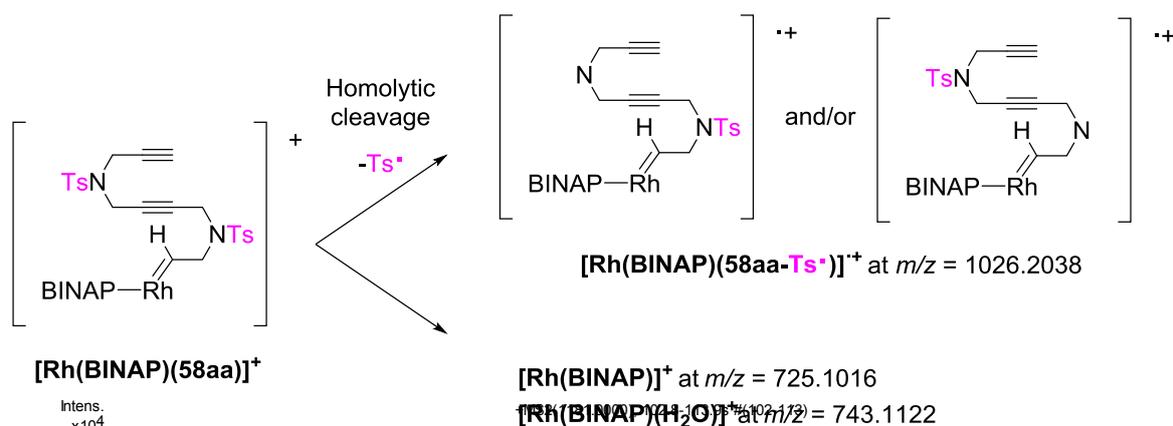


Figure 6.5 Experimental (top) and calculated (bottom) isotopic pattern for $[\text{Rh}(\text{BINAP})(58\text{aa})]^+$.

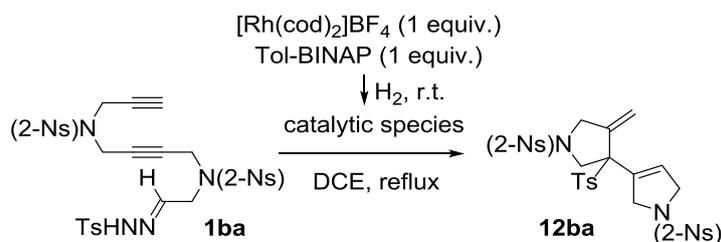
The MS/MS analysis showed that this peak suffered fragmentation resulting in a peak at 1026.2038 corresponding to a homolytic cleavage of the tosyl group of the tether $[\text{Rh}(\text{BINAP})(58\text{aa-Ts})]^{2+}$ (Scheme 6.8) and peaks at 725.1016 and 743.1122 corresponding to the fragment $[\text{Rh}(\text{BINAP})]^+$ and $[\text{Rh}(\text{BINAP})(\text{H}_2\text{O})]^+$.



In an attempt to detect the intermediate still presenting the Rh-H bond as a doubly charged cation, an experiment was carried out by cryospray ionisation mass spectrometry (CSI-MS) at -40°C . However, the Rh-H bond was broken and the peak at 1181.2226 m/z ratio that we assigned to

$[\text{Rh}(\text{BINAP})(\mathbf{58aa})]^+$ was again obtained. The analysis of the reaction mixture after 30 or 60 minutes gave analogous results.

In order to confirm the results obtained, we repeated the experiment changing both the substrate **1aa** and the BINAP ligand for the 2-Ns-linked substrate **1ba** and Tol-BINAP, respectively. The reaction was set up under the optimised reaction conditions using stoichiometric quantities of the catalytic system and analysed by HRMS-TOF (Scheme 6.9).



Scheme 6.9 Rhodium-catalysed cyclisation studied by ESI-HRMS.

The mixture of compound **1ba** and the catalyst was analysed under the same experimental conditions as above. The ESI-HRMS spectrum showed the signals expected for the catalytic species $[\text{Rh}(\text{Tol-BINAP})(\text{CH}_3\text{CN})]^+$ at 822.1846, $[\text{Rh}(\text{Tol-BINAP})(\text{cod})]^+$ at 889.2500 *m/z* ratio and $[\text{Rh}(\text{Tol-BINAP}=\text{O})(\text{cod})]^+$ at 905.2470 *m/z* ratio (Figure 6.6). In this case, a monocharged cationic species that was structurally analogous to the one previously observed at a *m/z* ratio of 1181.2206 for **1aa** and BINAP was detected with significantly increased intensity at a *m/z* ratio of 1299.2053.

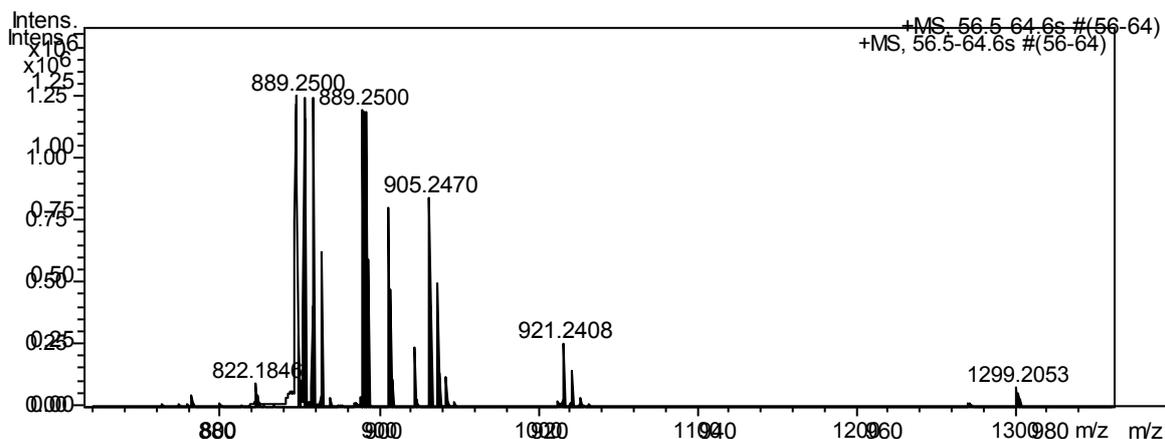
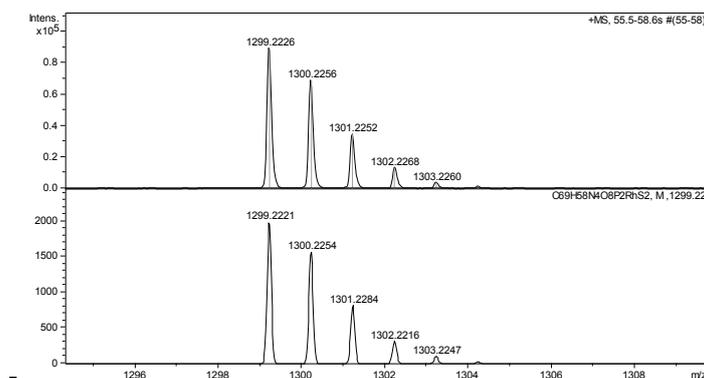
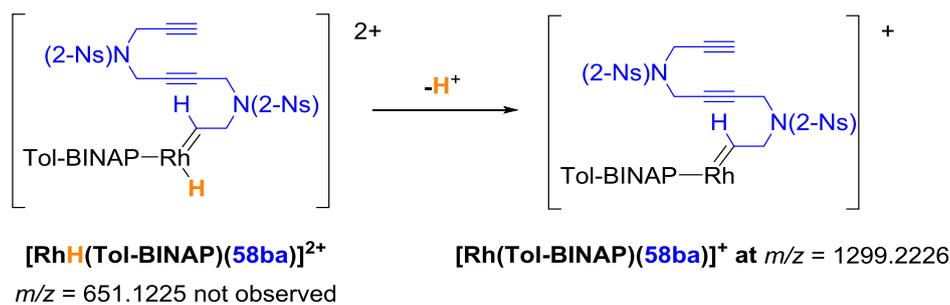


Figure 6.6 ESI-HRMS spectrum after 5 minutes of reaction.

The formation of the peak at 1299.2053 in the mass spectrum can again be explained by the loss of a H^+ from the Rh-H intermediate to give $[\text{Rh}(\text{Tol-BINAP})(\mathbf{58ba})]^+$. The isotopic distribution of this intermediate fits perfectly with the one that is theoretically predicted (Scheme 6.10).



Scheme 6.10 Observed fragmentations of the intermediate $[\text{RhH}(\text{Tol-BINAP})(\mathbf{58ba})]^{2+}$.

This peak at an m/z ratio of 1299.2226 was isolated and fragmented under CID. The fragmentation pattern, which is shown in Figure 6.7, is analogous to the one already discussed for substrate **1aa**: loss of the sulfonyl group on the tether to give $[\text{Rh}(\text{Tol-BINAP})(\mathbf{58ba})]^+$ at 1113.2194 and carbene decomplexation to form $[\text{Rh}(\text{Tol-BINAP})]^+$ at 781.1565.

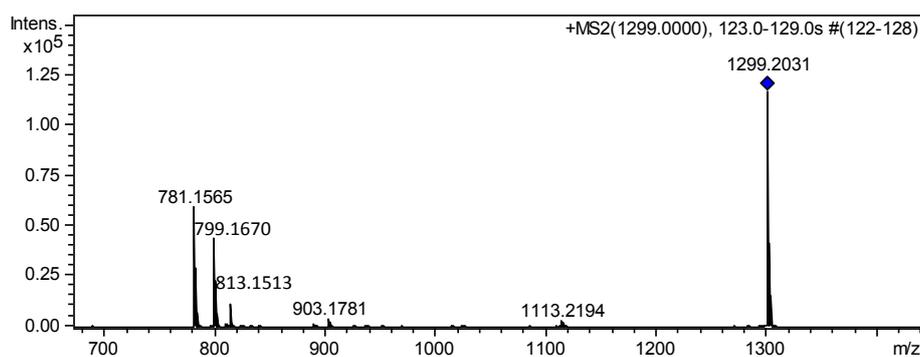
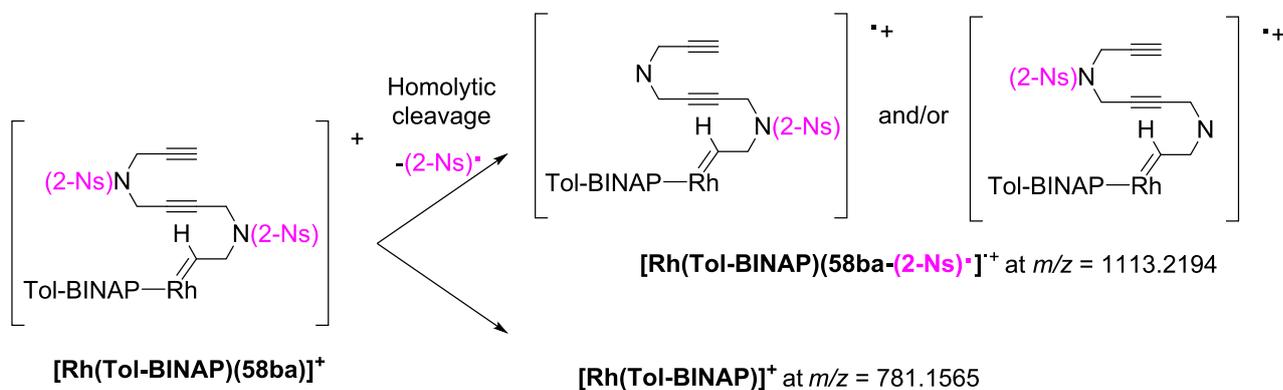
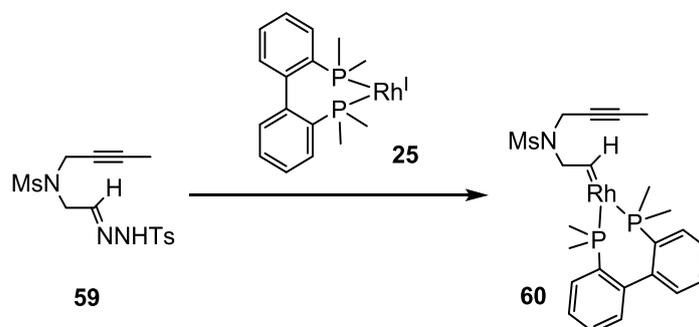


Figure 6.7 Expected fragmentations of the peak with $m/z = 1299.2031$.

In conclusion, ESI-HRMS experiments showed the presence of cationic rhodium carbene intermediates that we postulate as being formed by H^+ loss from the Rh-H intermediate species postulated in the catalytic cycle. Attempts to detect intermediates preserving the Rh-H bond have, for the moment, been unsuccessful.

6.4. DFT calculations

In order to obtain further insight into the reaction mechanism and complement the experimental evidence gained by NMR and ESI-HRMS studies, we performed B3LYP/cc-pVDZ calculations using simplified models of the $[Rh(BINAP)]^+$ (**25**) and the *N*-tosylhydrazone to reduce computational costs. In the case of the *N*-tosylhydrazone substrate, the simplification implied the consideration of only one non-terminal alkyne (Scheme 6.11).



Scheme 6.11 Rhodium-catalysed cyclisation studied by DFT.

Figure 6.8 shows the Gibbs energy profile for the formation of the simplified structure of the common intermediate **F** from Chapters 3, 4 and 5. The first step involves the coordination of the reagent with the catalyst to form a 16-electron rhodium(I) species in a square planar coordination geometry (**B**). This transformation is slightly exergonic by 6.4 kcal/mol. The hydrogen transfer from the *N*-tosylhydrazone to the rhodium with concomitant complexation of the negatively polarised carbon of the *pseudo*-diazo compound then occurs to deliver intermediate **C** with a Gibbs energy barrier of 26.7 kcal/mol. Two different pathways have been analysed from this intermediate **C** to form intermediate **F**. The first corresponds to a sequential dissociation of *p*-toluenesulfinate and nitrogen extrusion (analogous to the Bamford-Stevens reaction). A second option is an overall transformation in a concerted manner. In the sequential route, the first step consists of the *p*-toluenesulfinate anion dissociation to give an ionic pair (**D**) – a process which is endergonic by 7.6 kcal/mol – that afterwards completely dissociates to deliver diazoderivative **E**. N_2 extrusion from diazoderivative **E** then forms the rhodium carbene **F** in a process which is endergonic by 11.6 kcal/mol. The whole process from **C** to **F** has an energy barrier of 18.5 kcal/mol.

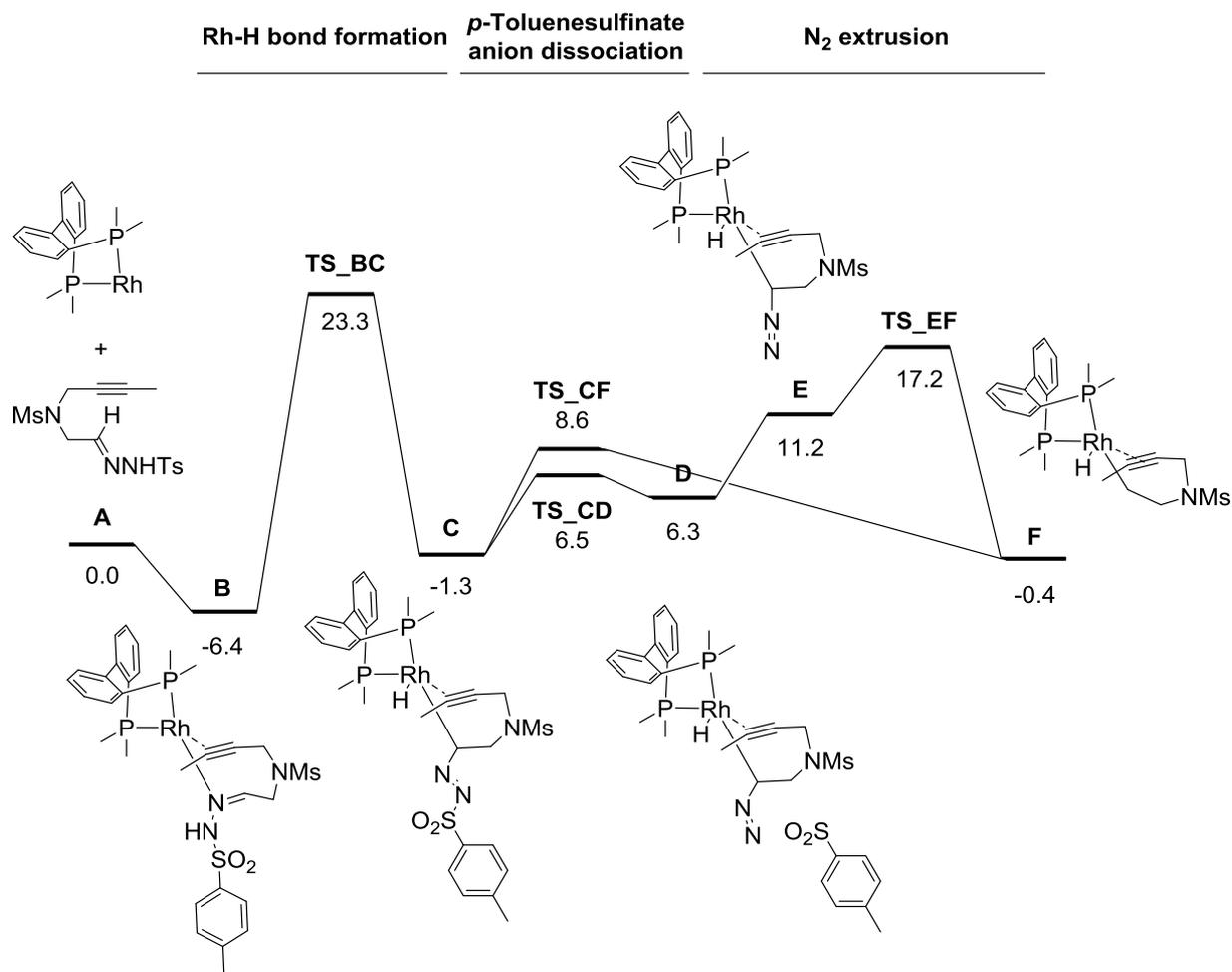


Figure 6.8 Gibbs energy profile (in kcal/mol) of the rhodium-carbene formation.

On the other hand, it was possible to accomplish the transformation of **C** to **F** in a concerted manner with a much more favourable Gibbs energy barrier of 9.9 kcal/mol that permits us to rule out the stepwise mechanism. This **TS_{CF}** transition state has a C-N distance of 1.725 Å, N-N of 1.195 Å and N-S of 2.027 Å, which indicates the formation and delivery of N₂ and *p*-toluenesulfinate (Figure 6.9).

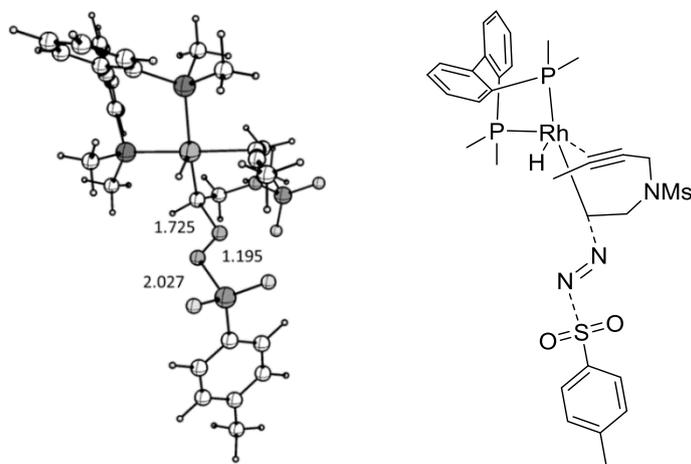


Figure 6.9 Optimised structure (B3LYP/cc-pVDZ) for **TS_{CF}**. Distances in Å.

In order to obtain more information about the oxidation state of the metal, the carbene behaviour of the carbon attached to the rhodium and the charges of the intermediates, the effective oxidation state (EOS) was evaluated with the method developed by Dr. Pedro Salvador from the University of Girona.¹¹⁰ The EOS analysis uses the so-called effective atomic orbitals and their occupations to distribute the integer electrons among the atoms or fragments. This method has been used in previous ruthenium studies with excellent results.¹¹¹ Intermediates **C** and **F** (Figure 6.10), which are representative of the intermediate structures in different parts of the catalytic cycle, were analysed. According to the requirements of the method, two fragments were defined in green and in purple in each of the intermediate structures. The analysis of **C** was obtained with a reliability of 90% (Figure 6.10, left). With regards to the purple fragment, the carbon attached to the rhodium shows an sp^3 hybridisation and a Rh-C distance of 2.154 Å, with the total charge of the fragment being -1. The green fragment of intermediate **C** shows a global +2 charge. Since the BINAP ligand is neutral, the charge of this fragment can be explained either by a rhodium in a +3 oxidation state and a hydride or by a +1 oxidation state for the rhodium and the hydrogen in the form of a proton.

On the other hand, the analysis of **F** was obtained with a reliability of 87% and a global charge of +2 (Figure 6.10, right). Due to the release of a molecular nitrogen and the *p*-toluenesulfonate anion, the carbon attached to the rhodium has changed its hybridisation into an sp^2 with a Rh-C distance of 2.234 Å. Whereas the purple fragment is now neutral, the green one maintains the +2 global charge. This can be again explained in two different scenarios: rhodium(III)/hydride or rhodium(I)/proton. The latter would explain the results obtained by ESI-HRMS, which show a proton loss that leads to the singly charged species that is observed. Looking closely at the effective atomic orbitals (eff-AO) of the rhodium and hydrogen moiety, the last occupied eff-AO for the rhodium is seen to have an occupation of 0.53 whereas the only eff-AO of the hydrogen has an occupation of 0.41, which is consistent with a rhodium(I)/proton with a reliability index of 62%. The rhodium(III)/hydride would have 38% reliability, pointing to the first scenario.

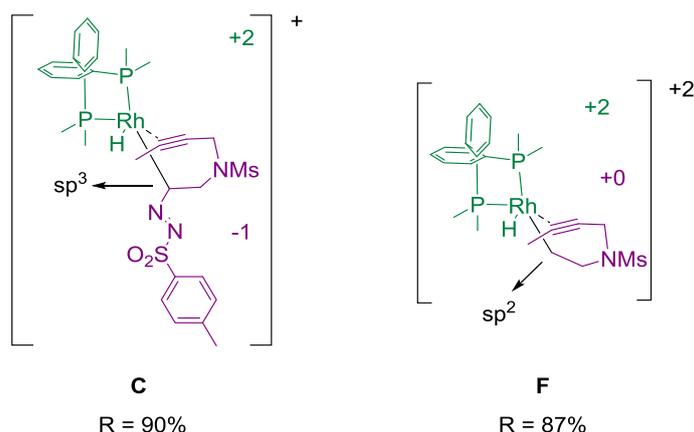


Figure 6.10 Effective oxidation state of intermediates **C** and **F**.

We finally evaluated the rhodium-carbene formation reaction through a model substrate that does not have an alkyne that could coordinate to rhodium and found that the barriers obtained by DFT methods were much higher, indicating the importance of the alkyne coordination to facilitate the formation of the rhodium carbene. In the reactions found in Chapters 3, 4 and 5, all substrates bear at least one alkyne

The experiments carried out demonstrate the feasibility of using this rhodium catalytic system to achieve sulfones when a base is present to affect *N*-tosylhydrazone decomposition, pointing to the different carbene formation mechanism operating when there is no alkyne chain present in the substrate that can coordinate to rhodium.

Overall, in this Chapter 6 we have demonstrated the presence of Rh-H intermediates in the catalytic cycle by direct detection in ^1H NMR, and ESI-HRMS experiments have shown intermediates that may be formed from these Rh-H intermediates and the loss of a H^+ . DFT studies indicate that the formation of the rhodium carbene takes place in a concerted manner through the release of N_2 and the *p*-toluenesulfinate and also highlights the importance of having an alkyne chain to obtain this base-free process.

Chapter 7. General conclusions

In Chapter 3 we have described the use of a catalytic system composed of a cationic rhodium source and BINAP as a ligand to generate a purely donor rhodium(I) carbene. The metal carbene formed in this way was involved in a cascade process that leads to the stereoselective formation of sulfonated azacyclic frameworks in a series of substrates. A plausible mechanism that accounts for all of the experimental data obtained was proposed based on the cooperative use of experimental and computational techniques. The work was pioneer in the generation and reactivity of rhodium(I) carbenes generated from arylsulfonylhydrazones for the preparation of complex molecular architectures in a stereoselective manner.

In Chapter 4 we describe the development of a cascade that explores the carbene/alkyne metathesis as an entry to rhodium vinyl carbenes that can cyclopropanate a tethered olefin. In this way we were able to enantioselectively synthesize various chiral vinylcyclopropane scaffolds in an efficient manner using again *N*-tosylhydrazones as an in situ source of the diazo compound.

In Chapter 5 we described the development of a cascade that explores the carbene/alkyne metathesis affording again rhodium vinyl carbenes and their further reactivity with allenes that leads to the stereoselective formation of methylenetetrahydropyran scaffolds. The use of *N*-tosylhydrazones also provided the diazo compound under base-free conditions, therefore generating purely donor rhodium(I) carbenes. Apart from the methodological development, the mechanism of the process has been studied both by means of experimental and theoretical tools. Rhodium-trimethylenemethane intermediates are proposed as key intermediates that shift the reactivity towards cyclisation. Improving our results from Chapter 3, the attack of the sulfinate was obtained in a regio- and enantioselective manner, even when its electronic properties are changed. This third contribution to the carbene/alkyne metathesis field, demonstrates the feasibility of the methodology.

Finally, in Chapter 6 we detected Rh-H intermediates by ^1H NMR, and ESI-HRMS experiments showed species that may be formed from these Rh-H intermediates and the loss of a H^+ . DFT studies indicate that the formation of the rhodium carbene takes place in a concerted manner through the release of N_2 and the *p*-toluenesulfinate, and also highlights the importance of having an alkyne chain to obtain this base-free process.

Chapter 8. Methods

8.1. General materials and instrumentation

8.1.1. General conditions

MATERIALS

Unless otherwise noted, materials were obtained from commercial suppliers and used without further purification. All reactions requiring anhydrous conditions were conducted in oven dried glassware under a dry nitrogen atmosphere. Dichloromethane and tetrahydrofuran were degassed and dried under nitrogen by passing through solvent purification columns (MBraun, SPS-800). Solvents were removed under reduced pressure with a rotary evaporator. When necessary, reaction mixtures were chromatographed on silica gel (230-400 mesh) using a gradient solvent system as the eluent. All cyclisation reactions were carried out using Schlenk techniques.

SPECTROSCOPY

- **NMR spectroscopy:** All ^1H and ^{13}C NMR spectra were recorded using Bruker Ultrashield AVANCE III 400 (400 MHz) and Bruker Ultrashield DPX300 (300 MHz) spectrometers of the Serveis Tècnics de Recerca of the University of Girona. Chemical shifts (δ) for ^1H and ^{13}C NMR were referenced to internal solvent resonances and reported relative to SiMe_4 .
- **Infrared spectra** were recorded on a Bruker Alpha FT-IR spectrometer with a DTGS detector and an ATR adapter or a FT-IR spectrophotometer Mattson-Galaxy Satellite, using a MKII Golden Gate Single Reflection ATR System of the Chemistry Department of the University of Girona.

SPECTROMETRY

- **Electrospray Mass Spectrometry** analyses were recorded on an Esquire 6000 Ion Trap Mass Spectrometer (Bruker) equipped with an electrospray ion source of the Serveis Tècnics de Recerca of the University of Girona.
- **High Resolution Mass Spectrometry** analyses were registered in Bruker Micro Q-TOF spectrometer with a Quadrupole-Time-Of-Flight hybrid analyser of the Serveis Tècnics de Recerca of the University of Girona.

CHROMATOGRAPHY

- **Thin Layer Chromatography (TLC)** were performed with pre-coated (0.20 mm width) chromatography plates Alugram Sil G/UV254.
- **Column Chromatography** were performed using silica gel SDS with a 35-70 μm mesh particle size.
- **High Performance Liquid Chromatography** were recorded with a CHIRALPAK AD-H column (4.6 x 250 mm, 5 μm) or CHIRALPAK IC column (4.6 x 250 mm, 5 μm) in a Spectra System Thermo (Shimadzu) apparatus equipped with an SN4000 connector, SCM1000 degasser, P2000 pump and UV6000LP detector with a 20 μL loop.

Elemental analyses were recorded on a Perkin Elmer EA2400 series II in the Serveis Tècnics of the University of Girona.

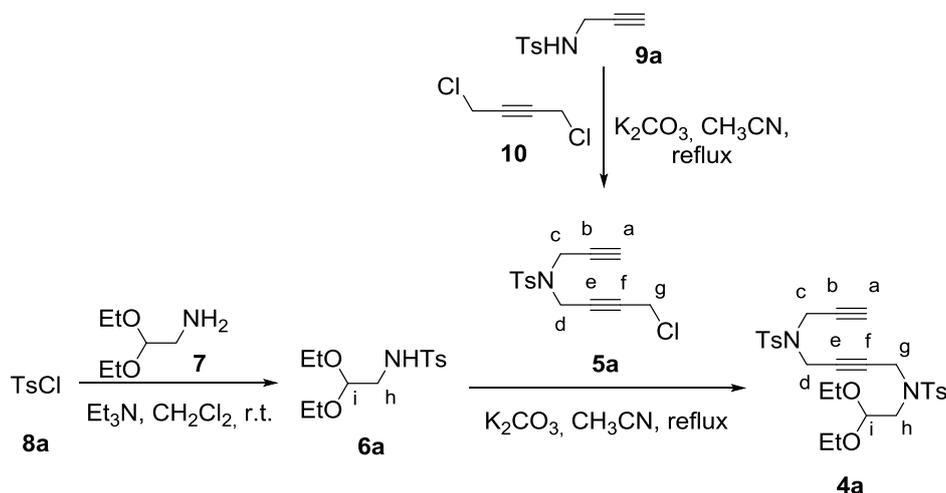
Optical rotations were recorded on a JASCO P-2000 polarimeter at the sodium K line at room temperature (concentration in g/100 mL) of the University of Barcelona.

Microwave heating: a CEM Discover S-Class microwave synthesizer was used (250 W/250psi). Microwave heated reactions were performed in sealed vials in an Ethos SEL Lab station Milestone INC.), a multimode microwave with a dual magnetron (1600 W). During the experiments, the time, temperature, and the power were measured with an "EasyControl" software package. The temperature was monitored and controlled throughout the reaction by an ATC-400FO Automatic Fiber Optic Temperature Control system. The wattage was automatically adjusted to maintain the desired temperature for the desired period of time.

8.2. Experimental procedure for the products synthesised in Chapter 3

8.2.1. Synthesis of substrates

8.2.1.1. Synthesis of acetal 4a



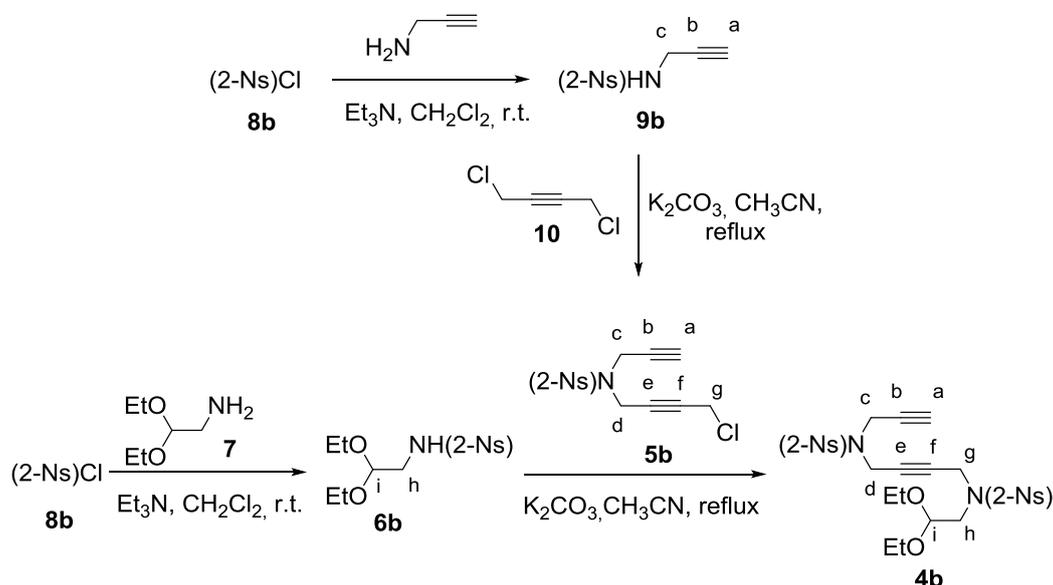
A mixture of *N*-tosylprop-2-yn-1-amine **9a**¹¹³ (1.76 g, 8.41 mmol), 1,4-dichloro-2-butyne (3.28 mL, 26.89 mmol) and anhydrous potassium carbonate (5.81 g, 42.04 mmol) in acetonitrile (250 mL) was stirred at refluxed for 3 hours (TLC monitoring). The mixture was cooled to room temperature, the salts were filtered off, and the solvent removed by vacuum evaporation. The oily residue was purified by column chromatography on silica gel (hexane/ethyl acetate, 10:0 to 7:3) to afford **5a** as a colourless oil (2.03 g, 82%). **MW**: 295.78 g/mol; **IR (ATR) ν (cm⁻¹)**: 2852, 1347, 1159; **¹H NMR (400 MHz, CDCl₃) δ (ppm)**: 2.19 (t, ⁴*J* = 2.4 Hz, 1H_a), 2.43 (s, 3H_{Ts}), 3.95 (t, ⁵*J* = 2.0 Hz, 2H_g), 4.12 (d, ⁴*J* = 2.4 Hz, 2H_c), 4.22 (t, ⁵*J* = 2.0 Hz, 2H_d), 7.31 (d, ³*J* = 8.0 Hz, 2H_{Ts}), 7.78 (d, ³*J* = 8.0 Hz, 2H_{Ts}); **¹³C NMR (100 MHz, CDCl₃) δ (ppm)**: 21.7 (C_{Ts}), 30.0 (C_g), 36.6 (C_c), 36.6 (C_d), 74.2 (C_a), 76.3 (C_f), 79.1 (C_b), 80.6 (C_e), 128.0 (2C_{Ts}), 129.8 (2C_{Ts}), 135.2 (C_{Ts}), 144.2 (C_{Ts}); **ESI-MS (m/z)**: 296.0 [M+H]⁺, 318.0 [M+Na]⁺, 334.0 [M+K]⁺; **EA**: calculated for C₁₄H₁₄ClNO₂S: C, 56.85; H, 4.77; N, 4.74; found: C, 56.35; H, 4.41; N, 4.64.

To a solution of tosyl chloride (5.02 g, 26.33 mmol) in anhydrous CH₂Cl₂ (175 mL) were added triethylamine (4.00 mL, 28.70 mmol) and 2,2-diethoxyethanamine **7** (4.25 mL, 29.23 mmol). The solution was stirred for 1 hour (TLC monitoring). The crude was subsequently washed with a 1M aqueous solution of hydrochloric acid (3 x 100 mL), a saturated aqueous solution of sodium bicarbonate (3 x 100 mL) and water (3 x 100 mL). The organic layer was dried (Na₂SO₄) and the solvent removed by vacuum evaporation to afford **6a** as a colourless solid (7.16 g, 95%). **MW**: 287.37 g/mol; **m.p.**: 71-73 °C; **IR (ATR) ν (cm⁻¹)**: 3255, 2919, 1324, 1167; **¹H NMR (400 MHz, CDCl₃) δ (ppm)**: 1.17 (t, ³*J* = 7.2 Hz, 6H_{OCH₂CH₃}), 2.43 (s, 3H_{Ts}), 3.03 (dd, ³*J* = 5.6 Hz / ³*J* = 6.4 Hz, 2H_h), 3.47 (dq, ²*J* = 9.6 Hz / ³*J* = 7.2 Hz, 2H_{OCH₂CH₃}), 3.64 (dq, ²*J* = 9.6 Hz / ³*J* = 7.2 Hz, 2H_{OCH₂CH₃}), 4.46 (t, ³*J* = 5.6 Hz, 2H_i), 4.66 (t, ³*J* = 6.4 Hz, 1H_{NH}), 7.29 (d, ³*J* = 8.0 Hz, 2H_{Ts}), 7.73 (d, ³*J* = 8.0 Hz, 2H_{Ts}); **¹³C**

NMR (75 MHz, CDCl₃) δ (ppm): 15.4 (2C_{OCH₂CH₃}), 21.6 (C_{Ts}), 45.6 (C_g), 63.3 (2C_{OCH₂CH₃}), 100.9 (C_i), 127.2 (2C_{Ts}), 129.9 (2C_{Ts}), 137.0 (C_{Ts}), 143.7 (C_{Ts}); **ESI-MS (m/z):** 310.1 [M+Na]⁺, 597.0 [2M+Na]⁺; **EA:** calculated for C₁₃H₂₁NO₄S: C, 54.33; H, 7.37; N, 4.87; found: C, 54.48 and 54.47; H, 7.41 and 7.59; N, 5.01 and 4.92.

A mixture of **5a** (0.19 g, 0.66 mmol), **6a** (0.18 g, 0.63 mmol) and anhydrous potassium carbonate (0.35 g, 2.52 mmol) in acetonitrile (12 mL) was stirred at reflux for 5 hours (TLC monitoring). The mixture was cooled to room temperature, the salts were filtered off, and the solvent removed by vacuum evaporation. The oily residue was purified by column chromatography on silica gel (hexane/ethyl acetate 7:3) to afford **4a** (0.25 g, 71%) as a colourless solid. **MW:** 546.70 g/mol; **m.p.:** 72-74 °C; **IR (ATR) ν (cm⁻¹):** 2981, 1329, 1161; **¹H NMR (300 MHz, CDCl₃) δ (ppm):** 1.21 (t, ³J = 7.2 Hz, 6H_{OCH₂CH₃}), 2.08 (t, ⁴J = 2.4 Hz, 1H_a), 2.43 (s, 3H_{Ts}), 2.44 (s, 3H_{Ts}), 3.12 (d, ³J = 5.6 Hz, 2H_h), 3.55 (dq, ²J = 9.6 Hz / ³J = 7.2 Hz, 2H_{OCH₂CH₃}), 3.73 (dq, ²J = 9.6 Hz / ³J = 7.2 Hz, 2H_{OCH₂CH₃}), 3.86 (d, ⁴J = 2.4 Hz, 2H_c), 3.88 (t, ⁵J = 1.8 Hz, 2H_d), 4.17 (t, ⁵J = 1.8 Hz, 2H_g), 4.64 (t, ³J = 5.6 Hz, 1H_i), 7.28 (d, ³J = 8.4 Hz, 2H_{Ts}), 7.31 (d, ³J = 8.4 Hz, 2H_{Ts}), 7.62 (d, ³J = 8.4 Hz, 2H_{Ts}), 7.69 (d, ³J = 8.4 Hz, 2H_{Ts}); **¹³C NMR (75 MHz, CDCl₃) δ (ppm):** 15.5 (2C_{OCH₂CH₃}), 21.7 (C_{Ts}), 36.1 (C_c), 36.3 (C_d), 38.6 (C_g), 48.8 (C_h), 63.8 (2C_{OCH₂CH₃}), 74.1 (C_a), 76.2 (C_b), 77.8 (C_f), 79.4 (C_e), 103.1 (C_i), 127.7 (2C_{Ts}), 127.9 (2C_{Ts}), 129.7 (2C_{Ts}), 135.3 (2C_{Ts}), 136.2 (2C_{Ts}), 143.9 (C_{Ts}), 144.2 (C_{Ts}); **ESI-MS (m/z):** 569.2 [M+Na]⁺, 585.1 [M+K]⁺; **EA:** calculated for C₂₇H₃₄N₂O₆S₂: C, 59.32; H, 6.27; N, 5.12; found: C, 59.58 and 59.41; H, 6.41 and 6.48; N, 5.12 and 5.12.

8.2.1.2. Synthesis of acetal **4b**



To a solution of 2-nitrobenzenesulfonyl chloride **8b** (1.00 g, 4.51 mmol) in anhydrous CH_2Cl_2 (30 mL) were added triethylamine (0.68 mL, 5.02 mmol) and propargylamine **11** (0.3 mL, 4.59 mmol). The solution was stirred for 1 hour (TLC monitoring). The crude was subsequently washed with a 1M aqueous solution of hydrochloric acid (3 x 20 mL), a saturated aqueous solution of sodium bicarbonate (3 x 20 mL) and water (3 x 20 mL). The organic layer was dried (Na_2SO_4) and the solvent removed by vacuum evaporation to afford **9b** as a colourless solid (0.87 g, 81%). **MW:** 240.23 g/mol; **m.p.:** 92-94

$^{\circ}\text{C}$; **IR (ATR) ν (cm^{-1}):** 3343, 3292, 1524, 1369, 1341, 1160; **$^1\text{H NMR}$ (400 MHz, CDCl_3) δ (ppm):** 1.98 (t, $^4J = 2.4$ Hz, 1H_a), 4.02 (d, $^4J = 2.4$ Hz, 2H_c), 5.71 (bs, 1H_{NH}), 7.74-7.80 (m, $2\text{H}_{2-\text{Ns}}$), 7.92 (m, $1\text{H}_{2-\text{Ns}}$), 8.20 (m, $1\text{H}_{2-\text{Ns}}$); **$^{13}\text{C NMR}$ (75 MHz, CDCl_3) δ (ppm):** 33.5 (C_c), 73.4 (C_a), 77.5 (C_b), 125.7 ($\text{C}_{2-\text{Ns}}$), 131.7 ($\text{C}_{2-\text{Ns}}$), 133.1 ($\text{C}_{2-\text{Ns}}$), 133.98 ($\text{C}_{2-\text{Ns}}$), 134.08 ($\text{C}_{2-\text{Ns}}$), 148.13 ($\text{C}_{2-\text{Ns}}$); **ESI-MS (m/z):** 241.0 [$\text{M}+\text{H}$] $^+$, 262.9 [$\text{M}+\text{Na}$] $^+$, 278.9 [$\text{M}+\text{K}$] $^+$; **EA:** calculated for $\text{C}_9\text{H}_8\text{N}_2\text{O}_4\text{S}$: C, 45.00; H, 3.36; N, 11.66; found: C, 44.79 and 44.99; H, 3.00 and 2.97; N, 11.59 and 11.59.

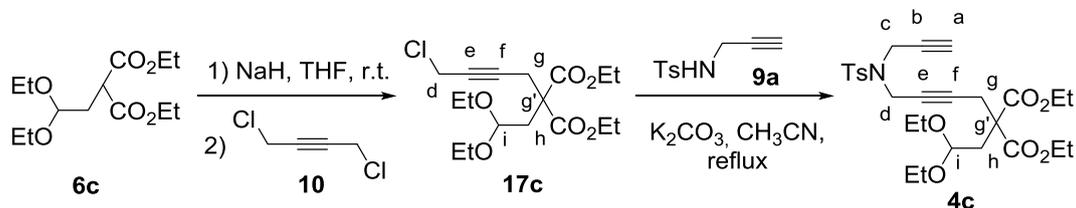
A mixture of **9b** (0.82 g, 3.43 mmol), 1,4-dichloro-2-butyne (1.33 mL, 13.72 mmol) and anhydrous potassium carbonate (2.37 g, 17.15 mmol) in acetonitrile (100 mL) was stirred at reflux for 1 hour (TLC monitoring). The mixture was cooled to room temperature, salts were filtered off, and the solvent removed by vacuum evaporation. The oily residue was purified by column chromatography on silica gel (hexane/ethyl acetate, 10:0 to 7:3) to afford **5b** as a waxy colourless solid (0.96 g, 86%). **MW:** 326.75 g/mol; **IR (ATR) ν (cm^{-1}):** 3306, 1540, 1352, 1166; **$^1\text{H NMR}$ (400 MHz, CDCl_3) δ (ppm):** 2.25 (t, $^4J = 2.4$ Hz, 1H_a), 4.03 (t, $^5J = 2.2$ Hz, 2H_g), 4.29 (d, $^4J = 2.4$ Hz, 2H_c), 4.36 (t, $^5J = 2.2$ Hz, 2H_d), 7.67-7.76 (m, $3\text{H}_{2-\text{Ns}}$), 8.08 (m, $1\text{H}_{2-\text{Ns}}$); **$^{13}\text{C NMR}$ (75 MHz, CDCl_3) δ (ppm):** 30.0 (C_g), 37.0 ($\text{C}_{c,d}$), 74.4 (C_a), 76.4 (C_f), 79.2 (C_b), 80.7 (C_e), 124.6 ($\text{C}_{2-\text{Ns}}$), 131.4 ($\text{C}_{2-\text{Ns}}$), 132.1 ($\text{C}_{2-\text{Ns}}$), 132.5 ($\text{C}_{2-\text{Ns}}$), 134.2 ($\text{C}_{2-\text{Ns}}$), 148.3 ($\text{C}_{2-\text{Ns}}$); **ESI-MS (m/z):** 327.0 [$\text{M}+\text{H}$] $^+$, 348.9 [$\text{M}+\text{Na}$] $^+$; **EA:** calculated for $\text{C}_{13}\text{H}_{11}\text{ClN}_2\text{O}_4\text{S}$: C, 47.79; H, 3.39; N, 8.57; found: C, 47.94 and 47.97; H, 3.05 and 3.26; N, 8.42 and 8.51.

To a solution of 2-nitrobenzenesulfonyl chloride **8b** (1.00 g, 4.51 mmol) in anhydrous CH_2Cl_2 (30 mL) were added triethylamine (0.7 mL, 5.02 mmol) and 2,2-diethoxyethanamine **7** (0.7 mL, 4.81 mmol). The solution was stirred for 1 hour (TLC monitoring). The crude was subsequently washed with a 1M aqueous solution of hydrochloric acid (3 x 20 mL), a saturated aqueous solution of sodium bicarbonate (3 x 20 mL) and water (3 x 20 mL). The organic layer was dried (Na_2SO_4) and the solvent removed by vacuum evaporation to afford **6b** as a waxy colourless solid (1.23 g, 86%). **MW:** 318.34 g/mol; **IR (ATR) ν (cm^{-1}):** 2978, 1538, 1342, 1165; **$^1\text{H NMR}$ (400 MHz, CDCl_3) δ (ppm):** 1.15 (t, $^3J = 7.2$ Hz, $6\text{H}_{\text{OCH}_2\text{CH}_3}$), 3.20 (d, $^3J = 5.6$ Hz, 2H_h), 3.47 (dq, $^2J = 9.6$ Hz / $^3J = 7.2$ Hz, $2\text{H}_{\text{OCH}_2\text{CH}_3}$), 3.64 (dq, $^2J = 9.6$ Hz / $^3J = 7.2$ Hz, $2\text{H}_{\text{OCH}_2\text{CH}_3}$), 4.51 (t, $^3J = 5.6$ Hz, 2H_i), 5.64 (bs, 1H_{NH}), 7.73-7.77 (m, 2H_{HAr}), 7.89 (m, 1H_{HAr}), 8.13 (m, 1H_{HAr}); **$^{13}\text{C NMR}$ (75 MHz, CDCl_3) δ (ppm):** 15.3 ($2\text{C}_{\text{OCH}_2\text{CH}_3}$), 46.2 (C_h), 63.4 ($2\text{C}_{\text{OCH}_2\text{CH}_3}$), 100.6 (C_i), 125.6 ($\text{C}_{2-\text{Ns}}$), 131.1 ($\text{C}_{2-\text{Ns}}$), 133.0 ($\text{C}_{2-\text{Ns}}$), 133.8 ($2\text{C}_{2-\text{Ns}}$), 148.1 ($\text{C}_{2-\text{Ns}}$); **ESI-MS (m/z):** 341.0 [$\text{M}+\text{Na}$] $^+$; **EA:** calculated for $\text{C}_{12}\text{H}_{18}\text{N}_2\text{O}_6\text{S}$: C, 45.28; H, 5.70; N, 8.80; found: C, 45.36; H, 5.91; N, 8.79.

A mixture of **5b** (0.69 g, 2.11 mmol), **6b** (0.67 g, 0.69 mmol) and anhydrous potassium carbonate (1.46 g, 3.45 mmol) in acetonitrile (45 mL) was stirred at reflux for 3 hours (TLC monitoring). The mixture was cooled to room temperature, salts were filtered off, and the solvent removed by vacuum evaporation. The oily residue was purified by column chromatography on silica gel (hexane/ethyl acetate 6:4) to afford **4b** (0.99 g, 77%) as a waxy colourless solid. **MW:** 608.64 g/mol; **IR (ATR) ν (cm^{-1}):** 2978, 1540, 1355, 1162; **$^1\text{H NMR}$ (300 MHz, CDCl_3) δ (ppm):** 1.19 (t, $^3J = 7.2$ Hz, $6\text{H}_{\text{OCH}_2\text{CH}_3}$), 2.19 (t, $^4J = 2.4$ Hz, 1H_a), 3.37 (d, $^3J = 5.2$ Hz, 2H_h), 3.53 (dq, $^2J = 9.2$ Hz / $^3J = 7.2$ Hz, $2\text{H}_{\text{OCH}_2\text{CH}_3}$), 3.70 (dq, $^2J = 9.2$ Hz / $^3J = 7.2$ Hz, $2\text{H}_{\text{OCH}_2\text{CH}_3}$), 4.10 (d, $^4J = 2.4$ Hz, 2H_c), 4.13 (t, $^5J = 2.0$ Hz, 2H_d), 4.31 (t, $^5J = 2.0$ Hz, 2H_g), 4.59 (t, $^3J = 5.2$ Hz, 1H_i), 7.65-7.67 (m, $2\text{H}_{2-\text{Ns}}$), 7.71-7.75 (m, $4\text{H}_{2-\text{Ns}}$), 8.00-8.02 (m, $2\text{H}_{2-\text{Ns}}$); **$^{13}\text{C NMR}$ (75 MHz, CDCl_3) δ (ppm):** 15.4 ($2\text{C}_{\text{OCH}_2\text{CH}_3}$), 36.6 (C_c), 36.8 (C_d), 38.79 (C_g), 49.1

(C_h), 63.9 (2C_{OCH₂CH₃}), 74.4 (C_a), 76.2 (C_b), 78.2 (C_f), 79.6 (C_e), 102.8 (C_i), 124.4 (C_{2-Ns}), 124.6 (C_{2-Ns}), 130.8 (C_{2-Ns}), 131.2 (C_{2-Ns}), 132.0 (C_{2-Ns}), 132.1 (C_{2-Ns}), 132.4 (C_{2-Ns}), 132.8 (C_{2-Ns}), 134.1 (C_{2-Ns}), 134.3 (C_{2-Ns}), 148.3 (C_{2-Ns}), 148.4 (C_{2-Ns}); **ESI-MS (m/z)**: 563.0 [M+Na]⁺; **EA**: calculated for C₂₅H₂₈N₄O₁₀S₂: C, 49.34; H, 4.64; N, 9.21; found: C, 49.20 and 49.35; H, 4.92 and 4.79; N, 8.98 and 8.99.

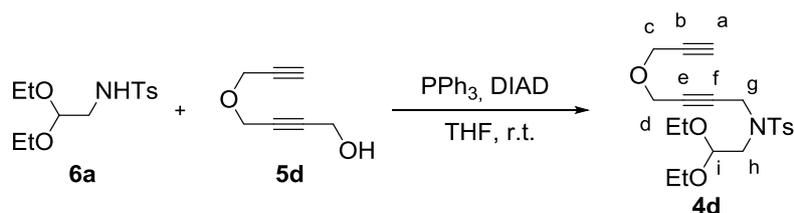
8.2.1.3. Synthesis of acetal **4c**



Diethyl 2-(2,2-diethoxyethyl)malonate **6c**¹¹⁴ (2.00 g, 7.23 mmol) in THF (15 mL) was added slowly to a suspension of NaH (60% dispersion in mineral oil, 0.35 g, 8.69 mmol) in THF (15 mL) at room temperature under N₂, and the mixture was then stirred at room temperature for 1h. 1,4-dichloro-2-butyne **10** (3.53 g, 28.9 mmol) in THF (15 mL) was added dropwise, and the mixture was stirred at room temperature for 24 hours. Water was added to quench the reaction, and the mixture was extracted with EtOAc (3 x 40 mL). The combined organic extracts were washed with brine, dried over Na₂SO₄, filtered and concentrated. The excess of 1,4-dichloro-2-butyne was removed by flash chromatography on silica gel using hexane:EtOAc (10:0 to 7:3) as eluent giving an inseparable mixture of non-reacted starting material and **17c** (1.6 g, 1:0.37 by NMR) which was used without further purification in the next reaction.

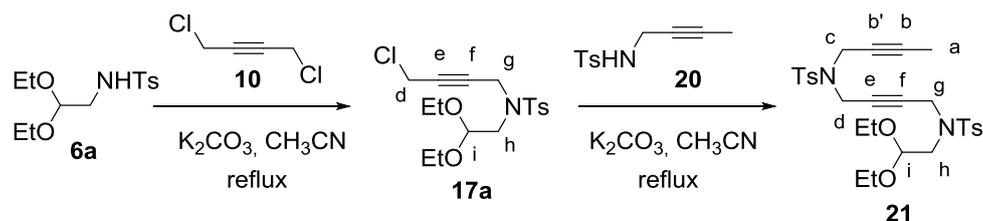
The previously obtained mixture of diethyl 2-(2,2-diethoxyethyl)malonate and **17c** (0.50 g) was reacted with *N*-tosylprop-2-yn-1-amine¹¹³ (1.30 g, 3.58 mmol) and anhydrous potassium carbonate (2.00 g, 14.34 mmol) in acetonitrile (30 mL) at reflux for 3 hours (TLC monitoring). The mixture was cooled to room temperature, the salts were filtered off, and the solvent removed by vacuum evaporation. The oily residue was purified by column chromatography on silica gel (hexane/ethyl acetate, 8:2) to afford **4c** as colourless oil (2.03 g, 84 %, 2 steps). **MW**: 535.65 g/mol; **IR (ATR) ν (cm⁻¹)**: 2978, 1731, 1351, 1161; **¹H NMR (300 MHz, CDCl₃) δ (ppm)**: 1.16 (t, ³J = 6.9 Hz, 6H_{OCH₂CH₃}), 1.23 (t, ³J = 7.1 Hz, 6H_{CO₂CH₂CH₃}), 2.09 (t, ⁴J = 2.4 Hz, 1H_a), 2.32 (d, ³J = 5.9 Hz, 2H_h), 2.43 (s, 3H_{Ts}), 2.77 (t, ⁴J = 2.1 Hz, 2H_g), 3.41 (dq, ²J = 9.2 Hz / ³J = 6.9 Hz, 2H_{OCH₂CH₃}), 3.73 (dq, ²J = 9.2 Hz / ³J = 6.9 Hz, 2H_{OCH₂CH₃}), 4.09 (t, ⁵J = 1.8 Hz, 2H_d), 4.13-4.14 (m, 2H_c), 4.10-4.20 (m, 4H_{CO₂CH₂CH₃}), 4.46 (t, ³J = 5.9 Hz, 1H_i), 7.31 (d, ³J = 8.4 Hz, 2H_{Ts}), 7.69 (d, ³J = 8.4 Hz, 2H_{Ts}); **¹³C NMR (75 MHz, CDCl₃) δ (ppm)**: 14.1 (2C_{OCH₂CH₃}), 15.3 (2C_{CO₂CH₂CH₃}), 21.7 (2C_{Ts}), 23.4 (C_g), 35.9 (C_h), 36.1 (C_d), 36.7 (C_c), 54.6 (C_g), 61.7 (2C_{OCH₂CH₃}), 62.2 (2C_{CO₂CH₂CH₃}), 74.0 (C_a), 75.74 (C_e), 79.3 (C_b), 81.2 (C_f), 100.2 (C_i), 128.0 (2C_{Ts}), 129.7 (2C_{Ts}), 135.3 (C_{Ts}), 144.0 (C_{Ts}), 170.0 (2C_{CO₂Et}); **ESI-MS (m/z)**: 558.2 [M+Na]⁺; **EA**: calculated for C₂₇H₃₇NO₈S(H₂O)_{0.5}: C, 59.54; H, 7.03; N, 2.57; found: C, 60.10 and 59.87; H, 6.68 and 6.52; N, 2.57 and 2.60.

8.2.1.4. Synthesis of acetal 4d



2,2-diethoxy-*N*-tosylethanamine, **6a** (0.43 g, 3.48 mmol) was added to a solution of 4-(prop-2-yn-1-yloxy)but-2-yn-1-ol **5d**¹¹⁵ (1 g, 3.48 mmol) and PPh₃ (1.19 g, 4.54 mmol) in THF (15 mL) at room temperature under N₂. After 10 minutes, diisopropyl azodicarboxylate (DIAD, 0.91 mL, 0.89 mmol) was added and the resulting reaction mixture was stirred for 24 hours. Water was then added followed by extraction with Et₂O (3 x 15 mL). The combined organic layers were washed with brine, dried over Na₂SO₄ and concentrated under reduce pressure. The oily residue was purified by column chromatography on silica gel (hexane/ethyl acetate, 8:2) to afford **4d** as colourless oil (0.78 g, 60 %). **MW**: 393.50 g/mol; **IR (ATR) v (cm⁻¹)**: 2977, 1343, 1159; **¹H NMR (400 MHz, CDCl₃) δ (ppm)**: 1.22 (t, ³J = 7.2 Hz, 6H_{OCH₂CH₃}), 2.42 (s, 3H_{Ts}), 2.46 (t, ⁴J = 2.4 Hz, 1H_a), 3.25 (d, ³J = 5.4 Hz, 2H_h), 3.57 (dq, ²J = 9.4 Hz / ³J = 7.2 Hz, 2H_{OCH₂CH₃}), 3.73 (dq, ²J = 9.4 Hz / ³J = 7.2 Hz, 2H_{OCH₂CH₃}), 3.97-3.98 (m, 2H_{c,d}), 4.33 (t, ⁵J = 2.0 Hz, 2H_g), 4.69 (t, ³J = 5.4 Hz, 1H_i), 7.30 (d, ³J = 8.2 Hz, 2H_{Ts}), 7.74 (d, ³J = 8.2 Hz, 2H_{Ts}); **¹³C NMR (75 MHz, CDCl₃) δ (ppm)**: 15.4 (2C_{OCH₂CH₃}), 21.6 (C_{Ts}), 38.6 (C_g), 48.6 (C_h), 56.1 (C_{c/d}), 56.3 (C_{c/d}), 63.5 (2C_{CO₂CH₂CH₃}), 75.0 (C_a), 78.8 (C_b), 80.3 (C_{e/f}), 80.3 (C_{e/f}), 102.8 (C_i), 127.7 (2C_{Ts}), 129.5 (2C_{Ts}), 136.1 (C_{Ts}), 143.6 (C_{Ts}); **ESI-MS (m/z)**: 416.1 [M+Na]⁺, 432.1 [M+K]⁺; **EA**: calculated for C₂₀H₂₇NO₅S: C, 61.05; H, 6.92; N, 3.56; found: C, 60.69 and 60.66; H, 7.00 and 7.04; N, 3.80 and 3.81.

8.2.1.5. Synthesis of acetal 21

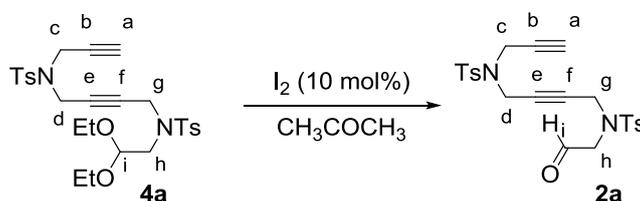


A mixture of 2,2-diethoxy-*N*-tosylethanamine **6a** (0.40 g, 1.44 mmol), 1,4-dichloro-2-butyne **10** (0.14 mL, 5.76 mmol) and anhydrous potassium carbonate (1.2 g, 7.2 mmol) in acetonitrile (15 mL) was stirred at refluxed for 2.5 hours (TLC monitoring). The mixture was cooled to room temperature, salts were filtered off, and the solvent removed by vacuum evaporation. The oily residue was purified by column chromatography on silica gel (hexane/ethyl acetate, 10:0 to 8:2) to afford **17a** as colourless oil (0.38 g, 71%). **MW**: 373.89 g/mol; **IR (ATR) v (cm⁻¹)**: 2976, 1347, 1159; **¹H NMR (300 MHz, CDCl₃) δ (ppm)**: 1.22 (t, ³J = 6.9 Hz, 6H_{OCH₂CH₃}), 2.43 (s, 3H_{Ts}), 3.22 (d, ³J = 5.6 Hz, 2H_h), 3.53 (dq, ²J = 9.3 Hz / ³J = 6.9 Hz, 2H_{OCH₂CH₃}), 3.74 (dq, ²J = 9.3 Hz / ³J = 6.9 Hz, 2H_{OCH₂CH₃}), 3.84 (t, ⁵J = 2.1 Hz, 2H_d), 4.33 (t, ⁵J = 2.1 Hz, 2H_g), 4.68 (t, ³J = 5.6 Hz, 1H_i), 7.31 (d, ³J = 8.4 Hz, 2H_{HAr}), 7.74 (d, ³J = 8.4 Hz, 2H_{HAr}); **¹³C NMR (75 MHz, CDCl₃) δ (ppm)**: 15.52 (2C_{OCH₂CH₃}), 21.66 (C_{Ts}), 38.59 (2C_{d,g}), 48.80 (C_h), 63.82 (2C_{OCH₂CH₃}), 78.78 (2C_{e,f}), 103.16 (C_i), 127.66 (2C_{Ts}), 129.64 (2C_{Ts}), 136.21 (C_{Ts}), 143.88 (C_{Ts}); **ESI-**

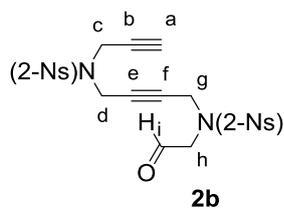
MS (m/z): 396.1 [M+Na]⁺; **EA:** calculated for C₁₇H₂₄ClNO₄S: C, 54.61; H, 6.47; N, 3.75; found: C, 54.93; H, 6.0; N, 3.75.

A mixture of **17a** (0.38 g, 1.02 mmol), N-(but-2-yn-1-yl)tosylamide **6a** (0.23 g, 1.02 mmol) and anhydrous potassium carbonate (0.84 g, 6.12 mmol) in acetonitrile (10 mL) was stirred at reflux for 3.5 h (TLC monitoring). The mixture was cooled to room temperature, salts were filtered off, and the solvent removed by vacuum evaporation. The oily residue was purified by column chromatography on silica gel (hexane/ethyl acetate 8:2) to afford **21** (0.243 g, 88%) as a colourless solid. **MW:** 560.72 g/mol; **m.p.:** 81-82 °C; **IR (ATR) v (cm⁻¹):** 2975, 1351, 1162; **¹H NMR (400 MHz, CDCl₃) δ (ppm):** 1.21 (t, ³J = 7.2 Hz, 6H_{OCH₂CH₃}), 1.60 (t, ⁵J = 2.4 Hz, 3H_a), 2.42 (s, 3H_{Ts}), 2.45 (s, 3H_{Ts}), 3.13 (d, ³J = 5.6 Hz, 2H_h), 3.55 (dq, ²J = 9.6 Hz / ³J = 7.2 Hz, 2H_{OCH₂CH₃}), 3.73 (dq, ²J = 9.6 Hz / ³J = 7.2 Hz, 2H_{OCH₂CH₃}), 3.79 (q, ⁵J = 2.4 Hz, 2H_c), 3.85 (t, ⁵J = 1.8 Hz, 2H_{d/g}), 4.18 (t, ⁵J = 1.8 Hz, 2H_{d/g}), 4.64 (t, ³J = 5.6 Hz, 1H_i), 7.29 (d, ³J = 8.4 Hz, 2H_{Ts}), 7.31 (d, ³J = 8.4 Hz, 2H_{Ts}), 7.62 (d, ³J = 8.4 Hz, 2H_{Ts}), 7.69 (d, ³J = 8.4 Hz, 2H_{Ts}); **¹³C NMR (75 MHz, CDCl₃) δ (ppm):** 3.5 (C_a), 15.5 (2C_{OCH₂CH₃}), 21.6 (C_{Ts}), 21.7 (C_{Ts}), 36.3 (C_{CH₂}), 36.6 (C_{CH₂}), 38.7 (C_{CH₂}), 48.8 (C_h), 63.8 (2C_{OCH₂CH₃}), 71.3 (C_{C≡C}), 78.1 (C_{C≡C}), 79.0 (C_{C≡C}), 82.0 (C_{C≡C}), 103.1 (C_i), 127.7 (2C_{Ts}), 127.9 (2C_{Ts}), 129.5 (2C_{Ts}), 129.7 (2C_{Ts}), 135.4 (C_{Ts}), 136.1 (C_{Ts}), 143.9 (C_{Ts}), 143.9 (C_{Ts}); **ESI-MS (m/z):** 578.2 [M+NH₄]⁺; **EA:** calculated for C₂₈H₃₆N₂O₆S₂: C, 59.98; H, 6.47; N, 5.00; found: C, 60.11 and 59.67; H, 6.18 and 5.91; N, 5.05 and 5.05.

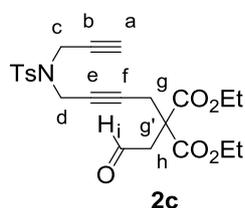
8.2.1.6. Synthesis of aldehydes **2** and **22**



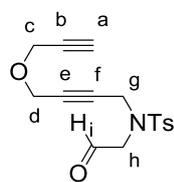
General procedure for **2 and **22**.**⁵⁰ A mixture of **4a** (0.50 g, 0.91 mmol) and iodine (75 mg, 0.3 mmol) in acetone (50 mL) was stirred at room temperature for 24 hours (TLC monitoring). Acetone was then removed under vacuum and the residue was diluted with CH₂Cl₂ (50 mL). The mixture was washed successively with 5% aqueous Na₂S₂O₃ (3 x 20 mL), H₂O (3 x 20 mL) and brine (3 x 20 mL). The organic layer was dried (Na₂SO₄), concentrated *in vacuo* and purified by column chromatography on silica gel (hexane/ethyl acetate 1:1) to afford **2a** (0.27 g, 62%) as a colourless solid. **MW:** 472.58 g/mol; **m.p.:** 96-97 °C; **IR (ATR) v (cm⁻¹):** 2924, 1726, 1346, 1156; **¹H NMR (300 MHz, CDCl₃) δ (ppm):** 2.12 (t, ⁴J = 2.4 Hz, 1H_a), 2.43 (s, 3H_{Ts}), 2.45 (s, 3H_{Ts}), 3.83 (d, ³J = 1.2 Hz, 2H_h), 3.92 (d, ⁴J = 2.4 Hz, 2H_c), 3.96 (t, ⁵J = 1.8 Hz, 2H_{d/g}), 4.05 (t, ⁵J = 1.8 Hz, 2H_{d/g}), 7.30 (d, ³J = 8.4 Hz, 2H_{Ts}), 7.34 (d, ³J = 8.4 Hz, 2H_{Ts}), 7.65 (d, ³J = 8.4 Hz, 2H_{Ts}), 7.67 (d, ³J = 8.4 Hz, 2H_{Ts}), 9.57 (t, ³J = 1.2 Hz, 1H_i); **¹³C NMR (75 MHz, CDCl₃) δ (ppm):** 21.7 (C_{Ts}), 21.7 (C_{Ts}), 36.3 (C_{d/g}), 36.4 (C_{d/g}), 38.9 (C_c), 55.9 (C_h), 74.3 (C_a), 76.1 (C_b), 78.1 (C_{e/f}), 79.5 (C_{e/f}), 127.7 (2C_{Ts}), 127.9 (2C_{Ts}), 129.8 (2C_{Ts}), 130.05 (2C_{Ts}), 134.94 (C_{Ts}), 135.14 (C_{Ts}), 144.35 (C_{Ts}), 144.64 (C_{Ts}), 197.18 (C_i); **ESI-MS (m/z):** 495.1 [M+Na]⁺, 511.1 [M+K]⁺, 527.1 [M+CH₃OH+Na]⁺, 543.1 [M+CH₃OH+K]⁺; **EA:** calculated for C₂₃H₂₄N₂O₅S₂: C, 58.46; H, 5.12; N, 5.93; found: C, 58.30 and 58.13; H, 4.84 and 4.96; N, 5.81 and 5.75.



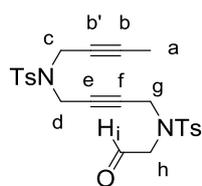
Compound **2b** (67% yield), colourless solid. **MW**: 534.51 g/mol; **m.p.**: 60-61 °C; **IR (ATR) ν (cm⁻¹)**: 3287, 1732, 1538, 1351, 1160; **¹H NMR (400 MHz, CDCl₃) δ (ppm)**: 2.22 (t, ⁴J = 2.4 Hz, 1H_a), 4.14 (d, ⁴J = 2.4 Hz, 2H_c), 4.19 (t, ⁵J = 1.6 Hz, 2H_{d/g}), 4.23 (t, ⁵J = 1.6 Hz, 2H_{d/g}), 4.25 (s, 2H_h), 7.68-7.70 (m, 2H_{2-Ns}), 7.72-7.77 (m, 4H_{2-Ns}), 8.02-8.06 (m, 2H_{2-Ns}), 9.59 (s, 1H_i); **¹³C NMR (75 MHz, CDCl₃) δ (ppm)**: 36.7 (C_{d/g}), 36.7 (C_{d/g}), 38.7 (C_c), 55.8 (C_h), 74.4 (C_a), 76.1 (C_b), 78.3 (C_{e/f}), 79.6 (C_{e/f}), 124.5 (C_{2-Ns}), 124.6 (C_{2-Ns}), 131.0 (C_{2-Ns}), 131.2 (C_{2-Ns}), 132.0 (C_{2-Ns}), 132.2 (C_{2-Ns}), 132.2 (C_{2-Ns}), 132.3 (C_{2-Ns}), 134.3 (C_{2-Ns}), 134.4 (C_{2-Ns}), 148.0 (C_{2-Ns}), 148.1 (C_{2-Ns}), 196.1 (C_i); **ESI-MS (m/z)**: 535.0 [M+H]⁺; **EA**: calculated for C₂₁H₁₈N₄O₉S₂: C, 47.19; H, 3.39; N, 10.48; found: C, 47.22 and 46.93; H, 3.55 and 3.48; N, 10.11 and 9.98.



Compound **2c** (85% yield), colourless oil. **MW**: 461.50 g/mol; **IR (ATR) ν (cm⁻¹)**: 2982, 1725, 1351, 1160; **¹H NMR (300 MHz, CDCl₃) δ (ppm)**: 1.24 (t, ³J = 7.2 Hz, 6H_{CO₂CH₂CH₃}), 2.12 (t, ⁴J = 2.4 Hz, 1H_a), 2.43 (s, 3H_{Ts}), 2.85 (t, ³J = 2.1 Hz, 2H_g), 3.07 (br abs, 2H_h), 4.10 (t, ³J = 2.1 Hz, 2H_d), 4.12 (d, ⁴J = 2.4 Hz, 2H_c), 4.20 (q, ³J = 7.2 Hz, 4H_{CO₂CH₂CH₃}), 7.30 (d, ³J = 8.2 Hz, 2H_{Ts}), 7.69 (d, ³J = 8.2 Hz, 2H_{Ts}), 9.68 (s, 1H_i); **¹³C NMR (75 MHz, CDCl₃) δ (ppm)**: 14.1 (2C_{CO₂CH₂CH₃}), 21.7 (C_{Ts}), 24.1 (C_g), 36.2 (C_d), 36.6 (C_c), 46.0 (C_h), 54.0 (C_g), 62.4 (2C_{CO₂CH₂CH₃}), 74.1 (C_a), 76.3 (C_b), 76.4 (C_e), 80.8 (C_f), 127.9 (2C_{Ts}), 129.7 (2C_{Ts}), 135.3 (C_{Ts}), 144.1 (C_{Ts}), 168.9 (2C_{CO₂Et}), 198.7 (C_i); **ESI-MS (m/z)**: 462.1 [M+H]⁺; **EA**: calculated for C₂₃H₂₇NO₇S: C, 59.86; H, 5.90; N, 3.03; found: C, 59.42 and 59.54; H, 5.97 and 5.93; N, 2.99 and 3.05.

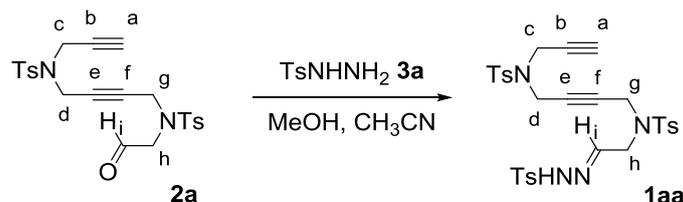


Compound **2d** (66% yield) colourless oil. **MW**: 319.38 g/mol; **IR (ATR) ν (cm⁻¹)**: 2923, 1731, 1342, 1157; **¹H NMR (400 MHz, CDCl₃) δ (ppm)**: 2.44 (s, 3H_{Ts}), 2.47 (t, ⁴J = 2.4 Hz, 1H_a), 3.95 (d, ³J = 1.2 Hz, 2H_h), 4.04 (d, ⁴J = 2.4 Hz, 2H_c), 4.05 (t, ⁵J = 1.8 Hz, 2H_g), 4.22 (t, ⁵J = 1.8 Hz, 2H_d), 7.34 (d, ³J = 8.4 Hz, 2H_{Ts}), 7.71 (d, ³J = 8.4 Hz, 2H_{Ts}), 9.66 (t, ³J = 1.2 Hz, 1H_i); **¹³C NMR (75 MHz, CDCl₃) δ (ppm)**: 21.6 (C_{Ts}), 39.0 (C_g), 56.0 (C_d), 56.35 (C_c), 56.5 (C_h), 75.33 (C_a), 78.6 (C_b), 79.1 (C_e), 81.8 (C_f), 127.7 (2C_{Ts}), 129.9 (2C_{Ts}), 134.8 (C_{Ts}), 144.4 (C_{Ts}), 197.3 (C_i); **ESI-MS (m/z)**: 320.1 [M+H]⁺, 342.1 [M+K]⁺; **EA**: calculated for C₁₆H₁₇NO₄S(H₂O)_{0.5}: C, 58.52; H, 5.53; N, 4.27; found: C, 58.48 and 58.28; H, 5.41 and 5.40; N, 4.44 and 4.40.

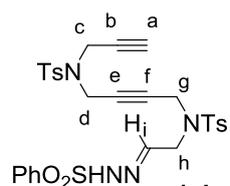


22 Compound **22** (65% yield), colourless oil. **MW**: 486.60 g/mol; **m.p.**: 56-58 °C; **IR (ATR) v (cm⁻¹)**: 2921, 1345, 1156; **¹H NMR (400 MHz, CDCl₃) δ (ppm)**: 1.62 (t, ⁵J = 2.0 Hz, 3H_a), 2.42 (s, 3H_{Ts}), 2.45 (s, 3H_{Ts}), 3.83 (d, ³J = 1.2 Hz, 2H_h), 3.85 (q, ⁴J = 2.0 Hz, 2H_c), 3.92 (t, ⁵J = 1.6 Hz, 2H_{d/g}), 4.05 (t, ⁵J = 1.6 Hz, 2H_{d/g}), 7.29 (d, ³J = 8.4 Hz, 2H_{Ts}), 7.34 (d, ³J = 8.4 Hz, 2H_{Ts}), 7.64 (d, ³J = 8.4 Hz, 2H_{Ts}), 7.65 (d, ³J = 8.4 Hz, 2H_{Ts}), 9.58 (t, ³J = 1.2 Hz, 1H_i); **¹³C NMR (100 MHz, CDCl₃) δ (ppm)**: 3.4 (C_a), 21.6 (C_{Ts}), 21.6 (2C_{Ts}), 36.2 (C_{CH2}), 38.8 (C_{CH2}), 38.8 (C_{CH2}), 55.9 (C_h), 71.1 (C_{C≡C}), 77.7 (C_{C≡C}), 79.7 (C_{C≡C}), 82.2 (C_{C≡C}), 127.6 (2C_{Ts}), 127.9 (2C_{Ts}), 129.5 (2C_{Ts}), 130.0 (2C_{Ts}), 134.9 (C_{Ts}), 135.2 (C_{Ts}), 144.0 (C_{Ts}), 144.6 (C_{Ts}), 197.2 (C_i); **ESI-MS (m/z)**: 487.1 [M+H]⁺; **EA**: calculated for C₂₄H₂₆N₂O₅S₂(H₂O)_{0.5}: C, 58.16; H, 5.49; N, 5.65; found: C, 58.14 and 58.26; H, 5.26 and 5.23; N, 5.55 and 5.51.

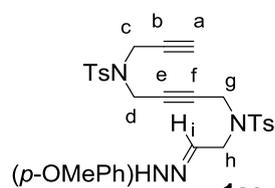
8.2.1.7. Synthesis of *N*-arylsulfonylhydrazones **1** and **23**



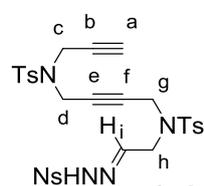
General procedure for 1 and 23. A solution of *p*-toluensulfonyl hydrazide (0.09 g, 0.47 mmol) in methanol (10 mL) was prepared. To this rapidly stirred mixture, a solution of **2a** (0.22 g, 0.47 mmol) in methanol (20 mL) and the minimum amount of acetonitrile to completely dissolve the product was added dropwise. The mixture was then stirred at room temperature for 1h (TLC monitoring). The solvent was removed by vacuum evaporation to afford **1aa** (0.28 g, 92%, *Z/E*:12/88)¹¹⁶ as a colourless solid. **MW**: 640.80 g/mol; **m.p.**: 74-76 °C; **IR (ATR) v (cm⁻¹)**: 3273, 3203, 2905, 1345, 1156; **¹H NMR (300 MHz, CDCl₃) δ (ppm)**: 2.14 (t, ⁴J = 2.4 Hz, 1H_a), 2.42 (s, 3H_{Ts}), 2.43 (s, 3H_{Ts}), 2.44 (s, 3H_{Ts}), 3.82-3.86 (m, 6H_{d,g,h}), 3.94 (d, ⁴J = 2.4 Hz, 2H_c), 7.10 (t, ³J = 5.4 Hz, 1H_i), 7.29-7.33 (m, 6H_{Ts}), 7.62 (d, ³J = 8.4 Hz, 2H_{Ts}), 7.68 (d, ³J = 8.4 Hz, 2H_{Ts}), 7.79 (d, ³J = 8.4 Hz, 2H_{Ts}), 8.24 (s, 1H_{NH}); **¹³C NMR (75 MHz, CDCl₃) δ (ppm)**: 21.8 (3C_{Ts}), 36.2 (C_{d/g}), 36.4 (C_{d/g}), 37.6 (C_h), 49.1 (C_c), 74.4 (C_a), 76.3 (C_b), 78.9 (C_{e/f}), 79.1 (C_{e/f}), 127.7 (2C_{Ts}), 127.9 (2C_{Ts}), 128.0 (2C_{Ts}), 129.8 (4C_{Ts}), 130.0 (2C_{Ts}), 135.0 (C_{Ts}), 135.4 (C_{Ts}), 135.5 (C_{Ts}), 144.5 (2C_{Ts} and C_i), 145.2 (C_{Ts}); **ESI-MS (m/z)**: 641.2 [M+H]⁺, 663.2 [M+Na]⁺; **EA**: calculated for C₃₀H₃₂N₄O₆S₃: C, 56.23; H, 5.03; N, 8.74; found: C, 55.84 and 55.79; H, 4.79 and 4.79; N, 8.85 and 8.81.



1ab Compound **1ab** (96% yield, *Z/E*:8/100)¹¹⁶, colourless solid. **MW**: 626.76 g/mol; **m.p.**: 58-60 °C; **IR (ATR) ν (cm⁻¹)**: 2923, 1344, 1154; **¹H NMR (400 MHz, CDCl₃) δ (ppm)**: 2.14 (t, ⁴*J* = 2.4 Hz, 1H_a), 2.42 (s, 3H_{Ts}), 2.44 (s, 3H_{Ts}), 3.82-3.85 (m, 6H_{d,g,h}), 3.94 (d, ⁴*J* = 2.4, 2H_c), 7.13 (t, ³*J* = 5.6 Hz, 1H_i), 7.29-7.32 (m, 4H_{HAr}), 7.49-7.54 (m, 2H_{HAr}), 7.57-7.70 (m, 3H_{HAr}), 7.66-7.69 (m, 2H_{HAr}), 7.90-7.92 (m, 2H_{HAr}), 8.55 (s, 1H_{NH}); **¹³C NMR (75 MHz, CDCl₃) δ (ppm)**: 21.7 (2C_{Ts}), 36.2 (C_{d/g}), 36.4 (C_{d/g}), 37.7 (C_h), 49.1 (C_c), 74.4 (C_a), 76.3 (C_b), 78.9 (C_{e/f}), 79.1 (C_{e/f}), 127.7 (2C_q), 127.9 (2C_q), 128.0 (2C_q), 129.2 (2C_q), 129.9 (2C_q), 130.0 (2C_q), 133.4 (C_q), 135.0 (C_q), 135.5 (C_q), 138.4 (C_q), 144.5 (C_q), 144.5 (C_i), 145.4 (C_q); **ESI-MS (m/z)**: 627.1 [M+H]⁺, 649.1 [M+Na]⁺; **EA**: calculated for C₂₉H₃₀N₄O₆S₃: C, 55.57; H, 8.94; N, 4.82; found: C, 55.13 and 55.52; H, 8.83 and 8.65; N, 4.95 and 4.96.

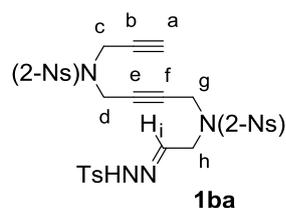


1ac Compound **1ac** (66% yield, *Z/E*:5/95)¹¹⁶, colourless solid. **MW**: 656.79 g/mol; **m.p.**: 68-70 °C; **IR (ATR) ν (cm⁻¹)**: 1329, 1155; **¹H NMR (400 MHz, CDCl₃) δ (ppm)**: 2.14 (t, ⁴*J* = 2.4 Hz, 1H_a), 2.43 (s, 3H_{Ts}), 2.44 (s, 3H_{Ts}), 3.82-3.87 (m, 6H_{d,g,h}), 3.86 (s, 3H_{p-OMePh}), 3.94 (d, ⁴*J* = 2.4, 2H_c), 6.96 (d, ³*J* = 9.2 Hz, 2H_{p-OMePh}), 7.10 (t, ³*J* = 5.2 Hz, 1H_i), 7.31 (d, ³*J* = 8.4 Hz, 2H_{Ts}), 7.31 (d, ³*J* = 8.0 Hz, 2H_{Ts}), 7.62 (d, ³*J* = 8.0 Hz, 2H_{Ts}), 7.67 (d, ³*J* = 8.4 Hz, 2H_{Ts}), 7.83 (d, ³*J* = 9.2 Hz, 2H_{p-OMePh}), 8.29 (s, 1H_{NH}); **¹³C NMR (75 MHz, CDCl₃) δ (ppm)**: 21.7 (2C_{Ts}), 36.2 (C_{d/g}), 36.4 (C_{d/g}), 37.6 (C_h), 49.0 (C_c), 55.8 (C_{p-OMePh}), 74.4 (C_a), 76.3 (C_b), 78.8 (C_{e/f}), 79.1 (C_{e/f}), 114.4 (2C_{p-OMePh}), 127.7 (2C_{Ts}), 127.9 (2C_{Ts}), 129.8 (2C_{p-OMePh}), 129.9 (2C_{Ts}), 130.0 (2C_{Ts}), 130.2 (C_{p-OMePh}), 135.0 (C_{Ts}), 135.4 (C_{Ts}), 144.4 (C_i), 144.5 (C_{Ts}), 145.1 (C_{Ts}), 163.6 (C_{p-OMePh}); **ESI-MS (m/z)**: 657.1 [M+H]⁺, 679.1 [M+Na]⁺, 695.1 [M+K]⁺; **EA**: calculated for C₃₀H₃₂N₄O₇S₃: C, 54.86; H, 4.91; N, 8.53; found: C, 55.26 and 55.16; H, 4.76 and 4.81; N, 8.07 and 8.09.

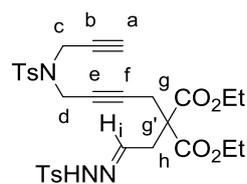


1ad Compound **1ad** (42% yield, *Z/E*:8/92)¹¹⁶, colourless solid. **MW**: 671.76 g/mol; **m.p.**: 70-72 °C; **IR (ATR) ν (cm⁻¹)**: 1346, 1156; **¹H NMR (300 MHz, CDCl₃) δ (ppm)**: 2.14 (t, ⁴*J* = 2.4 Hz, 1H_a), 2.44 (s, 3H_{Ts}), 2.44 (s, 3H_{Ts}), 3.85-3.88 (m, 6H_{d,g,h}), 3.94 (d, ⁴*J* = 2.4, 2H_c), 7.24 (t, ³*J* = 5.1 Hz, 1H_i), 7.32 (d, ³*J* = 8.0 Hz, 4H_{Ts}), 7.62 (d, ³*J* = 8.0 Hz, 2H_{Ts}), 7.67 (d, ³*J* = 8.0 Hz, 2H_{Ts}), 8.10 (d, ³*J* = 9.0 Hz, 2H_{Ns}), 8.30 (d, ³*J* = 9.0 Hz, 2H_{Ns}), 8.95 (s, 1H_{NH}); **¹³C NMR (75 MHz, CDCl₃) δ (ppm)**: 21.8 (2C_{Ts}), 36.2 (C_{d/g}), 36.6 (C_{d/g}), 38.3 (C_h), 49.72 (C_c), 74.5 (C_a), 79.2 (C_b), 79.1 (C_{e/f}), 79.5 (C_{e/f}), 124.3 (2C_{Ns}), 127.6 (2C_{Ts}), 127.9 (2C_{Ts}), 129.4 (2C_{Ts}), 130.0 (2C_{Ts}), 130.1 (2C_{Ns}), 134.8 (C_{Ts}), 135.4 (C_{Ts}),

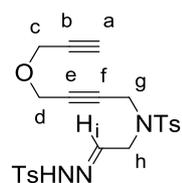
144.2 (C_i), 144.6 (C_{Ts}), 144.8 (C_{Ts}), 147.0 (C_{Ns}), 150.5 (C_{Ns}); **ESI-MS (m/z)**: 672.1 [M+H]⁺, 694.1 [M+Na]⁺; **ESI-HRMS (m/z)**: calculated for [M+Na]⁺: 694.1070; experimental: 694.1061.



Compound **1ba** (97% yield, *Z/E*:0/100)¹¹⁶, colourless solid. **MW**: 702.74 g/mol; **m.p.**: 62-63 °C; **IR (ATR) v (cm⁻¹)**: 3269, 1540, 1354, 1160; **¹H NMR (400 MHz, CDCl₃) δ (ppm)**: 2.23 (t, ⁴*J* = 2.2 Hz, 1H_a), 2.43 (s, 3H_{Ts}), 3.97 (t, ⁵*J* = 2.0 Hz, 2H_{d/g}), 4.03 (t, ³*J* = 5.2 Hz, 1H_h), 4.08 (t, ⁵*J* = 2.0 Hz, 2H_{d/g}), 4.09 (d, ⁴*J* = 2.2 Hz, 2H_c), 7.14 (t, ³*J* = 5.2 Hz, 1H_i), 7.31 (d, ³*J* = 8.4 Hz, 2H_{Ts}), 7.67-7.80 (m, 8H_{HAr}), 8.00 (m, 1H_{Ns}), 8.06 (m, 1H_{Ns}), 8.19 (s, 1H_{NH}); **¹³C NMR (75 MHz, CDCl₃) δ (ppm)**: 21.6 (C_{Ts}), 36.7 (C_d), 36.8 (C_g), 37.6 (C_h), 49.0 (C_c), 74.5 (C_a), 76.2 (C_b), 79.1 (C_{e/f}), 79.2 (C_{e/f}), 124.6 (C_{2-Ns}), 124.7 (C_{2-Ns}), 127.9 (2C_{Ts}), 129.8 (2C_{Ts}), 131.16 (C_{2-Ns}), 131.25 (C_{2-Ns}), 132.03 (C_{2-Ns}), 132.20 (C_{2-Ns}), 132.23 (C_{2-Ns}), 132.38 (C_{2-Ns}), 134.3 (C_{2-Ns}), 134.4 (C_{2-Ns}), 135.1 (C_{Ts}), 144.5 (C_i, C_{Ts}), 148.0 (C_{2-Ns}), 148.0 (C_{2-Ns}); **ESI-MS (m/z)**: 703.0 [M+H]⁺, 725.0 [M+Na]⁺; **EA**: calculated for C₂₈H₂₆N₆O₁₀S₃: C, 47.86; H, 3.73; N, 11.96; found: C, 47.91 and 48.07; H, 3.65 and 3.66; N, 11.60 and 11.66.

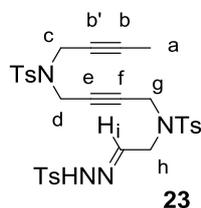


Compound **1ca** (100% yield, *Z/E*:23/77)¹¹⁶, waxy colourless solid. **MW**: 629.74 g/mol; **IR (ATR) v (cm⁻¹)**: 2926, 1730, 1327, 1158; **¹H NMR (400 MHz, CDCl₃) δ (ppm)**: 1.19 (t, ³*J* = 7.2 Hz, 6H_{CO₂CH₂CH₃}), 2.12 (t, ⁴*J* = 2.4 Hz, 1H_a), 2.41 (s, 3H_{Ts}), 2.43 (s, 3H_{Ts}), 2.63 (t, ⁵*J* = 2.1 Hz, 2H_g), 2.74 (d, ³*J* = 5.7 Hz, 2H_h), 4.00 (t, ⁵*J* = 2.1 Hz, 2H_d), 4.08-4.17 (m, 2H_c+4H_{CO₂CH₂CH₃}), 7.20 (t, ³*J* = 5.7 Hz, H_i), 7.29-7.33 (m, 4H_{Ts}), 7.70 (d, ³*J* = 8.4 Hz, 2H_{Ts}), 7.79 (d, ³*J* = 8.4 Hz, 2H_{Ts}), 8.10 (s, 1H_{NH}); **¹³C NMR (100 MHz, CDCl₃) δ (ppm)**: 14.0 (2C_{CO₂CH₂CH₃}), 21.6 (C_{Ts}), 21.7 (C_{Ts}), 23.7 (C_h), 35.9 (C_g), 36.1 (C_d), 36.4 (C_c), 55.9 (C_{g'}), 62.1 (2C_{CO₂CH₂CH₃}), 74.2 (C_a), 76.4 (C_b), 79.4 (C_e), 80.6 (C_f), 127.9 (2C_{Ts}), 128.0 (2C_{Ts}), 129.7 (2C_{Ts}), 129.8 (2C_{Ts}), 135.1 (C_{Ts}), 135.5 (C_{Ts}), 144.2 (C_{Ts}), 144.2 (C_i), 147.0 (C_{Ts}), 169.1 (2C_{CO₂Et}); **ESI-MS (m/z)**: 630.1 [M+H]⁺, 652.2 [M+Na]⁺; **EA**: calculated for C₃₀H₃₅N₃O₈S₂(H₂O)_{0.5}: C, 56.41; H, 5.68; N, 6.58; found: C, 56.26 and 56.25; H, 5.51 and 5.46; N, 6.69 and 6.68.



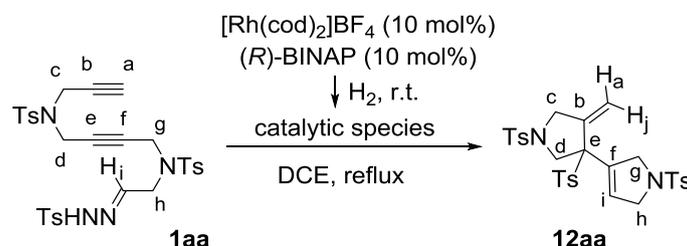
Compound **1da** (79% yield, *Z/E*:6/94)¹¹⁶, waxy colourless solid. **MW**: 487.59 g/mol; **IR (ATR) v (cm⁻¹)**: 2922, 1342, 1157; **¹H NMR (400 MHz, CDCl₃) δ (ppm)**: 2.40 (s, 3H_{Ts}), 2.42 (s, 3H_{Ts}), 2.50 (t, ⁴*J* = 2.4 Hz, 1H_a), 3.86-3.87 (m, 2H_{d/g}+2H_h), 3.95 (t, ⁵*J* = 1.6 Hz, 2H_{d/g}), 4.05 (d, ³*J* = 2.4 Hz, 2H_c), 7.11 (t, ³*J* = 5.2 Hz, 1H_i), 7.27-7.31 (m, 4H_{Ts}), 7.64 (d, ³*J* = 8.4 Hz, 2H_{Ts}), 7.77 (d, ³*J* = 8.4 Hz, 2H_{Ts}), 8.70 (s, 1H_{NH}); **¹³C NMR (100 MHz, CDCl₃) δ (ppm)**: 21.6 (C_{Ts}), 21.6 (C_{Ts}), 37.4 (C_g), 48.4 (C_h),

56.4 ($C_{c/d}$), 56.5 ($C_{c/d}$), 75.5 (C_a), 78.7 (C_b), 79.7 ($C_{e/f}$), 81.2 ($C_{e/f}$), 127.7 ($2C_{Ts}$), 127.9 ($2C_{Ts}$), 129.7 ($2C_{Ts}$), 129.8 ($2C_{Ts}$), 135.0 (C_{Ts}), 135.1 (C_{Ts}), 144.2 (C_{Ts}), 144.3 (C_i), 145.5 (C_{Ts}); **ESI-MS (m/z)**: 488.0 [$M+H$]⁺, 510.1 [$M+Na$]⁺; **EA**: calculated for $C_{23}H_{25}N_3O_5S_2$: C, 56.66; H, 5.17; N, 8.62; found: C, 56.14; H, 5.18; N, 8.35.



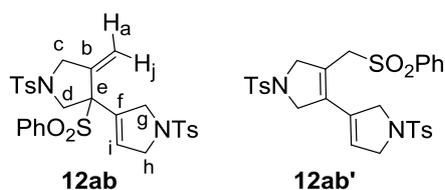
23 Compound **23** (100% yield, *Z/E*:10/90)¹¹⁶, colourless solid. **MW**: 654.82 g/mol; **m.p.**: 73-74 °C; **IR (ATR) ν (cm^{-1})**: 2923, 1344, 1155; **1H NMR (400 MHz, $CDCl_3$) δ (ppm)**: 1.64 (t, $^5J = 2.4$ Hz, 3H_a), 2.42 (s, 3H_{Ts}), 2.43 (s, 3H_{Ts}), 2.44 (s, 3H_{Ts}), 3.84-3.85 (m, 8H_{c,d,g,h}), 7.11 (t, $^3J = 5.4$ Hz, 1H_i), 7.29-7.32 (m, 6H_{Ts}), 7.62 (d, $^3J = 8.4$ Hz, 2H_{Ts}), 7.68 (d, $^3J = 8.4$ Hz, 2H_{Ts}), 7.79 (d, $^3J = 8.4$ Hz, 2H_{Ts}), 8.28 (s, 1H_{NH}); **^{13}C NMR (100 MHz, $CDCl_3$) δ (ppm)**: 3.5 (C_a), 21.7 (C_{Ts}), 21.7 (C_{Ts}), 21.8 (C_{Ts}), 36.2 (C_{CH_2}), 37.0 (C_{CH_2}), 37.9 (C_{CH_2}), 49.3 (C_h), 71.5 ($C_{C=C}$), 78.7 ($C_{C=C}$), 79.5 ($C_{C=C}$), 82.4 ($C_{C=C}$), 127.7 ($2C_{Ts}$), 128.0 ($4C_{Ts}$), 129.7 ($2C_{Ts}$), 129.8 ($2C_{Ts}$), 130.0 ($2C_{Ts}$), 135.3 (C_{Ts}), 135.5 (C_{Ts}), 135.5 (C_{Ts}), 144.2 (C_i), 144.4 ($2C_{Ts}$), 145.3 (C_{Ts}); **ESI-MS (m/z)**: 655.1 [$M+H$]⁺; **EA**: calculated for $C_{31}H_{34}N_4O_6S_3$: C, 56.86; H, 5.23; N, 8.56; found: C, 56.72; H, 4.73; N, 8.29.

8.2.2. Experimental procedure for the rhodium(I)-catalysed cyclization of *N*-arylsulfonylhydrazones **1** and **23**

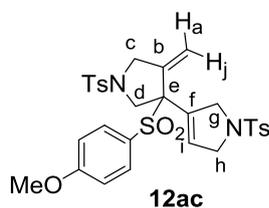


General procedure for 12 and 27. [Rh(cod)₂]BF₄ (0.0040 g, 0.01 mmol) and (*R*)-BINAP (0.0068 g, 0.01 mmol) were dissolved in dichloromethane (3 mL) under nitrogen. Hydrogen gas was bubbled to the stirred catalyst solution for 30 minutes and the resulting mixture was concentrated to dryness. The mixture was dissolved in 1,2-dichloroethane (1.5 mL) and a solution of **1aa** (0.0641 g, 0.10 mmol) in dichloroethane (1.5 mL) was added. The reaction mixture was heated at reflux for 1 hour (TLC monitoring). The solvent was evaporated and the residue was purified by column chromatography on silica gel (hexane/ethyl acetate, 6:4) to afford a colourless solid (0.0356 g, 58% yield, >99% ee) which was identified by spectroscopy data as compound **12aa**. **MW**: 612.77 g/mol; **m.p.**: 92-93 °C; **IR (ATR) ν (cm^{-1})**: 2920, 1343, 1159; **1H NMR (300 MHz, $CDCl_3$) δ (ppm)**: 2.43 (s, 3H_{Ts}), 2.45 (s, 3H_{Ts}), 2.47 (s, 3H_{Ts}), 3.33 (d, $^2J = 10.8$ Hz, 1H_d), 3.36 (dt, $^4J = 2.4$ Hz / $^2J = 13.5$ Hz, 1H_c), 3.70 (dt, $^4J = 1.8$ Hz / $^2J = 13.5$ Hz, 1H_c), 3.83 (d, $^2J = 10.8$ Hz, 1H_d), 4.08-4.13 (m, 2H_g), 4.18 (m, 1H_h), 4.37 (m, 1H_h), 5.41 (m, 1H_a), 5.66 (m, 2H_{i,j}), 7.19 (d, $^3J = 8.6$ Hz, 2H_{Ts}), 7.35 (d, $^3J = 8.6$ Hz, 2H_{Ts}), 7.38 (d, $^3J = 8.6$ Hz, 2H_{Ts}),

7.42 (d, $^3J = 8.6$ Hz, $2H_{Ts}$), 7.57 (d, $^3J = 8.6$ Hz, $2H_{Ts}$), 7.74 (d, $^3J = 8.6$ Hz, $2H_{Ts}$); ^{13}C NMR (75 MHz, $CDCl_3$) δ (ppm): 21.7 (C_{Ts}), 21.8 (C_{Ts}), 21.9 (C_{Ts}), 52.9 (C_c), 55.1 (C_g), 55.2 (C_d), 55.4 (C_h), 73.9 (C_e), 116.5 (C_{afj}), 127.7 ($2C_{Ts}$), 128.0 ($2C_{Ts}$), 129.1 (C_i), 129.6 ($2C_{Ts}$), 130.1 ($2C_{Ts}$), 130.1 ($2C_{Ts}$), 130.8 ($2C_{Ts}$), 131.4 (C_{Ts}), 132.2 (C_{Ts}), 132.4 (C_f), 133.8 (C_{Ts}), 139.0 (C_b), 144.1 (C_{Ts}), 144.7 (C_{Ts}), 145.9 (C_{Ts}); **ESI-MS (m/z)**: 613.0 $[M+H]^+$; **AE**: calculated for $C_{30}H_{32}N_2O_6S_3$: C, 58.80; H, 5.26; N, 4.57; found: C, 58.87 and 58.82; H, 5.13 and 5.22; N, 4.77 and 4.63. The enantiomeric excess has been determined by **HPLC** analysis using a CHIRALPAK AD-H column (4.6 x 250 mm, 5 μ m) with 10 % hexane / 90 % 2-PrOH mobile phase at a 1.0 mL/min flux rate, using a UV detector set up at $\lambda = 254$ nm. The retention time for the major isomer is 42.6 min and for the minor isomer is 37.1 min. $[\alpha]^{20}_D +15.74$ (c 0.18 g / 100 mL, CH_2Cl_2).

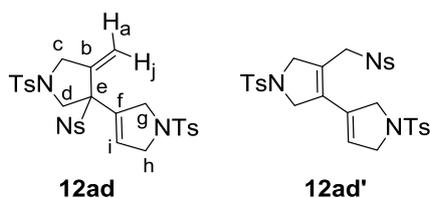


Compound **12ab** (41% yield¹¹⁷, ee >99%) and **12ab'** (13% yield¹¹⁷) were obtained as an inseparable mixture of colourless solids following the general cyclisation procedure. **MW**: 598.75 g/mol; **IR (ATR) ν (cm^{-1})**: 2922, 1341, 1158; 1H NMR (400 MHz, $CDCl_3$) δ (ppm): 2.45 (s, $3H_{Ts}$), 2.47 (s, $3H_{Ts}$), 3.29 (d, $^2J = 11.2$ Hz, $1H_d$), 3.38 (dt, $^4J = 2.0$ Hz / $^2J = 13.6$ Hz, $1H_c$), 3.65 (dt, $^4J = 2.0$ Hz / $^2J = 13.6$ Hz, $1H_c$), 3.91 (d, $^2J = 11.2$ Hz, $1H_d$), 4.08-4.13 (m, $2H_h$), 4.19 (m, $1H_g$), 4.37 (m, $1H_g$), 5.41 (m, $1H_a$), 5.66-5.67 (m, $2H_{ji}$), 7.33-7.39 (m, $6H_{HAr}$), 7.44 (m, $1H_{HAr}$), 7.56-7.59 (m, $4H_{HAr}$), 7.73-7.56 (m, $2H_{HAr}$); ^{13}C NMR (100 MHz, $CDCl_3$) δ (ppm): 21.7 (C_{Ts}), 21.8 (C_{Ts}), 52.8 (C_c), 55.2 (C_g), 55.3 (C_d), 55.4 (C_h), 74.1 (C_e), 116.7 (C_{afj}), 127.7 ($2C_q$), 128.0 ($2C_q$), 129.0 ($2C_q$), 129.3 (C_i), 129.7 (C_q), 130.2 ($4C_q$), 130.9 ($2C_q$), 132.2 (C_f), 133.9 ($2C_q$), 134.6 (C_q), 135.4 (C_q), 138.9 (C_b), 144.1 (C_q), 144.7 (C_q); **ESI-MS (m/z)**: 599.1 $[M+H]^+$, 621.1 $[M+Na]^+$, 637.0 $[M+K]^+$; **AE**: calculated for $C_{29}H_{30}N_2O_6S_3$: C, 58.17; H, 5.05; N, 4.68; found: C, 58.05 and 58.57; H, 5.62 and 5.62; N, 4.26 and 4.41. The enantiomeric excess has been determined by **HPLC** analysis using a CHIRALPAK AD-H column (4.6 x 250 mm, 5 μ m) with 10 % hexane / 90 % 2-PrOH mobile phase at a 1.0 mL/min flux rate, using a UV detector set up at $\lambda = 254$ nm. The retention time for the major isomer is 25.75 min and for the minor isomer is 34.40 min.

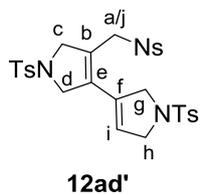


Compound **12ac** (33% yield, ee >99%), colourless solid. **MW**: 628.77 g/mol; **m.p.**: 100-102 $^{\circ}C$; **IR (ATR) ν (cm^{-1})**: 2921, 1340, 1157; 1H NMR (300 MHz, $CDCl_3$) δ (ppm): 2.45 (s, $3H_{Ts}$), 2.47 (s, $3H_{Ts}$), 3.31 (d, $^2J = 10.8$ Hz, $1H_d$), 3.39 (dt, $^4J = 2.1$ Hz / $^2J = 13.5$ Hz, $1H_c$), 3.67 (dt, $^4J = 2.1$ Hz / $^2J = 13.5$ Hz, $1H_c$), 3.88-3.90 (m, $3H_{OMe}+1H_d$), 4.07-4.13 (m, $2H_g$), 4.17 (m, $1H_h$), 4.33 (m, $1H_h$), 5.40 (m, $1H_a$), 5.63 (m, $1H_j$), 5.67 (m, $1H_i$), 6.85 (d, $^3J = 9.0$ Hz, $2H_{p-OMePh}$), 7.34 (d, $^3J = 8.4$ Hz, $2H_{Ts}$), 7.36 (d, $^3J = 8.4$ Hz, $2H_{Ts}$), 7.48 (d, $^3J = 9.0$ Hz, $2H_{p-OMePh}$), 7.57 (d, $^3J = 8.4$ Hz, $2H_{Ts}$), 7.74 (d, $^3J = 8.4$ Hz, $2H_{Ts}$); ^{13}C NMR (75 MHz, $CDCl_3$) δ (ppm): 21.7 (C_{Ts}), 21.8 (C_{Ts}), 52.9 (C_c), 55.3 (C_d), 55.9

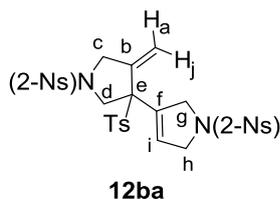
(C_g), 55.9 (C_{OMe}), 74.0 (C_{e,h}), 114.2 (2C_{p-OMePh}), 116.3 (C_{ajl}), 126.6 (C_q), 127.7 (2C_{Ts}), 128.0 (2C_{Ts}), 129.0 (C_i), 130.1 (4C_{Ts}), 131.5 (C_q), 132.6 (C_q), 133.1 (2C_{p-OMePh}), 133.8 (C_q), 139.2 (C_q), 144.1 (C_{Ts}), 144.7 (C_{Ts}), 164.8 (C_{p-OMePh}); **ESI-HRMS (m/z)**: calculated for [M+Na]⁺: 651.1264; experimental: 651.1286. The enantiomeric excess has been determined by **HPLC** analysis using a CHIRALPAK AD-H column (4.6 x 250 mm, 5 μm) with 10 % hexane / 90 % 2-PrOH mobile phase at a 1.0 mL/min flux rate, using a UV detector set up at λ = 254 nm. The retention time for the minor isomer is 33.77 min and for the major isomer is 44.69 min. [α]_D²⁰ +16.36 (c 0.22 g /100 mL, CH₂Cl₂).



Compound **12ad** (20% yield¹¹⁸, ee >99%) and **12ad'** (14% yield¹¹⁸) were obtained as an inseparable mixture of colourless solid. **MW**: 643.75 g/mol; **IR (ATR) ν (cm⁻¹)**: 2922, 1345, 1158; **¹H NMR (400 MHz, CDCl₃) δ (ppm)**: 2.45 (s, 3H_{Ts}), 2.46 (s, 3H_{Ts}), 3.15 (d, ²J = 11.3 Hz, 1H_d), 3.44 (dt, ⁴J = 2.0 Hz / ²J = 13.5 Hz, 1H_c), 3.48 (dt, ⁴J = 2.3 Hz / ²J = 13.5 Hz, 1H_c), 4.12 (d, ²J = 11.3 Hz, 1H_d), 4.13-4.17 (m, 2H_g), 4.42-4.38 (m, 2H_h), 5.50 (m, 1H_a), 5.72 (m, 1H_j), 5.86 (m, 1H_i), 7.33-7.38 (m, 4H_{Ts}), 7.53 (d, ³J = 8.4 Hz, 2H_{Ts}), 7.73 (d, ³J = 8.4 Hz, 2H_{Ts}), 7.90 (d, ³J = 9.0 Hz, 2H_{Ns}), 8.27 (d, ³J = 9.0 Hz, 2H_{Ns}); **ESI-HRMS (m/z)**: calculated for [M+Na]⁺: 666.1009; experimental: 666.0994. The enantiomeric excess has been determined by **HPLC** analysis using a CHIRALPAK AD-H column (4.6 x 250 mm, 5 μm) with 10 % hexane / 90 % 2-PrOH mobile phase at a 1.0 mL/min flux rate, using a UV detector set up at λ = 254 nm. The retention time for the major isomer is 27.9 min and for the minor isomer is 32.1 min.

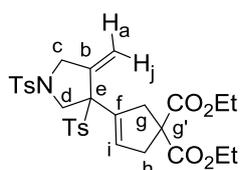


A small sample of pure **12ad'** could be isolated by column chromatography and characterised: **MW**: 643.75 g/mol; **m.p.**: 80-82°C; **¹H NMR (400 MHz, CDCl₃) δ (ppm)**: 2.44 (s, 3H_{Ts}), 2.45 (s, 3H_{Ts}), 3.87 (br s, 2H_{ajl}), 4.04-4.05 (m, 2H_h), 4.10-4.11 (m, 2H_g), 4.17-4.18 (m, 2H_{d/c}), 4.31-4.32 (m, 2H_{d/c}), 5.64 (m, 1H_i), 7.34-7.39 (m, 4H_{Ts}), 7.70 (d, ³J = 8.3 Hz, 2H_{Ts}), 7.72 (d, ³J = 8.3 Hz, 2H_{Ts}), 7.89 (d, ³J = 8.8 Hz, 2H_{Ns}), 8.28 (d, ³J = 8.8 Hz, 2H_{Ns}); **ESI-HRMS (m/z)**: calculated for [M+Na]⁺: 666.1009; experimental: 666.0994.

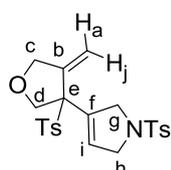


Compound **12ba** (43% yield, 69% ee), colourless solid. **MW**: 674.71 g/mol; **m.p.**: 112-114 °C; **IR (ATR) ν (cm⁻¹)**: 2921, 1540, 1352, 1164; **¹H NMR (300 MHz, CDCl₃) δ (ppm)**: 2.45 (s, 3H_{Ts}), 3.71 (d, ²J = 11.7 Hz, 1H_d), 3.78 (dt, ⁴J = 2.4 Hz / ²J = 13.8 Hz, 1H_c), 4.06 (dt, ⁴J = 2.1 Hz / ²J = 13.8 Hz, 1H_c), 4.27 (d, ³J = 11.7 Hz, 1H_d), 4.31-4.35 (m, 2H_g), 4.39 (m, 1H_h), 4.51 (m, 1H_h),

5.53 (m, 1H_a), 5.79-5.81 (m, 2H_{ij}), 7.31 (d, ³J = 8.4 Hz, 2H_{Ts}), 7.63-7.68 (m, 2H_{Ts}+2H_{2-Ns}), 7.72-7.77 (m, 4H_{2-Ns}), 7.92 (m, 1H_{2-Ns}), 8.00 (m, 1H_{2-Ns}); ¹³C NMR (75 MHz, CDCl₃) δ (ppm): 21.9 (C_{Ts}), 52.8 (C_c), 55.3 (C_d), 55.4 (C_{g/h}), 55.4 (C_{g/h}), 74.0 (C_e), 116.8 (C_{afj}), 124.4 (2C_{2-Ns}), 129.3 (C_i), 129.9 (2C_{Ts}), 130.3 (C_{2-Ns}), 130.6 (2C_{Ts}), 130.9 (C_{2-Ns}), 131.0 (C_q), 131.8 (C_q), 131.9 (C_{2-Ns}), 131.9 (C_{2-Ns}), 132.1 (C_q), 134.0 (2C_{2-Ns}), 138.7 (C_q), 146.3 (C_q), 148.4 (C_q), 148.5 (C_q); **ESI-MS (m/z)**: 675.0 [M+H]⁺, 697.0 [M+Na]⁺; **ESI-HRMS (m/z)**: calculated for [M+Na]⁺: 697.0703, for [M+K]⁺: 713.0443; experimental: 697.0708, 713.0434. The enantiomeric excess has been determined by **HPLC** analysis using a CHIRALPAK AD-H column (4.6 x 250 mm, 5 μm) with 70 % hexane / 30 % 2-PrOH mobile phase at a 1.0 mL/min flux rate, using a UV detector set up at λ = 254 nm. The retention time for the major isomer is 30.49 min and for the minor isomer is 21.14 min. [α]_D²⁰ +17.46 (c 0.35 g /100 mL, CH₂Cl₂).

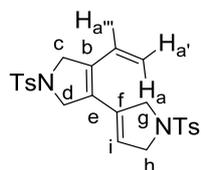
**12ca**

Compound **12ca** (45% yield, 96% ee), waxy colourless solid. **MW**: 601.73 g/mol; **IR (ATR) ν (cm⁻¹)**: 2922, 1728, 1347, 1159; **¹H NMR (400 MHz, CDCl₃) δ (ppm)**: 1.25 (t, ³J = 7.2 Hz, 3H_{CO₂CH₂CH₃}), 1.26 (t, ³J = 7.2 Hz, 3H_{CO₂CH₂CH₃}), 2.44 (s, 3H_{Ts}), 2.46 (s, 3H_{Ts}), 3.01-3.03 (m, 2H_g), 3.14-3.30 (m, 2H_h), 3.43 (dt, ⁴J = 2.0 Hz / ²J = 12.0 Hz, 1H_c), 3.45 (d, ²J = 10.8 Hz, 1H_d), 3.73 (dt, ⁴J = 2.0 Hz / ²J = 12.0 Hz, 1H_c), 3.92 (d, ²J = 10.8 Hz, 1H_d), 4.19 (q, ³J = 7.2, 2H_{CO₂CH₂CH₃}), 4.21 (q, ³J = 7.2, 4H_{CO₂CH₂CH₃}), 5.42 (m, 1H_a), 5.63 (m, 1H_i), 5.70 (m, 1H_j), 7.25 (d, ³J = 8.0 Hz, 2H_{Ts}), 7.33 (d, ³J = 8.0 Hz, 2H_{Ts}), 7.60 (d, ³J = 8.0 Hz, 4H_{Ts}); ¹³C NMR (75 MHz, CDCl₃) δ (ppm): 14.1 (2C_{CO₂CH₂CH₃}), 21.8 (2C_{Ts}), 40.4 (C_g), 41.5 (C_h), 53.0 (C_c), 55.1 (C_d), 59.2 (C_g), 61.9 (2C_{CO₂CH₂CH₃}), 75.0 (C_e), 116.4 (C_{afj}), 128.0 (2C_{Ts}), 129.4 (2C_{Ts}), 130.0 (2C_{Ts}), 131.0 (2C_{Ts}), 131.6 (C_i), 131.7 (C_q), 132.8 (C_q), 133.9 (C_q), 139.3 (C_b), 144.3 (C_q), 145.4 (C_{Ts}), 171.4 (C_{CO₂Et}), 171.7 (C_{CO₂Et}); **ESI-MS (m/z)**: 466.1 [M-TsH+H]⁺, 602.1 [M+H]⁺; **ESI-HRMS (m/z)**: calculated for [M+Na]⁺: 624.1696; experimental: 624.1704; The enantiomeric excess has been determined by **HPLC** analysis using a CHIRALPAK AD-H column (4.6 x 250 mm, 5 μm) with 70 % hexane / 30 % 2-PrOH mobile phase at a 1.0 mL/min flux rate, using a UV detector set up at λ = 254 nm. The retention time for the major isomer is 22.6 min and for the minor isomer is 20.6 min. [α]_D²⁰ +22.53 (c 0.25 g /100 mL, CH₂Cl₂).

**12da**

Compound **12da** (44% yield, 93% ee), colourless solid. **MW**: 459.57 g/mol; **m.p.**: 72-74 °C; **IR (ATR) ν (cm⁻¹)**: 2920, 1342, 1158; **¹H NMR (300 MHz, CDCl₃) δ (ppm)**: 2.43 (s, 3H_{Ts}), 2.45 (s, 3H_{Ts}), 3.85 (d, ²J = 10.5 Hz, 1H_d), 4.01 (dt, ⁴J = 2.1 Hz / ²J = 13.2 Hz, 1H_c), 4.14-4.22 (m, 3H_{c,g,g}), 4.32-4.39 (m, 2H_h), 3.54 (d, ²J = 10.5 Hz, 1H_d), 5.41 (m, 1H_a), 5.59 (m, 1H_j), 5.70 (m, 1H_i), 7.22 (d, ³J = 8.4 Hz, 2H_{Ts}), 7.37 (d, ³J = 8.1 Hz, 2H_{Ts}), 7.51 (d, ³J = 8.1 Hz, 2H_{Ts}), 7.76 (d, ³J = 8.4 Hz, 2H_{Ts}); ¹³C NMR (75 MHz, CDCl₃) δ (ppm): 21.6 (C_{Ts}), 21.7 (C_{Ts}), 55.1 (C_g), 55.5 (C_h), 72.6 (C_c), 74.8 (C_d), 75.0 (C_e), 113.4 (C_{afj}), 127.6 (2C_{Ts}), 128.3 (C_i), 129.3 (2C_{Ts}), 129.9 (2C_{Ts}), 130.7 (2C_{Ts}), 132.7 (C_{Ts}), 132.7 (C_q),

133.8 (C_q), 142.2 (C_q), 143.8 (C_q), 145.4 (C_q); **ESI-MS (m/z)**: 304.1 [M-TsH+H]⁺, 460.0 [M+H]⁺; **ESI-HRMS (m/z)**: calculated for [M+Na]⁺: 482.1066; experimental: 482.1075. The enantiomeric excess has been determined by **HPLC** analysis using a CHIRALPAK AD-H column (4.6 x 250 mm, 5 μm) with 60 % hexane / 40 % 2-PrOH mobile phase at a 1.0 mL/min flux rate, using a UV detector set up at λ = 254 nm. The retention time for the major isomer is 27.50 min and for the minor isomer is 22.52 min. **[α]_D²⁰** +16.36 (c 0.22 g /100 mL, CH₂Cl₂).



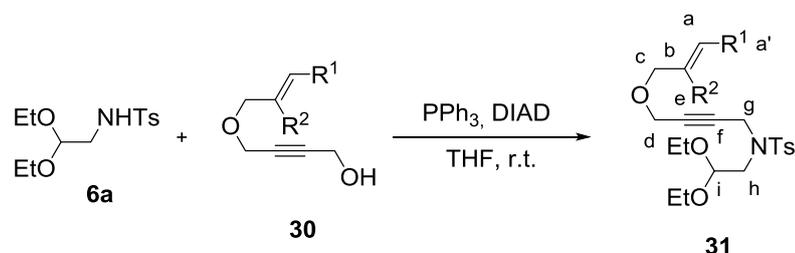
27

Compound **27**¹¹⁹ (63% yield), colourless solid. **MW**: 470.60 g/mol; **m.p.**: 110-111 °C; **IR (ATR) ν (cm⁻¹)**: 2922, 1337, 1158; **¹H NMR (400 MHz, CDCl₃) δ (ppm)**: 2.43 (s, 6H_{Ts}), 4.13-4.15 (m, 2H_h), 4.19-4.21 (m, 2H_d), 4.27-4.28 (m, 2H_c), 4.33-4.35 (m, 2H_g), 5.13 (d, ³J = 17.2 Hz, 1H_a), 5.29 (d, ³J = 11.0 Hz, 1H_{a'}), 5.54 (s, 1H_i), 6.45 (dd, ³J = 11.0 Hz / ³J = 17.2 Hz, 1H_{a''}), 7.32 (d, ³J = 8.0 Hz, 4H_{Ts}), 7.71 (d, ³J = 8.0 Hz, 4H_{Ts}); **¹³C NMR (100 MHz, CDCl₃) δ (ppm)**: 21.7 (2C_{Ts}), 54.2 (C_h), 55.3 (C_g), 55.5 (C_c), 56.6 (C_d), 119.5 (C_{a/a'}), 125.1 (C_i), 126.2 (C_e), 127.5 (2C_{Ts}), 127.6 (2C_{Ts}), 128.0 (C_{a''}), 130.1 (2C_{Ts}), 130.1 (2C_{Ts}), 131.8 (C_f), 132.8 (C_b), 133.7 (C_{Ts}), 134.0 (C_{Ts}), 144.0 (C_{Ts}), 144.0 (C_{Ts}); **ESI-MS (m/z)**: 471.1 [M+H]⁺; **ESI-HRMS (m/z)**: calculated for [M+Na]⁺: 493.1226; experimental: 493.1221.

8.3. Experimental procedure for the products synthesised in Chapter 4

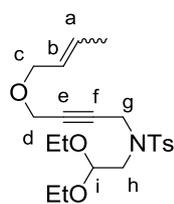
8.3.1. Synthesis of substrates

8.3.1.1. Synthesis of acetal 31a, 31i, 31j and 31k



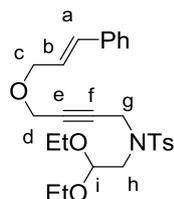
- 31a** ($R^1=R^2=H$), 74% yield
31i ($R^1=CH_3$, $R^2=H$), 65% yield
31j ($R^1=Ph$, $R^2=H$), 54% yield
31k ($R^1=H$, $R^2=CH_3$), 85% yield

General procedure for 31. 2,2-diethoxy-*N*-tosylethanamine **6a** (1.66 g, 5.76 mmol) was added to a solution of 4-(allyloxy)but-2-yn-1-ol **30**¹²⁰ (0.73 g, 5.76 mmol) and PPh_3 (1.97 g, 7.51 mmol) in THF (100 mL) at room temperature under N_2 . After 10 minutes, diisopropylazodicarboxylate (DIAD, 1.51 mL, 7.67 mmol) was added and the resulting reaction mixture was stirred for 24 hours. After adding water, extraction was performed with Et_2O (3 x 50 mL). The combined organic layers were washed with brine, dried over anhydrous Na_2SO_4 and concentrated under reduce pressure. The oily residue was purified by column chromatography on silica gel (hexane/ethyl acetate, 10:0 to 8:2) to afford **31a** as colourless oil (1.68 g, 74 %). R_f (hexane/ethyl acetat 7:3): 0.50; **MW**: 395.51 g/mol; **IR (ATR) v (cm⁻¹)**: 2976, 2915, 1347, 1160; **¹H NMR (300 MHz, CDCl₃) δ (ppm)**: 1.21 (t, $^3J = 7.2$ Hz, 6H_{OCH₂CH₃}), 2.40 (s, 3H_{TS}), 3.25 (d, $^3J = 5.7$ Hz, 2H_h), 3.56 (dq, $^2J = 9.3$ Hz / $^3J = 7.2$ Hz, 2H_{OCH₂CH₃}), 3.73 (dq, $^2J = 9.3$ Hz / $^3J = 7.2$ Hz, 2H_{OCH₂CH₃}), 3.81 (dt, $^3J = 5.7$ Hz / $^4J = 1.2$ Hz, 2H_c), 3.87 (t, $^5J = 1.8$ Hz, 2H_{d/g}), 4.33 (t, $^5J = 1.8$ Hz, 2H_{d/g}), 4.69 (t, $^3J = 5.7$ Hz, H_i), 5.16-5.25 (m, 2H_{a/a'}), 5.80 (ddt, $^3J = 5.7$ Hz / $^3J = 10.3$ Hz / $^3J = 17.1$ Hz, H_b), 7.28 (d, $^3J = 8.1$ Hz, 2H_{TS}), 7.74 (d, $^3J = 8.1$ Hz, 2H_{TS}); **¹³C NMR (75 MHz, CDCl₃) δ (ppm)**: 15.3 (2C_{OCH₂CH₃}), 21.5 (C_{TS}), 38.6 (C_g), 48.5 (C_h), 56.9 (C_d), 63.3 (2C_{OCH₂CH₃}), 70.2 (C_c), 79.6 (C_{e/f}), 81.2 (C_{e/f}), 102.7 (C_i), 117.6 (C_a), 127.7 (2C_{TS}), 129.4 (2C_{TS}), 133.8 (C_b), 136.1 (C_{TS}), 143.4 (C_{TS}); **ESI-MS (m/z)**: 418.2 [M+Na]⁺, 434.1 [M+K]⁺; **EA**: calculated for C₂₀H₂₉NO₅S: C, 60.74; H, 7.39; N, 3.54; found: C, 60.61 and 60.60; H, 7.12 and 7.45; N, 3.56 and 3.62.



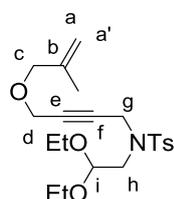
A mixture of (*Z*) and (*E*)-4-(but-2-en-1-yloxy)but-2-yn-1-ol **30i** starting material was prepared in a 1.0:5.1 ratio following a previously reported procedure.¹²¹

Using the same experimental procedure as for compound **31a**, **31i** was obtained as a colourless oil (1.77 g, 65% yield) after 3 hours. R_f (hexane/ethyl acetat 7:3): 0.71; **MW**: 409.54 g/mol; **IR (ATR) ν (cm^{-1})**: 2975, 2928, 2883, 1346, 1159; **$^1\text{H NMR}$ (400 MHz, CDCl_3) δ (ppm)**: 1.22 (t, $^3J = 6.8$ Hz, $6\text{H}_{\text{OCH}_2\text{CH}_3}$), 1.71 (d, $^3J = 6.4$ Hz 3H_{CH_3}), 2.41 (s, 3H_{Ts}), 3.25 (d, $^3J = 5.6$ Hz, 2H_h), 3.53-3.61 (m, $2\text{H}_{\text{OCH}_2\text{CH}_3}$), 3.72-3.77 (m, $4\text{H}_{\text{OCH}_2\text{CH}_3,c}$), 3.85 (s, 2H_g), 4.33 (s, 2H_d), 4.69 (t, $^3J = 5.6$ Hz, H_i), 5.49 (m, $\text{H}_{a/b}$), 5.66 (m, $\text{H}_{a/b}$), 7.29 (d, $^3J = 8.0$ Hz, 2H_{Ts}), 7.74 (d, $^3J = 8.0$ Hz, 2H_{Ts}); **$^{13}\text{C NMR}$ (100 MHz, CDCl_3) δ (ppm)**: 15.4 ($2\text{C}_{\text{OCH}_2\text{CH}_3}$), 17.9 (C_{CH_3}), 21.6 (C_{Ts}), 38.8 (C_g), 48.7 (C_h), 56.8 (C_d), 63.5 ($2\text{C}_{\text{OCH}_2\text{CH}_3}$), 70.1 (C_c), 79.6 (C_{eff}), 81.4 (C_{eff}), 102.9 (C_i), 130.5 (C_a), 127.8 (2C_{Ts}), 129.5 (2C_{Ts}), 130.5 (C_b), 136.3 (C_{Ts}), 143.5 (C_{Ts}); **ESI-HRMS (m/z)**: calculated for $[\text{M}+\text{Na}]^+$: 432.1815; experimental: 432.1823.



31j The starting material, 4-(cinnamyloxy)but-2-yn-1-ol **30j**, was prepared following a previously published procedure.¹²²

Using the same experimental procedure as for compound **31a**, **31j** was obtained as a colourless oil (1.12 g, 54% yield) after 24 hours. R_f (hexane/ethyl acetat 7:3): 0.46; **MW**: 471.61 g/mol; **IR (ATR) ν (cm^{-1})**: 2976, 2930, 2885, 1347, 1160; **$^1\text{H NMR}$ (400 MHz, CDCl_3) δ (ppm)**: 1.22 (t, $^3J = 6.9$ Hz, $6\text{H}_{\text{OCH}_2\text{CH}_3}$), 2.35 (s, 3H_{Ts}), 3.27 (d, $^3J = 5.6$ Hz, 2H_h), 3.56 (dq, $^2J = 9.4$ Hz / $^3J = 7.0$ Hz, $2\text{H}_{\text{OCH}_2\text{CH}_3}$), 3.75 (dq, $^2J = 9.4$ Hz / $^3J = 7.0$ Hz, $2\text{H}_{\text{OCH}_2\text{CH}_3}$), 3.92 (t, $^5J = 1.6$ Hz, 2H_g), 3.99 (d, $^3J = 7.2$ Hz, 2H_c), 4.35 (s, 2H_d), 4.70 (t, $^3J = 5.6$ Hz, H_i), 6.19 (dt, $^3J = 16.0$ Hz / $^3J = 6.0$ Hz, H_b), 6.55 (d, $^3J = 16.0$ Hz, H_a), 7.27 (d, $^3J = 7.4$ Hz, 2H_{Ts}), 7.28 (m, H_{Ph}), 7.30-7.34 (m, 2H_{Ph}), 7.38 (d, $^3J = 7.2$ Hz, 2H_{Ph}), 7.76 (d, $^3J = 7.4$ Hz, 2H_{Ts}); **$^{13}\text{C NMR}$ (100 MHz, CDCl_3) δ (ppm)**: 15.4 ($\text{C}_{\text{OCH}_2\text{CH}_3}$), 21.7 (C_{Ts}), 38.8 (C_g), 48.7 (C_h), 57.0 (C_d), 63.5 ($2\text{C}_{\text{OCH}_2\text{CH}_3}$), 72.3 (C_c), 79.9 (C_{eff}), 81.3 (C_{eff}), 103.9 (C_i), 125.0, 126.6, 127.8, 127.9, 128.7, 129.5, 133.3, 136.2, 136.5, 143.5; **ESI-MS (m/z)**: 494.2 $[\text{M}+\text{Na}]^+$; **ESI-HRMS (m/z)**: calculated for $[\text{M}+\text{Na}]^+$: 494.1972; experimental: 494.1992.

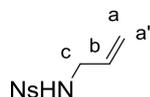


31k The starting compound, 4-((2-methylallyl)oxy)but-2-yn-1-ol **30k**, was prepared as described in a previous publication.¹²³

Using the same experimental procedure as for compound **31a**, **31k** was obtained as a colourless oil (1.77 g, 85% yield) after 2 hours. R_f (hexane/ethyl acetat 7:3): 0.54; **MW**: 409.54 g/mol; **IR (ATR) ν (cm^{-1})**: 2977, 2930, 1342, 1158; **$^1\text{H NMR}$ (400 MHz, CDCl_3) δ (ppm)**: 1.21 (t, $^3J = 7.2$ Hz, $6\text{H}_{\text{OCH}_2\text{CH}_3}$), 1.69 (s, 3H_{CH_3}), 2.40 (s, 3H_{Ts}), 3.25 (d, $^3J = 5.6$ Hz, 2H_h), 3.57 (dq, $^2J = 9.4$ Hz / $^3J = 7.2$ Hz, $2\text{H}_{\text{OCH}_2\text{CH}_3}$), 3.74 (dq, $^2J = 9.4$ Hz / $^3J = 7.2$ Hz, $2\text{H}_{\text{OCH}_2\text{CH}_3}$), 3.73 (s, 2H_g), 3.85 (t, $^4J = 1.6$ Hz, 2H_c), 4.33 (t, $^5J = 1.8$ Hz, 2H_d), 4.69 (t, $^3J = 5.6$ Hz, H_i), 4.88-4.89 (m, $2\text{H}_{a,a'}$), 7.28 (d, $^3J = 8.2$ Hz, 2H_{Ts}), 7.74

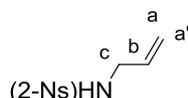
(d, $^3J = 8.2$ Hz, $2H_{Ts}$); ^{13}C NMR (100 MHz, $CDCl_3$) δ (ppm): 15.4 ($2C_{OCH_2CH_3}$), 19.5 (C_{CH_3}), 21.6 (C_{Ts}), 38.8 (C_g), 48.7 (C_h), 56.9 (C_d), 63.5 ($2C_{CO_2CH_2CH_3}$), 73.4 (C_c), 79.6 (C_{eff}), 81.4 (C_{eff}), 102.9 (C_i), 112.9 (C_a), 127.8 ($2C_{Ts}$), 129.5 ($2C_{Ts}$), 136.3 (C_{Ts}), 141.4 (C_b), 143.5 (C_{Ts}); **ESI-HRMS (m/z)**: calculated for $[M+Na]^+$: 432.1815; experimental: 432.1820.

8.3.1.2. Synthesis of acetals 31b, 31c and 31d



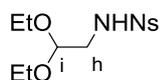
33d

General procedure for 33. Triethylamine (1.0 mL, 7.6 mmol) and allylamine (0.3 mL, 7.6 mmol) were added to a solution of 4-nitrobenzenesulfonyl chloride (1.53 g, 6.9 mmol) in anhydrous CH_2Cl_2 (30 mL) and the resulting solution was stirred at room temperature for 20 minutes (TLC monitoring). The crude was subsequently washed with a 1M aqueous solution of hydrochloric acid (3 x 50 mL), a saturated aqueous solution of sodium bicarbonate (3 x 50 mL) and water (3 x 50 mL), dried over anhydrous Na_2SO_4 and concentrated under reduced pressure to afford **33d** as a colourless solid (1.49 g, 89%). **MW**: 242.25 g/mol; **m.p.**: 114-116 °C; **IR (ATR) ν (cm^{-1})**: 3255, 3103, 1520, 1310, 1159; 1H NMR (300 MHz, $CDCl_3$) δ (ppm): 3.69 (dddd, $^3J = 6.0$ Hz / $^3J = 6.0$ Hz / $^4J = 1.5$ Hz / $^4J = 1.5$ Hz, $2H_c$), 4.77 (t, $^3J = 6.0$ Hz, H_{NH}), 5.11-5.16 (m, $2H_{a/a'}$), 5.70 (ddt, $^3J = 5.7$ Hz / $^3J = 10.2$ Hz / $^3J = 17.2$ Hz, H_b), 8.08 (d, $^3J = 9.0$ Hz, $2H_{Ns}$), 8.38 (d, $^3J = 9.0$ Hz, $2H_{Ns}$); ^{13}C NMR (75 MHz, $CDCl_3$) δ (ppm): 45.9 (C_c), 118.5 (C_a), 124.6 ($2C_{Ns}$), 128.5 ($2C_{Ns}$), 132.4 (C_b), 146.1 (C_{Ns}), 150.19 (C_{Ns}); **ESI-MS (m/z)**: 265.0 $[M+Na]^+$; **EA**: calculated for $C_9H_{10}N_2O_4S$: C, 44.62; H, 4.16; N, 11.56; found: C, 44.80 and 44.74; H, 3.93 and 3.92; N, 11.42 and 11.52.



33b

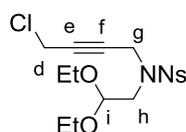
Using the same experimental procedure as for compound **33d**, **33b** was obtained as a colourless solid (0.82 g, 75% yield) after 1 hour. **MW**: 242.25 g/mol; **m.p.**: 71-72°C; **IR (ATR) ν (cm^{-1})**: 3341, 1549, 1409, 1346, 1172; 1H NMR (400 MHz, $CDCl_3$) δ (ppm): 3.77 (dddd, $^3J = 6.0$ Hz / $^3J = 5.7$ Hz / $^4J = 1.5$ Hz / $^4J = 1.5$ Hz, $2H_c$), 5.11 (ddt, $^3J = 10.2$ Hz / $^2J = 1.5$ Hz / $^4J = 1.5$ Hz, H_a), 5.21 (ddt, $^3J = 17.1$ Hz / $^2J = 1.5$ Hz / $^4J = 1.5$ Hz, H_a), 5.42 (t, $^3J = 6.0$ Hz, H_{NH}), 5.74 (ddt, $^3J = 17.1$ Hz / $^3J = 10.2$ Hz / $^3J = 5.7$ Hz, H_b), 7.73-7.78 (m, $2H_{2-Ns}$), 7.86 (m, H_{2-Ns}), 8,12 (m, H_{2-Ns}); ^{13}C NMR (75 MHz, $CDCl_3$) δ (ppm): 46.3 (C_c), 118.1 (C_a), 125.5 (C_{2-Ns}), 131.0 (C_{2-Ns}), 131.1 (C_{2-Ns}), 132.5 (C_b), 132.6 (C_{2-Ns}), 133.9 (C_{2-Ns}), 148.0 (C_{2-Ns}); **ESI-MS (m/z)**: 243.0 $[M+H]^+$, 265.0 $[M+Na]^+$; **EA**: calculated for $C_9H_{10}N_2O_4S$: C, 44.62; H, 4.16; N, 11.56; found: C, 44.69 and 44.84; H, 4.13 and 4.11; N, 11.28 and 11.35.



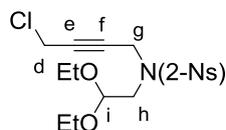
6d

Triethylamine (1.0 mL, 7.6 mmol) and aminoacetaldehyde diethyl acetal (1.1 mL, 7.6 mmol) were added to a solution of 4-nitrobenzenesulfonyl chloride (1.52 g, 6.9 mmol) in anhydrous CH_2Cl_2 (30 mL) and the resulting solution was stirred at room temperature for 20 minutes (TLC monitoring). The crude was subsequently washed with a 1M aqueous solution of hydrochloric acid (3 x

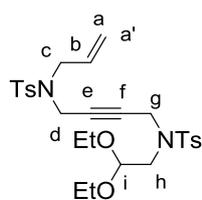
50 mL), a saturated aqueous solution of sodium bicarbonate (3 x 50 mL) and water (3 x 50 mL), dried over anhydrous Na_2SO_4 and concentrated under reduced pressure to afford **6d** as a colourless solid (2.02 g, 93%). **MW**: 318.34 g/mol; **m.p.**: 84–85°C; **IR (ATR) ν (cm^{-1})**: 3200, 3099, 2980, 2895, 1526, 1345, 1164; **$^1\text{H NMR}$ (300 MHz, CDCl_3) δ (ppm)**: 1.17 (t, $^3J = 7.2$ Hz, $6\text{H}_{\text{OCH}_2\text{CH}_3}$), 3.25 (dd, $^3J = 6.3$ Hz / $^3J = 5.6$ Hz, 2H_h), 3.48 (dq, $^2J = 9.3$ Hz / $^3J = 7.2$ Hz, $2\text{H}_{\text{OCH}_2\text{CH}_3}$), 3.66 (dq, $^2J = 9.3$ Hz / $^3J = 7.2$ Hz, $2\text{H}_{\text{OCH}_2\text{CH}_3}$), 4.50 (t, $^3J = 5.4$ Hz, H_i), 4.87 (t, $^3J = 5.6$ Hz, H_{NH}), 8.06 (d, $^3J = 9.0$ Hz, 2H_{Ns}), 8.37 (d, $^3J = 9.0$ Hz, 2H_{Ns}); **$^{13}\text{C NMR}$ (75 MHz, CDCl_3) δ (ppm)**: 15.3 ($\text{C}_{\text{OCH}_2\text{CH}_3}$), 45.9 (C_h), 63.4 ($2\text{C}_{\text{OCH}_2\text{CH}_3}$), 100.6 (C_i), 124.5 (2C_{Ns}), 128.4 (2C_{Ns}), 145.9 (C_{Ns}), 150.1 (C_{Ns}); **ESI-MS (m/z)**: 341.1 [$\text{M}+\text{Na}$] $^+$; **EA**: calculated for $\text{C}_{12}\text{H}_{18}\text{N}_2\text{O}_6\text{S}$: C, 45.28; H, 5.70; N, 8.80; found: C, 45.61 and 45.49; H, 5.73 and 5.75; N, 8.77 and 8.76.

**17d**

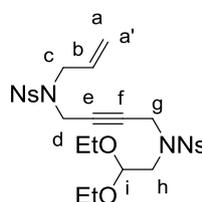
A mixture of **6d** (1.89 g, 5.9 mmol), 1,4-dichloro-2-butene (2.32 mL, 23.8 mmol) and anhydrous potassium carbonate (4.93 g, 35.7 mmol) in acetonitrile (100 mL) was stirred at reflux for 15 hours (TLC monitoring). The mixture was cooled to room temperature, salts were filtered off, and the solvent removed under reduced pressure. The oily residue was purified by column chromatography on silica gel (hexane/ethyl acetate, 10:0 to 7:3) to afford **17d** as a colourless oil (1.65 g, 68%). **R_f** (hexane/ethyl acetate 7:3): 0.55; **MW**: 404.86 g/mol; **IR (ATR) ν (cm^{-1})**: 2977, 2885, 1529, 1348, 1163; **$^1\text{H NMR}$ (300 MHz, CDCl_3) δ (ppm)**: 1.23 (t, $^3J = 7.2$ Hz, $6\text{H}_{\text{OCH}_2\text{CH}_3}$), 3.26 (d, $^3J = 5.6$ Hz, 2H_h), 3.58 (dq, $^2J = 9.3$ Hz / $^3J = 6.9$ Hz, $2\text{H}_{\text{OCH}_2\text{CH}_3}$), 3.76 (dq, $^2J = 9.3$ Hz / $^3J = 7.2$ Hz, $2\text{H}_{\text{OCH}_2\text{CH}_3}$), 3.87 (t, $^5J = 2.1$ Hz, $2\text{H}_{d/g}$), 4.41 (t, $^5J = 2.1$ Hz, $2\text{H}_{d/g}$), 4.69 (t, $^3J = 5.6$ Hz, H_i), 8.07 (d, $^3J = 9.0$ Hz, 2H_{Ns}), 8.37 (d, $^3J = 9.0$ Hz, 2H_{Ns}); **$^{13}\text{C NMR}$ (75 MHz, CDCl_3) δ (ppm)**: 15.3 ($\text{C}_{\text{OCH}_2\text{CH}_3}$), 15.4 ($\text{C}_{\text{OCH}_2\text{CH}_3}$), 29.7 (C_d), 38.9 (C_g), 48.9 (C_h), 63.8 ($2\text{C}_{\text{OCH}_2\text{CH}_3}$), 79.5 ($\text{C}_{e/f}$), 80.6 ($\text{C}_{e/f}$), 102.7 (C_i), 124.3 (2C_{Ns}), 129.0 (2C_{Ns}), 144.8 (C_{Ns}), 150.3 (C_{Ns}); **ESI-MS (m/z)**: 427.1 [$\text{M}+\text{Na}$] $^+$; **EA**: calculated for $\text{C}_{16}\text{H}_{21}\text{ClN}_2\text{O}_6\text{S}$: C, 47.47; H, 5.23; N, 6.92; found: C, 47.82; H, 5.31; N, 6.90.

**17b**

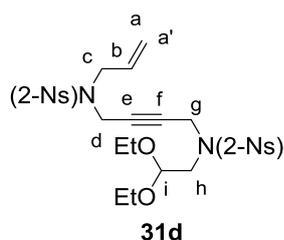
Using the same experimental procedure as for compound **17d**, **17b** was obtained as a waxy dark brown solid (1.45 g, 42% yield) after 3 hours. **R_f** (hexane/ethyl acetate 7:3): 0.58; **MW**: 404.86 g/mol; **IR (ATR) ν (cm^{-1})**: 2976, 2888, 1543, 1357, 1162, 1057; **$^1\text{H NMR}$ (300 MHz, CDCl_3) δ (ppm)**: 1.20 (t, $^3J = 6.9$ Hz, $6\text{H}_{\text{OCH}_2\text{CH}_3}$), 3.47 (d, $^3J = 5.7$ Hz, 2H_h), 3.53 (dq, $^2J = 9.3$ Hz / $^3J = 6.9$ Hz, $2\text{H}_{\text{OCH}_2\text{CH}_3}$), 3.73 (dq, $^2J = 9.3$ Hz / $^3J = 6.9$ Hz, $2\text{H}_{\text{OCH}_2\text{CH}_3}$), 3.97 (t, $^5J = 2.1$ Hz, 2H_g), 4.43 (t, $^5J = 2.1$ Hz, 2H_d), 4.63 (t, $^3J = 5.7$ Hz, H_i), 7.65 (m, $\text{H}_{2-\text{Ns}}$), 7.69–7.73 (m, $2\text{H}_{2-\text{Ns}}$), 8.05 (m, $\text{H}_{2-\text{Ns}}$); **$^{13}\text{C NMR}$ (75 MHz, CDCl_3) δ (ppm)**: 15.3 ($\text{C}_{\text{OCH}_2\text{CH}_3}$), 15.4 ($\text{C}_{\text{OCH}_2\text{CH}_3}$), 29.9 (C_d), 38.9 (C_g), 49.0 (C_h), 63.8 ($2\text{C}_{\text{OCH}_2\text{CH}_3}$), 80.2 ($\text{C}_{e/f}$), 80.3 ($\text{C}_{e/f}$), 102.7 (C_i), 124.3 ($\text{C}_{2-\text{Ns}}$), 130.7 ($\text{C}_{2-\text{Ns}}$), 131.7 ($\text{C}_{2-\text{Ns}}$), 132.8 ($\text{C}_{2-\text{Ns}}$), 133.7 ($\text{C}_{2-\text{Ns}}$), 148.4 ($\text{C}_{2-\text{Ns}}$); **ESI-MS (m/z)**: 427.1 [$\text{M}+\text{Na}$] $^+$; **ESI-HRMS (m/z)**: calculated for [$\text{M}+\text{Na}$] $^+$: 427.0701; experimental: 427.0696.

**31b**

General procedure for 31. A mixture of *N*-(4-chlorobut-2-yn-1-yl)-*N*-(2,2-diethoxyethyl)-4-methylbenzenesulfonamide **17a** (0.29 g, 0.08 mmol), *N*-allyltosylamide **33a**¹²⁴ (0.16 g, 0.08 mmol) and anhydrous potassium carbonate (0.65 g, 4.7 mmol) in acetonitrile (10 mL) was stirred at reflux for 24 hours (TLC monitoring). The mixture was cooled to room temperature, the salts were filtered off, and the solvent removed under reduced pressure. The oily residue was purified by column chromatography on silica gel (hexane/ethyl acetate 8:2) to afford **31b** (0.30 g, 70%) as a colourless waxy solid. **R_f** (hexane/ethyl acetate 8:2): 0.27; **MW**: 548.71 g/mol; **m.p.**: 62-63 °C; **IR (ATR) ν (cm⁻¹)**: 2976, 1345, 1157; **¹H NMR (400 MHz, CDCl₃) δ (ppm)**: 1.21 (t, ³J = 6.8 Hz, 6HOCH₂CH₃), 2.41 (s, 3H_{Ts}), 2.43 (s, 3H_{Ts}), 3.04 (d, ³J = 5.7 Hz, 2H_h), 3.54 (dq, ²J = 9.2 Hz / ³J = 6.8 Hz, 2HOCH₂CH₃), 3.58 (d, ³J = 4.0 Hz, 2H_c), 3.72 (dq, ²J = 9.2 Hz / ³J = 6.8 Hz, 2HOCH₂CH₃), 3.84 (t, ⁵J = 1.8 Hz, 2H_{d/g}), 4.06 (t, ⁵J = 1.8 Hz, 2H_{d/g}), 4.60 (t, ³J = 5.7 Hz, H_i), 5.08 (dd, ²J = 1.4 Hz / ³J = 17.2 Hz, H_a), 5.15 (dd, ²J = 1.4 Hz / ³J = 10.0 Hz, H_a), 5.61 (ddt, ³J = 4.0 Hz / ³J = 10.0 Hz / ³J = 17.2 Hz, H_b), 7.28-7.30 (m, 4H_{Ts}), 7.62-7.64 (m, 4H_{Ts}); **¹³C NMR (100 MHz, CDCl₃) δ (ppm)**: 15.3 (2COCH₂CH₃), 21.4 (2C_{Ts}), 35.7 (C_{d/g}), 38.3 (C_{d/g}), 48.5 (C_c), 48.8 (C_h), 63.6 (2COCH₂CH₃), 77.8 (C_{eff}), 78.9 (C_{eff}), 102.8 (C_i), 119.6 (C_a), 127.4 (2C_{Ts}), 127.5 (2C_{Ts}), 129.6 (2C_{Ts}), 129.5 (C_{Ts}), 131.7 (C_b), 135.8 (C_{Ts}), 136.1 (C_{Ts}), 143.7 (C_{Ts}), 143.7 (C_{Ts}); **ESI-MS (m/z)**: 571.2 [M+Na]⁺; **EA**: calculated for C₂₇H₃₆N₂O₆S₂: C, 59.10; H, 6.61; N, 5.11; found: C, 58.74 and 58.62; H, 6.64 and 6.19; N, 5.07 and 5.08.

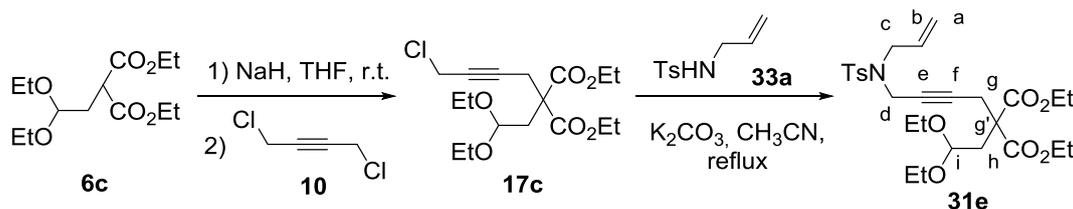
**31c**

Using the same experimental procedure as for compound **31b**, **31c** was obtained as a waxy dark brown solid (1.98 g, 84% yield) after 6 hours. **R_f** (hexane/ethyl acetate 7:3): 0.36; **MW**: 610.65 g/mol; **m.p.**: 100-102 °C; **IR (ATR) ν (cm⁻¹)**: 3103, 2975, 1537, 1529, 1349, 1163; **¹H NMR (300 MHz, CDCl₃) δ (ppm)**: 1.20 (t, ³J = 6.9 Hz, 6HOCH₂CH₃), 3.09 (d, ³J = 5.4 Hz, 2H_h), 3.51 (dq, ²J = 9.3 Hz / ³J = 6.9 Hz, 2HOCH₂CH₃), 3.72 (dq, ²J = 9.3 Hz / ³J = 6.9 Hz, 2HOCH₂CH₃), 3.81 (d, ³J = 5.4 Hz, 2H_c), 3.93 (t, ⁵J = 1.5 Hz, 2H_{d/g}), 4.15 (t, ⁵J = 1.5 Hz, 2H_{d/g}), 4.57 (t, ³J = 5.4 Hz, H_i), 5.12-5.522 (m, 2H_{a/a'}), 5.80 (m, H_b), 7.97 (d, ³J = 9.0 Hz, 2H_{Ns}), 8.01 (d, ³J = 9.0 Hz, 2H_{Ns}), 8.35 (d, ³J = 9.0 Hz, 2H_{Ns}), 8.37 (d, ³J = 9.0 Hz, 2H_{Ns}); **¹³C NMR (75 MHz, CDCl₃) δ (ppm)**: 15.3 (COCH₂CH₃), 15.4 (COCH₂CH₃), 36.0 (C_{d/g}), 38.6 (C_{d/g}), 48.9 (C_{c/h}), 49.4 (C_{c/h}), 64.2 (2COCH₂CH₃), 78.3 (C_{eff}), 79.3 (C_{eff}), 102.7 (C_i), 120.5 (C_a), 124.3, 124.5, 128.7, 128.8, 131.0, 131.1, 144.9, 145.0, 150.3; **ESI-MS (m/z)**: 633.2 [M+Na]⁺, 649.1 [M+K]⁺; **EA**: calculated for C₂₅H₃₀N₄O₁₀S₂: C, 49.17; H, 4.95; N, 9.18; found: C, 49.28 and 49.33; H, 4.90 and 4.91; N, 9.16 and 9.24.



Using the same experimental procedure as for compound **31b**, **31d** was obtained as a waxy dark brown oil (1.29 g, 86% yield) after 2 hours. R_f (hexane/ethyl acetat 7:3): 0.38; **MW**: 610.65 g/mol; **IR (ATR) ν (cm^{-1})**: 3096, 2977, 1542, 1355, 1162; **$^1\text{H NMR}$ (300 MHz, CDCl_3) δ (ppm)**: 1.17 (t, $^3J = 6.9$ Hz, $6\text{H}_{\text{OCH}_2\text{CH}_3}$), 3.31 (d, $^3J = 5.5$ Hz, 2H_h), 3.50 (dq, $^2J = 9.6$ Hz / $^3J = 6.9$ Hz, $2\text{H}_{\text{OCH}_2\text{CH}_3}$), 3.68 (dq, $^2J = 9.6$ Hz / $^3J = 6.9$ Hz, $2\text{H}_{\text{OCH}_2\text{CH}_3}$), 3.86 (d, $^3J = 6.3$ Hz, 2H_c), 4.01 (t, $^5J = 1.7$ Hz, $2\text{H}_{d/g}$), 4.26 (t, $^5J = 1.7$ Hz, $2\text{H}_{d/g}$), 4.56 (t, $^3J = 5.5$ Hz, H_i), 5.17 (m, $\text{H}_{a/a'}$), 5.22 (m, $\text{H}_{a/a'}$), 5.61 (ddt, $^3J = 17.4$ Hz / $^3J = 10.0$ Hz / $^3J = 6.3$ Hz, H_b), 7.62-7.65 (m, $2\text{H}_{2-\text{Ns}}$), 7.72-7.74 (m, $4\text{H}_{2-\text{Ns}}$), 7.79 - 8.01 (m, $2\text{H}_{2-\text{Ns}}$); **$^{13}\text{C NMR}$ (75 MHz, CDCl_3) δ (ppm)**: 15.3 ($2\text{C}_{\text{OCH}_2\text{CH}_3}$), 36.0 ($\text{C}_{d/g}$), 38.6 ($\text{C}_{d/g}$), 48.7 ($\text{C}_{c/h}$), 49.4 ($\text{C}_{c/h}$), 63.7 ($2\text{C}_{\text{OCH}_2\text{CH}_3}$), 78.6 ($\text{C}_{e/f}$), 79.2 ($\text{C}_{e/f}$), 102.4 (C_i), 120.4 (C_a), 124.2, 124.3, 130.6, 131.3, 131.9, 132.7, 132.8, 133.9, 134.0, 148.0, 148.2; **ESI-MS (m/z)**: 633.2 [$\text{M}+\text{Na}$] $^+$; **EA**: calculated for $\text{C}_{25}\text{H}_{30}\text{N}_4\text{O}_{10}\text{S}_2$: C, 49.17; H, 4.95; N, 9.18; found: C, 49.14 and 49.06; H, 4.79 and 4.93; N, 8.71 and 8.77.

8.3.1.3. Synthesis of acetal **31e**

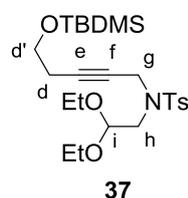
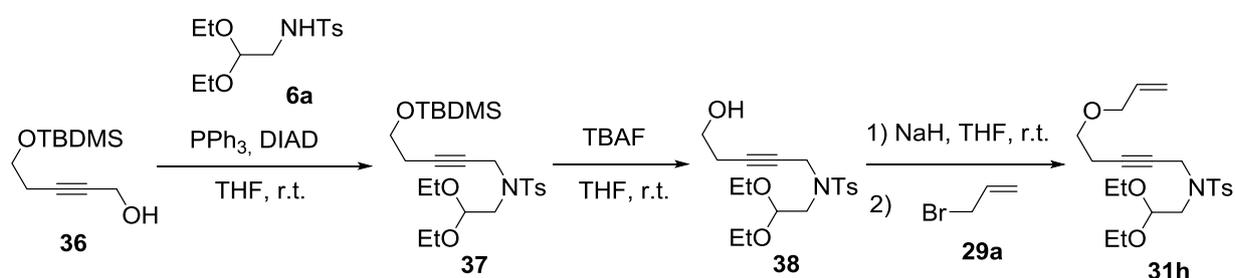


Diethyl 2-(2,2-diethoxyethyl)malonate **6c** (2.00 g, 7.23 mmol) in THF (15 mL) was added slowly to a suspension of NaH (60% dispersion in mineral oil, 0.35 g, 8.69 mmol) in THF (15 mL) at room temperature under N_2 and the mixture was stirred for 1 hour. 1,4-dichloro-2-butyne **10** (3.53 g, 28.9 mmol) in THF (15 mL) was then added dropwise, and the mixture was stirred at room temperature for 24 hours (TLC monitoring). Water was added to quench the reaction, and the mixture was extracted with EtOAc (3 x 40 mL). The combined organic extracts were washed with brine, dried over anhydrous Na_2SO_4 and concentrated under reduce pressure. The excess of 1,4-dichloro-2-butyne was removed by column chromatography on silica gel using hexane:EtOAc 10:0 as eluent, and a 7:3 mixture of this eluent was used to obtain an inseparable mixture of non-reacted starting material and **17c** (1.6 g, 1:0.37 by $^1\text{H NMR}$) which was used without further purification in the next reaction.

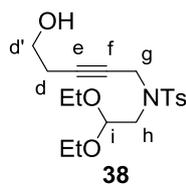
The previously obtained mixture of diethyl 2-(2,2-diethoxyethyl)malonate and **17c** (1.36 g) was reacted with *N*-allyltosylamide **33a** (0.48 g, 2.27 mmol) and anhydrous potassium carbonate (1.56 g, 11.29 mmol) in acetonitrile (30 mL) at reflux for 24 hours (TLC monitoring). The mixture was cooled to room temperature, the salts were filtered off, and the solvent was removed under reduced pressure. The oily residue was purified by column chromatography on silica gel (hexane/ethyl acetate, 9:1 to 7:3) to afford **31e** as colourless oil (1.05, g, 88 %, 2 steps). R_f (hexane/ethyl acetat 7:3): 0.50; **MW**: 537.67 g/mol; **IR (ATR) ν (cm^{-1})**: 2978, 1737, 1349, 1161; **$^1\text{H NMR}$ (400 MHz, CDCl_3) δ (ppm)**: 1.15 (t, $^3J =$

7.2 Hz, 6H_{OCH₂CH₃}), 1.22 (t, ³J = 7.2 Hz, 6H_{CO₂CH₂CH₃}), 2.26 (d, ³J = 5.6 Hz, 2H_h), 2.44 (s, 3H_{Ts}), 2.65 (t, ⁵J = 2.0 Hz, 2H_g), 3.40 (dq, ²J = 9.2 Hz / ³J = 7.2 Hz, 2H_{OCH₂CH₃}), 3.60 (dq, ²J = 9.2 Hz / ³J = 7.2 Hz, 2H_{OCH₂CH₃}), 3.77 (d, ³J = 6.4 Hz, 2H_c), 4.05 (t, ⁵J = 2.0 Hz, 2H_d), 4.13 (q, ³J = 7.2 Hz, 2H_{CO₂CH₂CH₃}), 4.14 (q, ³J = 7.2 Hz, 2H_{CO₂CH₂CH₃}), 4.40 (t, ³J = 5.6 Hz, H_i), 5.22 (dd, ²J = 1.2 Hz / ³J = 10.0 Hz, H_a), 5.29 (dd, ²J = 1.2 Hz / ³J = 17.0 Hz, H_a), 5.69 (ddt, ³J = 6.4 Hz / ³J = 10.0 Hz / ³J = 17.0 Hz, H_b), 7.31 (d, ³J = 8.2 Hz, 2H_{Ts}), 7.70 (d, ³J = 8.2 Hz, 2H_{Ts}); ¹³C NMR (100MHz, CDCl₃) δ (ppm): 14.1 (2C_{OCH₂CH₃}), 15.2 (2C_{CO₂CH₂CH₃}), 21.6 (C_{Ts}), 23.3 (C_g), 35.9 (C_{d/h}), 36.2 (C_{d/h}), 48.9 (C_c), 54.5 (C_g), 61.6 (2C_{OCH₂CH₃}), 62.1 (2C_{CO₂CH₂CH₃}), 76.1 (C_{eff}), 80.7 (C_{eff}), 100.1 (C_i), 120.0 (C_a), 127.7 (2C_{Ts}), 129.6 (2C_{Ts}), 132.1 (C_b), 136.4 (C_{Ts}), 143.5 (C_{Ts}), 169.9 (2C_{CO₂Et}); ESI-MS (m/z): 560.3 [M+Na]⁺; EA: calculated for C₂₇H₃₉NO₈S: C, 60.32; H, 7.31; N, 2.61; found: C, 60.52 and 60.40; H, 7.25 and 7.34; N, 2.62 and 2.63.

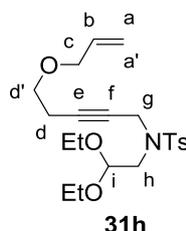
8.3.1.4. Synthesis of acetal 31h



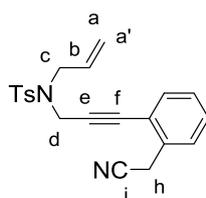
37 2,2-diethoxy-*N*-tosylethanamine **6a** (1.06 g, 3.69 mmol) was added to a solution of 5-(tert-butyldimethylsilyloxy)-2-pentyn-1-ol **36**¹²⁵ (0.79 g, 3.69 mmol) and PPh₃ (1.26 g, 4.80 mmol) in THF (50 mL) at room temperature under N₂. After 10 minutes, diisopropylazodicarboxylate (DIAD, 0.96 mL, 4.88 mmol) was added and the resulting reaction mixture was stirred for 2 hours (TLC monitoring). After adding water, extraction was performed with Et₂O (3 x 50 mL). The combined organic layers were washed with brine, dried over anhydrous Na₂SO₄ and concentrated under reduced pressure. The oily residue was purified by column chromatography on silica gel (hexane/ethyl acetate, 10:0 to 8:2) to afford **37** as colourless oil (1.49 g, 84 %). **R_f** (hexane/ethyl acetate 7:3): 0.64; **MW**: 483.74 g/mol; ¹H NMR (400 MHz, CDCl₃) δ (ppm): 0.03 (s, 6H_{TBDMS}), 0.09 (s, 9H_{TBDMS}), 1.21 (t, ³J = 7.2 Hz, 6H_{OCH₂CH₃}), 2.08-2.13 (m, 2H_d), 2.41 (s, 3H_{Ts}), 3.23 (d, ³J = 5.6 Hz, 2H_h), 3.45 (t, ³J = 7.4 Hz, 2H_{d'}), 3.57 (dq, ²J = 9.4 Hz / ³J = 7.4 Hz, 2H_{OCH₂CH₃}), 3.74 (dq, ²J = 9.4 Hz / ³J = 7.4 Hz, 2H_{OCH₂CH₃}), 4.24 (t, ⁵J = 2.2 Hz, 2H_g), 4.68 (t, ³J = 5.6 Hz, H_i), 7.27 (d, ³J = 8.4 Hz, 2H_{Ts}), 7.74 (d, ³J = 8.4 Hz, 2H_{Ts}); ¹³C NMR (100 MHz, CDCl₃) δ (ppm): -5.2 (2C_{TBDMS}), 15.5 (2C_{OCH₂CH₃}), 18.4 (C_d), 21.6 (C_{Ts}), 23.0 (3C_{TBDMS}), 26.0 (C_{TBDMS}), 39.0 (C_g), 48.6 (C_h), 61.7 (C_{d'}), 63.5 (2C_{OCH₂CH₃}), 74.5 (C_{eff}), 82.6 (C_{eff}), 103.0 (C_i), 128.0 (2C_{Ts}), 129.4 (2C_{Ts}), 136.5 (C_{Ts}), 143.4 (C_{Ts}).



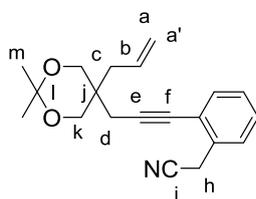
38 TBAF (1.27g, 4.01 mmol) was added to a degassed solution at 0°C of **37** (1.49g, 3.08 mmol) in THF (20 mL). After 1 hour (TLC monitoring), the solvent was removed by vacuum evaporation. The oily residue was purified by column chromatography on silica gel (hexane/ethyl acetate, 8:2 to 6:4) to afford **38** as a colourless solid (0.91, g, 80 %). R_f (hexane/ethyl acetat 1:1): 0.50; **MW**: 369.48 g/mol; $^1\text{H NMR}$ (400 MHz, CDCl_3) δ (ppm): 1.21 (t, $^3J = 7.2$ Hz, $6\text{H}_{\text{OCH}_2\text{CH}_3}$), 2.07 (bs, H_{OH}), 2.17-2.21 (m, 2H_d), 2.42 (s, 3H_{Ts}), 3.25 (d, $^3J = 5.5$ Hz, 2H_h), 3.46 (br t, $^3J = 6.0$ Hz, $2\text{H}_{d'}$), 3.57 (dq, $^2J = 9.2$ Hz / $^3J = 7.2$ Hz, $2\text{H}_{\text{OCH}_2\text{CH}_3}$), 3.74 (dq, $^2J = 9.2$ Hz / $^3J = 7.2$ Hz, $2\text{H}_{\text{OCH}_2\text{CH}_3}$), 4.23 (t, $^5J = 2.0$ Hz, 2H_g), 4.68 (t, $^3J = 5.5$ Hz, H_i), 7.30 (d, $^3J = 8.0$ Hz, 2H_{Ts}), 7.74 (d, $^3J = 8.0$ Hz, 2H_{Ts}); $^{13}\text{C NMR}$ (100 MHz, CDCl_3) δ (ppm): 15.4 ($2\text{C}_{\text{OCH}_2\text{CH}_3}$), 21.5 (C_{Ts}), 22.9 (C_d), 38.9 (C_g), 48.7 (C_h), 60.7 ($\text{C}_{d'}$), 63.5 ($2\text{C}_{\text{CO}_2\text{CH}_2\text{CH}_3}$), 75.2 ($\text{C}_{e/f}$), 82.6 ($\text{C}_{e/f}$), 102.8 (C_i), 127.8 (2C_{Ts}), 129.4 (2C_{Ts}), 136.2 (C_{Ts}), 143.7 (C_{Ts}).



31h Compound **38** (0.75 g, 2.03 mmol) in THF (20 mL) was added slowly to a suspension of NaH (60% dispersion in mineral oil, 0.12 g, 3.05 mmol) in THF (20 mL) at room temperature under N_2 and the mixture was stirred for 1 hour. Allylbromide **29a** (0.21 g, 2.44 mmol) in THF (20 mL) was added dropwise, and the mixture was stirred at room temperature for 15 hours (TLC monitoring). Water was added to quench the reaction, and the mixture was extracted with EtOAc (3 x 30 mL). The combined organic extracts were washed with brine, dried over anhydrous Na_2SO_4 , filtered and concentrated under reduce pressure. The residue was purified by column chromatography on silica gel using hexane:EtOAc (9:1 to 7:3) to afford **31h** as a palid yellow oil (0.62, g, 74 %). R_f (hexane/ethyl acetat 6:4): 0.55; **MW**: 409.54 g/mol; $^1\text{H NMR}$ (400 MHz, CDCl_3) δ (ppm): 1.29-1.23 (m, $6\text{H}_{\text{OCH}_2\text{CH}_3}$), 2.16-2.20 (m, $2\text{H}_{d'}$), 2.41 (s, 3H_{Ts}), 3.22-3.28 (m, $4\text{H}_{d,h}$), 3.54-3.59 (m, $2\text{H}_{\text{OCH}_2\text{CH}_3}$), 3.72-3.76 (m, $2\text{H}_{\text{OCH}_2\text{CH}_3}$), 3.91-3.92 (m, 2H_g), 4.24-4.24 (m, 2H_c), 5.23-5.27 (m, $2\text{H}_{a,a'}$), 5.85 (m, H_b), 7.28 (d, $^3J = 8.2$ Hz, 2H_{Ts}), 7.74 (d, $^3J = 8.2$ Hz, 2H_{Ts}); $^{13}\text{C NMR}$ (100 MHz, CDCl_3) δ (ppm): 15.4 ($2\text{C}_{\text{OCH}_2\text{CH}_3}$), 19.8 (C_d), 21.5 (C_{Ts}), 38.9 (C_g), 48.5 (C_h), 63.3 ($2\text{C}_{\text{CO}_2\text{CH}_2\text{CH}_3}$), 68.1 ($\text{C}_{d'}$), 71.8 (C_c), 74.3 ($\text{C}_{e/f}$), 82.4 ($\text{C}_{e/f}$), 102.8 (C_i), 117.1 (C_a), 127.8 (2C_{Ts}), 129.3 (2C_{Ts}), 134.5 (C_b), 136.3 (C_{Ts}), 143.3 (C_{Ts}).

8.3.1.5. Synthesis of cyano **41a** and **41b****41a**

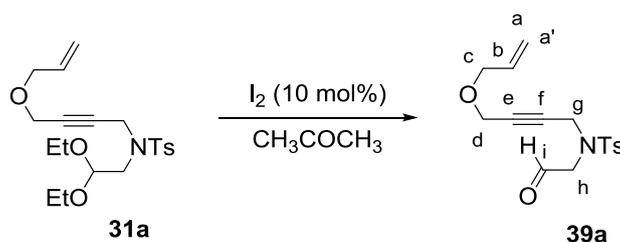
$\text{Pd}(\text{PPh}_3)_2\text{Cl}_2$ (0.30 g, 0.42 mmol), *N*-allyl-4-methyl-*N*-(prop-2-yn-1-yl)benzenesulfonamide **42** (3.14 g, 12.59 mmol) and CuI (0.08 g, 0.42 mmol) were added at room temperature a solution of 2-iodophenylacetonitrile **44** (2.04 g, 8.39 mmol) in triethylamine (4.0 mL) and the reaction mixture was stirred for 15 hours (TLC monitoring). Triethylamine was then evaporated off and the residue was concentrated in vacuo and purified by column chromatography on silica gel (hexane/ethyl acetate 9:1 to 1:1) to afford **41a** (2.68 g, 87%) as a dark brown oil. R_f (hexane/ethyl acetate 1:1): 0.80; **MW**: 364.46 g/mol; **IR (ATR) ν (cm^{-1})**: 1346, 1158; **$^1\text{H NMR}$ (300 MHz, CDCl_3) δ (ppm)**: 2.34 (s, 3 H_{Ts}), 3.50 (s, 2 H_h), 4.92 (d, $^3J = 6.3$ Hz, 2 H_c), 4.37 (s, 2 H_d), 5.68 (dd, $^3J = 17.1$ Hz / $^2J = 1.3$ Hz, H_a), 5.34 (dd, $^3J = 10.1$ Hz / $^2J = 1.3$ Hz, $\text{H}_{a'}$), 5.76 (ddt, $^3J = 6.3$ Hz / $^3J = 10.1$ Hz / $^3J = 17.1$ Hz, H_b), 7.13 (dd, $^3J = 7.5$ Hz / $^4J = 1.3$ Hz, H_{Ph}), 7.22-7.28 (m, 3 $\text{H}_{\text{Ts,Ph}}$), 7.34 (ddd, $^3J = 7.2$ Hz / $^3J = 1.5$ Hz / $^4J = 1.5$ Hz, H_{Ph}), 7.41 (m, H_{Ph}), 7.77 (d, $^3J = 8.4$ Hz, 2 H_{Ts}); **$^{13}\text{C NMR}$ (75 MHz, CDCl_3) δ (ppm)**: 21.6 (C_{Ts}), 22.4 (C_h), 36.7 (C_d), 49.6 (C_c), 82.5 (C_{eff}), 88.5 (C_{eff}), 117.29 (C_i), 120.2 ($\text{C}_{a/a'}$), 121.9, 127.9, 129.4, 129.7, 131.6, 132.1, 132.7, 136.2, 143.9; **ESI-HRMS (m/z)**: calculated for $[\text{M}+\text{Na}]^+$: 387.1138; experimental: 387.1148.

**41b**

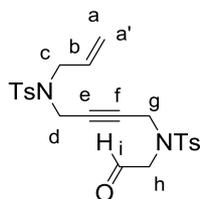
The starting compound, 5-allyl-2,2-dimethyl-5-(prop-2-yn-1-yl)-1,3-dioxane **43**, was prepared following a previously published procedure.¹²⁶

Using the same experimental procedure as for compound **41a**, **41b** was obtained as a brown oil (1.13 g, 88% yield) after 24 hours. R_f (hexane/ethyl acetate 1:1): 0.64; **MW**: 309.17 g/mol; **IR (ATR) ν (cm^{-1})**: 2991, 1371, 1197; **$^1\text{H NMR}$ (400 MHz, CDCl_3) δ (ppm)**: 1.43 (s, 3 H_m), 1.44 (s, 3 H_m), 2.21 (d, $^3J = 7.6$ Hz, 2 H_c), 2.71 (s, 2 H_d), 3.70 (d, $^2J = 11.6$ Hz, 2 H_k), 3.74 (d, $^2J = 11.6$ Hz, 2 H_k), 3.87 (s, 2 H_h), 5.15 (m, H_a), 5.19 (m, H_a), 5.80 (m, H_b), 7.29 (dd, $^3J = 7.2$ Hz / $^4J = 1.6$ Hz, H_{Ph}), 7.33 (ddd, $^3J = 7.2$ Hz / $^3J = 6.0$ Hz / $^4J = 6.0$ Hz, H_{Ph}), 7.44-7.46 (m, 2 H_{Ph}); **$^{13}\text{C NMR}$ (100 MHz, CDCl_3) δ (ppm)**: 21.3, 22.9, 23.6, 26.5, 36.1, 37.4, 67.0 (2 C_k), 80.2 (C_{eff}), 93.4 (C_{eff}), 98.4 (C_i), 117.6 (C_i), 119.3 (C_a), 123.4, 128.1, 128.2, 128.6, 131.7, 132.2, 132.8; **ESI-HRMS (m/z)**: calculated for $[\text{M}+\text{Na}]^+$: 332.1621; experimental: 332.1627.

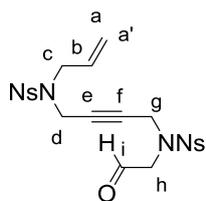
8.3.1.6 Synthesis of aldehydes 39 and 40



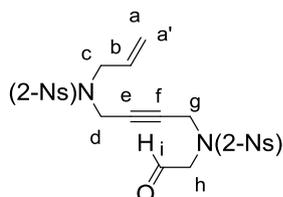
General procedure for 39.⁵⁰ A mixture of **31a** (1.53 g, 3.87 mmol) and iodine (0.10 mg, 0.4 mmol) in acetone (100 mL) was stirred at room temperature for 24 hours (TLC monitoring). Acetone was then removed under vacuum and the residue was dissolved in CH_2Cl_2 (50 mL). The mixture was washed successively with 5% aqueous $\text{Na}_2\text{S}_2\text{O}_3$ (3 x 20 mL), H_2O (3 x 20 mL) and brine (3 x 20 mL). The organic layer was dried over anhydrous Na_2SO_4 and the solvent removed by vacuum evaporation. The oily residue was purified by column chromatography on silica gel (hexane/ethyl acetate 8:2 to 6:4) to afford **39a** (0.86 g, 69%) as a colourless oil. R_f (hexane/ethyl acetate 1:1): 0.80; **MW**: 321.39 g/mol; **IR (ATR) ν (cm^{-1})**: 2925, 2848, 1732, 1346, 1158; **$^1\text{H NMR}$ (300 MHz, CDCl_3) δ (ppm)**: 2.44 (s, 3H_{Ts}), 3.88 (dt, $^3J = 7.5 \text{ Hz} / ^4J = 1.5 \text{ Hz}$, 2H_{c}), 3.93 (d, $^3J = 1.7 \text{ Hz}$, 2H_{h}), 3.95 (t, $^5J = 1.8 \text{ Hz}$, $2\text{H}_{\text{d/g}}$), 4.21 (t, $^5J = 1.8 \text{ Hz}$, $2\text{H}_{\text{d/g}}$), 5.19-5.28 (m, $2\text{H}_{\text{a/a'}}$), 5.83 (ddt, $^3J = 17.4 \text{ Hz} / ^3J = 10.5 \text{ Hz} / ^3J = 5.7 \text{ Hz}$, H_{b}), 7.33 (d, $^3J = 8.4 \text{ Hz}$, 2H_{Ts}), 7.71 (d, $^3J = 8.4 \text{ Hz}$, 2H_{Ts}), 9.67 (t, $^3J = 1.7 \text{ Hz}$, H_{i}); **$^{13}\text{C NMR}$ (75 MHz, CDCl_3) δ (ppm)**: 21.7 (C_{Ts}), 39.2 (C_{g}), 56.1 (C_{d}), 57.1 (C_{h}), 70.7 (C_{c}), 78.5 ($\text{C}_{\text{e/f}}$), 82.9 ($\text{C}_{\text{e/f}}$), 118.1 (C_{a}), 127.9 (2C_{Ts}), 129.9 (2C_{Ts}), 133.7 (C_{b}), 135.0 (2C_{Ts}), 144.4 (C_{Ts}), 197.5 (C_{i}); **ESI-MS (m/z)**: 344.1 [$\text{M}+\text{Na}$] $^+$, 360.1 [$\text{M}+\text{K}$] $^+$; **EA**: calculated for $\text{C}_{16}\text{H}_{19}\text{NO}_4\text{S} \cdot 0.5\text{H}_2\text{O}$: C, 58.16; H, 6.10; N, 4.24; found: C, 58.37 and 58.24; H, 6.06 and 6.12; N, 4.31 and 4.30.



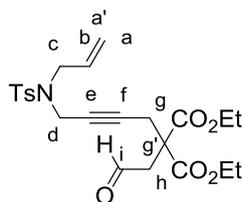
39b Using the same experimental procedure as for compound **39a**, **39b** was obtained as a colourless oil (0.16 g, 60% yield) after 24 hours. R_f (hexane/ethyl acetate 1:1): 0.74; **MW**: 474.59 g/mol; **m.p.**: 62-64 °C; **IR (ATR) ν (cm^{-1})**: 2923, 1726, 1344, 1154; **$^1\text{H NMR}$ (400 MHz, CDCl_3) δ (ppm)**: 2.43 (s, 6H_{Ts}), 3.64 (d, $^3J = 6.4 \text{ Hz}$, 2H_{c}), 3.73 (d, $^3J = 0.8 \text{ Hz}$, H_{h}), 3.89 (t, $^5J = 1.8 \text{ Hz}$, $2\text{H}_{\text{d/g}}$), 3.93 (t, $^5J = 1.8 \text{ Hz}$, $2\text{H}_{\text{d/g}}$), 5.12 (dd, $^3J = 16.8 \text{ Hz} / ^2J = 1.2 \text{ Hz}$, $\text{H}_{\text{a/a'}}$), 5.16 (dd, $^3J = 10.0 \text{ Hz} / ^2J = 1.2 \text{ Hz}$, $\text{H}_{\text{a/a'}}$), 5.61 (ddt, $^3J = 16.8 \text{ Hz} / ^3J = 10.0 \text{ Hz} / ^3J = 6.4 \text{ Hz}$, H_{b}), 7.30 (d, $^3J = 8.2 \text{ Hz}$, 2H_{Ts}), 7.32 (d, $^3J = 8.2 \text{ Hz}$, 2H_{Ts}), 7.63 (d, $^3J = 8.2 \text{ Hz}$, 2H_{Ts}), 7.66 (d, $^3J = 8.2 \text{ Hz}$, 2H_{Ts}), 9.51 (t, $^3J = 0.8 \text{ Hz}$, H_{i}); **$^{13}\text{C NMR}$ (75 MHz, CDCl_3) δ (ppm)**: 21.6 (C_{Ts}), 21.7 (C_{Ts}), 35.8 ($\text{C}_{\text{d/g}}$), 38.8 ($\text{C}_{\text{d/g}}$), 49.3 (C_{c}), 55.8 (C_{h}), 77.8 ($\text{C}_{\text{e/f}}$), 79.8 ($\text{C}_{\text{e/f}}$), 119.9 ($\text{C}_{\text{a/a'}}$), 127.7 (2C_{Ts}), 127.8 (2C_{Ts}), 129.7 (2C_{Ts}), 130.0 (2C_{Ts}), 131.9 (C_{b}), 134.9 (C_{Ts}), 136.1 (C_{Ts}), 144.0 (C_{Ts}), 144.5 (C_{Ts}), 197.1 (C_{i}); **ESI-MS (m/z)**: 475.1 [$\text{M}+\text{H}$] $^+$, 497.1 [$\text{M}+\text{Na}$] $^+$; **EA**: calculated for $\text{C}_{23}\text{H}_{26}\text{N}_2\text{O}_5\text{S}_2 \cdot 0.5\text{H}_2\text{O}$: C, 57.12; H, 5.63; N, 5.79; found: C, 57.42 and 57.60; H, 5.61 and 5.43; N, 5.60 and 5.59.



39c Using the same experimental procedure as for compound **39a**, **39c** was obtained as a pale orange solid (0.53 g, 45% yield) after 24 hours. R_f (hexane/ethyl acetat 6:4): 0.27; **MW**: 536.53 g/mol; **m.p.**: 123-125°C; **IR (ATR) ν (cm^{-1})**: 3104, 2868, 1732, 1527, 1349, 1165; **$^1\text{H NMR}$ (300 MHz, CDCl_3) δ (ppm)**: 3.79 (d, $^3J = 6.5$ Hz, 2H_c), 4.01 (s, $4\text{H}_{d,g}$), 4.09 (s, 2H_h), 5.20-5.27 (m, $2\text{H}_{a/a'}$), 5.62 (ddt, $^3J = 16.8$ Hz / $^3J = 10.1$ Hz / $^3J = 6.5$ Hz, H_b), 7.97 (d, $^3J = 8.7$ Hz, 2H_{Ns}), 7.99 (d, $^3J = 8.7$ Hz, 2H_{Ns}), 8.38 (d, $^3J = 8.7$ Hz, 4H_{Ns}), 9.51 (s, H_i); **$^{13}\text{C NMR}$ (75 MHz, CDCl_3) δ (ppm)**: 36.0 ($\text{C}_{d/g}$), 38.5 ($\text{C}_{d/g}$), 49.7 (C_c), 55.8 (C_h), 78.1 ($\text{C}_{e/f}$), 79.9 ($\text{C}_{e/f}$), 120.8 (C_a), 124.5 (2C_{Ns}), 124.7 (2C_{Ns}), 128.8 (C_b), 131.0 (2C_{Ns}), 131.1 (2C_{Ns}), 144.2 (C_{Ns}), 144.9 (C_{Ns}), 150.4 (C_{Ns}), 150.5 (C_{Ns}), 195.6 (C_i); **ESI-MS (m/z)**: 559.1 [$\text{M}+\text{Na}$] $^+$, 575.0 [$\text{M}+\text{K}$] $^+$; **EA**: calculated for $\text{C}_{21}\text{H}_{20}\text{N}_4\text{O}_9\text{S}_2$: C, 47.01; H, 3.76; N, 10.44; found: C, 47.09 and 47.09; H, 3.67 and 3.74; N, 10.22 and 10.28.

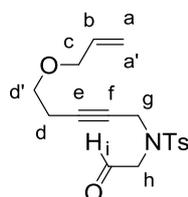


39d Using the same experimental procedure as for compound **39a**, **39d** was obtained as a orange solid (0.30 g, 41% yield) after 24 hours. R_f (hexane/ethyl acetat 1:1): 0.40; **MW**: 536.53 g/mol; **m.p.**: 124-125°C; **IR (ATR) ν (cm^{-1})**: 2981, 1537, 1351, 1160, 1125; **$^1\text{H NMR}$ (400 MHz, CDCl_3) δ (ppm)**: 3.89 (d, $^3J = 6.4$ Hz, 2H_c), 4.05 (s, $2\text{H}_{d/g}$), 4.19 (s, $2\text{H}_{d/g}$), 4.22 (s, 2H_h), 5.22-5.26 (m, $2\text{H}_{a,a'}$), 5.64 (ddt, $^3J = 17.2$ Hz / $^3J = 10.0$ Hz / $^3J = 6.4$ Hz, H_b), 7.72-7.74 (m, $2\text{H}_{2-\text{Ns}}$), 7.75-7.77 (m, $4\text{H}_{2-\text{Ns}}$), 8.00-8.04 (m, $2\text{H}_{2-\text{Ns}}$), 9.56 (s, H_i); **$^{13}\text{C NMR}$ (75 MHz, CDCl_3) δ (ppm)**: 36.0 ($\text{C}_{d/g}$), 38.6 ($\text{C}_{d/g}$), 49.6 (C_c), 55.6 (C_h), 77.9 ($\text{C}_{e/f}$), 80.2 ($\text{C}_{e/f}$), 120.5 (C_a), 124.5 ($\text{C}_{2-\text{Ns}}$), 129.7, 131.0, 131.3, 132.0, 132.3, 132.3, 132.4, 132.7, 134.2, 135.2, 144.3, 147.9, 196.2 (C_i); **ESI-MS (m/z)**: 537.0 [$\text{M}+\text{H}$] $^+$, 591.1 [$\text{M}+\text{MeOH}+\text{Na}$] $^+$; **ESI-HRMS (m/z)**: calculated for [$\text{M}+\text{Na}$] $^+$ and [$\text{M}+\text{MeOH}+\text{Na}$] $^+$: 559.0564 and 591.0826; experimental: 559.0549 and 591.0801.

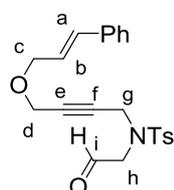


39e Using the same experimental procedure as for compound **39a**, **39e** was obtained as a colourless oil (0.73 g, 86% yield) after 24 hours. R_f (hexane/ethyl acetat 7:3): 0.16; **MW**: 463.55 g/mol; **IR (ATR) ν (cm^{-1})**: 2981, 1730, 1348, 1161; **$^1\text{H NMR}$ (400 MHz, CDCl_3) δ (ppm)**: 1.23 (t, $^3J = 7.2$ Hz, $6\text{H}_{\text{CO}_2\text{CH}_2\text{CH}_3}$), 2.44 (s, 3H_{Ts}), 2.74 (t, $^5J = 2.0$ Hz, 2H_g), 3.07 (d, $^3J = 1.2$ Hz, 2H_h), 3.77 (d, $^3J = 6.4$ Hz, 2H_c), 4.04 (t, $^5J = 2.0$ Hz, 2H_d), 4.19 (q, $^3J = 7.2$ Hz, $2\text{H}_{\text{CO}_2\text{CH}_2\text{CH}_3}$), 4.20 (q, $^3J = 7.2$ Hz, $2\text{H}_{\text{CO}_2\text{CH}_2\text{CH}_3}$), 5.22 (dd, $^3J = 10.0$ Hz / $^2J = 1.2$ Hz, H_a), 5.28 (dd, $^3J = 17.1$ Hz / $^2J = 1.2$ Hz, H_a), 5.70

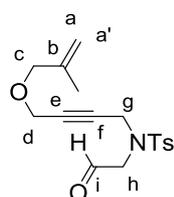
(ddt, $^3J = 17.1$ Hz / $^3J = 6.4$ Hz / $^3J = 10.0$ Hz, H_b), 7.30 (d, $^3J = 8.0$ Hz, 2H_{Ts}), 7.70 (d, $^3J = 8.0$ Hz, 2H_{Ts}), 9.63 (t, $^3J = 1.2$ Hz, H_i); **^{13}C NMR (100 MHz, CDCl₃) δ (ppm)**: 14.0 (2C_{CO₂CH₂CH₃}), 21.6 (C_{Ts}), 24.0 (C_g), 36.1 (C_d), 45.9 (C_h), 49.0 (C_c), 53.9 (C_{g'}), 62.3 (2C_{CO₂CH₂CH₃}), 76.8 (C_{eff}), 80.3 (C_{eff}), 119.9 (C_a), 127.8 (2C_{Ts}), 129.6 (2C_{Ts}), 132.1 (C_b), 136.3 (C_{Ts}), 143.7 (C_{Ts}), 168.8 (2C_{CO₂Et}), 198.5 (C_i); **ESI-MS (m/z)**: 464.1 [M+H]⁺, 486.2 [M+Na]⁺; **EA**: calculated for C₂₃H₂₉NO₇S: C, 59.60; H, 6.31; N, 3.02; found: C, 59.39 and 59.39; H, 6.25 and 6.42; N, 3.01 and 3.01.

**39h**

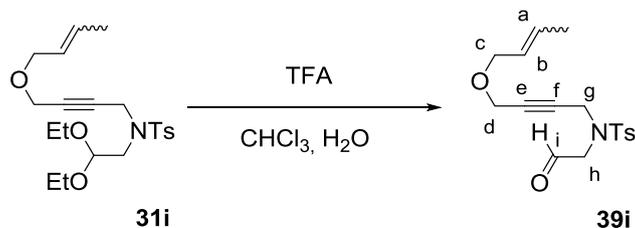
Compound **39h** was not isolated and was used without purification in the subsequent reaction.

**39j**

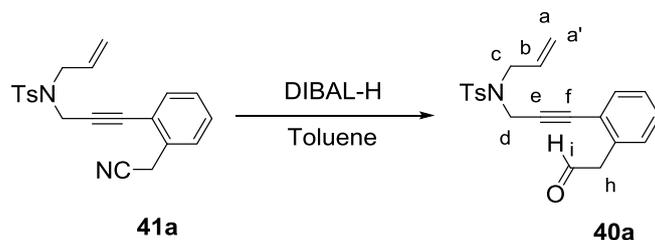
Using the same experimental procedure as for compound **39a**, **39j** was obtained as a colourless waxy solid (0.12 g, 15% yield) after 24 hours. **R_f** (hexane/ethyl acetat 7:3): 0.18; **MW**: 397.49 g/mol; **IR (ATR) ν (cm⁻¹)**: 2924, 1346, 1158; **^1H NMR (400 MHz, CDCl₃) δ (ppm)**: 2.38 (s, 3H_{Ts}), 3.93 (d, $^3J = 1.0$ Hz, 2H_h), 3.99 (t, $^5J = 1.8$ Hz, 2H_g), 4.03 (d, $^3J = 6.4$ Hz, 2H_c), 4.21 (t, $^5J = 1.8$ Hz, 2H_d), 6.19 (dt, $^3J = 16.2$ Hz / $^3J = 1.2$ Hz, H_b), 6.57 (d, $^3J = 16.2$ Hz, H_a), 7.24-7.38 (m, 9H_{Ts,Ph}), 9.51 (t, $^3J = 1.0$ Hz, H_i); **^{13}C NMR (100 MHz, CDCl₃) δ (ppm)**: 21.6 (C_{Ts}), 39.1 (C_g), 56.0 (C_d), 57.0 (C_h), 70.3 (C_c), 78.6 (C_{eff}), 82.9 (C_{eff}), 124.8, 126.5, 127.7, 128.0, 128.7, 129.9, 133.4, 136.4, 144.3, 197.4 (C_i); **ESI-HRMS (m/z)**: calculated for [M+Na]⁺: 420.1240; experimental: 420.1255.

**39k**

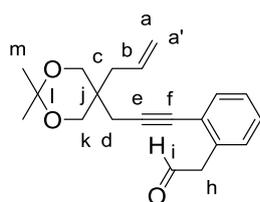
Using the same experimental procedure as for compound **39a**, **39k** was obtained as a colourless oil (0.74 g, 51% yield) after 24 hours. **R_f** (hexane/ethyl acetat 7:3): 0.55; **MW**: 335.42 g/mol; **IR (ATR) ν (cm⁻¹)**: 2931, 1345, 1159; **^1H NMR (300 MHz, CDCl₃) δ (ppm)**: 1.70 (t, $^4J = 1.5$ Hz, 3H_{CH₃}), 2.43 (s, 3H_{Ts}), 3.78 (s, 2H_g), 3.92 (d, $^3J = 2.1$ Hz, 2H_h), 3.93 (t, $^5J = 1.2$ Hz, 2H_d), 4.21 (t, $^4J = 1.6$ Hz, 2H_c), 4.90-4.92 (m, 2H_{a/a'}), 7.33 (d, $^3J = 7.8$ Hz, 2H_{Ts}), 7.71 (d, $^3J = 7.8$ Hz, 2H_{Ts}), 9.66 (t, $^3J = 1.6$ Hz, H_i); **^{13}C NMR (75 MHz, CDCl₃) δ (ppm)**: 19.5 (C_{CH₃}), 21.6 (C_{Ts}), 39.1, 56.0, 56.8, 73.7, 78.3, 82.9, 113.1 (C_a), 127.8 (2C_{Ts}), 129.9 (2C_{Ts}), 134.9 (C_{Ts}), 141.2 (C_{Ts}), 144.4 (C_b), 197.5 (C_i); **ESI-MS (m/z)**: 336.1 [M+H]⁺; **EA**: calculated for C₁₇H₂₁NO₄S.H₂O: C, 57.77; H, 6.56; N, 3.96; found: C, 57.99; H, 6.06; N, 4.21.



A solution of **31i** (1.48 g, 3.61 mmol) in trifluoroacetic acid (4.7 mL, 61.4 mmol), CHCl_3 (4.7 mL) and H_2O (2.3 mL) was stirred at room temperature for 24 hours. The mixture was diluted with CH_2Cl_2 and washed successively with 5% aqueous $\text{Na}_2\text{S}_2\text{O}_3$ (3 x 50 mL), H_2O (3 x 50 mL) and brine (3 x 50 mL). The organic layer was dried over anhydrous Na_2SO_4 and the solvent removed under reduced pressure. The oily residue was purified by column chromatography on silica gel (hexane/ethyl acetate 8:2 to 5:5) to afford **39i** (0.62 g, 51%) as a pale orange waxy solid. R_f (hexane/ethyl acetate 7:3): 0.54; **MW**: 335.42 g/mol; **IR (ATR) ν (cm^{-1})**: 2935, 1733, 1345, 1159; **$^1\text{H NMR}$ (400 MHz, CDCl_3) δ (ppm)**: 1.70-1.72 (m, 3H_{CH_3}), 2.43 (s, 3H_{Ts}), 3.78-3.81 (m, 2H_c), 3.90-3.94 (m, $4\text{H}_{d/g,h}$), 4.20-4.21 (m, $2\text{H}_{d/g}$), 5.50 (m, $\text{H}_{a/b}$), 5.68 (m, $\text{H}_{a/b}$), 7.32 (d, $^3J = 8.4$ Hz, 2H_{Ts}), 7.71 (d, $^3J = 8.0$ Hz, 2H_{Ts}), 9.66 (m, H_i); **$^{13}\text{C NMR}$ (100 MHz, CDCl_3) δ (ppm)**: 17.8 (C_{CH_3}), 21.6 (C_{Ts}), 39.1 (C_g), 56.0 (C_d), 56.6 (C_h), 70.4 (C_c), 78.3 ($\text{C}_{e/f}$), 83.0 ($\text{C}_{e/f}$), 126.5, 127.7, 129.8, 130.7, 134.9, 144.3, 197.4 (C_i); **ESI-HRMS (m/z)**: calculated for $[\text{M}+\text{Na}]^+$: 358.1083; experimental: 358.1090.

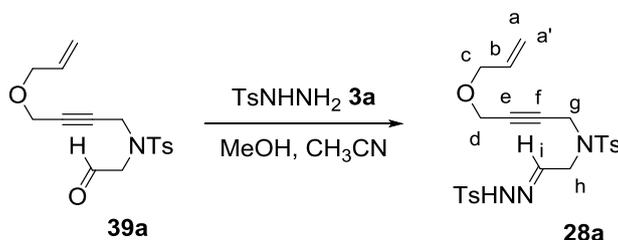


DIBAL-H (3.69 mL, 3.67 mmol) was added to a mixture of **41a** (1.03 g, 2.82 mmol) and anhydrous toluene (30 mL) at 0°C . The mixture was then stirred at room temperature for 2 hours (TLC monitoring). The mixture was washed successively with HCl (3 x 50 mL), H_2O (3 x 50 mL) and brine (3 x 50 mL). The organic layer was dried over anhydrous Na_2SO_4 and the solvent removed under reduced pressure. The oily residue was purified by column chromatography on silica gel (hexane/ethyl acetate 9:1 to 7:3) to afford **40a** (0.31 g, 30%) as a colourless solid. R_f (hexane/ethyl acetate 1:1): 0.60; **MW**: 367.46 g/mol; **m.p.**: 58-59 $^\circ\text{C}$; **IR (ATR) ν (cm^{-1})**: 2924, 1344, 1156; **$^1\text{H NMR}$ (400 MHz, CDCl_3) δ (ppm)**: 2.32 (s, 3H_{Ts}), 3.59 (d, $^3J = 2.0$ Hz, 2H_h), 3.88 (d, $^3J = 6.4$ Hz, 2H_c), 4.32 (s, 2H_d), 5.27 (dd, $^3J = 10.0$ Hz / $^2J = 1.4$ Hz, H_a), 5.32 (dd, $^3J = 17.2$ Hz / $^2J = 1.4$ Hz, H_a), 5.76 (ddt, $^3J = 17.2$ Hz / $^3J = 10.0$ Hz / $^3J = 6.4$ Hz, H_b), 7.71-7.30 (m, $6\text{H}_{\text{Ts, Ph}}$), 7.75 (d, $^3J = 8.2$ Hz, 2H_{Ts}), 9.56 (t, $^3J = 2.0$ Hz, H_i); **$^{13}\text{C NMR}$ (75 MHz, CDCl_3) δ (ppm)**: 21.6 (C_{Ts}), 36.7 (C_d), 49.1 ($\text{C}_{c/h}$), 49.5 ($\text{C}_{c/h}$), 83.8 ($\text{C}_{e/f}$), 86.9 ($\text{C}_{e/f}$), 120.2 ($\text{C}_{a/a'}$), 122.9, 127.4, 127.9, 129.2, 129.7, 130.1, 132.2, 132.8, 134.2, 136.2, 143.8, 198.8 (C_i); **ESI-HRMS (m/z)**: calculated for $[\text{M}+\text{Na}]^+$: 390.1134; experimental: 390.1147.

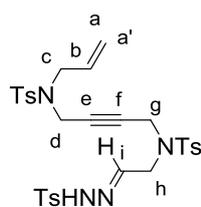


40b Using the same experimental procedure as for compound **40a**, **40b** was obtained as a colourless oil (0.39 g, 35% yield) after 24 hours. R_f (hexane/ethyl acetat 1:1): 0.64; **MW**: 312.41 g/mol; **IR (ATR) ν (cm^{-1})**: 2991, 1372, 1197; **$^1\text{H NMR}$ (400 MHz, CDCl_3) δ (ppm)**: 1.43-1.44 (m, 6H_m), 2.19 (d, $^3J = 8.4$ Hz, 2H_c), 2.65-2.71 (m, 2H_d), 3.67-3.74 (m, 4H_k), 3.84-3.88 (m, 2H_h), 5.13-5.18 (m, 2H_{a/a'}), 5.78 (m, H_b), 7.19-7.30 (m, 2H_{Ph}), 7.44-7.49 (m, H_{Ph}), 9.74 (t, $^3J = 2.4$ Hz, H_i); **$^{13}\text{C NMR}$ (100 MHz, CDCl_3) δ (ppm)**: 21.6, 23.6, 26.2, 36.1, 373, 49.5 (C_h), 67.0 (2C_k), 81.5 (C_{e/f}), 91.7 (C_{e/f}), 98.3 (C_l), 119.2 (C_a), 124.4, 127.6, 128.2, 128.2, 128.4, 128.7, 130.2, 132.2, 132.3, 132.8, 132.8, 134.2, 199.4 (C_i).

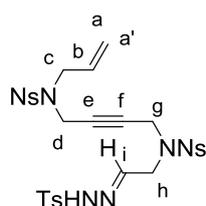
8.3.1.7. Synthesis of *N*-tosylhydrazones **28**



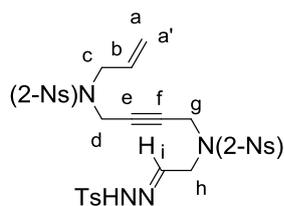
General procedure for 28. A solution of *p*-toluensulfonylhydrazide **3a** (0.46 g, 2.47 mmol) in methanol (10 mL) was prepared and stirred rapidly. A solution of **39a** (0.79 g, 2.46 mmol) in methanol (20 mL) and the minimum amount of acetonitrile to completely dissolve the product was then added dropwise. After the addition, the mixture was stirred at room temperature for 1 hour (TLC monitoring). The solvent was concentrated under reduced pressure and purified by column chromatography on silica gel (hexane/ethyl acetate 9:1 to 7:3) to afford **28a** (0.75 g, 63%, *Z/E*:14/86)¹¹⁶ as a waxy colourless solid. R_f (hexane/ethyl acetate 6:4): 0.33; **MW**: 489.61 g/mol; **IR (ATR) ν (cm^{-1})**: 3207, 2919, 1343, 1158; **$^1\text{H NMR}$ (300 MHz, CDCl_3) δ (ppm)**: 2.42 (s, 6H_{Ts,Ts}), 3.85 (t, $^5J = 1.8$ Hz, 2H_g), 3.88-3.92 (m, 6H_{c,d,h}), 5.23-5.30 (m, 2H_{a,a'}), 5.88 (ddt, $^3J = 17.1$ Hz / $^3J = 10.5$ Hz / $^3J = 5.3$ Hz, H_b), 7.05 (t, $^3J = 5.3$ Hz, H_i), 7.27-7.31 (m, 4H_{Ts}), 7.66 (d, $^3J = 8.4$ Hz, 2H_{Ts}), 7.79 (d, $^3J = 8.1$ Hz, 2H_{Ts}), 8.01 (br s, H_{NH}); **$^{13}\text{C NMR}$ (75 MHz, CDCl_3) δ (ppm)**: 21.3 (2C_{Ts}), 37.2 (C_g), 48.2 (C_h), 56.8 (C_d), 70.3 (C_c), 78.8 (C_{e/f}), 81.9 (C_{e/f}), 117.8 (C_a), 127.5 (2C_{Ts}), 127.6 (2C_{Ts}), 129.4 (2C_{Ts}), 129.5 (2C_{Ts}), 133.5 (C_b), 135.0 (C_{Ts}), 135.1 (C_{Ts}), 143.9 (2C_{Ts}), 145.3 (C_i); **ESI-MS (m/z)**: 512.2 [M+Na]⁺, 528.1 [M+K]⁺; **EA**: calculated for C₂₃H₂₇N₃O₅S₂: C, 56.42; H, 5.56; N, 8.58; found: C, 56.09 and 56.26; H, 5.44 and 5.71; N, 8.39 and 8.49.



28b Using the same experimental procedure as for compound **28a**, **28b** was obtained as a colourless solid (0.14 g, 93% yield, *Z/E*:7/93)¹¹⁶ after 1 hour. **R_f** (hexane/ethyl acetat 6:4): 0.24; **MW**: 642.80 g/mol; **m.p.**: 139-140 °C; **IR (ATR) v (cm⁻¹)**: 3188, 2920, 1341, 1158; **¹H NMR (400 MHz, CDCl₃) δ (ppm)**: 2.39 (s, 3H_{Ts}), 2.40 (s, 3H_{Ts}), 2.41 (s, 3H_{Ts}), 3.63 (d, ³*J* = 6.0 Hz, 2H_h), 3.73 (d, ³*J* = 5.2 Hz, H_c), 3.75 (s, 2H_{d/g}), 3.79 (s, 2H_{d/g}), 5.10-5.20 (m, 2H_{a,a'}), 5.56 (m, H_b), 7.12 (t, ³*J* = 6.0 Hz, H_i), 7.26-7.31 (m, 6H_{Ts}), 7.57 (d, ³*J* = 8.4 Hz, 2H_{Ts}), 7.65 (d, ³*J* = 8.4 Hz, 2H_{Ts}), 7.77 (d, ³*J* = 8.4 Hz, 2H_{Ts}), 8.73 (br s, H_{NH}); **¹³C NMR (75 MHz, CDCl₃) δ (ppm)**: 21.5 (C_{Ts}), 21.6 (C_{Ts}), 21.7 (C_{Ts}), 35.7 (C_{d/g}), 37.6 (C_{d/g}), 48.8 (C_c), 49.2 (C_h), 78.4 (C_{eff}), 79.3 (C_{eff}), 120.0 (C_a), 127.6 (2C_{Ts}), 127.7 (2C_{Ts}), 127.7 (2C_{Ts}), 129.7 (2C_{Ts}), 129.8 (2C_{Ts}), 129.8 (2C_{Ts}), 131.7 (C_b), 135.4 (C_{Ts}), 135.4 (C_{Ts}), 135.8 (C_{Ts}), 144.1 (C_{Ts}), 144.3 (2C_{Ts}), 145.3 (C_i); **ESI-MS (m/z)**: 643.1 [M+H]⁺; **EA**: calculated for C₃₀H₃₄N₄O₆S₃·0.5H₂O: C, 55.28; H, 5.41; N, 8.60; found: C, 55.14 and 55.31; H, 5.05 and 5.04; N, 8.31 and 8.32.

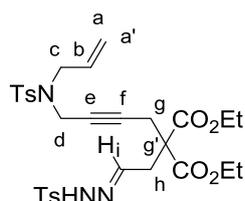


28c Using the same experimental procedure as for compound **28a**, **28c** was obtained as a pale orange solid (0.64 g, 100% yield, *Z/E*:9/91)¹¹⁶ after 1 hour. **R_f** (hexane/ethyl acetat 1:1): 0.32; **MW**: 704.74 g/mol; **m.p.**: 77-79°C; **IR (ATR) v (cm⁻¹)**: 1528, 1347, 1159; **¹H NMR (300 MHz, CDCl₃) δ (ppm)**: 2.44 (s, 3H_{Ts}), 3.77 (d, ³*J* = 6.3 Hz, 2H_c), 3.87 (s, 2H_{d/g}), 3.96-3.98 (m, 4H_{d/g,h}), 5.15-5.24 (m, 2H_{a/a'}), 5.49 (ddt, ³*J* = 16.8 Hz / ³*J* = 10.2 Hz / ³*J* = 6.3 Hz, H_b), 7.10 (t, ³*J* = 5.1 Hz, H_i), 7.33 (d, ³*J* = 8.4 Hz, 2H_{Ts}), 7.78 (d, ³*J* = 8.4 Hz, 2H_{Ts}), 7.93 (d, ³*J* = 8.7 Hz, 2H_{Ns}), 7.98 (d, ³*J* = 8.7 Hz, 2H_{Ns}), 8.31 (d, ³*J* = 8.7 Hz, 2H_{Ns}), 8.37 (br s, H_{NH}), 8.36 (d, ³*J* = 8.7 Hz, 2H_{Ns}); **¹³C NMR (100 MHz, CDCl₃) δ (ppm)**: 21.6 (C_{Ts}), 36.0 (C_{d/g}), 37.5 (C_{d/g}), 48.6 (C_c), 49.6 (C_h), 78.5 (C_{eff}), 79.4 (C_{eff}), 120.6 (C_a), 124.4, 124.5, 127.8, 128.7, 128.8, 129.8, 130.9, 135.0, 144.1, 144.3, 144.6, 144.7, 150.3, 150.3; **ESI-MS (m/z)**: 727.2 [M+Na]⁺, 743.1 [M+K]⁺; **EA**: calculated for C₂₈H₂₈N₆O₁₀S₃: C, 47.72; H, 4.00; N, 11.93; found: C, 47.62 and 47.43; H, 3.87 and 3.77; N, 11.75 and 11.76.



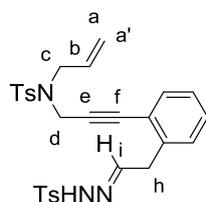
28d Using the same experimental procedure as for compound **28a**, **28d** was obtained as a pale orange solid (0.44 g, 100% yield, *Z/E*:6/94)¹¹⁶ after 1 hour. **R_f** (hexane/ethyl acetat 1:1): 0.38; **MW**: 704.74 g/mol; **m.p.**: 80-82°C; **IR (ATR) v (cm⁻¹)**: 3222, 2924, 1541, 1351, 1159; **¹H**

NMR (400 MHz, CDCl₃) δ (ppm): 2.42 (s, 3HTs), 3.84 (d, ³J = 6.4 Hz, 2H_c), 3.90 (s, H_{d/g}), 3.96 (s, H_{d/g}), 4.01 (d, ³J = 5.2 Hz, 2H_h), 5.19-5.24 (m, 2H_{a/a'}), 5.57 (ddt, ³J = 16.8 Hz / ³J = 10.0 Hz / ³J = 6.4 Hz, H_b), 7.18 (t, ³J = 5.2 Hz, H_i), 7.30 (d, ³J = 8.6 Hz, 2H_{Ts}), 7.65-7.90 (m, 6H_{2-Ns}), 7.69 (d, ³J = 8.6 Hz, 2H_{Ts}), 8.01 (m, H_{2-Ns}), 8.06 (m, H_{2-Ns}), 8.48 (br s, H_{NH}); **¹³C NMR (75 MHz, CDCl₃) δ (ppm):** 21.6 (CTs), 36.0, 37.5, 48.8, 49.5, 78.9 (C_{e/f}), 79.4 (C_{e/f}), 120.5 (C_a), 124.4, 124.7, 127.7, 128.0, 130.2, 130.9, 131.0, 131.1, 132.4, 132.5, 134.0, 135.2, 144.3, 149.9 (C_i); **ESI-MS (m/z):** 705.1 [M+H]⁺, 727.1 [M+Na]⁺; **EA:** calculated for C₂₈H₂₈N₆O₁₀S₃: C, 47.72; H, 4.00; N, 11.93; found: C, 48.13; H, 4.04; N, 11.42.



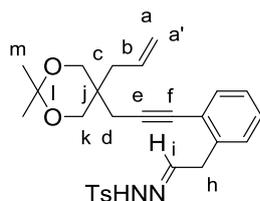
28e Using the same experimental procedure as for compound **28a**, **28e** was obtained

as a waxy colourless solid (0.84 g, 87% yield, *Z/E*:8/92)¹¹⁶ after 1 hour. **R_f** (hexane/ethyl acetat 1:1): 0.33; **MW:** 631.76 g/mol; **IR (ATR) ν (cm⁻¹):** 3208, 2975, 1737, 1721, 1322, 1159; **¹H NMR (400 MHz, CDCl₃) δ (ppm):** 1.14 (t, ³J = 7.0 Hz, 6H_{CO₂CH₂CH₃}), 2.38 (s, 3H_{Ts}), 2.41 (s, 3H_{Ts}), 2.54 (s, 2H_g), 2.61 (d, ³J = 5.2 Hz, 2H_h), 3.76 (d, ³J = 6.2 Hz, 2H_c), 3.99 (s, 2H_d), 4.04 (q, ³J = 7.0 Hz, 4H_{CO₂CH₂CH₃}), 5.19 (d, ³J = 10.2 Hz, H_a), 5.24 (d, ³J = 17.0 Hz, H_a), 5.65 (ddt, ³J = 6.2 Hz / ³J = 10.2 Hz / ³J = 17.0 Hz, H_b), 7.18 (t, ³J = 5.2 Hz, H_i), 7.16-7.30 (m, 4H_{Ts}), 7.68 (d, ³J = 8.0 Hz, 2H_{Ts}), 7.79 (d, ³J = 8.4 Hz, 2H_{Ts}), 8.81 (br s, H_{NH}); **¹³C NMR (100 MHz, CDCl₃) δ (ppm):** 13.8 (2C_{CO₂CH₂CH₃}), 21.3 (C_{Ts}), 21.4 (C_{Ts}), 23.5 (C_h), 35.4 (C_{d/g}), 35.9 (C_{d/g}), 48.7 (C_g), 55.5 (C_c), 61.8 (2C_{CO₂CH₂CH₃}), 76.4 (C_{e/f}), 80.0 (C_{e/f}), 119.8 (C_a), 127.4 (2C_{Ts}), 127.8 (2C_{Ts}), 129.4 (2C_{Ts}), 129.5 (2C_{Ts}), 131.7 (C_b), 135.4 (C_{Ts}), 135.8 (C_{Ts}), 143.6 (C_{Ts}), 143.8 (C_{Ts}), 146.8 (C_i), 168.8 (2C_{CO₂Et}); **ESI-MS (m/z):** 632.2 [M+H]⁺, 654.3 [M+Na]⁺; **EA:** calculated for C₃₀H₃₇N₃O₈S₂: C, 57.04; H, 5.90; N, 6.65; found: C, 57.07 and 56.77; H, 5.99 and 5.97; N, 6.75 and 6.68.

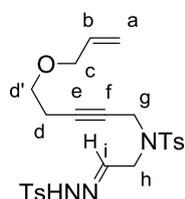


28f Using the same experimental procedure as for compound **28a**, **28f** was obtained as

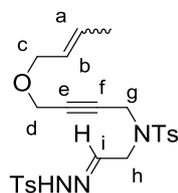
a pale yellow solid (0.30 g, 87% yield, *Z/E*:27/73)¹¹⁶ after 1 hour. **R_f** (hexane/ethyl acetat 1:1): 0.35; **MW:** 535.68 g/mol; **m.p.:** 60-61°C; **IR (ATR) ν (cm⁻¹):** 2920, 1345, 1325, 1156; **¹H NMR (400 MHz, CDCl₃) δ (ppm):** 2.32 (s, 3H_{Ts}), 2.42 (s, 3H_{Ts}), 3.47 (d, ³J = 5.6 Hz, 2H_h), 3.79 (d, ³J = 6.4 Hz, 2H_c), 4.25 (s, 2H_d), 5.20-5.26 (m, 2H_{a/a'}), 5.68 (m, H_b), 7.00-7.28 (m, 9H_{Ts,Ph,i}), 7.71-7.82 (m, 4H_{Ts}), 8.06 (br s, H_{NH}); **¹³C NMR (100 MHz, CDCl₃) δ (ppm):** 21.6 (C_{Ts}), 21.7 (C_{Ts}), 36.7 (C_{d/h}), 37.4 (C_{d/h}), 49.5 (C_c), 83.7 (C_{e/f}), 87.3 (C_{e/f}), 120.0 (C_a), 120.1, 122.2, 126.9, 127.8, 128.0, 128.1, 128.2, 129.0, 129.4, 129.7, 129.8, 132.1, 132.6, 135.5, 136.2, 138.0, 143.9, 144.2, 150.0 (C_i); **ESI-HRMS (m/z):** calculated for [M+Na]⁺: 558.1492; experimental: 558.1509.



28g Using the same experimental procedure as for compound **28a**, **28g** was obtained as a pale yellow waxy solid (0.38 g, 22% yield, *Z/E*:22/78)¹¹⁶ after 1 hour. **R_f** (hexane/ethyl acetat 1:1): 0.30; **MW**: 480.62 g/mol; **IR (ATR) v (cm⁻¹)**: 2923, 1163; **¹H NMR (400 MHz, CDCl₃) δ (ppm)**: 1.41 (s, 3H_m), 1.43 (s, 3H_m), 2.11 (d, ³J = 7.6 Hz, 2H_c), 2.61 (s, 2H_d), 3.59-3.69 (m, 6H_{h,k}), 5.09-5.13 (m, 2H_{a,a'}), 5.75 (m, H_b), 6.99-7.37 (m, 7H_{Ts,Ph,i}), 7.75 (d, ³J = 8.4 Hz, 2H_{Ts}), 8.30 (br s, H_{NH}); **¹³C NMR (100 MHz, CDCl₃) δ (ppm)**: 21.2, 21.6 (C_{Ts}), 23.3, 26.5, 36.0, 37.3, 37.5, 66.8 (2C_k), 81.5 (C_{eff}), 91.5 (C_{eff}), 98.4 (C_i), 119.1 (C_a), 123.4, 126.8, 127.9, 128.0, 128.1, 129.3, 129.6, 129.7, 132.1, 132.5, 135.5, 138.0, 143.9, 150.2 (C_i).

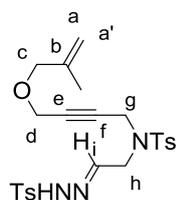


28h Using the same experimental procedure as for compound **28a**, **28h** was obtained as a colourless waxy solid (0.28 g, 59% yield, *Z/E*:7/93)¹¹⁶ after 1 hour. **R_f** (hexane/ethyl acetat 1:1): 0.49; **MW**: 503.63 g/mol; **¹H NMR (400 MHz, CDCl₃) δ (ppm)**: 2.14-2.17 (m, 2H_{d'}), 2.37 (s, 3H_{Ts}), 2.40 (s, 3H_{Ts}), 3.29 (t, ³J = 6.6 Hz, 2H_d), 3.79 (s, 2H_g), 3.87 (d, ³J = 5.6 Hz, 2H_h), 3.93 (dt, ²J = 6.0 Hz / ³J = 1.6 Hz, 2H_c), 5.17 (m, H_{a'}), 5.25 (m, H_a), 5.85 (ddt, ³J = 17.2 Hz / ³J = 10.4 Hz / ³J = 5.6 Hz, H_b), 7.13 (t, ³J = 5.6 Hz, H_i), 7.25 (d, ³J = 8.4 Hz, 2H_{Ts}), 7.27 (d, ³J = 8.4 Hz, 2H_{Ts}), 7.64 (d, ³J = 8.4 Hz, 2H_{Ts}), 7.76 (d, ³J = 8.4 Hz, 2H_{Ts}), 9.01 (br s, H_{NH}); **¹³C NMR (100 MHz, CDCl₃) δ (ppm)**: 19.6 (C_{d'}), 21.3 (C_{Ts}), 21.4 (C_{Ts}), 37.6 (C_g), 48.6 (C_h), 67.8 (C_d), 71.6 (C_c), 73.9 (C_{eff}), 83.4 (C_{eff}), 117.6 (C_a), 127.5 (2C_{Ts}), 127.6 (2C_{Ts}), 129.4 (2C_{Ts}), 129.5 (2C_{Ts}), 134.1 (C_b), 135.3 (C_{Ts}), 135.4 (C_{Ts}), 143.8 (C_{Ts}), 143.9 (C_{Ts}), 145.8 (C_i).



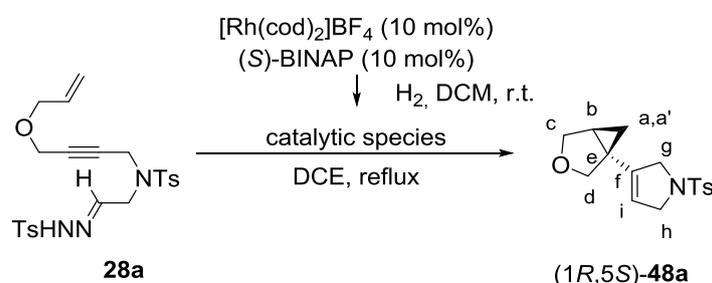
28i Using the same experimental procedure as for compound **28a**, **28i** was obtained as a colourless oil (0.76 g, 87% yield, *Z/E*:8/92)¹¹⁶ after 1 hour. **R_f** (hexane/ethyl acetat 1:1): 0.58; **MW**: 503.63 g/mol; **IR (ATR) v (cm⁻¹)**: 3209, 2920, 1345, 1158; **¹H NMR (400 MHz, CDCl₃) δ (ppm)**: 1.72-1.75 (m, 3H_{CH3}), 2.41 (s, 3H_{Ts}), 2.42 (s, 3H_{Ts}), 3.80-3.82 (m, 4H_{c,g}), 3.87 (t, ⁵J = 2.0 Hz, 2H_d), 3.89 (d, ³J = 5.2 Hz, 2H_h), 5.51 (m, H_{a/b}), 5.71 (m, H_{a/b}), 7.07 (t, ³J = 5.2 Hz, H_i), 7.27-7.30 (m, 4H_{Ts}), 7.65 (d, ³J = 8.4 Hz, 2H_{Ts}), 7.77 (d, ³J = 8.0 Hz, 2H_{Ts}), 8.35 (br s, H_{NH}); **¹³C NMR (100 MHz, CDCl₃) δ (ppm)**: 17.9 (C_{CH3}), 21.6 (C_{Ts}), 21.7 (C_{Ts}), 37.8 (C_g), 49.1 (C_h), 56.8 (C_d), 70.9 (C_c), 79.7 (C_{eff}), 82.5 (C_{eff}), 126.5 (C_a), 127.8 (2C_{Ts}), 128.0 (2C_{Ts}), 129.7 (2C_{Ts}), 129.8 (2C_{Ts}), 131.3 (C_b), 135.4 (C_{Ts}), 135.5 (C_{Ts}), 144.2

(C_{Ts}), 144.3 (C_{Ts}), 146.1 (C_i); **ESI-HRMS (m/z)**: calculated for [M+Na]⁺: 526.1441; experimental: 526.1415.



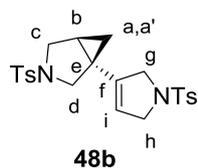
28k Using the same experimental procedure as for compound **28a**, **28k** was obtained as a colourless oil (0.84 g, 82% yield, *Z/E*: 6/94)¹¹⁶ after 1 hour. **R_f** (hexane/ethyl acetat 1:1): 0.53; **MW**: 503.63 g/mol; **IR (ATR) v (cm⁻¹)**: 3201, 2921, 1344, 1158; **¹H NMR (400 MHz, CDCl₃) δ (ppm)**: 1.71 (s, 3H_{CH3}), 2.40 (s, 3H_{Ts}), 2.40 (s, 3H_{Ts}), 3.79 (s, 2H_h), 3.81 (s, 2H_g), 3.86-3.88 (m, 4H_{c,d}), 4.91-4.92 (m, 2H_{a,a'}), 7.10 (t, ³*J* = 5.4 Hz, H_i), 7.27 (d, ³*J* = 8.4 Hz, 4H_{Ts}), 7.65 (d, ³*J* = 8.4 Hz, 2H_{Ts}), 7.77 (d, ³*J* = 8.4 Hz, 2H_{Ts}), 8.72 (br s, H_{NH}); **¹³C NMR (100 MHz, CDCl₃) δ (ppm)**: 19.5 (C_{CH3}), 21.5 (C_{Ts}), 21.6 (C_{Ts}), 37.5 (C_g), 48.4 (C_h), 56.9 (C_d), 73.8 (C_c), 79.2 (C_{eff}), 82.2 (C_{eff}), 113.3 (C_a), 127.7 (2C_{Ts}), 127.9 (2C_{Ts}), 129.6 (2C_{Ts}), 129.7 (2C_{Ts}), 135.2 (C_b), 141.1 (C_{Ts}), 141.3 (C_{Ts}), 144.1 (C_{Ts}), 144.2 (C_{Ts}), 145.6 (C_i); **ESI-MS (m/z)**: 504.1 [M+H]⁺, 526.2 [M+Na]⁺; **EA**: calculated for C₂₄H₂₉N₃O₅S₂·0.5H₂O: C, 56.23; H, 5.90; N, 8.20; found: C, 56.16 and 56.52; H, 5.86 and 6.06; N, 7.94 and 8.04.

8.3.2. Experimental procedure for the rhodium(I)-catalysed cyclisation of *N*-tosylhydrazone derivatives **28**

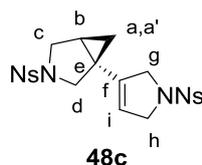


General procedure for 48. [Rh(cod)₂]BF₄ (0.0112 g, 0.028 mmol) and (S)-BINAP (0.0172 g, 0.028 mmol) were dissolved in CH₂Cl₂ (4 mL) under N₂. Hydrogen gas was bubbled to the stirred catalyst solution for 30 minutes and the resulting mixture was concentrated to dryness. The mixture was then dissolved in 1,2-dichloroethane (1.5 mL) and a solution of **28a** (0.1092 g, 0.28 mmol) in 1,2-dichloroethane (1.5 mL) was added. The reaction mixture was heated at reflux for 1.5 hours (TLC monitoring). The solvent was evaporated and the residue was purified by column chromatography on silica gel (hexane/ethyl acetate, 10:0 to 9:1) to afford **48a** (0.0599 g, 71% yield, 78% ee) as a colourless solid. **R_f** (hexane/ethyl acetat 1:1): 0.46; **MW**: 305.39 g/mol; **m.p.**: 101-103°C; **[α]_D²⁰** +40.25 (c 0.20 g / 100 mL, CH₃CN); **IR (ATR) v (cm⁻¹)**: 2928, 1333, 1160; **¹H NMR (300 MHz, CDCl₃) δ (ppm)**: 0.78-0.85 (m, 2H_{a/a'}), 1.61 (m, H_b), 2.44 (s, 3H_{Ts}), 3.69-3.73 (m, 2H_c), 3.78-3.83 (m, 2H_d), 3.92-3.94 (m, 2H_g), 4.10-4.12 (m, 2H_h), 5.33 (m, H_i), 7.34 (d, ³*J* = 8.4 Hz, 2H_{Ts}), 7.72 (d, ³*J* = 8.4 Hz, 2H_{Ts}); **¹³C NMR (75 MHz, CDCl₃) δ (ppm)**: 13.5 (C_{a/a'}), 21.1 (C_{Ts}), 24.4 (C_b), 27.9 (C_e), 55.1 (C_c), 55.3 (C_d),

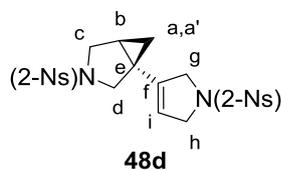
69.6 (C_g), 70.6 (C_h), 118.2 (C_i), 127.4 (C_{Ts}), 127.5 (C_{Ts}), 129.9 (2C_{Ts}), 134.1 (C_{Ts}), 137.6 (C_f), 143.6 (C_{Ts}); **ESI-MS (m/z)**: 306.1 [M+H]⁺, 328.1 [M+Na]⁺; **AE**: calculated for C₁₆H₁₉NO₃S: C, 62.93; H, 6.27; N, 4.59; found: C, 62.41 and 63.24; H, 6.20 and 6.21; N, 4.68 and 4.44. The enantiomeric excess has been determined by **HPLC** analysis using a CHIRALPAK AD-H column (4.6 x 250 mm, 5 μm) with 99% hexane / 1 % 2-PrOH mobile phase at a 1.0 mL/min flow rate, using a UV detector set up at λ = 254 nm. The retention time for the major isomer is 21.0 min and for the minor isomer is 22.0 min.



Using the same experimental procedure as for compound **48a**, **48b** was obtained as a colourless solid (0.0198 g, 74% yield, 88% ee) after 1 hour. **R_f** (hexane/ethyl acetat 6:4): 0.31; **MW**: 458.59 g/mol; **m.p.**: 79-82 °C; **[α]²⁰_D** -3.74 (c 0.17 g / 100 mL, CH₃CN); **IR (ATR) ν (cm⁻¹)**: 2922, 1327, 1159; **¹H NMR (400 MHz, CDCl₃) δ (ppm)**: 0.80 (dd, ²J = 8.0 Hz / ³J = 5.6 Hz, H_{a/a'}), 0.86 (dd, ²J = 8.0 Hz / ³J = 5.3 Hz, H_{a/a'}), 1.51 (ddt, ³J = 4.4 Hz / ³J = 4.4 / ³J = 4.4 Hz, H_b), 2.42 (s, 3H_{Ts}), 2.44 (s, 3H_{Ts}), 3.02-3.05 (m, 2H_c), 3.52-3.56 (m, 2H_{g/h}), 3.79-3.82 (m, 2H_{g/h}), 4.05-4.07 (m, 2H_h), 5.28 (m, H_i), 7.30-7.34 (m, 4H_{Ts}), 7.65-7.66 (m, 4H_{Ts}); **¹³C NMR (75 MHz, CDCl₃) δ (ppm)**: 14.1 (C_{a/a'}), 21.7 (C_{Ts}), 23.0 (C_{Ts}), 26.9 (C_e), 49.7 (C_d), 51.2 (C_d), 54.6 (C_h), 55.3 (C_g), 118.9 (C_i), 127.5 (2C_{Ts}), 127.6 (2C_{Ts}), 129.9 (2C_{Ts}), 130.0 (2C_{Ts}), 133.4 (C_{Ts}), 134.1 (C_{Ts}), 137.68 (C_f), 143.8 (C_{Ts}), 143.9 (C_{Ts}); **ESI-MS (m/z)**: 459.0 [M+H]⁺; **AE**: calculated for C₂₃H₂₆N₂O₄S₂·0.5H₂O: C, 59.08; H, 5.82; N, 5.99; found: C, 59.62; H, 5.94; N, 5.47. The enantiomeric excess has been determined by **HPLC** analysis using a CHIRALPAK AD-H column (4.6 x 250 mm, 5 μm) with 80 % hexane / 20 % 2-PrOH mobile phase at a 1.0 mL/min flow rate, using a UV detector set up at λ = 254 nm. The retention time for the major isomer is 40.2 min and for the minor isomer is 34.8min.

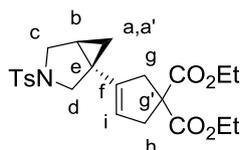


Using the same experimental procedure as for compound **48a**, **48c** was obtained as a colourless solid (0.0456 g, 100% yield) after 1 hour. **m.p.**: 203-205 °C (dec.); **R_f** (hexane/ethyl acetat 2:8): 0.52; **MW**: 520.53 g/mol; **[α]²⁰_D** +3.91 (c 0.12 g / 100 mL, CH₃CN); **IR (ATR) ν (cm⁻¹)**: 1528, 1346, 1161; **¹H NMR (400 MHz, CDCl₃) δ (ppm)**: 0.84-0.90 (m, 2H_{a/a'}), 1.61 (m, H_b), 3.12-3.17 (m, 2H_c), 3.61-3.66 (m, 2H_d), 3.88-3.90 (m, 2H_g), 4.10-4.15 (m, 2H_h), 5.36 (m, H_i), 7.96-7.99 (m, 4H_{Ns}), 8.36-8.38 (m, 4H_{Ns}); **AE**: calculated for C₂₁H₂₀N₄O₈S₂: C, 48.45; H, 3.87; N, 10.76; found: C, 48.74; H, 4.05; N, 10.31.

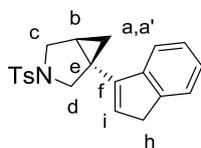


Using the same experimental procedure as for compound **48a**, **48d** was obtained as a dark brown waxy solid (0.0310 g, 71% yield) after 1 hour. **R_f** (hexane/ethyl acetat 2:8): 0.58; **MW**: 520.53 g/mol; **[α]²⁰_D** +5.21 (c 0.11 g / 100 mL, CH₃CN); **IR (ATR) ν (cm⁻¹)**: 2926, 1480,

1353, 1123; $^1\text{H NMR}$ (400 MHz, DMSO-d_6) δ (ppm): 0.51 (dd, $^2J = 5.6$ Hz / $^3J = 5.1$ Hz, H_a), 1.06 (dd, $^3J = 8.0$ Hz, $^2J = 5.6$ Hz, H_a), 1.89 (m, H_b), 3.39 (dd, $^2J = 10.0$ Hz / $^3J = 3.6$ Hz, H_c), 3.46 (d, $^2J = 10.0$ Hz, H_c), 3.50 (d, $^2J = 9.6$ Hz, H_d), 3.62 (d, $^2J = 9.6$ Hz, H_d), 4.05-4.07 (m, 2H_h), 4.16-4.18 (m, 2H_g), 5.63 (t, $^3J = 1.6$ Hz, H_i), 7.81-8.04 (m, $8\text{H}_{2-\text{Ns}}$); $^{13}\text{C NMR}$ (100 MHz, DMSO-d_6) δ (ppm): 13.2 (C_a), 22.4 (C_b), 26.4 (C_e), 49.7 (C_h), 51.0 (C_g), 54.6 (C_d), 55.3 (C_c), 118.7 ($\text{C}_{2-\text{Ns}}$), 124.3 ($\text{C}_{2-\text{Ns}}$), 124.4 ($\text{C}_{2-\text{Ns}}$), 129.5 (C_i), 129.6 ($\text{C}_{2-\text{Ns}}$), 129.8 ($\text{C}_{2-\text{Ns}}$), 130.3 ($\text{C}_{2-\text{Ns}}$), 132.4 ($\text{C}_{2-\text{Ns}}$), 132.6 ($\text{C}_{2-\text{Ns}}$), 134.7 ($\text{C}_{2-\text{Ns}}$), 134.9 ($\text{C}_{2-\text{Ns}}$), 136.9 (C_f), 147.6 ($\text{C}_{2-\text{Ns}}$), 147.9 ($\text{C}_{2-\text{Ns}}$); **ESI-MS** (m/z): 543.1 $[\text{M}+\text{Na}]^+$, 559.0 $[\text{M}+\text{K}]^+$; **ESI-HRMS** (m/z): calculated for $[\text{M}+\text{Na}]^+$: 543.0615; experimental: 543.0596.

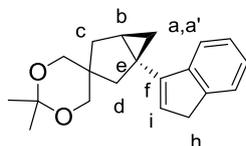
**48e**

Using the same experimental procedure as for compound **48a**, **48e** was obtained as a colourless waxy solid (0.0117 g, 53% yield, 81% ee) after 1 hour. R_f (hexane/ethyl acetat 1:1): 0.59; **MW**: 447.55 g/mol; $[\alpha]_D^{20}$ -6.27 (c 0.08 g / 100 mL, CH_3CN); **IR (ATR)** ν (cm^{-1}): 2924, 1729, 1344, 1161; $^1\text{H NMR}$ (400 MHz, CDCl_3) δ (ppm): 0.83 (m, $\text{H}_{a/a'}$), 0.91 (m, $\text{H}_{a/a'}$), 1.12-1.25 (m, $6\text{H}_{\text{CO}_2\text{CH}_2\text{CH}_3}$), 1.53 (m, H_b), 2.44 (s, 3H_{Ts}), 2.63-2.77 (m, 2H_h), 2.96-2.98 (m, 2H_g), 3.05 (dd, $^2J = 9.2$ Hz / $^3J = 3.6$ Hz, H_c), 3.09 (d, $^2J = 9.2$ Hz, H_c), 3.54 (d, $^2J = 9.4$ Hz, H_d), 3.58 (d, $^2J = 9.4$ Hz, H_d), 4.14 (q, $^3J = 7.2$ Hz, $2\text{H}_{\text{CO}_2\text{CH}_2\text{CH}_3}$), 4.16 (q, $^3J = 7.2$ Hz, $2\text{H}_{\text{CO}_2\text{CH}_2\text{CH}_3}$), 5.22 (m, H_i), 7.33 (d, $^3J = 8.2$ Hz, 2H_{Ts}), 7.67 (d, $^3J = 8.2$ Hz, 2H_{Ts}); $^{13}\text{C NMR}$ (75 MHz, CDCl_3) δ (ppm): 14.1 ($2\text{C}_{\text{CO}_2\text{CH}_2\text{CH}_3}$), 14.2 ($2\text{C}_{\text{CO}_2\text{CH}_2\text{CH}_3}$), 21.7 (C_{Ts}), 22.5 ($\text{C}_{a/a'}$), 28.4 (C_b), 29.8 (C_e), 40.8 ($\text{C}_{g/h}$), 40.8 ($\text{C}_{g/h}$), 49.9 ($\text{C}_{c/d}$), 51.5 ($\text{C}_{c/d}$), 58.6 (C_g), 61.8 ($2\text{C}_{\text{CO}_2\text{CH}_2\text{CH}_3}$), 120.9 (C_i), 127.8 (2C_{Ts}), 129.8 (2C_{Ts}), 133.3 (C_{Ts}), 139.6 (C_f), 134.7 (C_{Ts}), 171.9 ($\text{C}_{\text{CO}_2\text{Et}}$), 172.1 ($\text{C}_{\text{CO}_2\text{Et}}$); **ESI-HRMS** (m/z): calculated for $[\text{M}+\text{Na}]^+$: 470.1608; experimental: 470.1596. The enantiomeric excess has been determined by **HPLC** analysis using a CHIRALPAK AD-H column (4.6 x 250 mm, 5 μm) with 99 % hexane / 1 % 2-PrOH mobile phase at a 1.0 mL/min flow rate, using a UV detector set up at $\lambda = 220$ nm. The retention time for the major isomer is 23.9 min and for the minor isomer is 29.7 min.

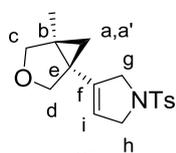
**48f**

Using the same experimental procedure as for compound **48a**, **48f** was obtained as a colourless solid (0.0314 g, 67% yield, 64% ee) after 1 hour. **m.p.**: 64-66 $^\circ\text{C}$; R_f (hexane/ethyl acetat 1:1): 0.40; **MW**: 351.46 g/mol; $[\alpha]_D^{20}$ +8.91 (c 0.44 g / 100 mL, CH_3CN); **IR (ATR)** ν (cm^{-1}): 2922, 1341, 1160; $^1\text{H NMR}$ (400 MHz, CDCl_3) δ (ppm): 0.99-1.05 (m, $2\text{H}_{a/a'}$), 1.71 (ddd, $^3J = 4.0$ Hz / $^3J = 4.0$ Hz / $^3J = 4.0$ Hz, H_b), 2.46 (s, 3H_{Ts}), 3.25-3.35 (m, $4\text{H}_{c,d}$), 3.69 (d, $^2J = 9.4$ Hz, H_d), 3.79 (d, $^2J = 9.4$ Hz, H_d), 6.23 (t, $^3J = 2.0$ Hz, H_i), 6.98 (m, H_{Ph}), 7.15-7.18 (m, 2H_{Ph}), 7.34 (d, $^3J = 8.1$ Hz, 2H_{Ts}), 7.43 (m, H_{Ph}), 7.72 (d, $^3J = 8.1$ Hz, 2H_{Ts}); $^{13}\text{C NMR}$ (100 MHz, CDCl_3) δ (ppm): 14.4 ($\text{C}_{a/a'}$), 21.7 (C_{Ts}), 21.9 (C_b), 26.8 (C_e), 37.7 (C_h), 50.5 (C_d), 52.9 (C_c), 119.7 (C_i), 124.2, 125.0, 126.2, 127.8, 129.8, 130.9, 133.3, 142.8, 143.7, 143.9, 144.7; **ESI-HRMS** (m/z): calculated for $[\text{M}+\text{Na}]^+$: 374.1185; experimental:

374.1181. The enantiomeric excess has been determined by **HPLC** analysis using a CHIRALPAK IA column (4.6 x 250 mm, 5 μ m) with 99% hexane / 1 % 2-PrOH mobile phase at a 0.5 mL/min flow rate, using a UV detector set up at λ = 240 nm. The retention time for the major isomer is 54.3 min and for the minor isomer is 58.3 min.

**48g**

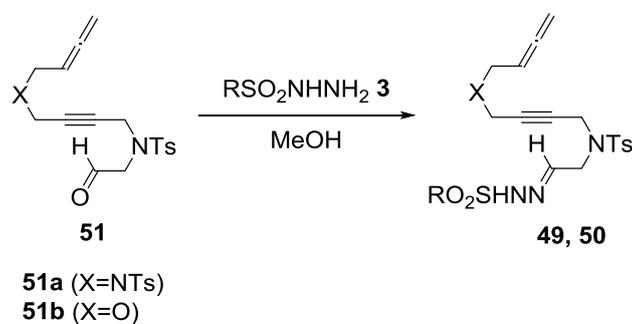
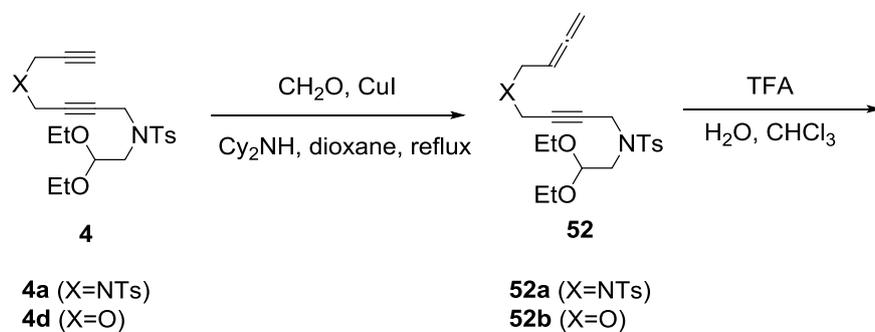
Using the same experimental procedure as for compound **48a**, **48g** was obtained as a colourless oil (0.0110g, 21% yield) after 3h. **R_f** (hexane/ethyl acetat 1:1): 0.54; **MW**: 296.41 g/mol; **¹H NMR (400 MHz, CDCl₃) δ (ppm)**: 0.58 (m, H_{a/a'}), 0.90 (m, H_{a/a'}), 1.06 (m, H_b), 1.38 (s, 3H_m), 1.41 (s, 3H_m), 1.73 (m, H_c), 1.81 (d, ²J = 14.0 Hz, H_c), 2.08 (s, 2H_d), 3.29 (d, ²J = 2.0 Hz, H_h), 3.64-3.66 (m, 4H_k), 6.19 (t, ³J = 2.0 Hz, H_i), 7.20 (m, H_{Ph}), 7.28 (m, 1H_{Ph}), 7.39-7.43 (m, 2H_{Ph}).

**48k**

Using the the optimised procedure described in Table 4.2, **48k** was obtained as a colourless waxy solid (0.0308 g, 63% yield, 74% ee) after 1 hour. **R_f** (hexane/ethyl acetat 1:1): 0.61; **MW**: 319.42 g/mol; **[α]²⁰_D** -13.58 (c 0.27 g / 100 mL, CH₃CN); **IR (ATR) ν (cm⁻¹)**: 2920, 1342, 1162; **¹H NMR (400 MHz, CDCl₃) δ (ppm)**: 0.64 (d, ²J = 4.8 Hz, H_{a/a'}), 0.88 (d, ²J = 4.8 Hz, H_{a/a'}), 1.00 (s, 3H_{CH3}), 2.43 (s, 3H_{Ts}), 3.51 (d, ²J = 8.4 Hz, H_c), 3.66 (d, ²J = 8.2 Hz, H_d), 3.72 (d, ²J = 8.2 Hz, H_d), 3.79 (d, ²J = 8.2 Hz, H_c), 3.93-4.16 (m, 4H_{g,h}), 5.35 (t, ³J = 2.0 Hz, H_i), 7.32 (d, ³J = 8.0 Hz, 2H_{Ts}), 7.72 (d, ³J = 8.0 Hz, 2H_{Ts}); **¹³C NMR (100 MHz, CDCl₃) δ (ppm)**: 13.0 (C_{CH3}), 17.8 (C_{a/a'}), 21.5 (C_{Ts}), 31.2 (C_{e/b}), 31.4 (C_{e/b}), 54.9 (C_h), 55.6 (C_g), 71.7 (C_d), 74.5 (C_c), 120.8 (C_i), 127.4 (2C_{Ts}), 129.8 (2C_{Ts}), 134.2 (C_{Ts}), 136.3 (C_f), 143.5 (C_{Ts}); **ESI-HRMS (m/z)**: calculated for [M+H]⁺ and [M+Na]⁺: 320.1315 and 342.1134; experimental: 320.1304 and 342.1131. The enantiomeric excess has been determined by **HPLC** analysis using a CHIRALPAK AD-H column (4.6 x 250 mm, 5 μ m) with 90 % hexane / 10 % 2-PrOH mobile phase at a 1.0 mL/min flow rate, using a UV detector set up at λ = 220 nm. The retention time for the major isomer is 15.4 min and for the minor isomer is 16.8 min.

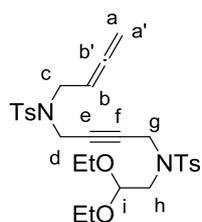
8.4. Experimental procedure for the products synthesised in Chapter 5

8.4.1. Synthesis of substrates



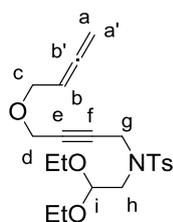
X	R	N-Sulfonylhydrazone
NTs	<i>p</i> -CH ₃ Ph	49
O	<i>p</i> -CH ₃ Ph	50a
O	Ph	50b
O	<i>p</i> -OCH ₃ Ph	50c
O	<i>p</i> -NO ₂ Ph	50d
O	<i>p</i> -IPh	50e
O	Naphthalene	50f
O	Dansyl	50g
O	CH ₃	50h
O	CH ₃ CH ₂ CH ₂ CH ₂	50i
O	2-Thiophene	50j

8.4.1.1. Synthesis of allenes 52



52a

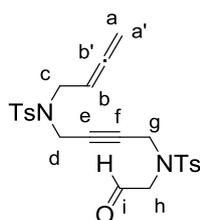
General procedure for 52. In a 250 mL 2-necked round bottom flask, a mixture of **4a** (3.01 g, 5.51 mmols), formaldehyde (0.41 g, 13.67 mmols) and copper(I) iodide (0.36 g, 2.76 mmols) in dioxane (100 mL) was heated to reflux. Dicyclohexylamine (1.4 mL, 10.00 mmols) was then added slowly to the reaction mixture. The mixture was stirred for 15 hours until completion (TLC monitoring). The insoluble salts were filtered off and the solvent was removed under reduced pressure. The reaction crude was purified by column chromatography on silica gel (hexane/ethyl acetate, 9:1 to 6:4) to afford **52a** as a dark brown waxy solid (2.46 g, 80% yield). **MW:** 560.72 g/mol; **IR (ATR) ν (cm^{-1}):** 2975, 2929, 1331, 1158; **$^1\text{H NMR}$ (400 MHz, CDCl_3) δ (ppm):** 1.20 (t, $^3J = 7.2$ Hz, $6\text{H}_{\text{OCH}_2\text{CH}_3}$), 2.43 (s, 6H_{Ts}), 3.06 (d, $^3J = 5.6$ Hz, 2H_h), 3.54 (dq, $^2J = 9.4$ Hz / $^3J = 7.2$ Hz, $2\text{H}_{\text{OCH}_2\text{CH}_3}$), 3.62 (dt, $^3J = 6.8$ Hz / $^5J = 2.4$ Hz, 2H_c), 3.72 (dq, $^2J = 9.4$ Hz / $^3J = 7.2$ Hz, $2\text{H}_{\text{OCH}_2\text{CH}_3}$), 3.90 (t, $^5J = 2.0$ Hz, $2\text{H}_{d/g}$), 4.10 (t, $^5J = 2.0$ Hz, $2\text{H}_{d/g}$), 4.61 (t, $^3J = 5.6$ Hz, H_i), 4.72 (dt, $^4J = 6.8$ Hz / $^5J = 2.4$ Hz, $2\text{H}_{a,a'}$), 4.89 (tt, $^3J = 6.8$ Hz, $^4J = 6.8$ Hz, H_b), 7.27-7.30 (m, 4H_{Ts}), 7.61 (d, $^3J = 8.4$ Hz, 2H_{Ts}), 7.66 (d, $^3J = 8.4$ Hz, 2H_{Ts}); **$^{13}\text{C NMR}$ (100 MHz, CDCl_3) δ (ppm):** 15.4 ($2\text{C}_{\text{OCH}_2\text{CH}_3}$), 21.5 (2C_{Ts}), 35.9 (C_g), 38.5 (C_d), 45.4 (C_c), 48.7 (C_h), 63.7 ($2\text{C}_{\text{CO}_2\text{CH}_2\text{CH}_3}$), 67.1 (C_a), 76.5 ($\text{C}_{e/f}$), 79.0 ($\text{C}_{e/f}$), 85.3 (C_b), 103.0 (C_i), 127.5 (2C_{Ts}), 127.6 (2C_{Ts}), 129.5 (2C_{Ts}), 129.6 (2C_{Ts}), 136.2 (C_{Ts}), 136.2 (C_{Ts}), 143.7 (2C_{Ts}), 209.6 (C_b); **ESI-MS (m/z):** 583.2 [$\text{M}+\text{Na}$] $^+$; **EA:** calculated for $\text{C}_{28}\text{H}_{36}\text{N}_2\text{O}_6\text{S}_2$: C, 59.98; H, 6.47; N, 5.00; found: C, 60.08 and 60.11; H, 6.62 and 6.54; N, 5.15 and 5.03.



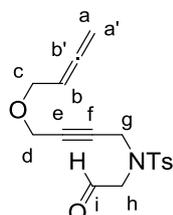
52b

Using the same experimental procedure as for compound **52a**, **52b** was obtained as a pale orange oil (1.85 g, 71% yield) after 15 hours. **MW:** 407.52 g/mol; **IR (ATR) ν (cm^{-1}):** 2976, 2931, 1346, 1159; **$^1\text{H NMR}$ (400 MHz, CDCl_3) δ (ppm):** 1.22 (t, $^3J = 7.2$ Hz, $6\text{H}_{\text{OCH}_2\text{CH}_3}$), 2.42 (s, 3H_{Ts}), 3.24 (d, $^3J = 5.6$ Hz, 2H_h), 3.57 (dq, $^2J = 9.4$ Hz / $^3J = 7.2$ Hz, $2\text{H}_{\text{OCH}_2\text{CH}_3}$), 3.75 (dq, $^2J = 9.4$ Hz / $^3J = 7.2$ Hz, $2\text{H}_{\text{OCH}_2\text{CH}_3}$), 3.85 (dt, $^3J = 6.6$ Hz, $^5J = 2.4$ Hz, 2H_c), 3.90 (t, $^5J = 2.0$ Hz, 2H_g), 4.33 (t, $^5J = 2.0$ Hz, 2H_d), 4.69 (t, $^3J = 5.6$ Hz, H_i), 4.80 (dt, $^4J = 6.6$ Hz / $^5J = 2.4$ Hz, $2\text{H}_{a,a'}$), 5.13 (tt, $^3J = 6.6$ Hz, $^4J = 6.6$ Hz, H_b), 7.28 (d, $^3J = 8.4$ Hz, 2H_{Ts}), 7.74 (d, $^3J = 8.4$ Hz, 2H_{Ts}); **$^{13}\text{C NMR}$ (100 MHz, CDCl_3) δ (ppm):** 15.5 ($2\text{C}_{\text{OCH}_2\text{CH}_3}$), 21.7 (C_{Ts}), 38.9 (C_g), 48.8 (C_h), 56.9 (C_d), 63.6 ($2\text{C}_{\text{CO}_2\text{CH}_2\text{CH}_3}$), 67.2 (C_c), 76.1 (C_a), 79.9 ($\text{C}_{e/f}$), 81.1 ($\text{C}_{e/f}$), 87.1 (C_b), 103.0 (C_i), 127.9 (2C_{Ts}), 129.6 (2C_{Ts}), 136.3 (C_{Ts}), 143.6 (C_{Ts}), 209.5 (C_b); **ESI-MS (m/z):** 430.1 [$\text{M}+\text{Na}$] $^+$, 446.1 [$\text{M}+\text{K}$] $^+$; **EA:** calculated for $\text{C}_{21}\text{H}_{29}\text{NO}_5\text{S}$: C, 61.89; H, 7.17; N, 3.44; found: C, 61.81; H, 6.93; N, 3.68.

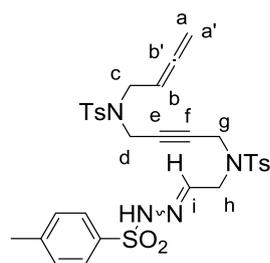
8.4.1.2. Synthesis of aldehydes 51

**51a**

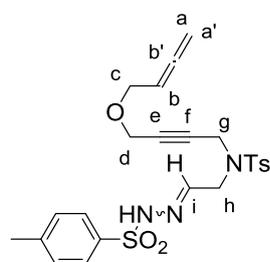
General procedure for 51. A solution of **52a** (2.09 g, 3.73 mmol) in trifluoroacetic acid (5 mL, 65.3 mmol), CHCl_3 (10 mL) and H_2O (5 mL) was stirred at room temperature for 24 hours (TLC monitoring). The mixture was diluted with CH_2Cl_2 and washed successively with 5% aqueous $\text{Na}_2\text{S}_2\text{O}_3$ (3 x 50 mL), H_2O (3 x 50 mL) and brine (3 x 50 mL). The organic layer was dried (Na_2SO_4), concentrated *in vacuo* and purified by column chromatography on silica gel (hexane/ethyl acetate 8:2 to 5:5) to afford **51a** (1.31 g, 73%) as a pale orange waxy solid. **MW**: 486.60 g/mol; **IR (ATR) ν (cm^{-1})**: 2922, 1342, 1156; **^1H NMR (400 MHz, CDCl_3) δ (ppm)**: 2.43 (s, 3H_{Ts}), 2.44 (s, 3H_{Ts}), 3.70-3.69 (m, $2\text{H}_{\text{d/g}}$), 3.75 (s, $2\text{H}_{\text{d/g}}$), 3.95 (s, $4\text{H}_{\text{c,h}}$), 4.74-4.75 (m, $2\text{H}_{\text{a,a'}}$), 4.93 (m, H_b), 7.29-7.33 (m, 4H_{Ts}), 7.62-7.66 (m, 4H_{Ts}), 9.52 (t, $^3J = 1.2$ Hz, H_i); **^{13}C NMR (100 MHz, CDCl_3) δ (ppm)**: 21.6 (2C_{Ts}), 35.9 (C_g), 38.5 (C_d), 45.8 (C_c), 55.8 (C_h), 76.6 (C_a), 77.7 (C_{eff}), 79.8 (C_{eff}), 85.3 (C_b), 127.6 (4C_{Ts}), 129.7 (2C_{Ts}), 130.0 (2C_{Ts}), 134.9 (C_{Ts}), 136.1 (C_{Ts}), 144.0 (C_{Ts}), 144.5 (2C_{Ts}), 197.1 (C_i), 209.7 (C_b); **ESI-HRMS (m/z)**: calculated for $[\text{M}+\text{Na}]^+$: 509.1175; experimental: 509.1162.

**51b**

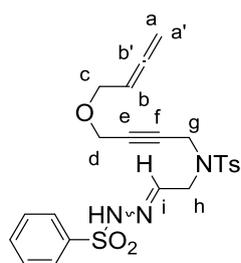
Using the same experimental procedure as for compound **51a**, **51b** was obtained as a colourless oil (1.26 g, 85% yield) after 24 hours. **MW**: 333.40 g/mol; **IR (ATR) ν (cm^{-1})**: 2926, 1344, 1157; **^1H NMR (400 MHz, CDCl_3) δ (ppm)**: 2.44 (s, 3H_{Ts}), 3.89-3.98 (m, 6H_{CH_2}), 4.20-4.21 (m, 2H_{CH_2}), 4.79-4.82 (m, $2\text{H}_{\text{a,a'}}$), 5.14 (m, H_b), 7.33 (d, $^3J = 8.0$ Hz, 2H_{Ts}), 7.71 (d, $^3J = 8.0$ Hz, 2H_{Ts}), 9.66 (t, $^3J = 1.2$ Hz, H_i); **^{13}C NMR (75 MHz, CDCl_3) δ (ppm)**: 21.6 (C_{Ts}), 39.1 (C_g), 56.0 (C_d), 56.7 (C_h), 67.4 (C_c), 76.0 ($\text{C}_{\text{a/a'}}$), 78.6 (C_{eff}), 82.7 (C_{eff}), 87.0 (C_b), 127.7 (2C_{Ts}), 129.9 (2C_{Ts}), 135.0 (C_{Ts}), 144.4 (C_{Ts}), 197.4 (C_i), 209.6 (C_b); **ESI-MS (m/z)**: 334.1 $[\text{M}+\text{H}]^+$; **EA**: calculated for $\text{C}_{17}\text{H}_{19}\text{NO}_4\text{S}$: C, 61.24; H, 5.74; N, 4.20; found: C, 61.01; H, 6.00; N, 4.28.

8.4.1.3. Synthesis of *N*-sulfonylhydrazones **49** and **50****49**

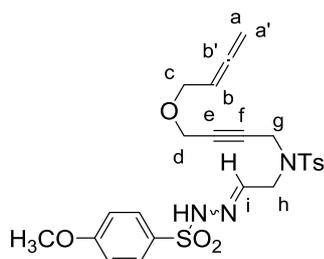
General procedure for 49. A solution of *p*-toluensulfonyl hydrazide (0.47 g, 2.53 mmol) in methanol (15 mL) was prepared. A solution of **51a** (1.23 g, 2.53 mmol) in methanol (15 mL) and the minimum amount of acetonitrile to completely dissolve the product was added dropwise to this mixture whilst it was being rapidly stirred. The mixture was then stirred at room temperature for 1 hour until completion (TLC monitoring). The solvent was removed under reduced pressure and the reaction crude was purified by column chromatography on silica gel (hexane/ethyl acetate, 9:1 to 6:4) to afford **49** (1.65 g, 73%, *Z/E*:8/92)¹¹⁶ as a colourless solid. **MW**: 654.82 g/mol; **IR (ATR) ν (cm⁻¹)**: 3197, 2922, 1342, 1155; **¹H NMR (400 MHz, CDCl₃) δ (ppm)**: 2.41-2.42 (m, 9H_{Ts}), 3.67-3.69 (m, 2H_c), 3.75 (d, ³*J* = 5.2 Hz, 2H_h), 3.77 (s, 2H_{d/g}), 3.85 (s, 2H_{d/g}), 4.71-4.73 (m, 2H_{a,a'}), 4.86 (tt, ³*J* = 6.8 Hz, ⁴*J* = 6.8 Hz, H_b), 7.11 (t, ³*J* = 5.2 Hz, H_i), 7.27-7.31 (m, 6H_{Ts}), 7.59 (d, ³*J* = 8.4 Hz, 2H_{Ts}), 7.65 (d, ³*J* = 8.4 Hz, 2H_{Ts}), 7.77 (d, ³*J* = 8.0 Hz, 2H_{Ts}), 8.60 (s, H_{NH}); **¹³C NMR (100 MHz, CDCl₃) δ (ppm)**: 21.5 (C_{Ts}), 21.5 (C_{Ts}), 21.6 (C_{Ts}), 35.8 (C_{d/g}), 37.4 (C_{d/g}), 45.6 (C_c), 48.4 (C_h), 76.7 (C_{a/a'}), 78.1 (C_{eff}), 79.1 (C_{eff}), 85.2 (C_b), 127.5 (6C_{Ts}), 129.8 (2C_{Ts}), 130.0 (2C_{Ts}), 135.2 (C_{Ts}), 135.3 (C_{Ts}), 135.9 (2C_{Ts}), 144.0 (C_{Ts}), 144.2 (C_{Ts}), 144.3 (C_{Ts}), 145.2 (C_i), 209.6 (C_{b'}); **ESI-MS (*m/z*)**: 655.1 [M+H]⁺, 677.2 [M+Na]⁺; **EA**: calculated for C₃₁H₃₄N₄O₆S₃·0.5H₂O: C, 56.09; H, 5.31; N, 8.44; found: C, 56.03 and 55.96; H, 5.36 and 5.24; N, 8.42 and 8.21.

**50a**

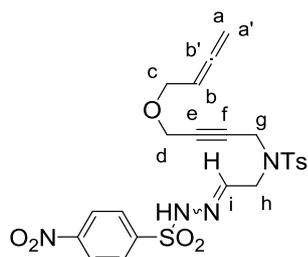
Using the same experimental procedure as for compound **49**, **50a** was obtained as a pale orange waxy solid (1.48 g, 85% yield, *Z/E*:6/94)¹¹⁶ after 1 hour. **MW**: 501.62 g/mol; **IR (ATR) ν (cm⁻¹)**: 3200, 2921, 1345, 1158; **¹H NMR (400 MHz, CDCl₃) δ (ppm)**: 2.41 (s, 3H_{Ts}), 2.42 (s, 3H_{Ts}), 3.87-3.87 (m, 4H_{d,g}), 3.89 (d, ³*J* = 5.2 Hz, 2H_h), 3.92 (dt, ³*J* = 6.8 Hz, ⁵*J* = 2.2 Hz, 2H_c), 4.82 (dt, ⁴*J* = 6.8 Hz, ⁵*J* = 2.2 Hz, 2H_{a/a'}), 5.19 (tt, ³*J* = 6.8 Hz, ⁴*J* = 6.8 Hz, H_b), 7.07 (t, ³*J* = 5.2 Hz, H_i), 7.28-7.30 (m, 4H_{Ts}), 7.65 (d, ³*J* = 8.4 Hz, 2H_{Ts}), 7.78 (d, ³*J* = 8.4 Hz, 2H_{Ts}), 8.30 (s, H_{NH}); **¹³C NMR (100 MHz, CDCl₃) δ (ppm)**: 21.5 (C_{Ts}), 21.6 (C_{Ts}), 37.4 (C_g), 48.5 (C_h), 56.7 (C_d), 67.4 (C_c), 76.1 (C_a), 79.2 (C_{eff}), 81.9 (C_{eff}), 86.9 (C_b), 127.7 (4C_{Ts}), 129.7 (4C_{Ts}), 135.1 (C_{Ts}), 135.2 (C_{Ts}), 144.1 (C_{Ts}), 144.6 (C_{Ts}), 145.6 (C_i), 209.5 (C_{b'}); **ESI-HRMS (*m/z*)**: calculated for [M+Na]⁺: 524.1284 and [M+K]⁺: 540.1024; experimental: 524.1282 and 540.1017.

**50b**

Using the same experimental procedure as for compound **49**, **50b** was obtained as a colourless waxy solid (0.10 g, 45% yield, *Z/E*:6/94)¹¹⁶ after 1 hour. **MW**: 487.59 g/mol; **IR (ATR) ν (cm^{-1})**: 3195, 2861, 1346, 1161; **$^1\text{H NMR}$ (400 MHz, CDCl_3) δ (ppm)**: 2.40 (s, 3 H_{Ts}), 3.86-3.88 (m, 4 $\text{H}_{\text{d,g}}$), 3.87 (d, $^3J = 5.2$ Hz, 2 H_h), 3.91 (dt, $^3J = 6.8$ Hz, $^5J = 2.4$ Hz, 2 H_c), 4.80 (dt, $^4J = 6.8$ Hz, $^5J = 2.4$ Hz, 2 $\text{H}_{\text{a/a'}}$), 5.16 (tt, $^3J = 6.8$ Hz, $^4J = 6.8$ Hz, H_b), 7.12 (t, $^3J = 5.2$ Hz, H_i), 7.28 (d, $^3J = 8.4$ Hz, 2 H_{Ts}), 7.48 (m, 2 H_{Ph}), 7.56 (m, H_{Ph}), 7.64 (d, $^3J = 8.4$ Hz, 2 H_{Ts}), 7.89 (m, 2 H_{Ph}), 8.82 (s, H_{NH}); **$^{13}\text{C NMR}$ (100 MHz, CDCl_3) δ (ppm)**: 21.5 (C_{Ts}), 37.5 (C_g), 48.6 (C_h), 56.7 (C_d), 67.5 (C_c), 76.1 (C_a), 79.4 (C_{eff}), 82.0 (C_{eff}), 86.8 (C_b), 127.7 (2 C_{Ph}), 127.8 (2 C_{Ph}), 129.0 (2 C_{Ts}), 129.7 (2 C_{Ts}), 133.2 (C_{Ph}), 135.2 (C_{Ts}), 138.1 (C_{Ph}), 144.1 (C_{Ts}), 145.9 (C_i), 209.5 (C_b); **ESI-HRMS (m/z)**: calculated for $[\text{M}+\text{Na}]^+$: 510.1128; experimental: 510.1130.

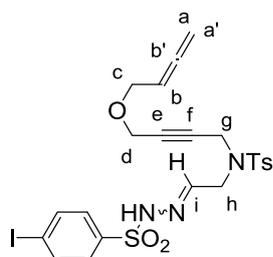
**50c**

Using the same experimental procedure as for compound **49**, **50c** was obtained as a colourless waxy solid (0.34 g, 63% yield, *Z/E*:7/93)¹¹⁶ after 1 hour. **MW**: 517.61 g/mol; **IR (ATR) ν (cm^{-1})**: 3191, 2928, 1344, 1155; **$^1\text{H NMR}$ (400 MHz, CDCl_3) δ (ppm)**: 2.41 (s, 3 H_{Ts}), 3.84 (s, 3 H_{OCH_3}), 3.86-3.88 (m, 6 $\text{H}_{\text{d,g,h}}$), 3.91 (dt, $^3J = 6.8$ Hz, $^5J = 2.4$ Hz, 2 H_c), 4.81 (dt, $^4J = 6.8$ Hz, $^5J = 2.4$ Hz, 2 $\text{H}_{\text{a/a'}}$), 5.17 (tt, $^3J = 6.8$ Hz, $^4J = 6.8$ Hz, H_b), 6.95 (d, $^3J = 8.8$ Hz, 2 $\text{H}_{\text{p-OCH}_3\text{Ph}}$), 7.10 (t, $^3J = 5.6$ Hz, H_i), 7.27-7.10 (m, 2 H_{Ts}), 7.65 (d, $^3J = 9.2$ Hz, 2 H_{Ts}), 7.82 (d, $^3J = 8.8$ Hz, 2 $\text{H}_{\text{p-OCH}_3\text{Ph}}$), 8.53 (s, H_{NH}); **$^{13}\text{C NMR}$ (100 MHz, CDCl_3) δ (ppm)**: 21.6 (C_{Ts}), 37.6 (C_g), 48.7 (C_h), 55.7 (C_{OCH_3}), 56.8 (C_h), 67.6 (C_c), 76.2 (C_a), 79.6 (C_{eff}), 82.1 (C_{eff}), 86.9 (C_b), 114.2 (2 $\text{C}_{\text{p-OCH}_3\text{Ph}}$), 127.7 (2 C_{Ts}), 129.7 (2 C_{Ts}), 129.8 (2 $\text{C}_{\text{p-OCH}_3\text{Ph}}$), 130.1 ($\text{C}_{\text{p-OCH}_3\text{Ph}}$), 135.4 (C_{Ts}), 144.1 (C_{Ts}), 145.8 (C_i), 163.5 ($\text{C}_{\text{p-OCH}_3\text{Ph}}$), 209.6 (C_b); **ESI-HRMS (m/z)**: calculated for $[\text{M}+\text{Na}]^+$: 540.1233; experimental: 540.1234.

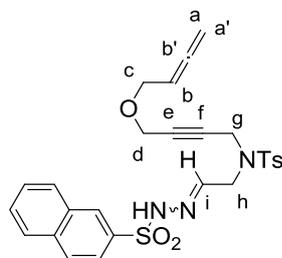
**50d**

Using the same experimental procedure as for compound **49**, **50d** was obtained as a colourless solid (0.28 g, 81% yield, *Z/E*:4/96)¹¹⁶ after 1 hour. **MW**: 532.59 g/mol; **IR**

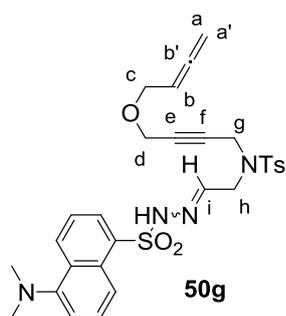
(ATR) v (cm⁻¹): 3238, 2862, 1529, 1346, 1307, 1158; **¹H NMR (400 MHz, CDCl₃) δ (ppm):** 2.40 (s, 3H_{TS}), 3.87-4.02 (m, 8H_{c,d,g,h}), 4.79-4.84 (m, 2H_{a,a'}), 5.17 (m, H_b), 7.18 (t, ³J = 6.2 Hz, H_i), 7.28-7.32 (m, 2H_{TS}), 7.60-7.63 (m, 2H_{TS}), 8.06-8.11 (m, 2H_{p-NO₂Ph}), 8.29 (d, ³J = 9.2 Hz, 2H_{p-NO₂Ph}), 9.00 (s, H_{NH}); **¹³C NMR (100 MHz, CDCl₃) δ (ppm):** 21.6 (C_{TS}), 37.9 (C_g), 48.8 (C_h), 56.8 (C_d), 67.8 (C_c), 76.2 (C_a), 79.5 (C_{e/f}), 82.3 (C_{e/f}), 86.8 (C_b), 124.2 (2C_{p-NO₂Ph}), 127.7 (2C_{TS}), 129.3 (2C_{p-NO₂Ph}), 129.9 (2C_{TS}), 134.9 (C_{TS}), 143.8 (C_{TS}), 144.5 (C_i), 147.5 (C_{p-NO₂Ph}), 150.4 (C_{p-NO₂Ph}), 209.7 (C_{b'}); **ESI-HRMS (m/z):** calculated for [M+Na]⁺: 555.0979; experimental: 555.0975.

**50e**

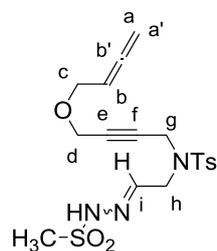
Using the same experimental procedure as for compound **49**, **50e** was obtained as a pale orange waxy solid (0.38 g, 85% yield, *Z/E*:7/93)¹¹⁶ after 1 hour. **MW:** 613.49 g/mol; **IR (ATR) v (cm⁻¹):** 3192, 2924, 1345, 1158; **¹H NMR (400 MHz, CDCl₃) δ (ppm):** 2.42 (s, 3H_{TS}), 3.86-3.91 (m, 8H_{c,d,g,h}), 4.80 (dt, ⁴J = 6.8 Hz, ⁵J = 2.4 Hz, 2H_{a/a'}), 5.17 (tt, ³J = 6.8 Hz, ⁴J = 6.8 Hz, H_b), 7.15 (t, ³J = 5.6 Hz, H_i), 7.29 (d, ³J = 8.6 Hz, 2H_{TS}), 7.58 (d, ³J = 8.6 Hz, 2H_{p-IPh}), 7.64 (d, ³J = 8.6 Hz, 2H_{TS}), 7.82 (d, ³J = 8.6 Hz, 2H_{p-IPh}), 8.92 (s, H_{NH}); **¹³C NMR (100 MHz, CDCl₃) δ (ppm):** 21.6 (C_{TS}), 37.6 (C_g), 48.6 (C_h), 56.7 (C_d), 67.5 (C_c), 76.2 (C_a), 79.3 (C_{e/f}), 82.1 (C_{e/f}), 86.9 (C_b), 100.9 (C_{p-IPh}), 127.7 (2C_{TS}), 129.2 (2C_{p-IPh}), 129.8 (2C_{TS}), 135.0 (C_{TS}), 137.8 (C_{p-IPh}), 138.2 (2C_{p-IPh}), 144.2 (C_{TS}), 146.4 (C_i), 209.5 (C_{b'}); **ESI-HRMS (m/z):** calculated for [M+Na]⁺: 636.0094; experimental: 636.0108.

**50f**

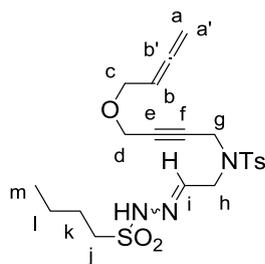
Using the same experimental procedure as for compound **49**, **50f** was obtained as a colourless waxy solid (0.25 g, 73% yield, *Z/E*:6/94)¹¹⁶ after 1 hour. **MW:** 537.65 g/mol; **IR (ATR) v (cm⁻¹):** 3211, 2923, 1343, 1157; **¹H NMR (400 MHz, CDCl₃) δ (ppm):** 2.35 (s, 3H_{TS}), 3.82-3.87 (m, 8H_{c,d,g,h}), 4.78 (dt, ⁴J = 6.8 Hz, ⁵J = 2.4 Hz, 2H_{a/a'}), 5.15 (tt, ³J = 6.8 Hz, ⁴J = 6.8 Hz, H_b), 7.14 (t, ³J = 5.2 Hz, H_i), 7.18 (d, ³J = 8.4 Hz, 2H_{TS}), 7.55-7.62 (m, 4H_{Naph}), 7.83-7.86 (m, 2H_{TS}+2H_{Naph}), 8.48 (s, H_{Naph}), 8.99 (s, H_{NH}); **¹³C NMR (100 MHz, CDCl₃) δ (ppm):** 21.5 (C_{TS}), 37.5 (C_g), 48.6 (C_h), 56.7 (C_d), 67.5 (C_c), 76.1 (C_a), 79.3 (C_{e/f}), 81.9 (C_{e/f}), 86.9 (C_b), 122.7 (C_{Naph}), 127.5 (C_{Naph}), 127.6 (2C_{TS}), 127.9 (C_{Naph}), 129.0 (C_{Naph}), 129.3 (C_{Naph}), 129.4 (C_{Naph}), 129.5 (C_{Naph}), 129.7 (2C_{TS}), 132.0 (C_{Naph}), 135.0 (C_{Naph}), 135.1 (C_{Naph}), 135.2 (C_{TS}), 144.0 (C_{TS}), 146.0 (C_i), 209.6 (C_{b'}); **ESI-HRMS (m/z):** calculated for [M+Na]⁺: 560.1284; experimental: 560.1276.



Using the same experimental procedure as for compound **49**, **50g** was obtained as a yellow fluorescent waxy solid (0.29 g, 86% yield, *Z/E*:9/91)¹¹⁶ after 1 hour. **MW**: 580.72 g/mol; **IR (ATR) ν (cm⁻¹)**: 3203, 2922, 2853, 1345, 1159; **¹H NMR (400 MHz, CDCl₃) δ (ppm)**: 2.38 (s, 3H_{TS}), 3.87 (s, 6H_{N(CH₃)₂}), 3.64 (t, ⁵*J* = 1.6 Hz, 2H_g), 3.76-3.79 (m, 4H_{d/h}), 3.87 (dt, ³*J* = 6.8 Hz, ⁵*J* = 2.4 Hz, 2H_c), 4.80 (dt, ⁴*J* = 6.8 Hz, ⁵*J* = 2.4 Hz, 2H_{a/a'}), 5.16 (tt, ³*J* = 6.8 Hz, ⁴*J* = 6.8 Hz, H_b), 7.02 (t, ³*J* = 5.6 Hz, H_i), 7.15 (m, H_{Dns}), 7.17 (d, ³*J* = 8.4 Hz, 2H_{TS}), 7.49-7.54 (m, 2H_{Dns}), 7.58 (d, ³*J* = 8.4 Hz, 2H_{TS}), 8.29 (m, H_{Dns}), 8.37 (m, H_{Dns}), 8.55 (m, H_{Dns}), 8.68 (s, H_{NH}); **¹³C NMR (100 MHz, CDCl₃) δ (ppm)**: 21.6 (C_{TS}), 37.4 (C_g), 45.5 (2C_{N(CH₃)₂}), 48.6 (C_h), 56.8 (C_d), 67.6 (C_c), 76.2 (C_a), 79.6 (C_{e/f}), 81.9 (C_{e/f}), 87.0 (C_b), 115.4 (C_{Dns}), 119.1 (C_{Dns}), 123.3 (C_{Dns}), 128.4 (2C_{TS}), 128.6 (C_{Dns}), 129.7 (2C_{TS}), 129.8 (C_{Dns}), 129.9 (C_{Dns}), 130.9 (C_{Dns}), 131.3 (C_{Dns}), 133.7 (C_{Dns}), 135.4 (C_{TS}), 144.0 (C_{TS}), 145.0 (C_i), 152.0 (C_{Dns}), 209.6 (C_{b'}); **EA**: calculated for C₂₉H₃₂N₄O₅S₂: C, 59.94; H, 5.55; N, 9.65; found: C, 59.94 and 59.98; H, 5.62 and 5.78; N, 9.43 and 9.49.

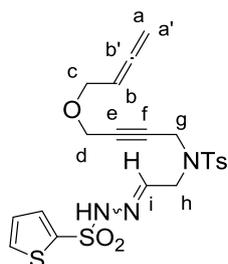


Using the same experimental procedure as for compound **49**, **50h** was obtained as a colourless waxy solid (0.11 g, 27% yield, *Z/E*:6/94)¹¹⁶ after 1 hour. **MW**: 425.52 g/mol; **IR (ATR) ν (cm⁻¹)**: 3205, 2926, 1343, 1158; **¹H NMR (400 MHz, CDCl₃) δ (ppm)**: 2.43 (s, 3H_{TS}), 3.05 (s, 3H_{SO₂CH₃}), 3.90-3.95 (m, 4H_{d/g, c}), 3.99 (d, ³*J* = 5.2 Hz, 2H_h), 4.12 (s, 2H_{d/g}), 4.80 (dt, ⁴*J* = 6.8 Hz, ⁵*J* = 2.4 Hz, 2H_{a/a'}), 5.19 (tt, ³*J* = 6.8 Hz, ⁴*J* = 6.8 Hz, H_b), 7.24 (t, ³*J* = 5.2 Hz, H_i), 7.33 (d, ³*J* = 8.2 Hz, 2H_{TS}), 7.73 (d, ³*J* = 8.2 Hz, 2H_{TS}), 8.63 (s, H_{NH}); **¹³C NMR (100 MHz, CDCl₃) δ (ppm)**: 21.6 (C_{TS}), 38.1 (C_g), 38.7 (C_{SO₂CH₃}), 48.9 (C_h), 56.8 (C_d), 67.6 (C_c), 76.1 (C_a), 79.7 (C_{e/f}), 82.2 (C_{e/f}), 86.9 (C_b), 127.7 (2C_{TS}), 129.8 (2C_{TS}), 135.2 (C_{TS}), 144.3 (C_{TS}), 146.5 (C_i), 209.6 (C_{b'}); **ESI-HRMS (*m/z*)**: calculated for [M+Na]⁺: 448.0971; experimental: 448.0979.



50i

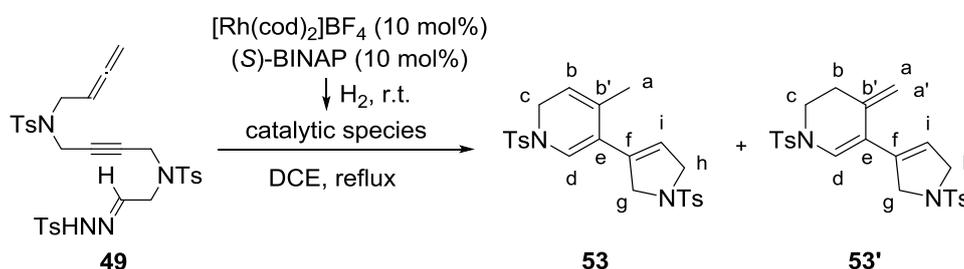
Using the same experimental procedure as for compound **49**, **50i** was obtained as a colourless waxy solid (0.32 g, 20% yield, *Z/E*:7/93)¹¹⁶ after 1 hour. **MW**: 467.60 g/mol; **IR (ATR) ν (cm^{-1})**: 3201, 2962, 1343, 1154; **$^1\text{H NMR}$ (400 MHz, CDCl_3) δ (ppm)**: 0.94 (t, $^3J = 7.4$ Hz, 3H_m), 1.46 (tt, $^3J = 7.2$ Hz / $^3J = 7.2$ Hz, 2H_l), 1.75-1.83 (m, 2H_k), 2.44 (s, 3H_{Ts}), 3.17-3.21 (m, 2H_j), 3.93 (dt, $^3J = 6.8$ Hz / $^5J = 2.4$ Hz, 2H_c), 3.95 (t, $^5J = 1.6$ Hz, 2H_{d/g}), 3.98 (d, $^3J = 5.2$ Hz, 2H_h), 4.11 (t, $^5J = 1.6$ Hz, 2H_{d/g}), 4.82 (dt, $^4J = 7.2$ Hz, $^5J = 2.4$ Hz, 2H_{a/a'}), 5.17 (tt, $^3J = 6.8$ Hz, $^4J = 6.8$ Hz, H_b), 7.21 (t, $^3J = 5.2$ Hz, H_i), 7.21 (d, $^3J = 8.4$ Hz, 2H_{Ts}), 7.73 (d, $^3J = 8.4$ Hz, 2H_{Ts}), 8.42 (s, H_{NH}); **$^{13}\text{C NMR}$ (100 MHz, CDCl_3) δ (ppm)**: 13.6 (C_m), 21.6 (C_{Ts}), 21.7 (C_l), 25.1 (C_k), 38.2 (C_g), 49.1 (C_h), 51.0 (C_j), 56.9 (C_d), 67.8 (C_c), 76.2 (C_a), 79.8 (C_{e/f}), 82.3 (C_{e/f}), 86.9 (C_b), 127.8 (2C_{Ts}), 129.9 (2C_{Ts}), 135.3 (C_{Ts}), 144.3 (C_{Ts}), 145.9 (C_i), 209.7 (C_{b'}); **ESI-HRMS (m/z)**: calculated for [M+Na]⁺: 490.1441; experimental: 490.1430.



50j

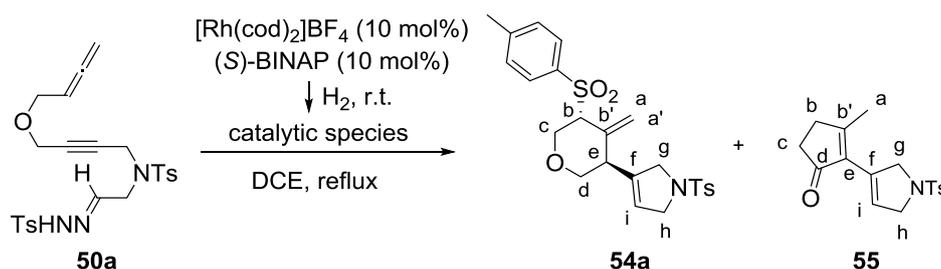
Using the same experimental procedure as for compound **49**, **50j** was obtained as a pale yellow oil (0.10 g, 18% yield, *Z/E*:6/94)¹¹⁶ after 1 hour. **MW**: 493.61 g/mol; **IR (ATR) ν (cm^{-1})**: 3200, 3102, 1342, 1159; **$^1\text{H NMR}$ (400 MHz, CDCl_3) δ (ppm)**: 2.42 (s, 3H_{Ts}), 3.87 (t, $^5J = 1.6$ Hz, 2H_{d/g}), 3.90-3.94 (m, 6H_{c/d,g,h}), 4.81 (dt, $^4J = 6.8$ Hz / $^5J = 2.4$ Hz, H_{a/a'}), 7.08 (dd, $^4J = 3.6$ Hz / $^3J = 4.8$ Hz, H_{thiophene}), 7.15 (t, $^3J = 5.2$ Hz, H_i), 7.62-7.64 (m, 2H_{Ts}), 7.66-7.68 (m, 3H_{Ts,thiophene}), 8.80 (s, H_{NH}); **$^{13}\text{C NMR}$ (100 MHz, CDCl_3) δ (ppm)**: 21.6 (C_{Ts}), 37.8 (C_g), 49.0 (C_h), 56.8 (C_d), 67.7 (C_c), 76.2 (C_a), 79.8 (C_{e/f}), 82.1 (C_{e/f}), 86.8 (C_b), 127.3 (C_{thiophene}), 127.7 (2C_{Ts}), 129.8 (2C_{Ts}), 133.0 (C_{thiophene}), 133.6 (C_{thiophene}), 135.2 (C_{thiophene}), 138.4 (C_{Ts}), 144.2 (C_{Ts}), 146.8 (C_i), 209.6 (C_{b'}); **ESI-HRMS (m/z)**: calculated for [M+Na]⁺: 516.0692; experimental: 516.0680.

8.4.2. Experimental procedure for the rhodium(I)-catalysed cyclisation of *N*-tosylhydrazone derivative **49**



A mixture of $[\text{Rh}(\text{cod})_2]\text{BF}_4$ (0.0052 g, 0.01 mmol) and BINAP (0.0079 g, 0.01 mmol) was dissolved in dichloromethane (4 mL) under nitrogen. Hydrogen gas was bubbled to the stirred catalytic solution for 30 minutes and the resulting mixture was concentrated to dryness. The mixture was dissolved in 1,2-dichloroethane (1.5 mL) and a solution of **49** (0.0818 g, 0.12 mmol) in dichloroethane (1.5 mL) was added. The reaction mixture was heated at reflux for 2 hours until completion (TLC monitoring). The solvent was evaporated and the residue was purified by column chromatography on silica gel (hexane/ethyl acetate, 7:3) to afford a mixture of compounds which was identified by spectroscopy data as **53** and **53'** (ratio 2:1) as a colourless solid (0.0164 g, 28% yield). **MW**: 470.60 g/mol; **$^1\text{H NMR}$ (400 MHz, CDCl_3) δ (ppm)**: 1.70-1.71 (m, 3 H_a , **53**), 2.34-2.41 (m, 2 H_b , **53'**), 2.44-2.44 (m, 12 H_{Ts} , **53/53'**), 3.43 (m, 2 H_c , **53'**), 3.90-3.93 (m, 2 H_c , **53**), 4.18-4.19 (m, 8 $\text{H}_{g,h}$, **53/53'**), 4.79 (m, $\text{H}_{a/a'}$, **53'**), 4.88 (m, $\text{H}_{a/a'}$, **53'**), 5.19 (m, H_b , **53**), 5.53 (s, H_i , **53**), 5.63 (s, H_i , **53'**), 6.52 (s, H_d , **53**), 6.61 (s, H_d , **53'**), 7.31-7.36 (m, 8 H_{Ts} , **53/53'**), 7.63-7.65 (m, 4 H_{Ts} , **53/53'**), 7.74-7.76 (m, 4 H_{Ts} , **53/53'**); **$^{13}\text{C NMR}$ (100 MHz, CDCl_3) δ (ppm)**: 20.5 (C_a , **53**), 21.7 (2C_{Ts} , **53** and **53'**), 21.8 (2C_{Ts} , **53** and **53'**), 30.5 (C_b , **53'**), 43.5 (C_c , **53**), 44.4 (C_c , **53'**), 55.3 ($\text{C}_{g/h}$, **53'**), 55.6 ($\text{C}_{g/h}$, **53'**), 55.7 ($\text{C}_{g/h}$, **53**), 55.8 ($\text{C}_{g/h}$, **53'**), 111.9 ($\text{C}_{a/a'}$, **53'**), 114.2 (C_f , **53'**), 114.6 (C_d , **53**), 116.9 (C_f , **53**), 121.0 (C_i , **53**), 121.6 (C_i , **53'**), 124.9 (C_d , **53'**), 125.7 (C_b , **53**), 127.1 (2C_{Ts} , **53'**), 127.3 (2C_{Ts} , **53'**), 127.7 (4C_{Ts} , **53** and **53'**), 130.0 (2C_{Ts} , **53**), 130.1 (2C_{Ts} , **53'**), 130.2 (2C_{Ts} , **53**), 130.3 (2C_{Ts} , **53'**), 131.4 ($\text{C}_{b'}$, **53**), 133.8 (C_e , **53**), 134.1 (C_{Ts} , **53**), 134.2 (C_{Ts} , **53'**), 134.5 (C_{Ts} , **53'**), 134.7 (C_e , **53'**), 134.8 (C_{Ts} , **53'**), 135.9 ($\text{C}_{b'}$, **53'**), 143.7 (2C_{Ts} , **53** and **53'**), 144.5 (C_{Ts} , **53**), 144.6 (C_{Ts} , **53'**); **ESI-MS (m/z)**: 471.1 $[\text{M}+\text{H}]^+$, 493.1 $[\text{M}+\text{Na}]^+$.

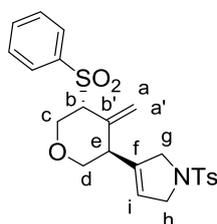
8.4.3. Experimental procedure for the rhodium(I)-catalysed cyclisation of *N*-sulfonylhydrazone derivatives **50**



General procedure for 54a and 55. A mixture of $[\text{Rh}(\text{cod})_2]\text{BF}_4$ (0.0101 g, 0.02 mmol) and BINAP (0.0156 g, 0.01 mmol) was dissolved in dichloromethane (4 mL) under nitrogen. Hydrogen gas was bubbled to the stirred catalytic solution for 30 minutes and the resulting mixture was concentrated to dryness. The mixture was dissolved in 1,2-dichloroethane (35 mL) and a solution of **50a** (0.1253 g, 0.25 mmol) in dichloroethane (35 mL) was added. The reaction mixture was heated at reflux for 2 hours until completion (TLC monitoring). The solvent was evaporated and the residue was purified by column chromatography on silica gel (hexane/ethyl acetate, 8:2) to afford a mixture of compounds, which were identified by spectroscopy data as **54a** and **55**.

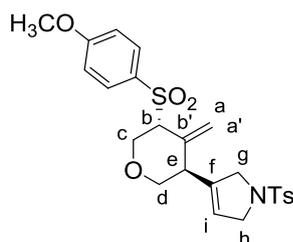
Compound **54a** was obtained as a colourless solid (0.0759 g, 64% yield, ee=83%). **MW:** 473.60 g/mol; **m.p.:** 132-133 °C; $[\alpha]_D^{20} +69.86$ (c 0.12 g / 100 mL, CH_3CN); **IR (ATR) ν (cm^{-1}):** 2922, 2852, 1335, 1160; **$^1\text{H NMR}$ (400 MHz, CDCl_3) δ (ppm):** 2.42 (s, 3 H_{Ts}), 2.45 (s, 3 H_{Ts}), 3.19 (dd, $^2J = 10.8$ Hz / $^3J = 10.8$ Hz, H_d), 3.51 (m, H_e), 3.57 (d, $^3J = 4.2$ Hz, H_b), 3.65 (dd, $^2J = 12.8$ Hz / $^3J = 4.2$ Hz, H_c), 3.87 (dd, $^2J = 10.8$ Hz / $^3J = 5.4$ Hz, H_d), 3.97-3.99 (m, 2 H_g), 4.12-4.13 (m, 2 H_h), 4.68 (d, $^2J = 2.0$ Hz, $\text{H}_{a/a'}$), 4.69 (d, $^2J = 2.0$ Hz, $\text{H}_{a/a'}$), 4.73 (d, $^2J = 12.8$ Hz, H_c), 5.44 (m, H_i), 7.31-7.35 (m, 4 H_{Ts}), 7.69-7.72 (m, 4 H_{Ts}); **$^{13}\text{C NMR}$ (100 MHz, CDCl_3) δ (ppm):** 21.6 (C_{Ts}), 21.7 (C_{Ts}), 39.8 (C_e), 54.6 ($\text{C}_{h/g}$), 54.9 ($\text{C}_{h/g}$), 66.3 (C_c), 67.7 (C_b), 71.0 (C_d), 119.2 ($\text{C}_{a/a'}$), 123.3 (C_i), 127.4 (2 C_{Ts}), 129.2 (2 C_{Ts}), 129.7 (2 C_{Ts}), 129.9 (2 C_{Ts}), 133.8 (C_{Ts}), 134.3 (C_{Ts}), 135.7 (C_f), 136.5 (C_b), 143.8 (C_{Ts}), 145.1 (C_{Ts}); **ESI-MS (m/z):** 474.2 $[\text{M}+\text{H}]^+$; **AE:** calculated for $\text{C}_{24}\text{H}_{27}\text{NO}_5\text{S}_2$: C, 60.87; H, 5.75; N, 2.96; found: C, 60.63; H, 5.58; N, 3.25. The enantiomeric excess has been determined by **HPLC** analysis using a CHIRALPAK IA column (4.6 x 250 mm, 5 μm) with 76 % hexane / 20 % 2-PrOH / 6 % acetonitrile mobile phase at a 1.0 mL/min flow rate, using a UV detector set up at $\lambda = 220$ nm. The retention time for the major isomer is 22.7 min and for the minor isomer is 17.0 min.

Compound **55** was obtained as a colourless solid (0.0088 g, 11 % yield). **MW:** 317.40 g/mol; **IR (ATR) ν (cm^{-1}):** 2922, 2849, 1686, 1337, 1159; **$^1\text{H NMR}$ (400 MHz, CDCl_3) δ (ppm):** 2.14 (s, 3 H_a), 2.38-2.38-2.41 (m, 2 H_b), 2.42 (s, 3 H_{Ts}), 2.56-2.57 (m, 2 H_c), 4.21-4.22 (m, 2 H_g), 4.40-4.43 (m, 2 H_h), 6.10 (m, H_i), 7.31 (d, $^3J = 8.4$ Hz, 2 H_{Ts}), 7.40 (d, $^3J = 8.4$ Hz, 2 H_{Ts}); **ESI-HRMS (m/z):** calculated for $[\text{M}+\text{Na}]^+$: 340.0978; experimental: 340.0976.

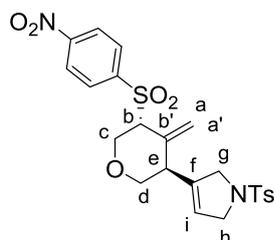
**54b**

Using the same experimental procedure as for compound **54a**, **54b** was obtained as a colourless solid (0.0479 g, 50% yield, ee=80%) after 1 hour. **MW:** 459.57 g/mol; **m.p.:** 82-84 °C; $[\alpha]_D^{20} +58.33$ (c 0.10 g / 100 mL, CH_3CN); **IR (ATR) ν (cm^{-1}):** 2921, 2852, 1594, 1130; **$^1\text{H NMR}$ (400 MHz, CDCl_3) δ (ppm):** 2.42 (s, 3 H_{Ts}), 3.20 (dd, $^2J = 10.6$ Hz / $^3J = 10.6$ Hz, H_d), 3.53 (m, H_e), 3.59 (d, $^3J = 3.6$ Hz, H_b), 3.66 (dd, $^2J = 12.8$ Hz / $^3J = 4.0$ Hz, H_c), 3.89 (dd, $^2J = 10.6$ Hz / $^3J = 5.2$ Hz, H_d), 3.97-4.00 (m, 2 H_g), 4.11-4.15 (m, 2 H_h), 4.67 (d, $^2J = 2.0$ Hz, $\text{H}_{a/a'}$), 4.70 (d, $^2J = 2.0$ Hz, $\text{H}_{a/a'}$), 4.76 (d, $^2J = 12.8$ Hz, H_c), 5.44 (m, H_i), 7.32 (d, $^3J = 7.4$ Hz, 2 H_{Ts}), 7.54-7.58 (m, 2 H_{Ph}), 7.66 (m, H_{Ph}), 7.70 (d,

$^3J = 7.4$ Hz, $2H_{Ts}$), 7.83-7.86 (m, $2H_{Ph}$); ^{13}C NMR (100 MHz, $CDCl_3$) δ (ppm): 21.6 (C_{Ts}), 39.8 (C_e), 54.7 ($C_{h/g}$), 54.9 ($C_{h/g}$), 66.3 (C_c), 67.8 (C_b), 71.1 (C_d), 119.3 ($C_{a/a'}$), 123.5 (C_i), 127.6 ($2C_{Ph}$), 129.1 ($2C_{Ts}$), 129.3 ($2C_{Ph}$), 130.0 ($2C_{Ts}$), 133.9 (C_{Ph}), 134.1 (C_{Ts}), 135.7 (C_f), 136.5 ($C_{b'}$), 137.3 (C_{Ph}), 143.9 (C_{Ts}); **ESI-MS (m/z)**: 460.1 $[M+H]^+$; **AE**: calculated for $C_{23}H_{25}NO_5S_2$: C, 60.11; H, 5.48; N, 3.05; found: C, 59.67; H, 5.44; N, 3.33. The enantiomeric excess has been determined by **HPLC** analysis using a CHIRALPAK IA column (4.6 x 250 mm, 5 μ m) with 70 % hexane / 20 % 2-PrOH / 10 % acetonitrile mobile phase at a 1.0 mL/min flow rate, using a UV detector set up at $\lambda = 220$ nm. The retention time for the major isomer is 9.4 min and for the minor isomer is 8.2 min.

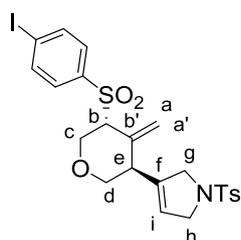
**54c**

Using the same experimental procedure as for compound **54a**, **54c** was obtained as a colourless solid (0.0238 g, 55% yield, ee=88%) after 1 hour. **MW**: 489.60 g/mol; **m.p.**: 86-87 °C; $[\alpha]_D^{20} +112.92$ (c 0.04 g / 100 mL, CH_3CN); **IR (ATR) ν (cm^{-1})**: 2920, 2851, 1339, 1304, 1159; 1H NMR (400 MHz, $CDCl_3$) δ (ppm): 2.43 (s, $3H_{Ts}$), 3.20 (dd, $^2J = 10.8$ Hz / $^3J = 10.8$ Hz, $1H_d$), 3.50 (m, H_e), 3.55 (d, $^3J = 4.0$ Hz, H_b), 3.65 (dd, $^2J = 12.8$ Hz / $^3J = 4.0$ Hz, H_c), 3.87 (dd, $^2J = 10.4$ Hz / $^3J = 5.6$ Hz, H_d), 3.90 (s, $3H_{OCH_3}$), 3.97-4.00 (m, $2H_g$), 4.12-4.14 (m, $2H_h$), 4.72-4.76 (m, $3H_{a,a',c}$), 5.43 (m, H_i), 7.00 (d, $^3J = 9.2$ Hz, $2H_{p-OCH_3Ph}$), 7.32 (d, $^3J = 8.4$ Hz, $2H_{Ts}$), 7.70 (d, $^3J = 8.4$ Hz, $2H_{Ts}$), 7.75 (d, $^3J = 9.2$ Hz, $2H_{p-OCH_3Ph}$); ^{13}C NMR (100 MHz, $CDCl_3$) δ (ppm): 21.7 (C_{Ts}), 39.8 (C_e), 54.7 ($C_{h/g}$), 54.9 ($C_{h/g}$), 55.8 (C_{OCH_3}), 66.5 (C_c), 68.0 (C_b), 71.0 (C_d), 114.3 ($2C_{p-OCH_3Ph}$), 119.2 ($C_{a/a'}$), 123.4 (C_i), 127.6 ($2C_{Ts}$), 128.9 (C_{p-OCH_3Ph}), 130.0 ($2C_{Ts}$), 131.4 ($2C_{p-OCH_3Ph}$), 134.0 (C_{p-OCH_3Ph}), 135.8 (C_{Ts}), 135.9 (C_f), 136.7 ($C_{b'}$), 143.9 (C_{Ts}), 164.0 (C_{p-OCH_3Ph}); **ESI-MS (m/z)**: 490.1 $[M+H]^+$; **AE**: calculated for $C_{24}H_{27}NO_6S_2$: C, 58.88; H, 5.56; N, 2.86; found: C, 58.79 and 58.99; H, 5.58 and 5.82; N, 3.18 and 3.31. The enantiomeric excess has been determined by **HPLC** analysis using a CHIRALPAK IA column (4.6 x 250 mm, 5 μ m) with 70 % hexane / 20 % 2-PrOH / 10 % acetonitrile mobile phase at a 1.0 mL/min flow rate, using a UV detector set up at $\lambda = 220$ nm. The retention time for the major isomer is 10.9 min and for the minor isomer is 9.8 min. min.

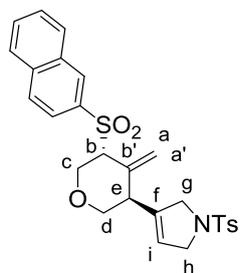
**54d**

Using the same experimental procedure as for compound **54a**, **54d** was obtained as a colourless solid (0.0451 g, 43% yield, ee=92%) after 24 hours. **MW**: 504.57 g/mol; **m.p.**: 122-124 °C; $[\alpha]_D^{20} +89.79$ (c 0.28 g / 100 mL, CH_3CN); **IR (ATR) ν (cm^{-1})**: 2922, 1530, 1347, 1303, 1158, 1105; 1H NMR (400 MHz, $CDCl_3$) δ (ppm): 2.43 (s, $3H_{Ts}$), 3.21 (dd, $^2J = 10.8$ Hz / $^3J = 10.8$ Hz,

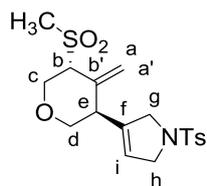
1H_d), 3.57 (m, H_e), 3.66 (d, ³J = 4.0 Hz, H_b), 3.72 (dd, ²J = 12.8 Hz / ³J = 4.0 Hz, H_c), 3.91 (dd, ²J = 10.8 Hz / ³J = 5.2 Hz, H_d), 3.97-4.01 (m, 2H_g), 4.13-4.14 (m, 2H_h), 4.70-4.81 (m, 3H_{a,a',c}), 5.50 (m, H_i), 7.33 (d, ³J = 8.0 Hz, 2H_{TS}), 7.70 (d, ³J = 8.0 Hz, 2H_{TS}), 8.05 (d, ³J = 8.6 Hz, 2H_{p-NO₂Ph}), 8.39 (d, ³J = 8.6 Hz, 2H_{p-NO₂Ph}); ¹³C NMR (75 MHz, CDCl₃) δ (ppm): 21.7 (C_{TS}), 39.9 (C_e), 54.5 (C_{h/g}), 54.8 (C_{h/g}), 66.0 (C_c), 68.0 (C_b), 71.0 (C_d), 120.2 (C_{a/a'}), 124.1 (C_i), 124.3 (2C_{p-NO₂Ph}), 127.6 (2C_{TS}), 130.0 (2C_{TS}), 130.7 (2C_{p-NO₂Ph}), 133.7 (C_{TS}), 135.2 (C_f), 136.1 (C_{b'}), 142.9 (C_{p-NO₂Ph}), 143.9 (C_{TS}), 151.0 (C_{p-NO₂Ph}); **ESI-HRMS (m/z)**: calculated for [M+Na]⁺: 527.0917; experimental: 527.0915. The enantiomeric excess has been determined by **HPLC** analysis using a CHIRALPAK IA column (4.6 x 250 mm, 5 μm) with 50 % hexane / 50 % 2-PrOH mobile phase at a 1.0 mL/min flow rate, using a UV detector set up at λ = 220 nm. The retention time for the major isomer is 20.6 min and for the minor isomer is 17.5 min.

**54e**

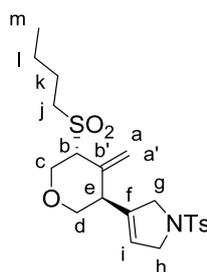
Using the same experimental procedure as for compound **54a**, **54e** was obtained as a colourless solid (0.0436 g, 41% yield, ee=87%) after 24 hours. **MW**: 585.47 g/mol; **m.p.**: 168-170°C; [α]_D²⁰ +64.19 (c 0.16 g / 100 mL, CH₃CN); **IR (ATR) ν (cm⁻¹)**: 2918, 2850, 1336, 1307, 1142, 1099; ¹H NMR (400 MHz, CDCl₃) δ (ppm): 2.43 (s, 3H_{TS}), 3.20 (dd, ²J = 10.8 Hz / ³J = 10.8 Hz, 1H_d), 3.51 (m, H_e), 3.57 (d, ³J = 4.2 Hz, H_b), 3.66 (dd, ²J = 12.8 Hz / ³J = 4.2 Hz, H_c), 3.89 (dd, ²J = 10.8 Hz / ³J = 5.2 Hz, H_d), 3.96-4.00 (m, 2H_g), 4.13-4.14 (m, 2H_h), 4.69-4.77 (m, 3H_{a,a',c}), 5.45 (m, H_i), 7.33 (d, ³J = 8.2 Hz, 2H_{TS}), 7.53 (d, ³J = 8.6 Hz, 2H_{p-IPh}), 7.70 (d, ³J = 8.2 Hz, 2H_{TS}), 7.91 (d, ³J = 8.6 Hz, 2H_{p-IPh}); ¹³C NMR (75 MHz, CDCl₃) δ (ppm): 21.7 (C_{TS}), 39.8 (C_e), 54.6 (C_{h/g}), 54.9 (C_{h/g}), 66.2 (C_c), 67.8 (C_b), 71.0 (C_d), 102.2 (C_{p-IPh}), 119.7 (C_{a/a'}), 123.7 (C_i), 127.6 (2C_{TS}), 130.0 (2C_{TS}), 130.5 (2C_{p-IPh}), 133.8 (C_{TS}), 135.5 (C_f), 136.3 (C_{b'}), 136.9 (C_{p-IPh}), 138.4 (2C_{p-IPh}), 143.9 (C_{TS}); **ESI-HRMS (m/z)**: calculated for [M+Na]⁺: 608.0033; experimental: 608.0023. The enantiomeric excess has been determined by **HPLC** analysis using a CHIRALPAK IA column (4.6 x 250 mm, 5 μm) with 70 % hexane / 20 % 2-PrOH / 10 % acetonitrile mobile phase at a 1.0 mL/min flow rate, using a UV detector set up at λ = 220 nm. The retention time for the major isomer is 10.7 min and for the minor isomer is 9.6 min.

**54f**

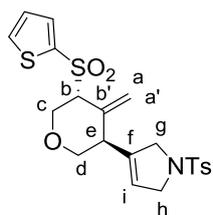
Using the same experimental procedure as for compound **54a**, **54f** was obtained as a colourless solid (0.0443 g, 47% yield, ee=82%) after 1 hour together with traces of compound **55** which could not be separated. **MW**: 509.63 g/mol; ¹H NMR (400 MHz, CDCl₃) δ (ppm): 2.39 (s, 3H_{TS}),

**54h**

Using the same experimental procedure as for compound **54a**, **54h** was obtained as a pale orange solid (0.0496 g, 72% yield, ee=86%) after 2.5 hours. **MW**: 397.50 g/mol; **m.p.**: 52-53°C; $[\alpha]_D^{20} +51.46$ (c 0.18 g / 100 mL, CH₃CN); **IR (ATR) v (cm⁻¹)**: 2928, 2856, 1336, 1299, 1159, 1107; **¹H NMR (400 MHz, CDCl₃) δ (ppm)**: 2.44 (s, 3H_{TS}), 2.93 (s, 3H_{SO₂CH₃}), 3.25 (dd, ²J = 10.8 Hz / ³J = 10.8 Hz, H_d), 3.61 (d, ³J = 4.0 Hz, H_b), 3.69-3.73 (m, 2H_{c,e}), 3.93 (dd, ²J = 10.4 Hz / ³J = 5.2 Hz, H_d), 4.01-4.07 (m, 2H_g), 4.15-4.17 (m, 2H_h), 4.78 (d, ²J = 12.8 Hz, H_c), 4.96 (d, ²J = 2.0 Hz, H_{a/a'}), 5.23 (d, ²J = 2.0 Hz, H_{a/a'}), 5.53 (m, H_i), 7.36 (d, ³J = 8.4 Hz, 2H_{TS}), 7.71 (d, ³J = 8.4 Hz, 2H_{TS}); **¹³C NMR (100 MHz, CDCl₃) δ (ppm)**: 21.6 (C_{TS}), 39.2 (C_{e/SO₂CH₃}), 39.9 (C_{e/SO₂CH₃}), 54.6 (C_{h/g}), 54.9 (C_{h/g}), 65.6 (C_c), 66.4 (C_b), 71.0 (C_d), 119.2 (C_{a/a'}), 123.9 (C_i), 127.5 (2C_{TS}), 130.0 (2C_{TS}), 133.7 (C_{TS}), 135.4 (C_f), 137.6 (C_{b'}), 143.9 (C_{TS}); **ESI-HRMS (m/z)**: calculated for [M+Na]⁺: 420.0910; experimental: 420.0918. The enantiomeric excess has been determined by **HPLC** analysis using a CHIRALPAK IA column (4.6 x 250 mm, 5 μm) with 76 % hexane / 20 % 2-PrOH / 4 % acetonitrile mobile phase at a 1.0 mL/min flow rate, using a UV detector set up at λ = 220 nm. The retention time for the major isomer is 19.8 min and for the minor isomer is 18.0 min.

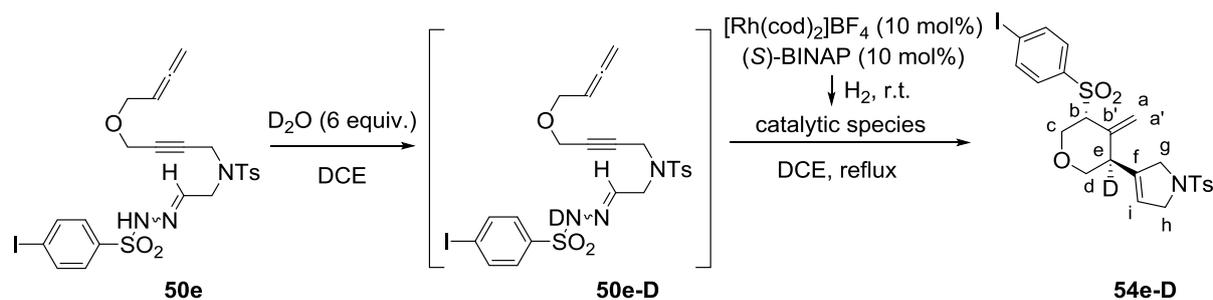
**54i**

Using the same experimental procedure as for compound **54a**, **54i** was obtained as a colourless solid (0.0437 g, 92% yield, ee=96%) after 2 hours. **MW**: 439.58 g/mol; **m.p.**: 56-58°C; $[\alpha]_D^{20} +80.54$ (c 0.25 g / 100 mL, CH₃CN); **IR (ATR) v (cm⁻¹)**: 2960, 2871, 1339, 1295, 1159, 1106; **¹H NMR (400 MHz, CDCl₃) δ (ppm)**: 0.96 (t, ³J = 7.6 Hz, 3H_m), 1.47 (tq, ³J = 7.6 Hz / ³J = 7.6 Hz, 2H_l), 1.80-1.83 (m, 2H_k), 2.44 (s, 3H_{TS}), 2.98-3.06 (m, 2H_j), 3.25 (dd, ²J = 10.8 Hz / ³J = 10.8 Hz, 1H_d), 3.57 (d, ³J = 3.6 Hz, H_b), 3.67-3.71 (m, 2H_{c,e}), 3.94 (dd, ²J = 10.8 Hz / ³J = 5.6 Hz, H_d), 4.03-4.05 (m, 2H_g), 4.15-4.16 (m, 2H_h), 4.79 (d, ²J = 12.8 Hz, H_c), 4.95 (d, ²J = 2.0 Hz, H_{a/a'}), 5.17 (d, ²J = 2.0 Hz, H_{a/a'}), 5.52 (m, H_i), 7.34 (d, ³J = 8.0 Hz, 2H_{TS}), 7.72 (d, ³J = 8.0 Hz, 2H_{TS}); **¹³C NMR (100 MHz, CDCl₃) δ (ppm)**: 13.7 (C_m), 21.7 (C_{TS}), 21.9 (C_l), 23.6 (C_k), 40.1 (C_e), 50.5 (C_j), 54.7 (C_{h/g}), 54.9 (C_{h/g}), 64.8 (C_c), 65.8 (C_b), 71.2 (C_d), 118.5 (C_{a/a'}), 123.7 (C_i), 127.6 (2C_{TS}), 130.0 (2C_{TS}), 133.9 (C_{TS}), 135.6 (C_f), 138.3 (C_{b'}), 143.9 (C_{TS}); **ESI-HRMS (m/z)**: calculated for [M+Na]⁺: 462.1379; experimental: 462.1373. The enantiomeric excess has been determined by **HPLC** analysis using a CHIRALPAK IA column (4.6 x 250 mm, 5 μm) with 78 % hexane / 20 % 2-PrOH / 2 % acetonitrile mobile phase at a 1.0 mL/min flow rate, using a UV detector set up at λ = 220 nm. The retention time for the major isomer is 21.9 min and for the minor isomer is 25.1 min.

**54j**

Using the same experimental procedure as for compound **54a**, **54j** was obtained as a colourless solid (0.0437 g, 40% yield, ee=91%) after 24 hours. **MW**: 465.60 g/mol; **m.p.**: 74-76°C; $[\alpha]_D^{20} +86.47$ (c 0.09 g / 100 mL, CH₃CN); **IR (ATR) v (cm⁻¹)**: 2959, 2860, 1307, 1159, 1141, 1106; **¹H NMR (400 MHz, CDCl₃) δ (ppm)**: 2.43 (s, 3H_{TS}), 3.22 (dd, ²J = 10.8 Hz / ³J = 10.8 Hz, H_d), 3.55 (m, H_e), 3.68-3.73 (m, 2H_{c,b}), 3.90 (dd, ²J = 10.4 Hz / ³J = 4.8 Hz, H_d), 4.00-4.02 (m, 2H_g), 4.13-4.15 (m, 2H_h), 4.77-4.80 (m, 3H_{a,a',c}), 5.46 (m, H_i), 7.17 (dd, ³J = 5.2 Hz / ³J = 3.8 Hz, H_{thiophene}), 7.33 (d, ³J = 8.4 Hz, 2H_{TS}), 7.64 (dd, ³J = 3.8 Hz / ⁴J = 1.4 Hz, H_{thiophene}), 7.71 (d, ³J = 8.4 Hz, 2H_{TS}), 7.75 (dd, ³J = 5.2 Hz / ⁴J = 1.4 Hz, H_{thiophene}); **¹³C NMR (100 MHz, CDCl₃) δ (ppm)**: 21.7 (C_{TS}), 39.8 (C_e), 54.7 (C_{h/g}), 54.9 (C_{h/g}), 66.4 (C_c), 69.1 (C_b), 71.1 (C_d), 119.5 (C_{a/a'}), 123.5 (C_i), 127.6 (2C_{TS}), 128.0 (C_{thiophene}), 130.0 (2C_{TS}), 133.9 (C_{TS}), 134.8 (C_{thiophene}), 135.5 (C_f), 135.7 (C_{thiophene}), 136.6 (C_{b'}), 138.2 (C_{thiophene}), 143.9 (C_{TS}); **ESI-MS (m/z)**: 466.1 [M+H]⁺; **AE**: calculated for C₂₁H₂₃NO₅S₃: C, 54.17; H, 4.98; N, 3.01; found: C, 54.39 and 54.21; H, 5.09 and 4.97; N, 3.35 and 3.29. The enantiomeric excess has been determined by **HPLC** analysis using a CHIRALPAK IA column (4.6 x 250 mm, 5 μm) with 78 % hexane / 20 % 2-PrOH / 2 % acetonitrile mobile phase at a 1.0 mL/min flow rate, using a UV detector set up at λ = 220 nm. The retention time for the major isomer is 28.8 min and for the minor isomer is 25.9 min.

8.4.4. Deuterium labelling experiment



Compound **54e-D** was obtained following the same procedure as for compound **54a** but stirring D₂O (6 eq.) in DCE before adding the catalytic system. The compound **54e-D** was obtained as a colourless solid (0.0169 g, 31% yield). **MW**: 586.48 g/mol; **¹H NMR (400 MHz, CDCl₃) δ (ppm)**: 2.45 (s, 3H_{TS}), 3.19 (d, ²J = 10.4 Hz, H_d), 3.56 (d, ³J = 4.0 Hz, H_b), 3.66 (dd, ²J = 13.2 Hz / ³J = 4.4 Hz, H_c), 3.89 (d, ²J = 10.4 Hz, H_d), 3.95-4.01 (m, 2H_g), 4.13-4.14 (m, 2H_h), 4.70-4.77 (m, 3H_{a,a',c}), 5.45 (m, H_i), 7.34 (d, ³J = 8.4 Hz, 2H_{TS}), 7.53 (d, ³J = 8.6 Hz, 2H_{p-IPh}), 7.71 (d, ³J = 8.4 Hz, 2H_{TS}), 7.92 (d, ³J = 8.6 Hz, 2H_{p-IPh}); **²H NMR (400 MHz, CHCl₃) δ (ppm)**: 3.48 (s, D_e); **¹³C NMR (100 MHz, CDCl₃) δ (ppm)**: 21.7 (C_{TS}), 39.3 (C_e), 54.6 (C_{h/g}), 54.9 (C_{h/g}), 66.2 (C_c), 67.9 (C_b), 71.0 (C_d), 102.2 (C_{p-IPh}), 119.7 (C_{a/a'}), 123.7 (C_i),

127.6 ($2C_{Ts}$), 130.0 ($2C_{Ts}$), 130.6 ($2C_{p-IPh}$), 133.9 (C_{Ts}), 135.5 (C_f), 136.3 (C_b), 137.0 (C_{p-IPh}), 138.5 (C_{p-IPh}), 143.9 (C_{Ts}); **ESI-HRMS (m/z)**: calculated for $[M+Na]^+$: 609.0096; experimental: 609.0094.

BIBLIOGRAPHY

- ¹ a) Davies, H. M. L.; Hedley, S. J. *Chem. Soc. Rev.* **2007**, *36*, 1109; b) Davies, H. M. L.; Denton, J. R. *Chem. Soc. Rev.* **2009**, *38*, 3061.
- ² a) Gutekunst, W. R.; Baran, P. S. *Chem. Soc. Rev.* **2011**, *40*, 1976; b) McMurray, L.; O'Hara, F.; Gaunt, M. J. *Chem. Soc. Rev.* **2011**, *40*, 1885.
- ³ Koizumi, Y.; Kobayashi, J.; Wakimoto, T.; Furuta, T.; Fukuyama, T.; Kan, T. *J. Am. Chem. Soc.* **2008**, *130*, 16854.
- ⁴ Jia, M.; Ma, S. *Angew. Chem. Int. Ed.* **2016**, *55*, 9134.
- ⁵ Bamford, W. R.; Stevens, T. S. *J. Am. Chem. Soc.* **1952**, 4735-4740. Carey, F. A.; Sundberg, R. J. *Advanced Organic Chemistry (Third Edition). Part B: Reactions and Synthesis.* Plenum Press; New York: **1991**.
- ⁶ Fulton, J. R.; Aggarwal, V. K.; Vicente, J. *Eur. J. Org. Chem.* **2005**, 1479.
- ⁷ Kulinkovich, O. G. *Cyclopropanes in Organic Synthesis*, John Wiley & Sons, Inc. Hoboken, NJ, **2015**.
- ⁸ a) Jones, V. K.; Deutschman Jr., A. J.; *J. Org. Chem.* **1965**, *30*, 3978; b) Vidal, M.; Vincens, M.; Arnaud, P. *Bull. Soc. Chim. Fr.* **1972**, 657; c) Dolgii, I. E.; Shapiro, E. A.; Nefedov, O. M. *Bull. Acad. Sci. USSR Div. Chem. Sci. (Engl. Transl.)* **1974**, *23*, 929; d) Shapiro, E. A.; Dolgii, I. E.; Nefedov, O. M. *Bull. Acad. Sci. USSR Div. Chem. Sci. (Engl. Transl.)* **1980**, *29*, 1493; e) Baikov, V. E.; Danilkina, L. P.; Ogloblin, K. A. *Russ. J. Gen. Chem.* **1983**, *53*, 2172.
- ⁹ Suárez, A.; Fu, G. C. *Angew. Chem. Int. Ed.* **2004**, *43*, 3580.
- ¹⁰ Hassink, M.; Liu, X.; Fox, J. M. *Org. Lett.* **2011**, *13*, 2388.
- ¹¹ a) Zhou, L.; Ma, J.; Zhang, Y.; Wang, J. *Tetrahedron Lett.* **2011**, *52*, 5484; b) Zhou, L.; Ma, J.; Zhang, Y.; Wang, J. *Tetrahedron Lett.* **2013**, *54*, 2558.
- ¹² Xiao, Q.; Xia, Y.; Li, H.; Zhang, Y.; Wang, J. *Angew. Chem. Int. Ed.* **2011**, *50*, 1114.
- ¹³ Hossain, M. L.; Ye, F.; Zhang, Y.; Wang, J. *J. Org. Chem.* **2013**, *78*, 1236.
- ¹⁴ a) Zhou, L.; Shi, Y.; Xiao, Q.; Liu, Y.; Ye, F.; Zhang, Y.; Wang, J. *Org. Lett.* **2011**, *13*, 968; b) Liu, G.; Xu, G.; Li, J.; Ding, D.; Sun, J. *Org. Biomol. Chem.* **2014**, *12*, 1387.
- ¹⁵ Ye, F.; Shi, Y.; Zhou, L.; Xiao, Q.; Zhang, Y.; Wang, J. *Org. Lett.* **2011**, *13*, 5020.
- ¹⁶ Paul, N. D.; Mandal, S.; Otte, M.; Cui, X.; Zhang, X. P.; de Bruin, B. *J. Am. Chem. Soc.* **2014**, *136*, 1090.
- ¹⁷ Helan, V.; Gulevich, A. V.; Gevorgyan, V. *Chem. Sci.*, **2015**, *6*, 1928.
- ¹⁸ a) Marek, I.; Simaan, S.; Masarwa, A. *Angew. Chem. Int. Ed.* **2007**, *46*, 7364-7376; b) Zhu, Z.-B.; Wei, Y.; Shi, M. *Chem. Soc. Rev.* **2011**, *40*, 5534.
- ¹⁹ Uehara, M.; Suematsu, H.; Yasutomi, Y.; Katsuki, T. *J. Am. Chem. Soc.* **2011**, *133*, 170.
- ²⁰ Cui, X.; Xu, X.; Lu, H.; Zhu, S.; Wojtas, L.; Zhang, X. P. *J. Am. Chem. Soc.* **2011**, *133*, 3304.
- ²¹ Lindsay, V. N. G.; Fiset, D.; Gritsch, P. J.; Azzi, S.; Charette, A. B. *J. Am. Chem. Soc.* **2013**, *135*, 1463.
- ²² Briones, J. F.; Davies, H. M. L. *Org. Lett.* **2011**, *13*, 3984.
- ²³ Briones, J. F.; Davies, H. M. L. *J. Am. Chem. Soc.* **2012**, *134*, 11916.

- ²⁴ Swenson, A. K.; Higgins, K. E.; Brewer, M. G.; Brennessel, W. W.; Coleman, M. G. *Org. Biomol. Chem.*, **2012**, *10*, 7483.
- ²⁵ Thomas, T. J.; Merritt, B. A.; Lemma, B. E.; McKoy, A. M.; Nguyen, T.; Swenson, A. K.; Mills, J. L., Coleman M. G. *Org. Biomol. Chem.* **2016**, *14*, 1742.
- ²⁶ Gulevich, A.V.; Dudnik, A. S.; Chernyak, N.; Gevorgyan, V. *Chem. Rev.* **2013**, *113*, 3084.
- ²⁷ Cui, X.; Xu, X.; Wojtas, L.; Kim, M. M.; Zhang, X. P. *J. Am. Chem. Soc.* **2012**, *134*, 19981.
- ²⁸ Xia, L.; Lee, Y. R. *Eur. J. Org. Chem.* **2014**, 3430.
- ²⁹ Hossain, M. L.; Ye, J.; Zhang, Y.; Wang, J. *Tetrahedron* **2014**, *70*, 6957.
- ³⁰ Kurandina, D.; Gevorgyan, V. *Org. Lett.* **2016**, *18*, 1804.
- ³¹ Tietze, L. F.; Beifuss, U. *Angew. Chem. Int. Ed. Engl.* **1993**, *32*, 131.
- ³² a) Korkowski, P. F.; Hoye, T. R.; Rydberg, D. B. *J. Am. Chem. Soc.* **1988**, *110*, 2676. b) Hoye, T. R.; Chen, K.; Vyvyan, J. R. *Organometallics* **1993**, *12*, 2806.
- ³³ Harvey, D. F.; Brown, M. F. *J. Org. Chem.* **1992**, *57*, 5559.
- ³⁴ Hoye, T. R.; Dinsmore, C. J.; Johnson, D.S.; Korkowski, P. F. *J. Org. Chem.* **1990**, *55*, 4518.
- ³⁵ a) Padwa, A.; Krumpke, K. E.; Gareau, Y.; Chiacchio, U. *J. Org. Chem.* **1991**, *56*, 2523; b) Padwa, A.; Dean, D. C.; Fairfax, D. J.; Xu, S. L. *J. Org. Chem.* **1993**, *58*, 4646.
- ³⁶ Padwa A.; Weingarten, M. D. *J. Org. Chem.* **2000**, *65*, 3722.
- ³⁷ Padwa, A.; Weingarten, M. D. *Chem. Rev.* **1996**, *96*, 223-269.
- ³⁸ a) Jansone-Popova, S., May, J. A. *J. Am. Chem. Soc.* **2012**, *134*, 17877; b) Jansone-Popova, S.; Le, P. Q.; May, J. A. *Tetrahedron* **2014**, *70*, 4118.
- ³⁹ Le, P. Q.; May, J. A. *J. Am. Chem. Soc.* **2015**, *137*, 12219.
- ⁴⁰ Shi, Y.; Gevorgyan, V. *Org. Lett.* **2013**, *15*, 5394.
- ⁴¹ Zheng, Y.; Mao, J.; Weng, Y.; Zhang, X.; Xu, X. *Org. Lett.* **2015**, *17*, 5638.
- ⁴² Yao, R.; Rong, G.; Yan, B.; Qiu, L.; Xu, X. *ACS Catal.* **2016**, *6*, 1024.
- ⁴³ Zhang, C.; Chang, S.; Qiu, L.; Xu, X. *Chem. Commun.* **2016**, *52*, 12470.
- ⁴⁴ a) Le Paih, J.; Dérien, S.; Özdemir, I.; Dixneuf, P. H. *J. Am. Chem. Soc.* **2000**, *122*, 7400; b) Vovard-Le Bray, C.; Dérien, S.; Dixneuf, P. H. *Angew. Chem. Int. Ed.* **2009**, *48*, 1439; c) Moulin, S.; Zhang, H.; Raju, S.; Bruneau, C.; Dérien, S. *Chem. Eur. J.* **2013**, *19*, 3292.
- ⁴⁵ a) Monnier, F.; Castillo, D.; Dérien, S.; Toupet, L.; Dixneuf, P. H. *Angew. Chem. Int. Ed.* **2003**, *42*, 5474; b) Monnier, F.; Vovard-Le Bray, C.; Castillo, D.; Aubert, V.; Dérien, S.; Dixneuf, P. H.; Toupet, L.; Ienco, A.; Mealli, C. *J. Am. Chem. Soc.* **2007**, *129*, 6037; c) Eckert, M.; Monnier, F.; Shchetnikov, G. T.; Titanyuk, I. D.; Osipov, S. N.; Toupet, L.; Dérien, S.; Dixneuf, P. H. *Org. Lett.* **2005**, *17*, 3741.
- ⁴⁶ Vovard-Le Bray, C.; Dérien, S.; Dixneuf, P. F.; Murakami, M. *Synlett* **2008**, 193.
- ⁴⁷ a) Ni, Y.; Montgomery, J. *J. Am. Chem. Soc.* **2004**, *126*, 11162; b) Ni, Y.; Montgomery, J. *J. Am. Chem. Soc.* **2006**, *128*, 2609.
- ⁴⁸ Panne, P.; Fox, J. M. *J. Am. Chem. Soc.* **2007**, *129*, 22.
- ⁴⁹ a) Cambeiro, F.; López, S.; Varela, J. A.; Saá, C. *Angew. Chem. Int. Ed.* **2012**, *51*, 723; b) Cambeiro, F.; López, S.; Varela, J. A.; Saá, C. *Angew. Chem. Int. Ed.* **2014**, *53*, 5959; c) González-Rodríguez, C.; Suárez, J. R.; Varela, J. A.; Saá, C. *Angew. Chem. Int. Ed.* **2015**, *54*, 2724.
- ⁵⁰ Sun, J.; Dong, Y.; Cao, L.; Wang, X.; Wang, S.; Hu, Y. *J. Org. Chem.* **2004**, *69*, 8932.

- ⁵¹ For selected recent examples, see: a) Qiu, H.; Li, M.; Jiang, L.-Q.; Lv, F.-P.; Zan, L.; Zhai, C.-W.; Doyle, M. P.; Hu, W.-H. *Nature Chem.* **2012**, *4*, 733; b) Wang, H.; Guptill, D. M.; Varela-Alvarez, A.; Musaev, D. G.; Davies, H. M. L. *Chem. Sci.*, **2013**, *4*, 2844; c) Parr, B. T.; Davies, H. M. L. *Angew. Chem. Int. Ed.* **2013**, *52*, 10044; d) Xu, X.; Zavalij, P. Y.; Doyle, M. P. *J. Am. Chem. Soc.* **2013**, *135*, 12439; e) Kwok, S. W.; Zhang, L.; Grimster, N. P.; Fokin, V. V. *Angew. Chem. Int. Ed.* **2014**, *53*, 3452; f) Qin, C.; Davies, H. M. L. *J. Am. Chem. Soc.* **2014**, *136*, 9792.
- ⁵² a) Aggarwal, V. K.; de Vicente, J.; Bonnert, R. V. *J. Org. Chem.* **2003**, *68*, 5381; b) Pérez-Aguilar M. C.; Valdés, C. *Angew. Chem. Int. Ed.* **2013**, *52*, 7219.
- ⁵³ *Modern Rhodium-Catalyzed Organic Reactions* (Ed.: P. A. Evans), Wiley-VCH, Weinheim, **2005**.
- ⁵⁴ Nishimura, T.; Maeda, Y.; Hayashi, T. *Angew. Chem. Int. Ed.* **2010**, *49*, 7324.
- ⁵⁵ Ma, X.; Jiang, J.; Lv, S.; Yao, W.; Yang, Y.; Liu, S.; Xia, F.; Hu, W. *Angew. Chem. Int. Ed.* **2014**, *53*, 13136.
- ⁵⁶ Yada, A.; Fujita, S.; Murakami, M. *J. Am. Chem. Soc.* **2014**, *136*, 7217.
- ⁵⁷ Chen, D.; Zhang, X.; Qi, W.-Y.; Xu, B.; Xu, M.-H. *J. Am. Chem. Soc.* **2015**, *137*, 5268.
- ⁵⁸ Chen, D.; Zhu, D.-X.; Xu, M.-H. *J. Am. Chem. Soc.* **2016**, *138*, 1498.
- ⁵⁹ Wang, X.; Zhou, Y.; Qiu, L.; Yao, R.; Zheng, Y.; Zhang, C.; Bao, X.; Xu, X. *Adv. Synth. Catal.* **2016**, *358*, 1571.
- ⁶⁰ Wermuth, C.-G.; Bourguignon, J.-J.; Schlewer, G.; Gies, J.-P.; Schoenfelder, A.; Melikian, A.; Bouchet, M.-J.; Chantreux, D.; Molimard, J.-C.; Heaulme, M.; Chambon, J.-P.; Biziere, K. *J. Med. Chem.* **1987**, *30*, 239.
- ⁶¹ Banti, D.; Groaz, E.; North, M. *Tetrahedron* **2004**, *60*, 8043.
- ⁶² O'Connor, J. M.; Baldridge, K. K.; Vélez, C. L.; Rheingold, A. L.; Moore, C. E. *J. Am. Chem. Soc.* **2013**, *135*, 8826.
- ⁶³ Kozuch, S.; Shaik, S. *Acc. Chem. Res.* **2011**, *44*, 101.
- ⁶⁴ Chen, D. Y.-K.; Pouwer, R. H.; Richard, J.-A. *Chem. Soc. Rev.* **2012**, *41*, 4631.
- ⁶⁵ Monn, J. A.; Valli, M. J.; Massey, S. M.; Wright, R. A.; Salhoff, C. R.; Johnson, B. G.; Howe, T.; Alt, C. A.; Rhodes, G. A.; Robey, R. L.; Griffey, K. R.; Tizzano, J. P.; Kallman, M. J.; Helton, D. R.; Schoepp, D. D.; *J. Med. Chem.* **1997**, *40*, 528.
- ⁶⁶ a) Sorbera, L. A.; Castaner, J.; Leeson, P. A. *Drugs Future* **2005**, *30*, 7; b) Skolnick, P.; Popik, P.; Janowsky, A.; Beer, B.; Lippa, A. S.; *Eur. J. Pharmacol.* **2003**, *461*, 99.
- ⁶⁷ Liu, M.-L.; Duan, Y.-H.; Hou, Y.-L.; Li, C.; Gao, H.; Dai, Y.; Yao, X.-S. *Org. Lett.* **2013**, *15*, 1000.
- ⁶⁸ He, X.-F.; Yin, S.; Ji, Y.-C.; Su, Z.-S.; Geng, M.-Y.; Yue, J.-M. *J. Nat. Prod.* **2010**, *73*, 45.
- ⁶⁹ Kulinkovich, O. G. in *Cyclopropanes in Organic Synthesis*, John Wiley & Sons, Inc, Hoboken, NJ, **2015**.
- ⁷⁰ For reviews, see: a) Wender, P. A.; Gamber, G. G.; Williams, T. J. Rhodium(I)-catalyzed [5+2], [6+2], and [5+2+1] Cycloadditions: New Reactions for Organic Synthesis in *Modern Rhodium-Catalyzed Organic Reactions* (Ed.: Evans, P.A.), **2005**, Wiley-VCH, Weinheim; b) Hudlicky, T.; Reed, J. W. *Angew. Chem. Int. Ed.* **2010**, *49*, 4864; c) Jiao, L.; Yu, Z.-X. *J. Org. Chem.* **2013**, *78*, 6842. For selected recent examples, see: d) Taber, D. F.; Guo, P.; Guo, N. *J. Am. Chem. Soc.* **2010**, *132*, 11179; e) Garayalde, D.; Krüger, K.; Nevado, C. *Angew. Chem. Int. Ed.* **2011**, *50*, 911; f) Laugeois, M.; Ponra, S.; Ratovelomana-Vidal, V.; Michelet, V.; Vitale, M. R. *Chem. Commun.* **2016**, *52*, 5332; g)

Zell, D.; Bu, Q.; Feldt, M.; Ackermann, L. *Angew. Chem. Int. Ed.* **2016**, *55*, 7408; h) Mita, T.; Tanaka, H.; Higuchi, Y.; Sato, Y. *Org. Lett.* **2016**, *18*, 2754.

⁷¹ Lebel, H.; Marcoux, J.-F.; Molinaro, C.; Charette, A. B. *Chem. Rev.* **2003**, *103*, 977; b) Pellissier, H. *Tetrahedron* **2008**, *64*, 7041; c) Hodgson, D. M.; Salik, S. *Curr. Org. Chem.* **2016**, *20*, 4.

⁷² a) Zhang, Z.; Wang, J. *Tetrahedron*, **2008**, *64*, 6577; b) Jia, M.; Ma, S. *Angew. Chem. Int. Ed.* **2016**, *55*, 9134.

⁷³ Davies, H. M. L.; Huby, N. J. S.; Cantrell Jr., W. R.; Olive, J. L. *J. Am. Chem. Soc.* **1993**, *115*, 9468.

⁷⁴ For reviews, see: a) Davies, H. M. L. *Aldrichimica Acta* **1997**, *30*, 107; b) Davies, H. M. L. *Eur. J. Org. Chem.* **1999**, 2459. For selected recent examples, see: c) Deng, L.; Giessert, A. J.; Gerlitz, O. O.; Dai, X.; Diver, S. T.; Davies, H. M. L. *J. Am. Chem. Soc.* **2005**, *127*, 1342; d) Lian, Y.; Miller, L. C.; Born, S.; Sarpong, R.; Davies, H. M. L. *J. Am. Chem. Soc.* **2010**, *132*, 12422; e) Xu, J.; Caro-Diaz, E. J. E.; Theodorakis, E. A. *Org. Lett.* **2010**, *12*, 3708; f) Parr, B. T.; Davies, H. M. L. *Angew. Chem. Int. Ed.* **2013**, *52*, 10044.

⁷⁵ For selected recent references, see: a) Benitez, D.; Shapiro, N. D.; Tkatchouk, E.; Wang, Y.; Doddard III, W. A.; Toste, F. D.; *Nat. Chem.* **2009**, *1*, 482; b) Miege, F.; Meyer, C.; Cossy, J. *Org. Lett.* **2010**, *12*, 4144; c) Miege, F.; Meyer, C.; Cossy, J. *Angew. Chem. Int. Ed.* **2011**, *50*, 5932; d) Miege, F.; Meyer, C.; Cossy, J. *Chem. Eur. J.* **2012**, *18*, 7810; e) Zhang, H.; Wang, B.; Wang, K.; Xie, G.; Li, C.; Zhang, Y.; Wang, J. *Chem. Comm.* **2014**, *50*, 8050.

⁷⁶ For selected references, see: a) Miki, K.; Ohe, K.; Uemura, S. *J. Org. Chem.* **2003**, *68*, 8505; b) Harrak, Y.; Blaszykowski, C.; Bernard, M.; Cariou, K.; Mainetti, E.; Mouriès, V.; Dhimane, A.-L.; Fensterbank, L.; Malacria, M. *J. Am. Chem. Soc.* **2004**, *126*, 8656; c) Moreau, X.; Goddard J.-P.; Bernard, M.; Lemièrre, G.; López-Romero, J. M.; Mainetti, E.; Marion, N.; Mouriès, V.; Thorimbert, S.; Fensterbank, L.; Malacria, M. *Adv. Synth. Catal.* **2008**, *350*, 43; d) Gorin, D. J.; Watson, I. D. G.; Toste, F. D. *J. Am. Chem. Soc.* **2008**, *130*, 3736; e) Sperger, C. A.; Tungen, J. E.; Fiksdahl, A. *Eur. J. Org. Chem.* **2011**, 3719.

⁷⁷ a) Johansson, M. J.; Gorin, D. J.; Staben, S. T.; Toste, F. D. *J. Am. Chem. Soc.* **2005**, *127*, 18002; b) Watson, I. D. G.; Ritter, S.; Toste, F. D. *J. Am. Chem. Soc.* **2009**, *131*, 2056.

⁷⁸ Zhu, D.; Ma, J.; Luo, K.; Fu, J.; Zhang, L.; Zhu, S. *Angew. Chem. Int. Ed.* **2016**, *55*, 8452.

⁷⁹ Zhang, L. *Acc. Chem. Res.* **2014**, *47*, 877; b) Zheng, Z.; Wang, Z.; Wang, Y.; Zhang, L. *Chem. Soc. Rev.* **2016**, *45*, 4448.

⁸⁰ a) Geny, A.; Gaudre, S.; Slowinski, F.; Amatore, M.; Chouraqui, G.; Malacria, M.; Aubert, C.; Gandon, V. *Adv. Synth. Cat.* **2009**, *351*, 271; b) Zuercher, W.J.; Scholl, M.; Grubbs, R. H. *J. Org. Chem.* **1998**, *63*, 4291; b) Araya, M.; Gulías, M.; Fernández, I.; Bhargava, G.; Castedo, L.; Mascareñas, J. L.; López, F. *Chem. Eur. J.* **2014**, *20*, 10225; d) Padwa, A.; Lipka, H.; Watterson, S. H.; Murphree, S. S. *J. Org. Chem.* **2003**, *68*, 6238.

⁸¹ Mukai, C.; Yamashita, H.; Hanaoka, M. *Org. Lett.* **2001**, *3*, 3385.

⁸² Lee, Y.-J.; Schrock, R. R.; Hoveyda, M. H. *J. Am. Chem. Soc.* **2009**, *131*, 10652.

⁸³ CCDC 1484927 (compound (1*R*,5*S*)-**48a**) contains the supplementary crystallographic data. These data can be obtained free of charge from The Cambridge Crystallographic Data Centre via www.ccdc.cam.ac.uk/data_request/cif. The thermal ellipsoids in the ORTEP plot of the X-ray structure of (1*R*,5*S*)-**48a** are drawn at 50% probability.

- ⁸⁴ Doyle, M. P.; Duffy, R.; Ratnikov, M.; Zhou, L. *Chem. Rev.* **2010**, *110*, 704.
- ⁸⁵ Preetz, A.; Fischer, C.; Kohrt, C.; Drexler, H.-J.; Baumann, W.; Heller, D. *Organometallics* **2011**, *30*, 5155.
- ⁸⁶ Hong, Y.-S.; Kim, H.-M.; Kim, H.-S.; Park, Y.-T. *Bull. Korean Chem. Soc.* **1999**, *20*, 1524.
- ⁸⁷ For selected reviews, see: a) Audran, G.; Pellissier, H. *Adv. Synth. Catal.* **2010**, *352*, 575; b) Adams, C. S.; Weatherly, C. D.; Burke, E. G.; Schomaker, J. M. *Chem. Soc. Rev.* **2014**, *43*, 3136; c) Brandi, A.; Cicchi, S.; Cordero, F. M.; Goti, A. *Chem. Rev.* **2014**, *114*, 7317. For selected papers, see: d) Lautens, M.; Meyer, C.; van Oeveren, A. *Tet. Lett.* **1997**, *38*, 3833; e) Vovard-Le Bray, C.; Dérien, S.; Dixneuf, P. H.; Murakami, M. *Synlett* **2008**, 193; f) Gregg, T. M.; Farrugia, M. K.; Frost, J. R. *Org. Lett.* **2009**, *11*, 4434; g) Lindsay, V. N. G.; Fiset, D.; Gritsch, P. J.; Azzi, S.; Charette, A. B. *J. Am. Chem. Soc.* **2013**, *135*, 1463; h) Phelps, A. M.; Dolan, N. S.; Connell, N. T.; Schomaker, J. M. *Tetrahedron* **2013**, *69*, 5614; h) Chanthamath, S.; Chua, H. W.; Kimura, S.; Shibatomi, K.; Iwasa S. *Org. Lett.* **2014**, *16*, 3408.
- ⁸⁸ Yao, T.; Hong, A.; Sarpong, R. *Synthesis* **2006**, 3605.
- ⁸⁹ Chanthamath, S.; Chua, H. W.; Kimura, S.; Shibatomi, K.; Iwasa, S. *Org. Lett.* **2014**, *16*, 3408.
- ⁹⁰ López, E.; Lonzi, G.; González, J.; López, L. A. *Chem. Commun.* **2016**, *52*, 9398.
- ⁹¹ Singh, R. R.; Pawar, S. K.; Huang, M.-J.; Liu, R.-S. *Chem. Commun.* **2016**, *52*, 11434.
- ⁹² a) Crabbé, P.; André, D.; Fillion, H. *Tetrahedron Lett.* **1979**, *10*, 893; b) Crabbé, P.; Fillion, H.; André, D.; Luche, J.-L. *J. Chem. Soc. Chem. Commun.* **1979**, 859; c) Rona, P.; Crabbé, P. *J. Am. Chem. Soc.* **1969**, *91*, 3289.
- ⁹³ González, M.; Rodríguez, R. A.; Cid, M. M.; López, C. S. *J. Comput. Chem.* **2012**, *33*, 1236-1239.
- ⁹⁴ Kuang, J.; Ma, S. *J. Org. Chem.* **2009**, *74*, 1763.
- ⁹⁵ CCDC 1493176 (compound (*R,R*)-**54a**) and CCDC 1493175 (compound **55**) contains the supplementary crystallographic data for this paper. These data can be obtained free of charge from The Cambridge Crystallographic Data Centre via www.ccdc.cam.ac.uk/data_request/cif. The thermal ellipsoids in the ORTEP plot of the X-ray structure of compound (*R,R*)-**54a** and **55** are drawn at 50% probability.
- ⁹⁶ Cossy, J.; Guérinot, A. *Adv. Heterocycl. Chem.* **2016**, *119*, 107-142.
- ⁹⁷ For the isolation of bryostatin 1, see: a) Pettit, G. R.; Herald, C. L.; Doubek, D. L.; Herald, D. L.; Arnold, E.; Clardy, J. *J. Am. Chem. Soc.* **1982**, *104*, 6846-6848; For a recent review on the bryostatins, see: b) Hale, K. J.; Manaviazar, S. *Chem. - Asian J.* **2010**, *5*, 704-754. For a recent total synthesis of bryostatins, see: c) Lu, Y.; Woo, S. K.; Krische, M. J. *J. Am. Chem. Soc.* **2011**, *133*, 13876-13879.
- ⁹⁸ For the isolation, see: a) Searle, P. A.; Molinski, T. F. *J. Am. Chem. Soc.* **1995**, *117*, 8126-8131; For a total synthesis, see: b) Smith III, A. B.; Verhoest, P. R.; Minbiole, K. P.; Schelhaas, M. *J. Am. Chem. Soc.* **2001**, *123*, 4834-4836.
- ⁹⁹ For the isolation, see: a) Cutignano, A.; Bruno, I.; Bifulco, G.; Casapullo, A.; Debitus, C.; Gomez-Paloma, L.; Riccio, R. *Eur. J. Org. Chem.* **2001**, 775-778; For a total synthesis, see: b) Hoye, T. R.; Hu, M. *J. Am. Chem. Soc.* **2003**, *125*, 9576-9577.

- ¹⁰⁰ For the isolation, see: a) Ohta, S.; Uy, M. M.; Yanai, M.; Ohta, E.; Hirata, T.; Ikegami, S. *Tetrahedron Lett.* **2006**, *47*, 1957-1960; For a recent total synthesis, see: b) Zhang, Z.; Xie, H.; Li, H.; Gao, L. Z. Song, *Org. Lett.* **2015**, *17*, 4706-4709.
- ¹⁰¹ a) Backes, G. L.; Jursic, B. S.; Neumann, D. M. *Bioorg. Med. Chem.* **2015**, *23*, 3397; b) Ozdemir, U. O.; Ilbiz, F.; Gunduzalp, A. B.; Ozbek, N.; Genç, Z. K.; Hamurcu, F.; Tekin, S. *J. Mol. Struct.* **2015**, *1100*, 464.
- ¹⁰² Lee, H.-Y. *Acc. Chem. Res.* **2015**, *48*, 2308.
- ¹⁰³ a) Kawakami, K.; Ishii, K.; Tanaka, T. *Bull. Chem. Soc. Jpn.* **1975**, *48*, 1051; b) Chiu, N.-S.; Schäfer, L.; Seip, R. *J. Organomet. Chem.* **1975**, *101*, 331.
- ¹⁰⁴ Maxwell, J. L.; Brown, K. C.; Bartley, D. W.; Kodadek, T. *Science* **1992**, *256*, 1544.
- ¹⁰⁵ a) Anciciaux, A. J.; Hubert, A. J.; Noels, A. F.; Petiniot, N.; Teyssie, P. *J. Org. Chem.* **1980**, *45*, 695; b) Alonso, M. E.; García, M.; Del, C. *Tetrahedron* **1989**, *45*, 69; c) Pirrung, M. C.; Morehead Jr, A. T. *J. Am. Chem. Soc.* **1996**, *118*, 8162; d) Pirrung, M. C.; Liu, H.; Morehead Jr, A. T. *J. Am. Chem. Soc.* **2002**, *124*, 1014; e) Wong, F. M.; Wang, J.; Hengge, A. C.; Wu, W. *Org. Lett.* **2007**, *9*, 1663.
- ¹⁰⁶ Qu, Z.; Shi, W.; Wang, J. *J. Org. Chem. Soc.* **2001**, *66*, 8139.
- ¹⁰⁷ a) Nowlan III, D. T.; Gregg, T. M.; Davies, H. M. L.; Singleton, D. A. *J. Am. Chem. Soc.* **2003**, *125*, 15902. b) Nakamura, E.; Yoshikai, N.; Yamanaka, M. *J. Am. Chem. Soc.* **2002**, *124*, 7181.
- ¹⁰⁸ All of the species detected in the present study were assigned by comparison of the experimentally obtained isotopic pattern and the theoretically calculated one. Only the most relevant spectra are shown in this chapter.
- ¹⁰⁹ a) Williams, V.; Kong, J. R.; Ko, B. J.; Mantri, Y.; Broadbelt, J. S.; Baik, M. H.; Krische, M. J. *J. Am. Chem. Soc.* **2009**, *131*, 16054; b) Parera, M.; Dachs, A.; Solà, M.; Pla-Quintana, A.; Roglans, A. *Chem. Eur. J.* **2012**, *18*, 13097.
- ¹¹⁰ Ramon-Córdoba, E.; Postils, V.; Salvador, P. *J. Chem. Theor. Comput.* **2015**, *11*, 1501.
- ¹¹¹ Skara, G.; Gimferrer, M.; De Proft, F.; Salvador, P.; Pinter, B. *Inorg. Chem.* **2016**, *55*, 2185.
- ¹¹² a) Feng, X.-W.; Wang, J.; Zhang, J.; Yang, J.; Wang, N.; Yu, X.-Q. *Org. Lett.* **2010**, *12*, 4408; b) Barluenga, J.; Tomás-Gamasa, M.; Aznar, F.; Valdés, C. *Eur. J. Org. Chem.* **2011**, 1520.
- ¹¹³ Deng, J.; Tabei, J.; Shiotsuki, M.; Sanda, F.; Masuda, T. *Macromolecules* **2004**, *37*, 5538.
- ¹¹⁴ Wermuth, C.-G.; Bourguignon, J.-J.; Schlewer, G.; Gies, J.-P.; Schoenfelder, A.; Melikian, A.; Bouchet, M.-J.; Chantreux, D.; Molimard, J.-C.; Heaulme, M.; Chambon, J.-P.; Biziere, K. *J. Med. Chem.* **1987**, *30*, 239.
- ¹¹⁵ Banti, D.; Groaz, E.; North, M. *Tetrahedron* **2004**, *60*, 8043.
- ¹¹⁶ Hydrazone derivatives were obtained as a mixture of *E/Z* isomers. Only the *E* isomer, which is the major product obtained, is described but the ratio of isomers as determined by ¹H NMR integration is given for completeness.
- ¹¹⁷ Calculated by ¹H NMR. Only the major compound **12ab** is fully described.
- ¹¹⁸ Calculated by ¹H NMR. Only the major compound **12ad** is fully described.
- ¹¹⁹ Yuan, W.; Wei, Y.; Shi, M. *ChemistryOpen* **2013**, *2*, 63-68.
- ¹²⁰ Geny, A.; Gaudre, S.; Slowinski, F.; Amatore, M.; Chouraqui, G.; Malacria, M.; Aubert, C.; Gandon, V. *Adv. Synth. Cat.* **2009**, *351*, 271.
- ¹²¹ Zuercher, W. J.; Scholl, M.; Grubbs, R. H. *J. Org. Chem.* **1998**, *63*, 4291.

- ¹²² Araya, M.; Gulías, M.; Fernández, I.; Bhargava, G.; Castedo, L.; Mascareñas, J. L.; López, F.; *Chem. Eur. J.* **2014**, *20*, 10225.
- ¹²³ Padwa, A.; Lipka, H.; Watterson, S. H.; Murphree, S. S. *J. Org. Chem.* **2003**, *68*, 6238.
- ¹²⁴ Brun, S.; Torres, Ò.; Pla-Quintana, A.; Roglans, A.; Goddard, R.; Pörschke, R. K. *Organometallics*, **2013**, *32*, 1710.
- ¹²⁵ Mukai, C.; Yamashita, H.; Hanaoka, M. *Org. Lett.* **2001**, *3*, 3385.
- ¹²⁶ Lee, Y.-J.; Schrock, R. R.; Hoveyda, M. H. *J. Am. Chem. Soc.* **2009**, *131*, 10652.